The Effects of LPS plus Pro-Inflammatory Cytokines on Glycogen Synthesis in C2C12 Myocytes

Xavier Roeseler

Thesis submitted for the degree of Doctor of Philosophy

University of Sussex

September 2010

Declaration

I hereby declare that this thesis has not been submitted, either in the same or different form, to this or any other University for a degree.

Signature:

Date:

Contents

The Effects of LPS plus Pro-Inflammatory Cytokines on Glycogen Synthesis in C2C12 Myocytes 1
Declaration 2
Contents 3
Acknowledgements 8
Abstract 9
Abbreviations 10
Chapter One - Introduction 12
1.1 Sepsis 13
1.2 LPS recognition by TLR4 and the Induction of the Inflammatory Response 14
1.3 The Key Pro-Inflammatory Cytokines: TNF-α, IL-1β and IFN-γ 17
1.3.1 TNF-α Signalling 18
1.3.2 IFN-γ Signalling 21
1.3.3 IL-1β Signalling 23
1.4 Nitric Oxide and Nitric Oxide Synthase 24
1.4.1 Nitric Oxide in the Innate Immune Response and Sepsis 25
1.5 Effects of Endotoxic Shock on Host Tissue 26
1.6 Glycogen and its Metabolism 27
1.6.1 Skeletal Muscle Glycogen Synthesis Regulation 29
1.6.2 Glucose transport 29
1.6.3 Muscle Glycogen Synthase 30
1.6.4 Glycogen Stores 31
1.6.5 Insulin Action on Muscle Glycogen Synthesis 31
1.7 Endotoxic Shock and Hepatic Glycogen Metabolism 33
1.8 Effects of Sepsis, Nitric Oxide, and In Vitro Inflammatory Models on Skeletal Muscle Glycogen Metabolism 34
1.8.1 In Vivo Models of Sepsis and Endotoxic Shock 35
1.8.2 The use of LPS and Pro-Inflammatory Cytokines in In Vitro Models 36
1.8.3 Investigating Insulin Resistance under Septic, Endotoxic and Inflammatory Conditions 36
1.8.4 The Role of Nitric Oxide 37
1.9 In Vitro Model of Skeletal Muscle: C2C12 Cells 38
1.10 Aims 39
Chapter Two – Materials and Methods 40
2.1 Materials 41

2.2 Cell Culture 42
2.2.1 Growth of C2C12 Myocytes 42
2.2.2 Cell Counting 44
2.2.3 Cryogenic Preservation 45
2.2.4 Determination of Cell Viability 45
2.2.5 Basis of In Vitro Model of Endotoxic Shock 47
2.2.6 Mouse Hind Limb Skeletal Muscle Extract 48
2.3 Determination of Nitrate and Nitrite 48
2.3.1 Preparation of Samples 49
2.3.2 Determination of Nitrite 49
2.3.3 Conversion of Nitrate 50
2.3.4 Procedure for the Conversion of Nitrate to Nitrite 50
2.3.5 Preparation of Formate Nitrate Reductase 51
2.4 Determination of Protein 51
2.4.1 Procedure for BCA method 52
2.4.2 Procedure for Bio-Rad Protein Assay (Bradford) Method 52
2.5 Determination of Glycogen 53
2.5.1 Conversion of Glycogen to Glucose 53
2.5.2 Determination of Glucose produced from Glycogen Breakdown 54
2.6 [U-^{14}C] Glucose Incorporation into Glycogen 54
2.6.1 Perfection of the Method 55
2.6.2 Sample Preparation 56
2.6.3 Procedure 56
2.7 Determination of Glucose Transport 57
2.7.1 Sample preparation and Procedure 57
2.8 Determination of Glycogen Phosphorylase Activity 57
2.8.1 Sample Preparation 58
2.8.2 Procedure 58
2.9 Determination of Glycogen Synthase Activity 59
2.9.1 Procedure 59
2.10 Determination of Glucose-6-Phosphate Concentration 60
2.10.1 Sample Preparation 60
2.10.2 Procedure 60
2.11 Determination of UDP-Glucose Concentration 61
2.11.1 Procedure 61
2.12 [^{35}S] Methionine Incorporation into Protein 61
2.12.1 Sample Preparation 62
2.12.2 Procedure 62

2.13 SDS-PAGE and Western Blotting 62
2.13.1 Sample Preparation 63
2.13.2 Preparation of the Polyacrylamide Gel 63
2.13.3 Loading of the Samples 64
2.13.4 Transfer of the Proteins 64
2.13.5 Immunodetection 65
2.13.6 Western Blot Detection Using ECL 68
2.13.7 Re-probing the Membrane 68
2.13.8 Analysis of Western Blots 68
2.14 Statistical Analysis 69
Chapter Three – Effects of LPS plus Pro-Inflammatory Cytokines on Nitric Oxide Production and Glycogen Synthesis in C2C12 Myocytes 70
3.1 Introduction 71
3.2 Effect of LPS plus Cytokine Treatment on Protein Content, Cell Viability and Nitric Oxide Levels in C2C12 Myocytes 72
3.2.1 Protein Content 72
3.2.2 Ethidium Homodimer-1 Cell Viability Assay 73
3.2.3 Nitric Oxide Levels 74
3.3 Effect of LPS plus Cytokine Treatment on Glycogen Synthesis in C2C12 Myocytes 78
3.3.1 Effect of LPS plus Cytokine Treatment on Basal Glycogen Synthesis in C2C12 Myocytes 80
3.3.2 Effects of LPS plus Cytokine Treatment on Insulin-Stimulated Glycogen Synthesis 81
3.3.3 Role of Nitric Oxide on LPS plus Cytokine-Induced Changes in Basal Glycogen Synthesis 87
3.3.4 Role of Nitric Oxide on LPS plus Cytokine-Induced Impairment of Insulin-Stimulated Glycogen Synthesis 92
3.3.5 Time-Dependent Changes in Glycogen Metabolism in Response to LPS plus Cytokines 96
3.4 Summary 101
Chapter Four – The Effects of LPS plus Pro-Inflammatory Cytokines on the Regulatory Steps Governing Glycogen Synthesis in C2C12 Myocytes 105
4.1 Introduction 106
4.2 Effect Of LPS plus Cytokine Treatment on Glucose Uptake in C2C12 Myocytes 108
4.2.1 Effects of LPS plus Cytokine Treatment on Basal Glucose Uptake in C2C12 Myocytes 109
4.2.2 Effects of LPS Plus Cytokine Treatment on Insulin-Stimulated Glucose Uptake in C2C12 Myocytes 111
4.2.3 Role of Nitric Oxide on LPS plus Cytokine-Induced Changes in Glucose Uptake 114

4.2.4 Role of Reactive Oxygen Species on LPS plus Cytokine-Induced Changes in Myoblast Glucose Uptake 117

4.2.5. Effects of LPS plus Cytokines on GLUT1 and GLUT4 Transporters..... 121

4.3 Effects of LPS plus Cytokines Treatment on Total Glycogen Stores in C2C12 Myocytes122

4.4 Effects of LPS plus Cytokines Treatment on Glycogen Synthase and Glycogen Phosphorylase in C2C12 Myocytes 124

4.5 Effect of LPS plus Cytokine Treatment on Levels of Glucose-6-Phosphate and UDP-Glucose in C2C12 Myocytes 135

4.6 Summary 137

Chapter Five – The State of the Signalling Machinery Following LPS plus Pro-Inflammatory Cytokine Treatment in C2C12 Myocytes..... 141

5.1 – Introduction 142

5.2 Effects of LPS plus Cytokine Treatment on AMPK Levels and Activity in C2C12 Cells... 144

5.2.1 Effects of LPS plus Cytokine Treatment on AMPK Levels and Activity in Myoblasts..... 144

5.2.2 Effects of LPS plus Cytokine Treatment on AMPK Levels and Activity in Myotubes 148

5.3 Effects of LPS plus Cytokine Treatment On Akt And GSK3 Levels and Activity in C2C12 Cells 150

5.3.1 Effects of LPS plus Cytokine Treatment on Akt and GSK3 Levels and Activity in Myoblasts..... 150

5.3.2 Effects of LPS plus Cytokine Treatment on Akt and GSK3 Levels and Activity in Myotubes 155

5.3.3 Comparison of the Akt and GSK3 Activity Between Myoblasts and Myotubes 161

5.4 Effects of LPS plus Cytokine Treatment on p38 and ERK Levels and Activity in C2C12 Cells 167

5.4.1 Effects of LPS plus Cytokine Treatment on p38 and ERK Levels and Activity in Myoblasts..... 167

5.4.2 Effects of LPS plus Cytokine Treatment on p38 and ERK Levels and Activity in Myotubes 173

5.5 Summary 180

Chapter Six – Effects of LPS plus Pro-Inflammatory Cytokines on Protein Synthesis in C2C12 Myocytes..... 185

6.1 Introduction 186

6.2 Effects of LPS plus Cytokines on Protein Synthesis in C2C12 Myocytes 189

6.2.1 Effects of LPS plus Cytokines on Basal Protein Synthesis in C2C12 Myocytes 190

6.2.2 Effects of LPS plus Cytokines on Insulin-Stimulated Protein Synthesis in C2C12 Myocytes..... 192

6.2.3 Role of Nitric Oxide on LPS plus Cytokine Induced Effects on Basal and Insulin-Stimulated Protein Synthesis 195

6.3 Effects of LPS plus Cytokine Treatment on 4E-BP1 Phosphorylation 199
6.4 LPS plus Cytokine-Induced Time-Dependent Changes on Basal and Insulin-Stimulated Protein Synthesis in Myoblasts 201
6.5 Effects of LPS and Pro-Inflammatory Cytokine Combinations on Protein Synthesis 206
6.6 Summary 209
Chapter Seven - Conclusion 213
7.1 Overview of the Present Studies 214
7.2 Future Work 220
Chapter Eight - Bibliography 223

Acknowledgements

I do not think I can thank Dr. Mike Titheradge enough. Not because of the standard polite gratitude given to supervisors in acknowledgements, but because I have tremendous respect for Mike as he has truly had a profound and positive impact on me as a person, and as a scientist. In addition I thank him especially for his patience and never ending time for my questions regarding anything from work to photography.

I would also like to thank Prof. Simon Morley and his laboratory (Dr. Mark Coldwell, Dr. Mark Willett, Dr. Michèle Brocard, Dr. Markete Vlasak and Jed MacDonald) who kindly responded to my regular queries regarding laboratory methods, as well as making my days in the lab incredibly fun. I must also thank Prof. Simon Morley for the countless laboratory equipment he let me use.

I would also like to thank the University of Sussex for the graduate teaching assistantship that allowed this work to be carried out.

Finally I would like to thank my friends and family who maintained my emotional network throughout the four year period; especially my parents, Fani Gamon, Yalda Javadi, Fred Gamper, Norfolk Square crew (Urielito y Greggy) and the BXL crew.

Abstract

Culturing C2C12 myoblasts and myotubes with a combination of LPS, TNF-α, IFN-γ and IL1β for 18 hours was used to determine the effects of endotoxic shock on possible causes of the dysregulation of glucose homeostasis associated with the syndrome. The in vitro model was confirmed by the significant production of NO in both myoblasts and myotubes following treatment. The treatment resulted in significantly different results between both myocyte preparations with regards to the regulation of glycogen synthesis.

In the myoblasts, the treatment significantly increased myoblast glycogen synthesis, in a NO-independent manner, as seen by the inclusion of the NO synthase inhibitor L-NAME. This stimulation was unlikely to be due to a change in either GS or Phosphorylase activity. However it may have been caused by a significant increase in glucose transport induced by the treatment. This latter increase was also NO-independent, as well as not requiring reactive oxygen species. Insulin-induced myoblast protein synthesis was impaired by the treatment, which is likely due to an impairment of insulin-stimulated ERK1/2 phosphorylation.

In the myotubes the case was different, as the treatment significantly reduced glycogen synthesis in a NO-dependent manner. This correlated with a NO-dependent increase in GS phosphorylation, indicating it was less active, however measurements of GS fractional activity failed to confirm this. Insulin stimulation of myotube glycogen synthesis was impaired by the treatment in a NO-independent manner, which may have involved an impairment of the insulin signal to ERK1/2. However the latter impairment was NO-dependent, suggesting other contributory mechanisms.

Endotoxic treatment significantly increased myoblast protein content, but failed to do so in myotubes. This effect in the myoblasts may be explained by a significant increase in protein synthesis between 6 and 12 hours of treatment. None of the effects observed in the study were due to the treatment compromising cell viability.

Abbreviations

2DOG	2-deoxyglucose
ADP	adenosine diphosphate
AMP	adenosine monophosphate
AMPK	AMP activated protein kinase
ATP	adenosine triphosphate
BCA	bicinchoninic acid
BP-1	eIF4E binding protein 1
DMEM	dulbecco's modified eagle medium
DTT	dithiothreitol
ECL	enhanced chemiluminescence
EDTA	ethylenediaminetetraacetic acid
EGTA	ethylene glycol tetracetic acid
eIF2	eukaryotic initiation factor 2
eIF4E	eukaryotic initiation factor 4 E
eNOS	endothelial nitric oxide synthase
ERK	extracellular signal-regulated kinase
EthD-1	ethidium homo-dimer 1
FMN	flavin mononucleotide
FNR	formate nitrate reductase
G-1-P	glucose-1-phosphate
G-6-P	glucose-6-phosphate
GDP	guanine diphosphate
GLUT1	glucose transporter 1
GLUT4	glucose transporter 4
GS	glycogen synthase
GS-a	glycogen synthase (dephosphorylated, active)
GS-b	glycogen synthase (phosphorylated, less active)
GSK3	Glycogen synthase kinase 3
GTP	guanine triphosphate
GTPase	GTP-hydrolysing enzyme
HEPES	4-(2-hydroxyethyl)-1-piperazineethanesulfonic acid
HK	hexokinase
IFN	interferon
IL-1	interleukin-1
iNOS	inducible nitric oxide synthase
IRS1	insulin receptor substrate-1
JNK	c-Jun N-terminal kinase
L-NAME	N-G-nitro-L-arginine methyl ester
LPS	lipopolysaccharide
MAPK	mitogen-activated protein kinase
MEM	minimal essential medium
MHC	myosin heavy chain

Mnk	MAPK signal-integrating kinase-1
MODS	multiple organ dysfunction
mTOR	mammalian target of rapamycin
NAD^+	nicotinamide adenine dinucleotide (oxidised)
NADH	nicotinamide adenine dinucleotide (reduced)
$NADP^+$	nicotinamide adenine dinucleotide phosphate (oxidised)
NADPH	nicotinamide adenine dinucleotide phosphate (reduced)
NFκB	nuclear factor κB
nNOS	neuronal nitric oxide synthase
NO	nitric oxide
NOx	nitrate and nitrite
P38	p38 mitogen activated protein kinase
PABP	poly-a-binding protein
PBS	phosphate buffered saline
PCA	perchloric acid
PDTC	pyrrolidine dithiocarbamate
Phosphorylase	glycogen phosphorylase
Phosphorylase-a	glycogen phosphorylase (dephosphorylated, active)
Phosphorylase-b	glycogen phosphorylase (phosphorylated, less active)
PI3K	phosphatidyl-inositol-3-kinase
PK	pyruvate kinase
PP-1	protein phosphatase 1
PVDF	polyvinylidene fluoride
RNS	reactive nitrogen species
ROS	reactive oxygen species
SNP	sodium nitro prusside
TBA	tris buffered saline
TCA	trichloro acetic acid
TEMES	N, N, N',N'-tetramethylenediamine
TLR	toll-like receptors
TNF	tumor necrosis factor
Tris	tris[hydroxymethyl] aminomethane
TSC2	tuberous sclerosis complex protein 2
Tween	polyoxyethylene sorbitan monolaurate

Chapter One - Introduction

1.1 Sepsis

In order to combat local infections, mammals have evolved to detect foreign pathogens and to initiate rapid host defence, via the innate immune system (Guha and Mackman 2001; Beutler 2003; Kumar et al. 2009). The innate immune system achieves this via highly conserved receptors called the Toll-like receptors (TLRs) (reviewed in (Kumar et al. 2009). Different TLR's can distinguish between, and recognize, different specific bacterial, viral or fungal components and induce an appropriate response (Kumar et al. 2009). The response initiated by the innate immune system is a powerful one, with the aim of quickly neutralising localised infections, eliminating the pathogens from the tissue and removal of damaged or dead host cells (Lydyard 2000; Beutler 2003). This response relies on the activation of specific transcription factors which mediate the production of a variety of factors such as prostaglandins, platelet activating factor, pro-inflammatory cytokines, nitric oxide (NO - via inducible nitric oxide synthase (iNOS)) and reactive oxygen species (Lydyard 2000; Annane et al. 2005). Dealing with a local infection is possible via this mechanism as the pathogens are neutralised and contained within the localised area (Beutler 2003). However, if a systemic infection arises, often by the contamination of the blood with the pathogen, the immune system can over-react, leading to sepsis and septic shock, which may then result in death (Guha and Mackman 2001; Victor et al. 2004).

Sepsis is defined as the systemic response to infection, resulting in a systemic inflammation which arises due to the overproduction of pro-inflammatory cytokines (Titheradge 1999; Annane et al. 2005). Sepsis is the leading cause of mortality in critically ill patients, it is estimated to have a mortality rate of 40-60%, and have an incidence of 50-95 cases per 100,000, which is rising by 9% each year (Titheradge 1999; Annane et al. 2005; Dauphinee and Karsan 2006). Sepsis can quickly escalate to septic shock, which is characterised by various symptoms including hypothermia, hypotension, tachycardia, failure to regulate blood glucose, and eventually leads to low tissue and organ perfusion, which can result in multiple organ dysfunction (MODS), causing death (Kilbourn et al. 1997; Titheradge 1999; Victor et al. 2004). Despite the dangers of a blood infection, not all pathogens cause septic shock; the majority of cases used to be attributed to gram-negative bacteria, however in recent years the figures have changed, and now it appears as though gram-positive bacterial sepsis is more prominent (Titheradge 1999; Guha and Mackman 2001; Annane et al. 2005). Due to this, research into sepsis often used the gram-negative bacterial outer-membrane component known to be important for the onset of gram-negative sepsis: lipopolysaccharide

(LPS), also known as endotoxin (Geppert et al. 1994; Novogrodsky et al. 1994; Virkamaki and Ykijarvinen 1994; Vary et al. 1995; Lang et al. 1996a). Of the TLRs it was discovered that TLR4 was the receptor responsible for inducing the intracellular signal that initiated gram-negative sepsis (Heyneman and Vercauteren 1997; Poltorak et al. 1998).

1.2 LPS recognition by TLR4 and the Induction of the Inflammatory Response

The TLR receptor family is widely expressed in immune cells as well as non-immune cells such as fibroblast, epithelial, endothelial, hepatic and muscle cells (Frost et al. 2004; Wallington et al. 2008; Kumar et al. 2009; Bryant et al. 2010). TLR4 is a type 1 transmembrane protein composed of an ectodomain containing a cystein-rich domain and various leucine-rich repeats important for protein-protein interactions (O'Neill 2006; Bryant et al. 2010). The intracellular domain of TLR's is homologous to that of the interleukin-l receptor (IL-1R) family, which is termed the Toll/IL-1R homology (TIR) domain (O'Neill 2006). LPS recognition by TLR4 (Figure 1.2a) is accomplished with the help of the primary sensing molecules: LPS binding protein (LBP) and CD14 (Wong, Chung et al. 2000; Guha and Mackman 2001; Lu, Yeh et al. 2008). CD14 is present in two isoforms, a membrane bound and a soluble form (sCD14) (Palsson-McDermott and O'Neill 2004; Lu et al. 2008). LBP extracts and solubilises LPS by binding to it and then facilitates LPS recognition by transferring it to CD14 (Lu et al. 2008; Bryant et al. 2010). CD14 raises the sensitivity to LPS, thus enhancing the efficiency of the host's response to LPS (Bryant et al. 2010). In addition to LBP, CD14 and TLR4, myeloid differentiation protein 2 (MD2) – an extracellular adaptor glycoprotein that binds to the leucine rich repeats of TLR4 – is indispensable for LPS signalling (Palsson-McDermott and O'Neill 2004; O'Neill 2006). CD14 transfers LPS to the TLR4/MD2 complex (Lu et al. 2008; Kumar et al. 2009), which causes TLR4 dimerisation or oligomerisation, and subsequent activation of the receptor-ligand complex, resulting in recruitment of the downstream components via TIR-TIR protein interactions (Palsson-McDermott and O'Neill 2004; O'Neill 2006; Lu et al. 2008). The LPS/TLR4 pathway consists of two signalling cascades that are termed the MyD88-dependent (myeloid differentiation primary response gene 88) and MyD88-independent pathway, or also known as the early and late phase response to LPS, respectively (Palsson-McDermott and O'Neill 2004; Lu et al. 2008). The early phase response results in the recruitment of a dimer composed of Mal (MyD88 adaptor-like) and MyD88 that can then initiate the rapid host response to LPS (Uematsu and Akira 2007; Lu et al. 2008;

Kumar et al. 2009; Bryant et al. 2010). The MyD88-independent cascade on the other hand is initiated by another dimer, consisting of TRIF (TIR domain-containing adaptor inducing IFN-β) and TRAM (TRIF-related adaptor molecule) (Lu et al. 2008; Bryant et al. 2010).

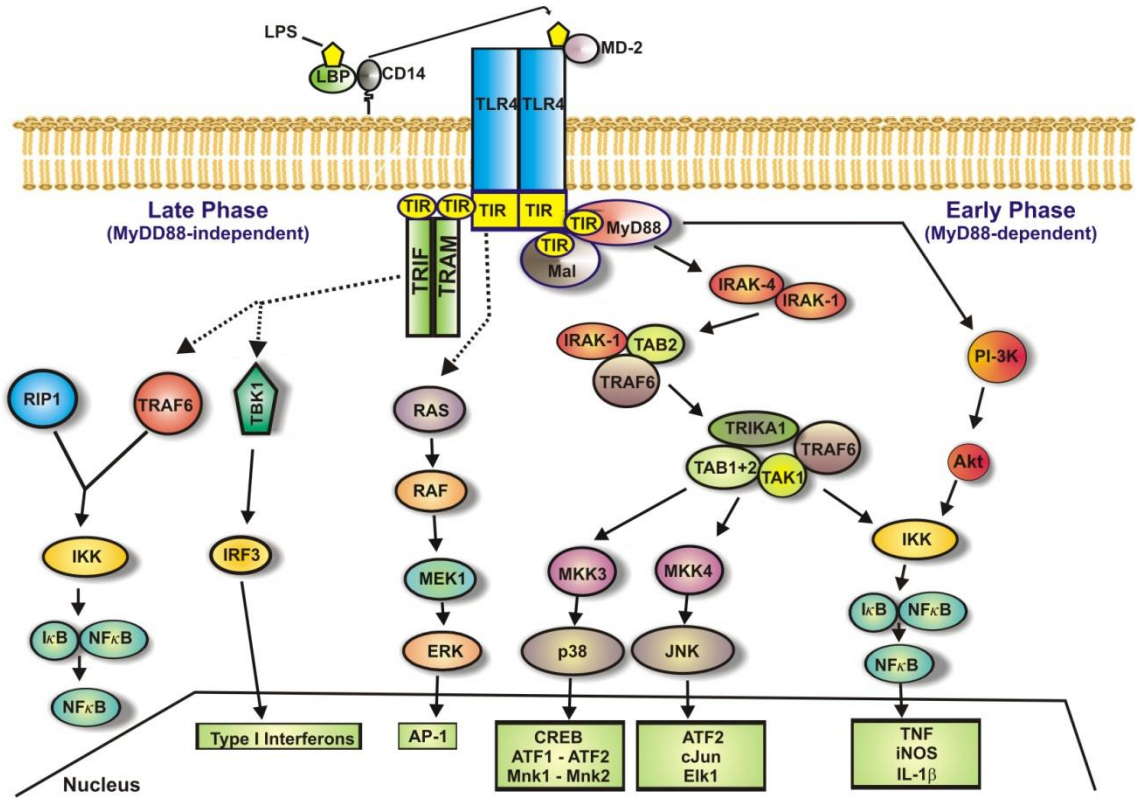

Figure 1.2a. LPS recognition by TLR4, and the subsequent signalling cascade.

The transduction of the early phase signal relies on the N-terminal death domain (DD) of MyD88 which recruits IL-1 receptor associated kinase-4 (IRAK-4) via its DD (Guha and Mackman 2001; Palsson-McDermott and O'Neill 2004; Lu et al. 2008). IRAK-1 is the next protein to be phosphorylated and activated in the pathway, achieved by active IRAK-4 (Lu et al. 2008). IRAK-1 then transduces the signal to TNF-α receptor associated factor 6 (TRAF6) which can then associate with TAK1 binding proteins 1 and 2 (TAB1, TAB2) (Dauphinee and Karsan 2006). The active TRAF6/TAB1+2 complex then associates with TAK1 (transforming growth factor-β-activated kinase), followed by association with the E2 ubiquitin-conjugating enzyme dimer Ubc13/Uev1A (known as TRAF6-regulated IKK activator -TRIKA1) (Dauphinee and Karsan 2006; O'Neill 2006). This induces the ubiquitination of TRAF6, which results in TAK-1 mediated phosphorylation of the IκB kinase signalosome (IKK), thereby activating it (Dauphinee and

Karsan 2006; O'Neill 2006). Activated IKK then phosphorylates members of the IκB family of inhibitors of NFκB, which in the unstimulated state bind to NFκB, concealing the nuclear localisation sequence, thus maintaining it in the cytoplasm (Bubici et al. 2004; Verstrepen et al. 2008). Phosphorylation of IκB results in the release of NFκB, which can then translocate to the nucleus to regulate genes such as upregulating the expression of iNOS, IL-1β (interleukin-1β) and TNF-α (tumor necrosis factor α) (Bubici et al. 2004; Annane et al. 2005; Verstrepen et al. 2008).

Mitogen-activated protein kinases (MAPK) are another set of important molecules that are activated during LPS stimulation, together they regulate the expression of various cytokines such as TNF-α, IL-1β, IL-6 and IL-8 as well as other transcription factors such as activator protein-1 (AP-1) (Guha and Mackman 2001; Palsson-McDermott and O'Neill 2004; Dauphinee and Karsan 2006; Lu et al. 2008). Their activation is induced in an MyD88/Mal-dependent fashion, although MyD88 or Mal-deficient mice displayed a delayed MAPK activation, suggesting other routes exist (Dauphinee and Karsan 2006; Lu et al. 2008). The MAPKs activated are ERK1/2 (extracellular signal-regulated kinase), JNK (c-Jun N-terminal kinase) and p38 (Guha and Mackman 2001; Palsson-McDermott and O'Neill 2004; Dauphinee and Karsan 2006; Lu et al. 2008). JNK and p38 are activated following activation of their kinases (MAPK Kinase – MAPKK) which is achieved by TAK1 (Guha and Mackman 2001; Palsson-McDermott and O'Neill 2004; Dauphinee and Karsan 2006). ERK activation on the other hand requires the activation of the small GTP binding protein Ras, which then transduces the signal to the serine/threonine kinase raf, which itself phosphorylates MEK1/2 (a MAPKK), thereby activating ERK1/2 (Dauphinee and Karsan 2006).

The MyD88-independent pathway is equally important as it results in the induction of the interferon-inducible genes, type I interferons (such as IFN-β), which then mediate indispensible anti-viral and anti-bacterial responses (Dauphinee and Karsan 2006; Lu et al. 2008). Instead of the Mal/MyD88 complex being recruited to the receptor, the MyD88-independent pathway relies on an adaptor molecule complex of TRIF and TRAM (Palsson-McDermott and O'Neill 2004; Akira et al. 2006; Dauphinee and Karsan 2006; Lu et al. 2008). The recruitment of the TRIF/TRAM complex to the ligand bound TLR4 receptor results in the activation of two subsequent signalling pathways (Dauphinee and Karsan 2006; Lu et al. 2008). The first results in the activation of TBK1 (TANK binding kinase 1, leading to the activation of IRF3 (interferon regulatory factor 3) which translocates to the nucleus to upregulate the IFN inducible genes and Type I interferons (Palsson-McDermott and O'Neill 2004; Akira et al. 2006; Dauphinee and Karsan 2006; Lu et al. 2008). The serine/threonine kinase RIP1 (receptor

interacting protein 1) is recruited to the TRIF/TRAM complex by binding to a RHIM sequence (RIP homotypic interacting motif) present on TRIF (Palsson-McDermott and O'Neill 2004; Dauphinee and Karsan 2006; Lu et al. 2008). Active RIP1 is responsible for the late-phase activation of NFκB, with the help of TRAF6, which is said to also induce the Type I interferons similarly to IRF3 (Dauphinee and Karsan 2006; Lu et al. 2008).

As Figure 1.2a displays, the stimulation of TLR4 activates a complicated signalling cascade that has a wide-range of targets. The key consequences lie in the activation of various transcription factors that mediate the next phase of the immunological response to LPS (Titheradge 1999; Guha and Mackman 2001; Palsson-McDermott and O'Neill 2004; Annane et al. 2005; Lu et al. 2008). LPS induction brings about the activation of NFκB, IRF3 and the MAPKs (Guha and Mackman 2001; Palsson-McDermott and O'Neill 2004; Annane et al. 2005; Lu et al. 2008; Kumar et al. 2009; Bryant et al. 2010). The modulation of the transcription factors induced by LPS signalling brings about the pro-inflammatory response which involves numerous mediators such as cytokines, chemokines, adhesion molecules, apoptotic factors and iNOS (Guha and Mackman 2001; Palsson-McDermott and O'Neill 2004; Victor et al. 2004; Annane et al. 2005). Evidence shows that TNF-α and IL-1β – two of the pro-inflammatory cytokines induced during the MyD88-dependent TLR4 cascade – are enough to bring about septic shock (Natanson et al. 1989; Rees et al. 1990). Moreover, pre-treatment of animals with anti- TNF-α antibodies or IL-1β receptor antagonists can protect them from the development of septic shock, although cannot aid if shock has already occurred suggesting the importance of IL-1β and TNF-α in mediating the primary stages of sepsis (Novogrodsky et al. 1994; Kilbourn et al. 1997). One pro-inflammatory cytokine not yet mentioned is IFN-γ, which is induced by the first wave of pro-inflammatory cytokines, such as IL-18 which is itself secreted in response to the MyD88-dependent LPS stimulation of NFκB (Schroder et al. 2004). IFN-γ is believed to be an important mediator of the progression of sepsis, as patients displaying septic shock show increased levels of IFN-γ, as well as TNF-α and IL-1β (Ertel et al. 1991), and experiments looking at mice treated with LPS and IFN-γ compared to mice only treated with LPS showed more pronounced mortality rates (Silva and Cohen 1992). In addition, it was shown that LPS-induced lethal toxicity requires the synergistic effect of TNF-α, IL-1β, IFN-γ and NO, thus further emphasising the key role played by the pro-inflammatory cytokines in sepsis (Novogrodsky et al. 1994).

1.3 The Key Pro-Inflammatory Cytokines: TNF-α, IL-1β and IFN-γ

Pro-inflammatory cytokines are important mediators of immunological responses as they allow communication with immunological cells, recruiting different members of the immune system to the site of infection as well as binding to non-immune cells inducing various responses such as cell survival, growth, differentiation and apoptosis (Thain 2000; Annane et al. 2005). Despite the fact that the range of inflammatory mediators induced by endotoxin is large, as discussed in Section 1.2, TNF-α, IL-1β and IFN-γ appear to be critical in the progression and development of sepsis.

1.3.1 TNF-α Signalling

Tumour necrosis factor (TNF) is a pleiotropic cytokine family involved in cellular proliferation, differentiation, inflammation, tumourigenesis, viral replication, and causing necrotic or apoptotic cell death (MacEwan 2002). In addition, it plays an important role in the pathogenesis of several disorders such as rheumatoid arthritis, asthma, septic shock and cachexia (MacEwan 2002). The TNF family includes over a dozen homologous ligands such as TNF-α, TNFβ and Fas ligand, however TNF-α appears to be the important ligand when considering the development of the inflammatory response and septic shock (MacEwan 2002). There are two known TNF-α receptors: TNFR1 and TNFR2; and they are expressed on virtually all cells except erythrocytes (Tracey and Cerami 1994; MacEwan 2002; Wallach 2002; Dempsey et al. 2003). Despite having related extracellular domains including the pre-ligand-binding assembly domain (PLAD) which promotes receptor trimerization upon TNF ligand binding, their intracellular domains lack homology (MacEwan 2002).

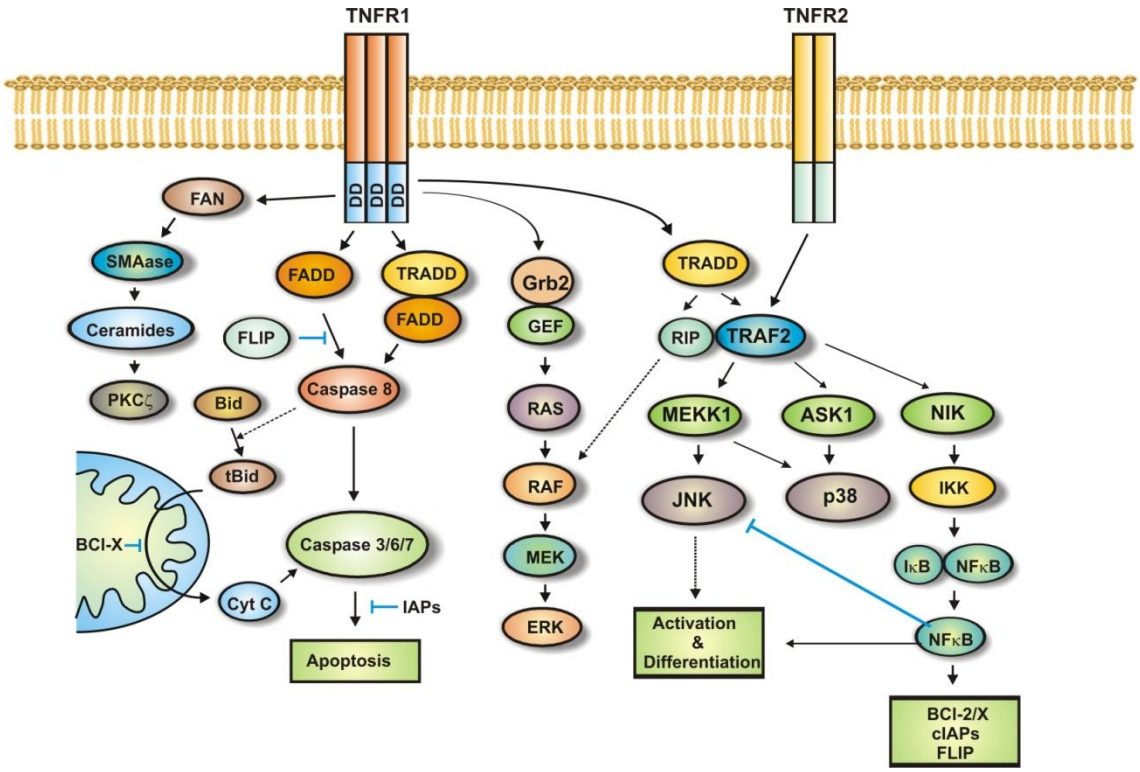

Figure 1.3.1a. Signalling cascades induced by TNFR1 and TNFR2 activation.

TNFR1 has an intracellular death domain (DD), important for transducing the signal downstream (Figure 1.3a) (Verstrepen et al. 2008). In the unstimulated state, the binding of silencer of DD (SODD) to the receptor prevents non-specific activation of the signal (MacEwan 2002; Dempsey et al. 2003). Upon TNF stimulation, the receptor trimerizes, disrupting the SODD interaction, thereby freeing the receptor DD that can now recruit downstream adaptor proteins such as FADD (Fas associated death domain) and TRADD (TNFR associated death domain) (MacEwan 2002; Dempsey et al. 2003; Verstrepen et al. 2008). FADD recruitment results in the formation of the death-inducing signalling complex (DISC), which is achieved via the association of FADD and caspase-8, through a death effector domain (DED) interaction (Dempsey et al. 2003). This results in the activation of caspase-8 which can then transduce the apoptotic signal via two separate routes (MacEwan 2002; Dempsey et al. 2003). Type I apoptosis refers to the processing and activation of caspases 3, 6 and 7 in the cytoplasm, whereas Type II apoptosis involves the release of cytochrome c from the mitochondria (Dempsey et al. 2003).

Receptor recruitment of TRADD induces an anti-apoptotic and inflammatory pathway, via the recruitment of RIP and TRAF2 (Dempsey et al. 2003). The TRADD/RIP/TRAF2 complex

bound to the active receptor can then activate NFκB, JNK and p38 (MacEwan 2002; Dempsey et al. 2003; Verstrepen et al. 2008). In order to activate NFκB, NIK (NFκb inducing kinase) is recruited to the receptor complex along with RIP-recruitment of the IKK signalosome, leading to phosphorylation and hence activation of the IκB kinases (MacEwan 2002; Wallach 2002; Dempsey et al. 2003). ERK can also be stimulated via the recruitment of the Grb2/SOS complex, which promotes the replacement of GDP for GTP in Ras (MacEwan 2002). Activated Ras in turn activates Raf, leading to MEK and finally ERK activation (MacEwan 2002).

There are various well-documented negative regulators of the TNF-α pathway. Evidence suggests that JNK activation is a pro-apoptotic signal when NFκB activation is hindered or protein synthesis is inhibited (Bubici et al. 2004). NFκB activation leads to the expression of certain proteins - such as A20, X-IAP and GADD45b – that are involved in negatively regulating the JNK pathway, leading to the anti-apoptotic transient activation of JNK as opposed to the pro-apoptotic sustained JNK activation signal (Dempsey et al. 2003; Bubici et al. 2004). In addition, many negative regulators of the apoptotic caspase-dependent pathway are upregulated by NFκB activation, such as the Bcl-2 (B cell lymphoma-2) family of proteins which are involved in sequestering Bak (Bcl-2 homologous antagonist killer) in the mitochondria, preventing the activation of the Type II caspase pathway (Dempsey et al. 2003). FLICE-inhibitory protein (FLIP), another NFκB induced gene, binds to FADD and caspase-8 with the result of inhibiting caspase-8 activation (Dempsey et al. 2003). Finally, the IAP proteins (inhibitor of apoptosis) inactivate the effector caspases 3/6/7 (Dempsey et al. 2003).

As well as negatively regulating the apoptotic signal, the reverse occurs as well. The anti-apoptotic signal is inhibited in various ways. Caspase-8 can cleave RIP into two molecules, generating RIPc, thereby disrupting the anti-apoptotic signalling cascade via RIP and TRAF2 (Dempsey et al. 2003). In addition, RIPc has been shown to enhance DD interactions between TRADD and FADD, thus promoting the caspase pathway (Dempsey et al. 2003). IKKβ is also subject to inhibition, via caspase-3, which cleaves IKKβ, thus ablating kinase activity and hence NFκB activation (Dempsey et al. 2003). The down-regulation of NFκB activation by these two similar mechanisms also reduces the expression of negative regulators of the apoptotic pathway, thus promoting TNF-α induced apoptosis. Together these facts show that TNF-α signalling activates several different opposing cellular cascades. The overall outcome is down to where the balance lies; if more anti-apoptotic/survival signals are activated, then the caspase cascade is prevented, however if the survival signals induced by NFκB and MAPK's are not strong enough to inhibit caspase-dependent apoptosis, the cell undergoes programmed cell death.

1.3.2 IFN-γ Signalling

Similarly to the signals induced by TNF-α, the Interferon-γ lymphokine exhibits a wide variety of biological functions such as macrophage activation (and hence the innate response), anti-viral, immunomodulatory effects and effects on cell proliferation and apoptosis (Boehm et al. 1997; Takaoka and Yanai 2006; Gough et al. 2008). This family of structurally related cytokines is divided into three types: type I IFN's comprise, among others, IFN-α, IFN-β, IFN-ω and IFN-κ; IFN-γ is the only type II IFN; and finally the type III IFN's comprise three sub-types of IFN-λ (Schroder et al. 2004; Takaoka and Yanai 2006; Gough et al. 2008). This division is based on the types of receptors the ligands bind to (Schroder et al. 2004). IFN-γ binds a heterodimeric receptor (IFNGR1/IFNGR2), which is expressed on all nucleated cells (Valente et al. 1992; Schroder et al. 2004; Takaoka and Yanai 2006).

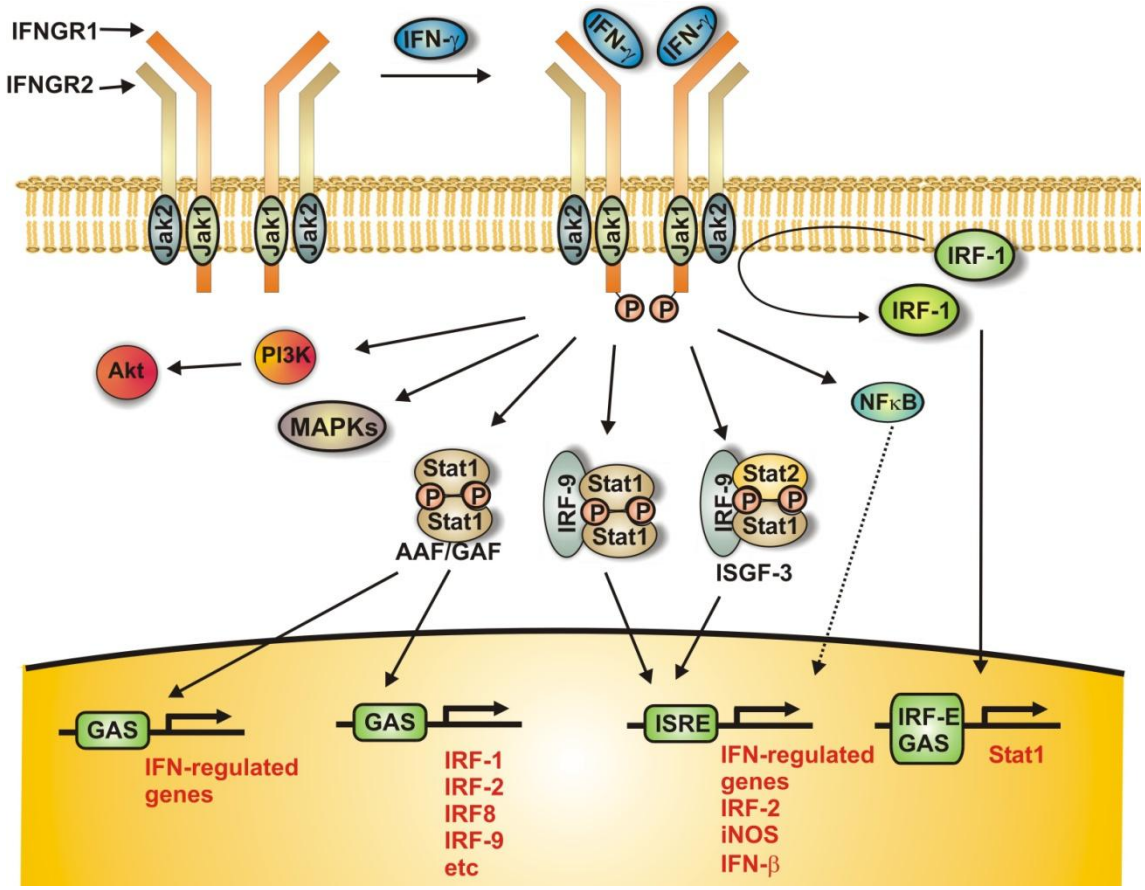

Figure 1.3.2a. IFN-γ stimulated pathway.

In the unstimulated state IFNGR1 and IFNGR2 are constitutively associated with Jak1 (janus tyrosine kinase 1) and Jak2, respectively (Schroder et al. 2004; Takaoka and Yanai 2006; Gough et al. 2008). Both Jaks are important in transducing the intracellular signal. Upon IFN-γ receptor binding, intracellular receptor domains open up and lead to the autophosphorylation and subsequent activation of Jak2 (Schroder et al. 2004; Gough et al. 2008). Activated Jak2 then phosphorylates and activates Jak1, which in turn phosphorylates both IFNGR1 receptors on tyrosine residues (Schroder et al. 2004; Gough et al. 2008). Both phosphotyrosine residues are important for transducing the signal as they form docking sites for the transcription factors Stat1 and Stat2 (signal transducer and activator of transcription 1/2) (Schroder et al. 2004; Takaoka and Yanai 2006; Gough et al. 2008). The Stat proteins are recruited via their SH2 domain (src homology 2 protein domain), and upon receptor binding are then phosphorylated by one of the Jak proteins (Schroder et al. 2004; Takaoka and Yanai 2006). This causes dissociation and homodimerisation of the Stat proteins, generating Stat1 homodimers (AAF) and to a lesser extent heterotrimers consisting of Stat1/Stat2/IRF9 (ISGF3) and Stat1/Stat1/IRF9 (Schroder et al. 2004; Takaoka and Yanai 2006). These transcription factors are important for activating the IFN-γ response, by binding to GAS elements (AAF action), and interferon sensitive response elements (ISRE) (heterotrimer action) (Schroder et al. 2004; Takaoka and Yanai 2006; Gough et al. 2008). Although the Jak-Stat signalling cascade is the most documented pathway stimulated by IFN-γ, alternative Stat1-independent cascades have recently been elucidated which result in the activation of PI3K (phosphatidyl-inositol-3-kinase), MAPKs and NFκB (Gough et al. 2008).

There are several mechanisms that down-regulate the IFN-γ pathway at different points in the signalling cascade. One such mechanism is the internalisation of the IFNGR-IFN-γ complex into the endosomal pathway (Schroder et al. 2004). This can either lead to receptor recycling and degradation of the ligand or, in some cell types, to degradation of the receptor itself (Schroder et al. 2004). Another important set of molecules is that of the suppressors of cytokine signalling (SOCS): SOCS1 and SOCS3 (Schroder et al. 2004; Gough et al. 2008). These molecules are induced by IFN-γ signalling and when expressed, associate with Jak1/2, hindering their tyrosine kinase activity thus inhibiting the IFN-γ signal cascade (Ueki et al. 2004). In addition, it is suggested that SOCS1 may also target the signal machinery for degradation via the proteasome pathway (Schroder et al. 2004). The Jak proteins are also subject to dephosphorylation by protein tyrosine phosphatases (PTP) Shp1 and Shp2 (SH2 domain-containing protein), thereby down-regulating the recruitment of Stat transcription factors to the receptor complex (Schroder et al. 2004). Stat1 homodimers associate through

their phosphotyrosine residues, and as a result, when they undergo dephosphorylation by nuclear PTPs, they dissociate from the DNA and from each other (Schroder et al. 2004).

1.3.3 IL-1β Signalling

Interleukin-1 is another pleiotropic cytokine that can affect almost every cell type in the body (O'Neill 2008). It is involved in numerous processes such as the inflammatory response, B-cell growth and differentiation and the stress responses (Subramaniam et al. 2004). IL-1α and IL-1β are ligands for the IL-1 receptor 1 (IL-1RI) which is a member of the IL-1R/TLR superfamily (McGettrick and O'Neill 2004; Subramaniam et al. 2004). This receptor superfamily has a characteristic TIR domain on the intracellular segment of the receptor, which is indispensable for signalling as it recruits and associates with TIR domain containing adaptor proteins via TIR-TIR domain interactions (McGettrick and O'Neill 2004; Subramaniam et al. 2004; Verstrepen et al. 2008; O'Neill 2008). The IL-1RI associates with the IL-1 receptor accessory protein (IL-1 RAcP) at the membrane, which is necessary for initiating the intracellular signal (Subramaniam et al. 2004; Verstrepen et al. 2008; O'Neill 2008).

The signalling cascade stimulated by IL-1RI is virtually the same as the TLR4 early phase (or MyD88-dependent) response to LPS stimulation presented in Section 1.2 (McGettrick and O'Neill 2004; Subramaniam et al. 2004; Verstrepen et al. 2008). Upon binding of IL-1 to its receptor (via extracellular immunoglobulin-like domains on the receptor) and IL-1RAcP, a conformational change occurs within the TIR domain of the receptor, allowing it to recruit MyD88 (via TIR-TIR domain interactions) (McGettrick and O'Neill 2004; Subramaniam et al. 2004; Verstrepen et al. 2008; O'Neill 2008). MyD88 recruits IRAK4, which in turn recruits IRAK-1, leading to its phosphorylation and activation which causes IRAK1 dissociation thereby enabling its interaction with TRAF6 and TAB2 (McGettrick and O'Neill 2004; Subramaniam et al. 2004; Verstrepen et al. 2008; O'Neill 2008). Studies have put forward two extra adaptor molecules called TIFA and Pellino1 which mediate the association of IRAK1 and TRAF6 (Subramaniam et al. 2004; Verstrepen et al. 2008). This association leads to the activation of TRAF6, and in turn TAK1, which then phosphorylates IκB kinase and MKK6, thus leading to the activation of NFκB and p38 and JNK, respectively (McGettrick and O'Neill 2004; Subramaniam et al. 2004; Verstrepen et al. 2008; O'Neill 2008).

Similarly to the other cytokine signalling cascades, negative regulators play an important part in controlling the signal and making sure IL-1 over stimulation does not occur. IL-1RII is a similar receptor to IL-1RI except that it lacks the functional TIR domain meaning that

it cannot transduce an intracellular signal (Subramaniam et al. 2004; O'Neill 2008). This receptor not only acts to sequester IL-1, but it also binds IL-1RAcP, pro-IL-1β (preventing its processing), and shows low affinity for IL-1 receptor antagonists (IL-1ra) (Subramaniam et al. 2004; O'Neill 2008). In addition to IL-1RII, another important negative regulator of the IL-1 system is IL1ra, which competes with IL-1 for IL-1RI binding (Subramaniam et al. 2004; O'Neill 2008).

1.4 Nitric Oxide and Nitric Oxide Synthase

Nitric oxide (NO) was originally discovered and defined as the endothelium derived relaxing factor (EDRF), until it was then recognized as NO (Furchgott and Zawadzki 1980; Fleming and Busse 1999). NO is a free radical gas responsible for many different functions in the body (Groves and Wang 2000; Alderton et al. 2001; Fleming and Busse 1999; Kleinert et al. 2004). These roles include: neuronal signal transmission; coordination of heart rhythm; regulation of vascular tone; and cytotoxicity against pathogens and tumours (Groves and Wang 2000; Bonavida et al. 2006). There are three isoforms of nitric oxide synthase (NOS), neuronal NOS (nNOS), inducible NOS (iNOS) and endothelial NOS (eNOS) (Groves and Wang 2000; Alderton et al. 2001). Both nNOS and eNOS are constitutive enzymes, which produce NO for short periods of time at picomolar concentrations, whereas iNOS is only expressed under particular stimulations, and produces NO in nanomolar concentrations for longer periods of time (Titheradge 1999; Bonavida et al. 2006; Jobgen et al. 2006). Calcium calmodulin associates with the NOS enzymes, regulating nNOS and eNOS especially, as opposed to iNOS which is primarily regulated at the transcriptional level (Alderton et al. 2001; Lee et al. 2003; Bonavida et al. 2006). During muscle contraction, Ca^{2+} levels oscillate in the cell, and activate eNOS (via the calmodulin subunit) which causes the release of NO and subsequent activation of soluble guanylate cyclase (sGC) (Bonavida et al. 2006). Activated sGC generates cGMP, which lowers Ca^{2+} levels, dilates the blood vessels and lowers blood pressure thereby relaxing the muscle and promoting perfusion of oxygen to the contracting cells (Bonavida et al. 2006). The NOS enzymes catalyse the oxidation of one of the guanidino nitrogen atoms of L-arginine, producing citrulline and NO (Groves and Wang 2000).

1.4.1 Nitric Oxide in the Innate Immune Response and Sepsis

Besides the basal roles played by NO in the body, it is a fundamental tool used by the immune system to fight off pathogens (Kilbourn et al. 1997; Titheradge 1999; Kleinert et al. 2004). The generation of NO in this respect is accomplished by the activation of the inducible form of NOS (iNOS) which is upregulated by LPS, TNF-α, IL-1β and IFN-γ among other factors (Kilbourn et al. 1997; Titheradge 1999; Kleinert et al. 2004; Annane et al. 2005; Bonavida et al. 2006). NO has this immunological function due to its highly reactive nature (also a property of its derivatives), which post-translationally modify proteins, reversibly and irreversibly depending on the reaction (Mannick and Schonhoff 2002; Bonavida et al. 2006). NO will readily bind transition metals present in prosthetic groups within proteins, which can either have a basal signalling role (such as the binding of NO to Fe^{3+} in sGC) or can abolish the protein's functions, such as the binding of NO to certain iron-sulphur complexes (Mannick and Schonhoff 2002). Binding of NO to cytochrome c oxidase present in the mitochondrial respiratory chain results in the inhibition of electron transport within the membrane leading to the build up of electron charge within the membrane, and subsequent production of superoxide (O_2^-) (Mannick and Schonhoff 2002; Bonavida et al. 2006). Peroxynitrite ($ONOO^-$), a highly oxidising and nitrating reactive nitrogen species (RNS) formed when NO reacts with O_2^-, is responsible for activating an apoptotic pathway by inducing mitochondrial dysfunction and cytochrome c release leading to the formation of the Apaf-1 apoptosome complex (apoptotic protease activating factor 1), which is critical for mediating this type of apoptosis (Mannick and Schonhoff 2002; Bonavida et al. 2006). Peroxynitrite is accountable for much of the cytotoxicity induced by high concentrations of NO during an immune response since it induces DNA damage, reacts with free thiol groups, forms disulphide linkages and can inhibit protein function (Bonavida et al. 2006).

It is clear that NO is a toxic molecule, which is why the innate immune system evolved to utilise it so as to induce damage to the invading microorganisms, and help in the combat of the infection before the adaptive immune response is initiated. This, together with the cytokine signalling cascades activated in response to endotoxin, is highly important in mediating the primary stages of the innate immune response and in successfully communicating the infection to the rest of the immune system (Lydyard 2000; Gough et al. 2008; O'Neill 2008; Verstrepen et al. 2008; Kumar et al. 2009; Bryant et al. 2010). During an infection, the innate immune system, via TLRs, will recognize and react accordingly to the invading microorganism. Host tissue and cells in proximity to a local infection undergo damage

and possibly apoptosis due to relatively high local concentrations of NO and cytokines (Lydyard 2000; Ulloa and Tracey 2005). If on the other hand a pathogen gains access to the blood stream, and is not apprehended quick enough, it can lead to a systemic infection. This in turn means that an innate immune response is mounted systemically, leading to an overwhelming production of NO and cytokines throughout the body thus likely leading to sepsis, and potentially MODS (Titheradge 1999; Ulloa and Tracey 2005; Annane et al. 2005; Bryant et al. 2010). Indeed it has been established that NO contributes to the pathophysiology of endotoxic shock due to its dilatory effects on blood circulation, which if uncontrolled can lead to massive vascular leakage and impaired circulation (Kilbourn et al. 1997; Titheradge 1999).

1.5 Effects of Endotoxic Shock on Host Tissue

Although NO production is a tool utilised by the innate immune response, the induction of iNOS is not restricted to immune cells such as macrophages or monocytes. Indeed TLR4 receptors are ubiquitously expressed and similarly iNOS is induced in a multitude of different tissues in the body such as endothelial cells, hepatocytes, vascular smooth muscle cells, skeletal muscle cells, kidney cells and fibroblasts (Titheradge 1999; Frost et al. 2004). This gives an indication of the extent of NO production induced during an infection, and explains why a systemic presence of endotoxin can lead to uncontrollable levels of NO in the body. The cytokines secreted during the MyD88-dependent TLR4 activation such as TNF-α and IL-1β, along with the second wave of inflammatory mediators such as IFN-γ, which are critical for the progression of sepsis, also widely activate different tissues in the body. IL-1β, TNF-α and IFN-γ receptors are present on almost all tissue (Valente et al. 1992; Tracey and Cerami 1994; O'Neill 2008). The progression of endotoxic shock results in a multitude of different effects and symptoms which have been documented, however due to the fact that LPS and pro-inflammatory cytokines induce responses in most tissues, the underlying causes for the range of symptoms associated with endotoxic shock become more complex. Tissue-specific studies can provide valuable insight into the progression of the syndrome.

Studies of the tissue-specific effects of endotoxic shock have generated some interesting studies and have attracted attention for the past couple of decades due to the growing occurrence of sepsis and it's high mortality rate among critically ill patients (Lang et al. 1990; Vary et al. 1995; Gamelli et al. 1996; Ceppi et al. 1997; Lang et al. 2007; Wallington et al. 2008; Maitra et al. 2000; Feingold et al. 2008; Huber-Lang et al. 2009). One of the symptoms associated with septic and endotoxic shock is a disruption to glucose homeostasis

characterised by an initial hyperglycaemic phase followed by a hypoglycaemic phase during the later stages (Lee et al. 1987; Virkamaki and Ykijarvinen 1995; Khanna et al. 1999; Titheradge 1999; Maitra et al. 2000; Wallington et al. 2008). The various symptoms associated with endotoxic shock already put a strain on the individual's system, which is then exacerbated by the disruption of glucose homeostasis as it is made more difficult for the tissues to function adequately, let alone combat the infection. These symptoms were recognized over two decades ago, resulting in research conducted to try and determine the causes; however each underlying mechanism has not yet been clearly established. The liver and peripheral tissues play an important function on the overall homeostasis of glucose. On the one hand the liver is important in maintaining blood glucose levels and providing glucose for the rest of the body, while on the other hand glucose disposal is undertaken by the peripheral tissues such as skeletal muscle and adipose tissue, which clearly affect glucose homeostasis (Azpiazu et al. 2000; Roach 2002). As a result it is essential to study the effects of endotoxic shock on different tissue; although some signalling pathways from one tissue to the next will be similar, tissues perform different functions and as a result express varying amounts of receptors and intracellular signalling molecules, suggesting they will respond distinctly to the bacterial endotoxin and pro-inflammatory mediators.

1.6 Glycogen and its Metabolism

Glycogen is a polymer of glucose, serving as an efficient store of energy providing readily accessible glucose during times of energy shortage (Roach 2002; Hargreaves 2004). When blood sugar levels are high, after a meal for example, insulin promotes the incorporation of glucose into glycogen, particularly in the skeletal muscle (Roach 2002; Hargreaves 2004). Although numerous cells have stores of glycogen, there are two main deposits of glycogen in mammals: in the liver and in skeletal muscle (Roach 2002). Both deposits play very different roles in the body however: skeletal muscle cells store glucose as glycogen in order to sustain muscle contraction, whereas the liver stores fuel the rest of the body when blood sugar levels decrease, thus maintaining glucose homeostasis (Roach et al. 2004; Greenberg et al. 2006). Due to these differences, the metabolic pathways regulating carbohydrate entry and storage in skeletal muscle cells are distinct to those present in the liver (Gomis et al. 2002; Ferrer et al. 2003; Jensen 2009). Although the general mechanism of glucose storage is the same in the liver and skeletal muscle, the isoforms of some of the enzymes expressed are different (Gomis

et al. 2002; Ferrer et al. 2003; Jensen 2009). These differences are highlighted in Figure 1.6a by an asterisk (*).

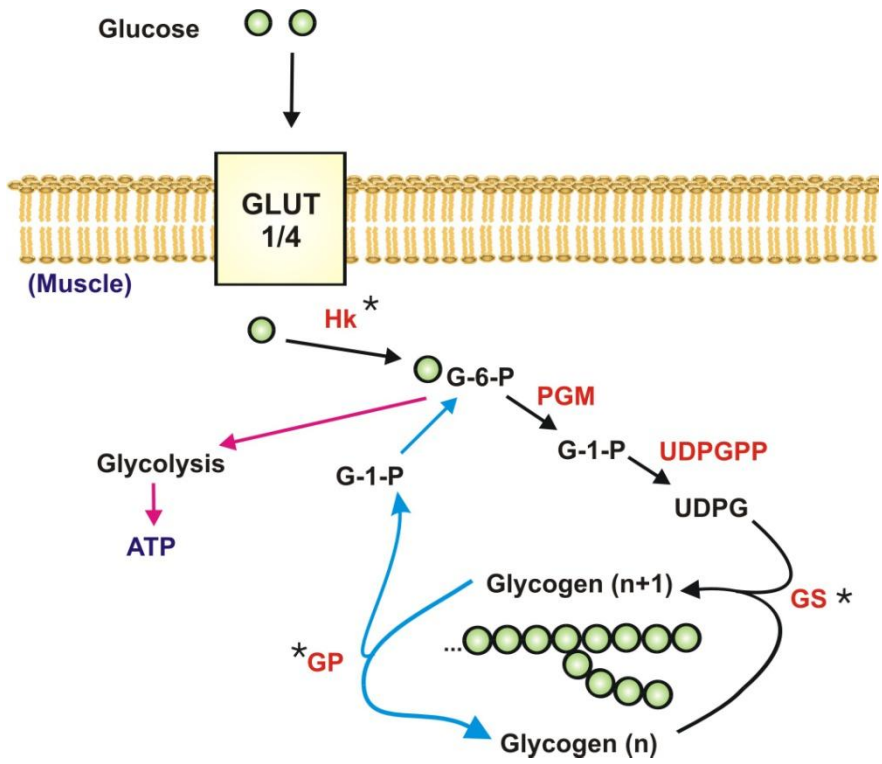

Figure 1.6a. Glycogen synthesis in muscles (black arrows). Blue arrows correspond to glycogenolysis, while the pink arrows specify glucose oxidation via glycolysis. GP = glycogen Phosphorylase.

Glucose is taken up by facilitative diffusion via the GLUT transporters; skeletal muscle express the constitutive transporter GLUT1 and insulin-dependent GLUT4 isoforms (Barnard and Youngren 1992; Greenberg et al. 2006; Nedachi and Kanzaki 2006). Upon entry, glucose is very quickly phosphorylated to glucose-6-phosphate (G-6-P) by hexokinase (Hk), then converted to glucose-1-phosphate (G-1-P) by phosphoglucomutase (PGM) and finally to UDP-glucose by UDP-glucose pyrophosphorylase (UDPGPP). UDP-glucose is the substrate for glycogen synthase (GS), which catalyses the final step in glycogen synthesis, and is another enzyme which is present as a liver and muscle isoform (VillarPalasi and Guinovart 1997; Roach 2002; Ferrer et al. 2003; Roach et al. 2004; Jensen 2009). The reverse of this process involves the breakdown of glycogen by glycogen Phosphorylase (Phosphorylase) to G-1-P, which is then converted to G-6-P in order to then feed into glycolysis, generating ATP (Roach 2002; Ferrer et al. 2003; Roach et al. 2004). G-6-P also elicits a feed forward mechanism promoting glycogen storage, by allosterically regulating GS which increases its affinity for UDP-glucose (VillarPalasi

and Guinovart 1997; Jensen 2009). There are key stages in the synthetic pathway that are tightly controlled in order to prevent futile cycling of carbohydrates: they lie at the beginning and end of the cascade (Manchester et al. 1996; VillarPalasi and Guinovart 1997; Azpiazu et al. 2000; Jensen et al. 2006; Lai et al. 2007).

1.6.1 Skeletal Muscle Glycogen Synthesis Regulation

There are three main factors affecting the rate of glycogen synthesis in skeletal muscle: the transport of glucose into the cell; the activity ratio of GS; and the amount of glycogen store present in the cell (Manchester et al. 1996; VillarPalasi and Guinovart 1997; Azpiazu et al. 2000; Jensen et al. 2006; Lai et al. 2007). In addition to this, skeletal muscle is insulin-sensitive: mainly activating GS and increasing glucose transport. Skeletal muscle makes up about 40% of total body weight, and accounts for approximately 80% of insulin-induced glucose disposal, further emphasising its role in glucose homeostasis (Azpiazu et al. 2000; Nedachi and Kanzaki 2006; Jensen 2009). The remaining components of the synthetic pathway, PGM and UDPGPP, are not subject to regulation, which explains why both the liver and skeletal muscle express the same forms of these enzymes (Ferrer et al. 2003).

1.6.2 Glucose transport

The entrance of glucose into the cell greatly influences the rate of glycogen stored (Ren et al. 1993; Hansen et al. 1995). Over-expressing GLUT1 or GLUT4 transporters in skeletal muscle of transgenic mice resulted in a significant increase in glucose uptake, and glycogen deposition, demonstrating the influence glucose transport has on glycogen synthesis (Ren et al. 1993; Hansen et al. 1995). The increase in glucose transport also increases levels of G-6-P as hexokinase has a high affinity for glucose meaning that it is instantly phosphorylated, which in turn feeds forward by allosterically regulating GS (VillarPalasi and Guinovart 1997; Gomis et al. 2002; Jensen 2009). In the resting state, skeletal muscle cells have constitutively present GLUT1 transporters at the membrane that sustain basal glucose uptake (Barnard and Youngren 1992 434; Greenberg et al. 2006 428; Nedachi and Kanzaki 2006 472). However upon insulin secretion after a meal or during exercise, GLUT4 transporters are translocated from intracellular pools to the outer membrane, allowing an increased uptake of glucose (Barnard and Youngren 1992; Roach 2002; Huang and Czech 2007). The translocation of GLUT4

transporters to the membrane greatly increases G-6-P levels which feeds forwards by activating GS to promote glycogen storage (VillarPalasi and Guinovart 1997; Roach 2002; Jensen 2009).

1.6.3 Muscle Glycogen Synthase

GS is the next stage at which tight regulation occurs (Manchester et al. 1996; Azpiazu et al. 2000; Jensen 2009). GS is an allosteric protein, present in two populations: an a-form that is more active and a less active b-form (VillarPalasi and Guinovart 1997; Jensen 2009). The ratio of the a-form to the b-form signifies the activity ratio, or fractional activity. The allosteric regulation involves G-6-P, as discussed in Section 1.6. When G-6-P levels increase, GS activity is enhanced which results in an increased rate of muscle glycogen synthesis (VillarPalasi and Guinovart 1997). In addition to allosteric regulation, muscle GS is subject to covalent regulation by phosphorylation, which is governed by several kinases and muscle specific protein phosphatase-1 (PP-1) (Aschenbach et al. 2001; Roach 2002; Jensen 2009). Muscle GS is important for metabolic homeostasis due to the critical role played by skeletal muscle in storing a large proportion of carbohydrates in the form of glycogen (Azpiazu et al. 2000; Nedachi and Kanzaki 2006; Jensen 2009). As a result it is not surprising that GS is tightly regulated, indeed there are numerous regulators that affect the level of enzyme phosphorylation and the concentration of G-6-P (VillarPalasi and Guinovart 1997; Roach 2002; Ferrer et al. 2003; Hargreaves 2004; Cohen 2006; Jensen 2009). GS has 9 well documented phosphorylation sites that have displayed physiological significance, up to 6 others have been revealed to be phosphorylated in vitro but failed to show any relevance in vivo (Roach 1990; Cohen 1993; VillarPalasi and Guinovart 1997). The covalent modification of GS is quite complex, some sites strongly inhibit it's activity (Sites 3a, 3b, 3c and 4), some mildly inactivate it (Sites 2a and 2b), while the rest induce little or no inactivation (Sites 1a, 1b and 5) (Roach 1990; Halse, Fryer et al. 2003; Skurat and Dietrich 2004; Jensen 2009). Phosphorylated GS is less active than the dephosphorylated form however allosteric activation by G-6-P can occur even if GS is phosphorylated, and in addition G-6-P promotes PP-1-mediated dephosphorylation (VillarPalasi and Guinovart 1997; Greenberg et al. 2006; Jensen 2009). Insulin plays an important role in skeletal muscle glycogen storage, as it activates GS in various ways: via the inhibition of GS kinases; the activation of GS phosphatases; and in increasing glucose transport thereby generating more G-6-P (Greenberg et al. 2006).

1.6.4 Glycogen Stores

Another crucial factor regulating glycogen synthesis is the amount of glycogen present in the cell itself; it is able to modulate the rate of glucose transport, the activity of GS and insulin signalling (Danforth 1965; Jensen et al. 2006; Lai et al. 2007). Mice with low, normal and high glycogen stores were used in order to determine any difference in basal and insulin stimulated aspects of glycogen synthesis (Jensen et al. 2006; Lai et al. 2007). Low glycogen stores correlated with an increase in: overall glycogen synthesis, basal and insulin-stimulated glucose transport, GLUT4 expression, GS affinity for UDP-glucose, and GS fractional activity (Jensen et al. 2006; Lai et al. 2007). By increasing GLUT4 expression and basal/insulin stimulated glucose transport, the entry of glucose into the cell was promoted, which would result in an increase in glycogen synthesis substrates (UDP-glucose) and allosteric activation of GS by G-6-P. While the increase in GS affinity for UDP-glucose would enhance the channelling of carbohydrate into glycogen, with the end result of increasing glycogen stores (Jensen et al. 2006; Lai et al. 2007). The reverse was also true, high glycogen stores increased GS phosphorylation and reduced: insulin-stimulated glycogen synthesis, GS activation and GS affinity for UDP-glucose (Jensen et al. 2006; Lai et al. 2007). Therefore when glycogen stores are high, the regulatory steps governing GS and its activity will switch off glycogen synthesis so as to slow down the rate of glucose incorporation into glycogen. These results show the importance of glycogen stores in regulating glycogen storage in skeletal muscle. The regulation of glycogen synthesis and breakdown is a crucial process for general metabolic control since glucose can be stored in only one form – glycogen. It is thus indispensable to have a tight regulation of GS and Phosphorylase, allowing glucose homeostasis to be maintained (Jensen 2009).

1.6.5 Insulin Action on Muscle Glycogen Synthesis

Insulin is a hormone that plays an important part in the regulation of skeletal glycogen metabolism, as it promotes the incorporation of glucose into glycogen by regulating the key steps governing glycogen synthesis, as shown in Figure 1.6.5a (Cohen 2006).

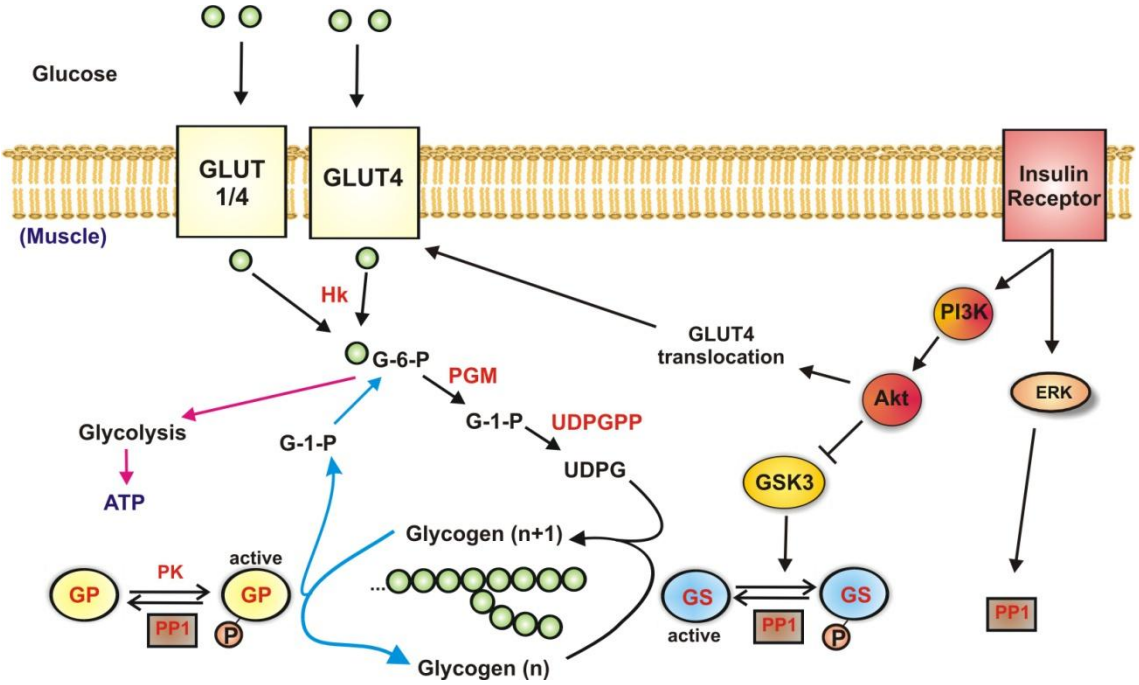

Figure 1.6.5a. Glycogen synthesis pathway showing the steps regulated by insulin. PK=phosphorylase kinase, GP = glycogen Phosphorylase.

During insulin stimulation, PI3K is recruited to the insulin receptor by binding to phospho-tyrosine residues on insulin receptor substrate-1 (IRS1), resulting in its activation (Cohen 2006). Once activated, PI3K catalyses the formation of PIP_3 (phosphatidylinositol-3-phosphate) resulting in the recruitment of Akt and PDK1 (PH domain-containing protein serine kinase 1) (Pirola et al. 2004). This leads to the activation of Akt, resulting from recruitment to PIP_3 and phosphorylation induced by PDK1 (Pirola et al. 2004; Cohen 2006). Akt then transduces the signal by activating AS160 (Akt substrate of 160Kda) which results in the translocation of GLUT4 receptor-containing vesicles to the plasma membrane, thereby increasing the transport of glucose into the cell (Kramer et al. 2006). This effect leads to an increase in the concentration of G-6-P which, as discussed in Section 1.6, results in the allosteric activation of GS, promoting glycogen synthesis (VillarPalasi and Guinovart 1997). Akt plays another pivotal role in the insulin response: to phosphorylate and inhibit GSK3 (glycogen synthase kinase 3), thus releasing GS from GSK3-mediated inhibition (Jope et al. 2007). Another mechanism by which insulin regulates glycogen synthesis is via activation of PP-1, via the activation of ERK (Ragolia and Begum 1998; Toole and Cohen 2007). PP-1 activation leads to the dephosphorylation of GS, Phosphorylase and phosphorylase kinase (PK) (Dent et al. 1990; Ragolia and Begum 1998; Aschenbach et al. 2001). This effect results in the activation of GS, and inhibition of Phosphorylase and PK (Dent et al. 1990; Aschenbach et al. 2001).

Together these effects ensure that the synthesis of glycogen is promoted, from the influx of glucose into the cell, to the activity of GS, while glycogen breakdown is inhibited, preventing the futile cycling of energy.

1.7 Endotoxic Shock and Hepatic Glycogen Metabolism

As mentioned in Section 1.5, endotoxic shock rapidly induces a hyperglycaemic phase (lasting for approximately 3 hours), followed by a profound hypoglycaemic phase during the terminal phases of the disease (Kelleher et al. 1982). The former phase is largely due to a rapid breakdown of hepatic glycogen stores and increased hepatic gluconeogenesis, whereas the latter phase occurs due to the failure to resynthesise the depleted stores of glycogen, an increase in peripheral glucose uptake and a failure of hepatic gluconeogenesis to maintain blood glucose concentrations (Knowles et al. 1986; Knowles et al. 1987; Liu and Kang 1987). Various suggestions have been put forward trying to explain these effects and determine the key underlying mechanisms, however some conflicting results have emerged (Liu and Kang 1987; Bagby et al. 1988; Casteleijn et al. 1988; Hill and McCallum 1991; Maitra et al. 1999; Maitra et al. 2000; Wallington et al. 2008). One important point to address is whether the alterations induced by endotoxic shock are: direct effects of the inflammatory insult; changes in glucoregulatory hormones caused by the syndrome; or whether it's a combination of the two. Following endotoxin administration, the levels of insulin, glucagon, corticosteroids and catecholamines are known to change (Kelleher et al. 1982). Due to the rise in blood glucose levels during the initial hyperglycaemic phase insulin secretion is stimulated, leading to high levels of insulin in the blood, while glucagon secretion is also significantly elevated (Kelleher et al. 1982; Maitra et al. 2000). As the glycogen stores are depleted, glucose homeostasis is not maintained due to the disruptions of glucoregulatory controls induced by sepsis and endotoxic shock resulting in even higher levels of glucagon and a significant decrease in plasma insulin levels (Kelleher et al. 1982; Maitra et al. 2000). Corticosterone and adrenalin on the other hand are significantly elevated relative to control levels 2 hours following sepsis and are maintained high up until 24 hours (Maitra et al. 2000).

Research into the underlying mechanisms of these effects has included in vivo and in vitro studies. For example one in vivo study prevented the increase in glucagon that occurs within the first hour of endotoxic shock and still noted elevated glucose levels in the blood, suggesting that alterations in glucagon concentration was not the only contributing factor to the changes in carbohydrate metabolism during endotoxic shock (Spitzer et al. 1989b). In vitro

studies are important for determining specific effects of mediators of endotoxic shock on tissue as they preclude alterations in the glucoregulatory hormones. An in vitro study of rat hepatocytes discovered that IL-1β treatment decreased the formation of glycogen, indicating a direct link between a mediator of endotoxic shock and hepatic glycogen metabolism (Lee et al. 1993). Finally, in a more recent study using an in vitro model of endotoxic shock, the effects of LPS plus cytokines on hepatic glycogen metabolism was determined using a combinations of LPS, TNF-α, IL-1β and IFN-γ (Wallington et al. 2008). The treatment resulted in an inhibition of glucose output from glycogen and an inhibition of glycogen repletion, which displays direct effects of the LPS plus cytokines on carbohydrate metabolism independent of changes in glucoregulatory hormones (Wallington et al. 2008).

These hepatic-specific studies which have contributed to the understanding of the potential causes relating to the disruption in glucose homeostasis observed during endotoxic shock, however only shed light onto one aspect of the problem. As mentioned in Section 1.5, the disposal of glucose into peripheral tissues such as skeletal muscle plays an important part in glucose homeostasis. Since some of the enzymes governing glycogen metabolism are different between liver and skeletal muscle, the effects observed in liver will not necessarily correlate with potential effects in skeletal muscle. As a result there have been studies that have tried to determine the effects of LPS and cytokines on various aspects of skeletal muscle glycogen metabolism (Lee et al. 1987; Virkamaki and Ykijarvinen 1994; Vary et al. 1995; Begum and Ragolia 1996; Lang et al. 1996a; Bedard et al. 1997; Ciaraldi et al. 1998; Halse et al. 2001; Wiernan et al. 2007).

1.8 Effects of Sepsis, Nitric Oxide, and In Vitro Inflammatory Models on Skeletal Muscle Glycogen Metabolism

Studies addressing skeletal muscle metabolic regulation during sepsis rarely follow the same experimental model, which can often lead to conflicting results, making it hard to reach a consensus. Nevertheless it is important to try and encompass each one in order to build a better picture of the situation at hand. Some studies have taken the in vivo approach, inducing endotoxic shock in animals via LPS injection (Lang et al. 1990; Virkamaki and Ykijarvinen 1994; Vary et al. 1995; Fan et al. 1996; Crossland et al. 2008). Others have used LPS and/or pro-inflammatory cytokines to elucidate the precise effects of these factors on specific aspects of skeletal muscle carbohydrate metabolism in vitro (Lee et al. 1987; Begum and Ragolia 1996; Bedard et al. 1997; Furnsinn et al. 1997; Ciaraldi et al. 1998; Del Aguila et al. 1999; Khanna et

al. 1999; Halse et al. 2001). As discussed in Section 1.4.1, NO plays a role in the pathophysiology of sepsis and endotoxic shock, making it an important molecule to consider during such studies, and as a result the effects of NO on glycogen metabolism have been studied (Bedard et al. 1997; Roberts 1997; Khanna et al. 1999; Adams et al. 2002; Sugita et al. 2002; Nishiki et al. 2008). The insulin response is strongly believed to be impaired during endotoxic shock and acute systemic inflammation, which has resulted in numerous studies trying to elucidate the precise mechanisms governing this problem (Virkamaki and Ykijarvinen 1994; Begum and Ragolia 1996; Del Aguila et al. 1999; Plomgaard et al. 2005; Sugita et al. 2005; Lorenzo 2008; Feve and Bastard 2009). Despite the numerous studies that have taken place, the exact underlying mechanisms and indeed the effects of endotoxic shock on skeletal muscle glycogen metabolism remain disputed.

1.8.1 In Vivo Models of Sepsis and Endotoxic Shock

In vivo models of endotoxic shock have reported a significant reduction in glycogen stores: one study looked at up to 300 minutes after LPS injection in rats (Virkamaki and Ykijarvinen 1994), the other over 24 hours (Crossland et al. 2008). In contrast with this however, Vary et. al. observed no change in glycogen stores in response to acute endotoxaemia (Vary et al. 1995). In vivo experiments looking at glucose disposal during sepsis or endotoxic shock are important, as they give primary results regarding tissue behaviour during the progression of such situations. One such study conducted by Maitra et. al. looked at tissue glucose uptake during the hyperglycaemic and hypoglycaemic phases of sepsis after a caecal ligation and puncture treatment in rats (Maitra et al. 2000). The studies found that skeletal muscle glucose uptake was significantly elevated during the hyperglycaemic phase, up to 6 hours post-infection, but then significantly decreased compared to control at 24 hours (Maitra et al. 2000). The latter result does not correlate with another in vivo study of sepsis which observed no change to skeletal muscle glucose transport 24 hours after the induction of endotoxic shock (Fan et al. 1996). Under insulin stimulation, endotoxaemia significantly decreased glucose uptake in rats, following 300 minutes of LPS treatment, indicating insulin resistance (Virkamaki and Ykijarvinen 1994).

1.8.2 The use of LPS and Pro-Inflammatory Cytokines in In Vitro Models

Some of the in vitro models cited in this section do not necessarily refer to endotoxic conditions, but are nevertheless equally important as they can provide insight into specific links between mediators of endotoxic shock and glycogen metabolism. For example much emphasis has been placed on TNF-α with regards to insulin resistance, and although TNF-α on its own cannot induce endotoxic shock, the results obtained from such studies can help in determining the potential underlying causes of a symptom. An important factor to note when discussing in vitro experiments is that they often differ in the parameters used, indeed the quantities of stimulants used (such as LPS, TNF-α, IFN-γ or IL-1β) do not correlate, which can therefore bring about conflicting results. A significant increase in basal glucose transport was observed in response to a 24 hour treatment with: TNF-α, IFN-γ and LPS in L6 rat skeletal muscle cells (Bedard et al. 1997; Khanna et al. 1999); TNF-α in human primary skeletal muscle cells (Ciaraldi et al. 1998); and L6 cells treated with monokines obtained from LPS-treated macrophages (Lee et al. 1987). This is however in contrast to two other studies using TNF-α where 5days exposure caused a 7% decrease in human skeletal muscle basal glucose uptake and 12h exposure to the cytokine caused a 100% decrease in L6 cells (Begum and Ragolia 1996; Halse et al. 2001). A reason for these discrepancies could be due to the varied times of treatment and the stimulants used.

1.8.3 Investigating Insulin Resistance under Septic, Endotoxic and Inflammatory Conditions

Since insulin signalling has been observed to be impaired in inflammatory conditions (Lang et al. 1990; Lang 1992; Hotamisligil et al. 1994; Virkamaki and Ykijarvinen 1994; Fan et al. 1996; Kroder et al. 1996; Ranganathan and Davidson 1996; Carlson 2004; Ueki et al. 2004; Plomgaard et al. 2005; Lorenzo 2008; Feve and Bastard 2009), numerous studies have tried to elucidate whether sepsis or endotoxin-induced insulin-resistance is brought on by the fluctuation in glucoregulatory hormones or if the specific mediators of inflammation are responsible. The in vitro studies have focused mainly on TNF-α, yet some results are slightly conflicting. Insulin-mediated glycogen synthesis in rat L6 myotubes was found to be inhibited by 60 minutes of treatment with TNF-α (Begum and Ragolia 1996), while a study using primary

rat skeletal muscle cells observed no change to insulin-mediated glycogen synthesis after 24 hours of TNF-α treatment (Furnsinn et al. 1997). The differences in results noted here could be due to the different times of treatment as well as the fact that Furnsinn et. al. used primary rat skeletal muscle cells compared to the L6 in vitro model. Insulin-mediated glucose uptake was significantly impaired in L6 myotubes in response to a 12 hour TNF-α treatment (Begum and Ragolia 1996), or a 24 hour TNF-α, IFN-γ and LPS treatment (Bedard et al. 1997). Similarly, this process was significantly impaired in human primary muscle cells in response to TNF-α treatment for 24 hours (Ciaraldi et al. 1998) of for 5 days (Halse et al. 2001). In contrast to these studies, a study observed an increased insulin-dependent upregulation of glucose transport after 1 hour of TNF-α treatment in C2C12 myotubes (Del Aguila et al. 1999). The variability in the experimental conditions may be the source of the inconsistencies, however it is quite clear that mediators of endotoxic shock affect the insulin-dependent signalling mechanisms in skeletal muscle (Marette 2002; Ueki et al. 2004; Khamzina et al. 2005; Plomgaard et al. 2005; Ghosh et al. 2007; Lorenzo 2008; Grzelkowska-Kowalczyk and Wieteska-Skrzeczynska 2009).

1.8.4 The Role of Nitric Oxide

Nitric oxide is systemically generated and released during sepsis and endotoxic shock which, as discussed in Section 1.4, can be very dangerous for the host tissue. Due to the significant presence of NO in such states, sepsis and endotoxic shock-related studies must take into account the reactive potential of this molecule as it can contribute to the results observed. Such conclusions tend to be drawn by two main routes, either inhibiting the NOS enzymes, or using NO-donors such as sodium nitro prusside (SNP). NO has been implicated in exercise/contraction mediated stimulation of glucose transport (Roberts 1997), however it was noted by Higaki et. al. that exercise-mediated glucose uptake and NO-mediated glucose uptake were additive (Higaki et al. 2001), implying that NO increases glucose transport in an exercise-independent manner. A dose-dependent increase in glucose transport was observed in cells treated with SNP (which releases a large amount of NO in a short space of time), suggesting higher levels of NO may be an important stimulator of glucose uptake as well (Balon and Nadler 1997; Etgen et al. 1997; Young et al. 1997; Higaki et al. 2001). As mentioned in Section 1.8.2, two groups treated L6 cells with TNF-α, IFN-γ and LPS for 24h and observed a significant upregulation in glucose transport (Bedard et al. 1997; Khanna et al. 1999). They also both treated the cells with N-G-nitro-L-arginine methyl ester (L-NAME – a NOS inhibitor), to deduce

the role of NO, and observed distinct results. L-NAME had no effect on the treatment-induced upregulation of glucose transport, implying NO was not responsible (Khanna et al. 1999), whereas the other group found that L-NAME completely abrogated the stimulation of glucose transport, suggesting NO plays a critical role in the process (Bedard et al. 1997). These two studies are very interesting because the conditions were almost identical, the same cell type were used and the same stimulants. The only difference was the quantities of each stimulant used, which highlights the possible variability between apparent similar experiments.

As portrayed in this Section (1.8), there may be some corroborating studies regarding the effects observed within skeletal muscle cells during sepsis or inflammatory stimulation, but many areas still require light to be shed on the underlying causes of many of these effects. Despite the disagreements presented, it is clear that NO can elicit effects on skeletal muscle glycogen metabolism.

1.9 In Vitro Model of Skeletal Muscle: C2C12 Cells

C2C12 cells are an in vitro model for skeletal muscle research. The cell line was initially isolated from the leg of an adult C3H mouse (Yaffe and Saxel 1977). C2C12 cells have been appropriately used for the analysis of: glycogen synthesis (Schmitz-Peiffer et al. 1999; Cazzolli et al. 2002; Doi et al. 2003); glucose transport (Liu et al. 1994; Del Aguila et al. 1999; Tortorella and Pilch 2002; Doi et al. 2003; Nedachi and Kanzaki 2006); and glycogen metabolism-related insulin signalling (Palmer et al. 1997; Tognarini and Villa-Moruzzi 1998; Del Aguila et al. 1999; Cazzolli et al. 2002; Doi et al. 2003; Lorenzo 2008; Grzelkowska-Kowalczyk and Wieteska-Skrzeczynska 2009). In addition C2C12 cells have been shown to be responsive to LPS and pro-inflammatory cytokines such as TNF-α, IFN-γ and IL-1: affecting glucose uptake (Del Aguila et al. 1999; Grzelkowska-Kowalczyk and Wieteska-Skrzeczynska 2009), protein synthesis (Li et al. 1998; Plaisance et al. 2008) or inducing iNOS expression (Williams et al. 1994; Gath et al. 1999; Frost et al. 2003a). Although primary cell lines can also be used to study skeletal muscle tissue, primary tissue is often ‘contaminated’ with resident macrophages or endothelial cells (Williams et al. 1994), which would prevent establishing precise links between stimulants and skeletal muscle signalling. This makes it clear that C2C12 cells are a good model system to study the effects of LPS and pro-inflammatory cytokines on glycogen metabolism in a basal or insulin-stimulated setting.

1.10 Aims

As observed with the studies relating to liver glycogen metabolism during endotoxic shock, the signalling machinery undergoes alterations that contribute to some of the symptoms associated with the syndrome such as the initial hyperglycaemic phase followed by the hypoglycaemic phase. It is evident that skeletal muscle glycogen metabolism contributes to these symptoms as it is also affected during endotoxic shock – for example peripheral glucose uptake is increased during the hypoglycaemic phase of endotoxic shock (Knowles et al. 1986) – but the primary causes for these effects are not yet clear. The project will use an established in vitro model of endotoxic shock, which was previously developed in other laboratories as well as ours (Curran et al. 1990; Ceppi et al. 1996; Wallington et al. 2008). The C2C12 skeletal muscle cell line will be treated with LPS, TNF-α, IFN-γ and IL-1β for 18 hours, after which measurements of various glycogen metabolic steps will be assayed and the activity of proteins determined. The synthesis of glycogen after treatment will be assayed and form the initial step towards elucidating the effects of LPS plus pro-inflammatory cytokines on glycogen synthesis. As highlighted in Section 1.6, muscle glycogen synthesis regulation involves a few key steps, of which the important ones are: glucose entry into the cell, glycogen stores, and GS activity. As a result, the glycogen synthesis results will be compared in parallel with differences in these regulatory steps. Although much research has focused on the increased rate of glucose uptake by skeletal muscle during endotoxic shock, the precise underlying mechanisms remain disputed. Similarly, previous research has measured glycogen stores in skeletal muscle cells during endotoxic shock or inflammatory conditions but failed to coincide. It is therefore still necessary to determine if such changes are occurring, and if they are, attempt to shed light on the principal causes.

Moreover, studies relating endotoxic shock to skeletal muscle glycogen metabolism have rarely tried to accommodate for each regulatory step within one process, making it hard to formulate an overall picture, this will be attempted in this study. Finally, insulin elicits important changes on skeletal muscle glycogen metabolism and has been shown to have impaired activity during endotoxic shock and inflammatory conditions. Consequently the insulin-stimulation of each of the aforementioned regulatory steps within glycogen metabolism will also be addressed, thus deducing whether or not insulin-resistance occurs and enabling to shed light on possible underlying mechanisms.

Chapter Two – Materials and Methods

2.1 Materials

The C2C12 myocytes were obtained from ECACC (European Collection of Cell Cultures), UK. All cell culture plates used were of the CELLSTAR variety obtained from Greiner-Bio-One, UK.

The following was obtained from PAA (The Cell Culture Company), UK : MEM (minimal essential medium), penicillin, streptomycin, FCS (fœtal calf serum), trypsin, PBS (phosphate buffered saline). DMEM (dulbecco's modified eagle medium) was obtained from GIBCO, UK .

The following was obtained from Sigma-Aldrich Company Limited, UK. : Insulin, LPS (lipopolysaccharide), N-(1-napthyl)ethyl-enediamine hydrochloride, sulphanilamide, FMN (flavin mono-nucleotide), kanamycin, ampicilin, LB base (lysogeny broth base), BCA reagents A and B (bicinchoninic acid), amyloglucosidase, hexokinase, glucose-6-phosphate dehydrogenase, BSA (bovin serum albumin), DTT (dithiothreitol), ATP (adenosine triphosphate), AMP (adenosine monophosphate), glucose-1-phosphate, glucose-6-phosphate, UDP-glucose (uridine diphosphate-glucose), $NADP^+$ (oxidised, nicotinamide adenine dinucleotide phosphate), NAD^+ (oxidised, nicotinamide adenine dinucleotide), NADH (reduced, nicotinamide adenine dinucleotide), glycogen, benzamidine, leupeptin, PMSF (phenylmethylsulfonyl fluoride), caffeine, microcystin, luminol, coumaric acid, TCA (trichloro acetic acid), imidazole, PCA (perchloric acid), PDTC (pyrrolidine dithiocarbamate), L-NAME (N (G)-nitro-L- arginine methyl ester), glutaraldehyde. DMSO (dimethyl sulphoxide), EthD-1 (ethidium homo-dimer-1), anti-iNOS (inducible nitric oxide synthase) primary antibody. The protease inhibitor (minus EDTA) was obtained from Roche Diagnostics, UK. While Euk8 was obtained from Richard Noles, GlaxoSmithKline, UK. Bradford reagent and SDS molecular weight standards were obtained from Bio-Rad, UK.

The following radio-labelled compounds were obtained from Perkin-Elmer, UK: [U-^{14}C]-Glucose (319mCi/ml), 2-deoxy-D-[^{3}H]glucose (20 Ci/ml), [U-^{14}C] UDP-Glucose (302mCi/mmol), [U-^{14}C] Glucose-1-Phosphate (200mCi/ml). While [^{35}S] Methionine (1175Ci/ml) was obtained from Molecular Probe, UK. Whatman 3MM paper and Whatman GF/C filters was obtained from Whatman, UK. The scintillation fluid was obtained from Fischer Scientific, UK. While the scintillation minivials were obtained from Beckman, UK.

Acrylamide was obtained from National Diagnostics, UK. The PVDF (Polyvinylidene Fluoride) was obtained from Amersham, UK. The X-Ray film was obtained from Jet X-Ray, UK.

E-coli strain JCB 387 pcnB ∆nrf, used for the preparation of formate nitrate reductase was a gift from Prof. J. A. Cole, University of Birmingham, UK. The pro-inflammatory cytokines (TNF-α, IFN-γ and IL-1β) were obtained from Autogen Bioclear, UK.

The following primary antibodies were obtained from Cell Signalling Technology, UK: glycogen synthase, phosphorylated-glycogen synthase (Ser641), AMP activated protein kinase (AMPK), phosphorylated-AMPK (Thr172), Akt, phosphorylated-Akt (Thr308), eukaryotic initiation factor 4 E binding protein 1 (4E-BP1), glycogen synthase kinase 3 (GSK3), phosphorylated GSK3 (Ser21/9), actin, extracellular signal regulated kinase (ERK), phosphorylated-ERK (Thr202/Tyr204), p38 mitogen activated protein kinase (p38), phosphorylated-p38 (Thr180/Tyr182), caveolin. The following primary antibodies were obtained from Santa Cruz Biotechnology, INC, Germany: glucose transporter 1 (GLUT1) and GLUT4. The secondary anti-rabbit and anti-mouse antibodies were obtained from GE Healthcare, UK.

Primary antibodies for myosin heavy chain (MHC) and poly-a-binding protein (PABP) were gifts from Prof. Simon J. Morley, University of Sussex.

All other products not outlined above were purchased from Sigma Aldrich Company Limited, UK. Those used for SDS-PAGE were of electrophoresis grade, and those used for culturing C2C12 were cell culture tested.

2.2 Cell Culture

2.2.1 Growth of C2C12 Myocytes

As discussed in Section 1.9, the C2C12 myocyte cell line was used during this thesis as it is an adequate model for the study of skeletal muscle metabolic regulation as well as responding to LPS plus cytokines, which will be described during the Model of Endotoxic Shock in Section 2.2.5. The C2C12 myoblasts (mononucleated cells) were cultured in 25cm² and 75cm² stock flasks in growth medium (GM: DMEM, supplemented with 20% FCS, 10^5U/litre penicillin and 100mg/litre streptomycin). All cells were incubated at 37˚C with 5% CO_2 humidified atmosphere. Stocks were allowed to grow for 2 days, reaching approximately 70% confluency, but never longer as this would entail changes in the cells due to contact inhibition promoting differentiation. As a result every 2 days the myoblasts were split with the use of the proteolytic enzyme trypsin and plated back into fresh stock flasks at a concentration of

175,000 cells/25cm². When needed, myoblasts were seeded in 6-well plates (9.6cm²) at a concentration of 100,000 cells (following counting Section 2.2.2) and left to grow for 24 hours in GM, at which point they were used for experiments as discussed in Section 2.2.5.

Upon the right conditions, C2C12 myoblasts can differentiate into myotubes and express mature muscle proteins. As a result, when needed, myoblasts were seeded in 6-well plates at a concentration of 175,000 cells and left to grow for 48 hours in GM at which point they were 90-100% confluent and contact inhibited. At this stage the cells were induced to differentiate (Day 0) by changing the medium to differentiation medium (DM: DMEM, supplemented with 2% horse serum, 10µg/ml insulin, 10^5U/litre penicillin and 100mg/litre streptomycin). The DM was changed every 24 hours until Day 3, at which point the cells displayed multinucleated myotubes (Figure 2.2.1a) and expressed mature muscle proteins relative to undifferentiated myoblasts (Figure 2.2.1b). At this point they were used for experiments as discussed in 2.2.5.

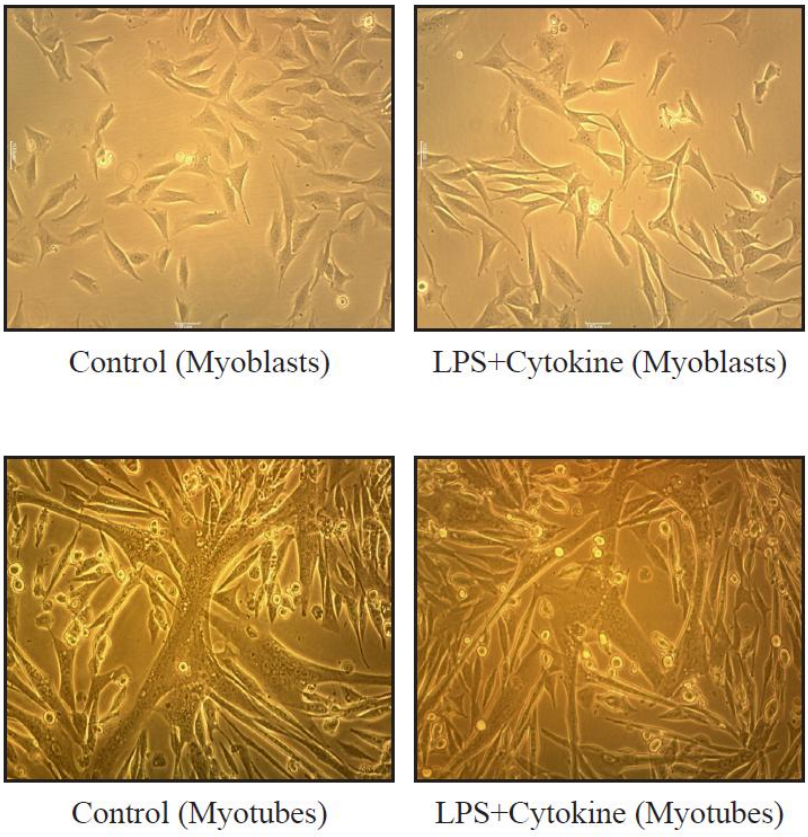

Figure 2.2.1a. Images taken down the microscope showing untreated and treated mononucleated myoblasts and differentiated myotubes. Cells were treated as described in Section 2.2.5.

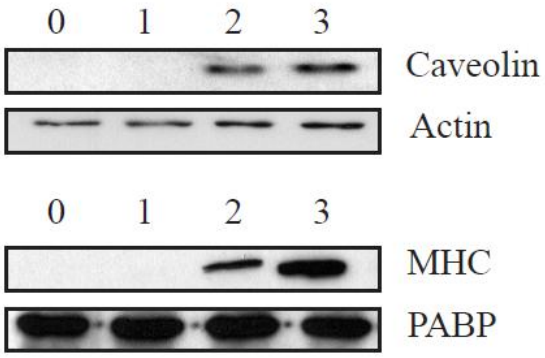

Figure 2.2.1b. Western blot displaying the levels of Caveolin and MHC with their respective loading controls (Actin, PABP) at 0, 1, 2 and 3 days following incubation in DM.

The method used to obtain the Western blot data is described in Section 2.13. As shown, after treatment in DM the myocytes expressed mature muscle fibres (Caveolin and MHC). In Figure 2.2.1a it is evident that the myoblasts formed multinucleated myotubes.

2.2.2 Cell Counting

Cell counting is generally done using a haemocytometer, which allows for the rough measurement of cell numbers (number of cells/ml). This was essential to ensure consistency when seeding the myoblasts for experiments, as described in Section 2.2.1. Cells were split as described above, spun at 12,000 RPM for 5 minutes in trypsin (containing 20% FCS) and the pellet re-suspended in 5ml of GM. 20µl of this was mixed with 20µl of trypan blue. A quartz cover slip was placed on top of the haemocytometer which allows for a 1mm gap. In Figure 2.2.2a the grids designated with a 'W' represent an area of 1mm by 1mm. The volume of liquid present within the grid between the haemocytometer and the cover slip is thus 0.1mm^3. By looking at the haemocytometer under the microscope and counting the cells within the grid, one can calculate the concentration of cells. Once the cover slip was in place, 20µl of the cell mixture was pipette between the haemocytometer and cover slip, and observed down the microscope.

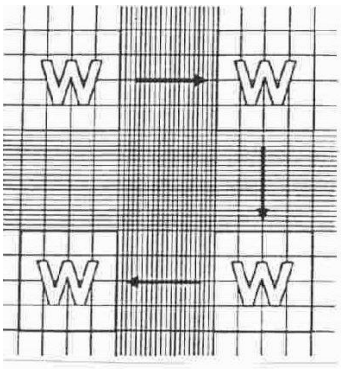

Figure 2.2.2a. Haemocytometer, used to count cells in suspension.

In order to calculate the number of cells/ml, the following calculation was performed:

$$\left(\frac{\text{Total number of cells}}{\text{Number of grids counted}} \times 10^4 \right) \times 2 = \text{cells/ml}$$

2.2.3 Cryogenic Preservation

In order to maintain reserve C2C12 myocytes from the same exact batch having been passaged the same number of times, thereby ensuring consistency with the cells used, cryogenic preservation was performed at regular points during this study, replenishing the stocks. Cells were replaced every 4-6 weeks during the duration of this study. Myoblasts were split as normal, spun at 12,000 RPM for 5 minutes in trypsin (containing 20% FCS) and the pellet re-suspended in freezing medium (90% FCS, 10% DMSO). Aliquots were quickly placed in cryotubes, then into a foam rack at -80°C for 24 hours, and finally transferred from the -80°C freezer to liquid nitrogen (-196°C).

2.2.4 Determination of Cell Viability

The cell viability assay was an important determination due to the potential cytotoxic conditions created by the in vitro model of endotoxic shock. Ethidum-Homodimer-1 (EthD-1) was used to determine cell viability, and is based on the method devised by Markovits et. al. (Markovits et al. 1979). EthD-1 readily binds nucleic acids and upon binding its fluorescence is enhanced by over 30 fold. As it is highly positively charged, it cannot diffuse across the cell membrane meaning that it cannot enter intact viable cells. The principle of determining the viability of cells in a well is done by comparing the fluorescence obtained from a particular

treatment to the fluorescence obtained from another well containing the same treatment and number of cells but treated with saponin (0.1%) prior to the EthD-1 assay. Saponin is a mild detergent that perforates holes through the plasma membrane. As a result, saponin treated wells will contain cells able to allow EthD-1 entry. The fluorescence obtained from this saponin-treated well represents the total cell number, which the non-saponin treated well can be compared to, thereby giving the proportion of viable cells, following treatment.

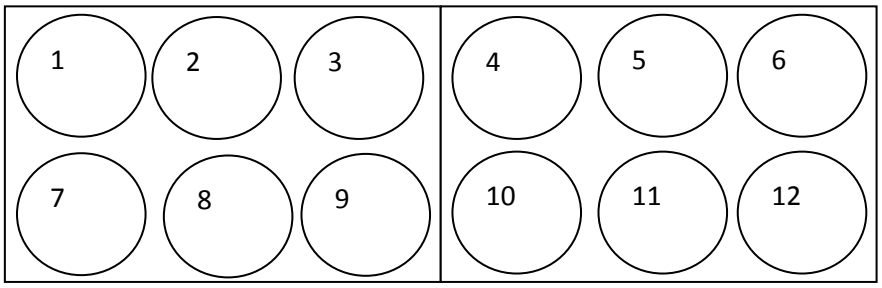

Figure 2.2.4a. 12 wells from a tissue culture plate

Figure 2.2.4a is shown to facilitate the explanation of this protocol: The wells 1-12 are identical in the sense that the cells were seeded at the same concentration. Wells 1-6 are control (untreated), while 7-12 are treated. Wells 1-3 and 7-9 were then incubated with 0.1% saponin but wells 4-6 and 10-12 were kept un-changed. The plate was then incubated at 37°C for 10 minutes to allow for the saponin to work. Following this incubation, all the wells were washed once in warm MEM, and then 100µl of MEM-EthD-1 (MEM containing 4µM EthD-1) was added, and incubated at 37°C for 20 minutes, allowing the EthD-1 to penetrate the cells and bind to the nucleic acids.

The fluorescence was then read at 645nm (with an excitation wavelength of 445nm). In addition to the wells shown above, wells without cells but with the MEM-EthD-1 were used as blanks. Before calculating the percentage viability of the cells on the plate, an average of the fluorescence of each set of treatments (with or without saponin – denoted '^{sap}') were calculated. Average of wells 1-3 = a^{sap}, average of wells 4-6 = b; the average of wells 7-9 = p^{sap} and average of wells 10-12 = q. From each of these (a^{sap}, b, p^{sap} and q) the average fluorescence obtained from the blank wells was subtracted, giving a^{*sap}, b*, p^{*sap} and q*. With these figures, the following calculation was made:

$$\frac{(a^{*sap} - b^{*})}{a^{*sap}} \times 100 = \% \text{ viable cells in control}$$

$$\frac{(p^{*sap} - q)}{p^{*sap}} \times 100 = \% \text{ viable cells in treated}$$

The two percentages are compared to assess if the treatment significantly decreased cell viability.

2.2.5 Basis of In Vitro Model of Endotoxic Shock

As described in Section 1.10 of the introduction, the established model of endotoxic shock used throughout this study was one developed by other laboratories including ours (Curran et al. 1990; Ceppi et al. 1996; Wallington et al. 2008). As discussed in Section 1.2, the presence of LPS in the blood results in the increased concentration of circulating cytokines including TNF-α, IFN-γ, IL-1β and IL-6 (Titheradge 1999). It has been established that the effect of NO is important for the pathophysiology of sepsis (Kilbourn et al. 1997), and together with the fact the presence of LPS, TNF-α, IFN-γ and IL-1β were required for NO production in vitro (Figure2.2.5a) (Curran et al. 1990; Ceppi et al. 1996), the C2C12 myocytes were treated for 18 hours with all 4 four stimulants. The conditions used for iNOS induction in C2C12 myocytes were: 1μg/ml LPS, 2ng/ml TNF-α, 10ng/ml IFN-γ and 0.1ng/ml IL-1β. Following seeding and growth, as described in Section 2.2.1, the myoblasts or myotubes were washed once in PBS, and then incubated for 18 hours in MEM (supplemented with 10% FCS, 10^5U/litre penicillin and 100mg/litre streptomycin) with the LPS plus cytokine treatment. Following treatment, the medium was sampled for the measurement of NOx (as described in Section 2.3), and the cells harvested as described for each protocol in this chapter.

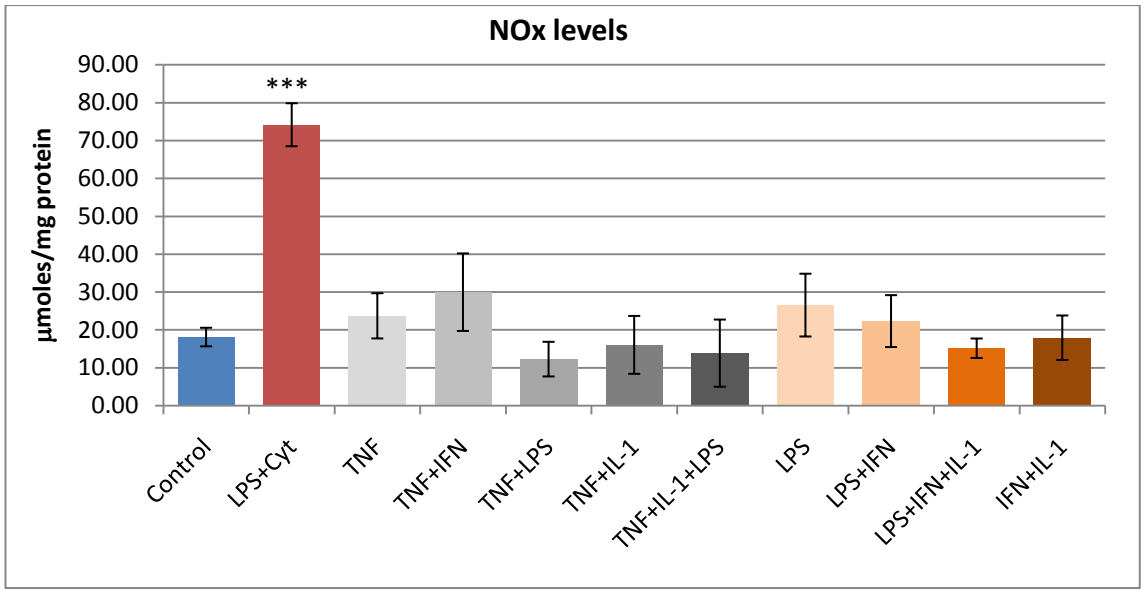

Figure 2.2.5a. Graph showing the levels of NOx (indicative of NO production described in Section 2.3) between 18 hour treatments with different combinations of LPS and cytokines. Results shown are the mean µmoles of NOx ± SEM from 8-12 determinations from 3 independent experiments. TNF = TNF-α, IFN = IFN-γ, IL-1 = IL-1β, LPS+Cyt = LPS+TNF-α+IFN-γ+IL-1β.
* = Significance from control
Statistical significance is as described in Section 2.14

As shown in the figure above, LPS plus all 3 cytokines was the only treatment that significantly increased NO production over 18 hours. Confirming previous results (Curran et al. 1990; Ceppi et al. 1996).

2.2.6 Mouse Hind Limb Skeletal Muscle Extract

At various points during the study, a skeletal muscle extract from the hind limb of 3 day old mice was used to compare with the C2C12 myocytes. These extracts were kindly given to us by Dr. Guy Richardson (University of Sussex, Brighton). The extracts were placed in tin foil as soon as they were excised from the bone and placed immediately in liquid nitrogen until the day of the assay, at which point they were thawed and ground in liquid nitrogen, then lysed depending on the assay they were used for.

2.3 Determination of Nitrate and Nitrite

As discussed in Section 1.1, nitric oxide (NO) levels increase drastically during sepsis, and can therefore be used as a positive assessment of the effect of the in vitro model of

endotoxic shock. NO has a short half-life (approximately 3 seconds), as a result in order to determine its concentration the levels of the stable derivatives generated during NO metabolism – nitrate (NO_3^-) and nitrite (NO_2^-) – were determined. The concentration of nitrate plus nitrite will be referred to as NOx throughout this report.

2.3.1 Preparation of Samples

Following the 18h incubation with LPS plus cytokines, a sample was taken from the cell medium in order to measure the levels of both nitrate and nitrite.

2.3.2 Determination of Nitrite

The concentration of nitrite was determined using a method first described by Griess (cited in (Green et al. 1982). The nitrite in the sample reacts with an aryl amine to produce a pink diazo dye (Azo product). The principle is shown in Figure 2.3.2a.

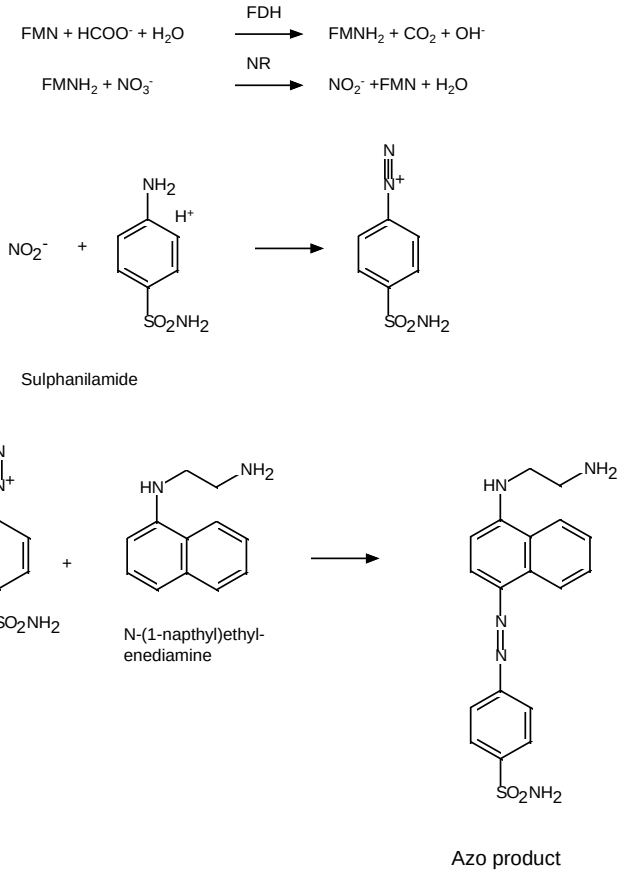

Figure 2.3.2a. Principle of the nitrite assay. FDH = formate dehydrogenase, NR = nitrate reductase.

50µl of sample/nitrite standard and 50µl of pure water were mixed with 100µl of Griess reagent in a 96 well ELISA microtitre plate. The Griess reagent consisted of equal volumes of solution A (1% (w/v) N-(1-napthyl)ethyl-enediamine hydrochloride) and solution B (1% (w/v) sulphanilamide in 5% (v/v) orthophosphoric acid) and was prepared immediately before use. The colour was allowed to develop at room temperature for approximately 10 minutes and the absorbance was then measured at 540nm. To determine the amount of nitrite in the samples, the absorbances were read against a standard curve prepared from sodium nitrite (0-100µM) in the same medium as the samples.

2.3.3 Conversion of Nitrate

The total level of NO can be assessed by converting the nitrate component of NO metabolism to nitrite. The original method, Taniguchi et. al., was modified by Titheradge (Taniguchi et al. 1985; Titheradge 1998). Formate nitrate reductase is used to reduce the nitrate to nitrite in the presence of FMN (flavin mono-nucleotide). FMN is added as an electron carrier and is reduced to $FMNH_2$ by formate dehydrogenase (formate: ferricytochrome b_1 oxidoreductase). The $FMNH_2$ is then used to reduce the nitrate to nitrite using nitrate reductase (ferrocytochrome: nitrate oxidoreductase). The concentration of nitrite formed is determined using the Griess reaction, as described in Section 2.3.2.

2.3.4 Procedure for the Conversion of Nitrate to Nitrite

The conversion buffer (0.5M phosphate buffer, 0.8M sodium formate, 0.4mM FMN buffer, pH 6.0) was diluted 2.8 times with pure water allowing 40µl per sample or nitrate standard. Formate nitrate reductase (FNR) enzyme was added to this buffer allowing 10µl of the diluted enzyme per sample or nitrate standard. 50µl of this buffer was added to 50µl of sample or nitrate standard and incubated in a 96 well ELISA microtitre plate for 1 hour at 37°C. Subsequent to this incubation, 100µl of Griess reagent was added to each well, and the absorbance measured at 540nm. In order to determine the levels of nitrate in the samples the concentration of nitrite measured in samples not containing FNR were subtracted from the levels of nitrite measured in samples with FNR (which would have included the nitrite and the nitrate converted to nitrite).

2.3.5 Preparation of Formate Nitrate Reductase

Kanamycin resistant Escherichia coli, strain JCB387 pcnB Δnrf (which contains FNR in its membranes), was grown on agar plates containing kanamycin (5μg/ml). A discrete kanamycin resistant colony was transferred aseptically to a 5ml bottle of LB media (2% (w/v) LB broth base, 1% (w/v) KNO_3, 1% (w/v) sodium formate, 0.1% w/v) K_2HPO_4, 10mM glycerol, pH 7.2) containing 5ml of 5% kanamycin solution to prevent contamination (kanamycin solution made up in 0.9% NaCl), and allowed to grow for several hours until cells were visible. 0.5ml of this E.coli culture was then transferred aseptically to several 500ml bottles of LB media and grown anaerobically overnight at 37°C in a shaking incubator. The media was centrifuged at 2000xg for 20 minutes at 4°C to collect the cells from the solution as a pellet. The pellet was re-suspended in 500ml of cold distilled water and centrifuged again. This re-suspension and centrifugation process was carried out two more times in order to remove any residual nitrite and nitrate from the medium. The pellet was then weighed and frozen overnight at -20°C, before being re-suspended in 5x its weight of ice-cold distilled water. The cells were disrupted by sonication for 5 minutes on ice (15 seconds on, 30 seconds off for 15 minutes) to prevent the cells warming up and denaturing the enzyme. The sonicated solution was centrifuged at 2000xg for 20 minutes to remove any un-broken cells. The pellet obtained can be sonicated again in order to maximise the yield of enzyme). The supernatant containing the cell membranes and FNR was then centrifuged at 20,000xg for 40 minutes to enable collection of the membranes in a pellet. This final pellet was re-suspended in 1ml of of cold distilled water and dialysed in a 5L beaker of water at 4°C overnight. The protein content of the dialysate was adjusted to 10mg/ml for use in the nitrate assay and then aliquoted, tested and stored at -80°C. Upon using the enzyme the aliquot was diluted 20 times with water and then used in the assay described in Section 2.3.3.

2.4 Determination of Protein

Two methods of protein determination were used, the BCA method and the Bio-Rad protein assay (Bradford). The BCA method is based on one conducted by Smith et. al. (Smith et al. 1985). BCA (bicinchoninic acid, disodium salt – BCA-Na_2) can form a stable coloured (purple) complex with cuprous ions (Cu^+) in an alkaline environment. Cu^+ is produced when proteins react with alkaline Cu^{2+} (the biuret reacton). Therefore, the quantity of protein in a sample dictates the level of Cu^+ produced which in turn determines the intensity of the colour. The

stable purple complex can be measured using a spectrophotometer at 540nm, which is read against a standard curve.

The Bio-Rad Protein Assay is based on the Bradford dye-binding method devised by Bradford (Bradford 1976). It is based on the colour change of Coomassie Brilliant Blue G-250 dye which turns towards a dark blue colour indicative of high levels of protein. The dye binds mainly basic and aromatic amino acid residues, the more residues it binds to, the darker the colour gets. The coloured samples can be measured using a spectrophotometer at 620nm with a reference filter of 405nm, and then compared to a standard curve.

2.4.1 Procedure for BCA method

A working reagent was made up consisting of 50 parts of solution A (BCA-A reagent: 1% (w/v) BCA-Na_2, 2% (w/v) $Na_2CO_3.H_2O$, 0.16% (w/v) Na_2 Tartrate, 0.4% NaOH, 0.95% $NaHCO_3$, pH 11.25) with 1 part of solution B (4% (w/v) CuSO4). 200µl of this working reagent was added to 20µl of sample or standard in a 96 well ELISA plate, mixed by shaking on a microplate shaker and incubated for 30 minutes at 37°C. The absorbance was then recorded at 540nm and the concentration of protein calculated against a standard (0-12µg/10µl of the appropriate buffer). For the determination of cellular protein from a 6 well plate, the cells were solubilised in 500µl of 1M KOH; this ensured that the results obtained fell within the range of the standard curve.

2.4.2 Procedure for Bio-Rad Protein Assay (Bradford) Method

A working reagent was prepared consisting of 4 parts Bio-Rad Bradford reagent and 1 part pure water. 200µl of this reagent was added to 5µl of sample in an eppendorf tube, and 150µl of the mixture was transferred to a 96 well ELISA plate at which point the absorbance was recorded at 620nm (with a reference filter of 405nm). The values were then compared to a standard curve which was prepared from a 10mg/ml BSA solution in pure water. 0, 1, 2, 4 and 8µl of this BSA solution was mixed with 200µl of the Bio-Rad reagent prepared, being equivalent to 0, 0.5, 1, 2 and 4µg of protein/well. For the determination of cellular protein from a 10 cm plate, the cells were harvested as described in Section 2.13.1. 2µl of the cell extract was diluted in 18µl of pure water, and 5µl of this dilution was mixed with the working

Bio-Rad reagent prepared, ensuring the values obtained fell within the range of the standard curve.

2.5 Determination of Glycogen

The glycogen content present in the cells was determined using a modification of the method described by Passoneau and Lowry (Passonneau and Lowry 1993). The principle of this assay is described below:

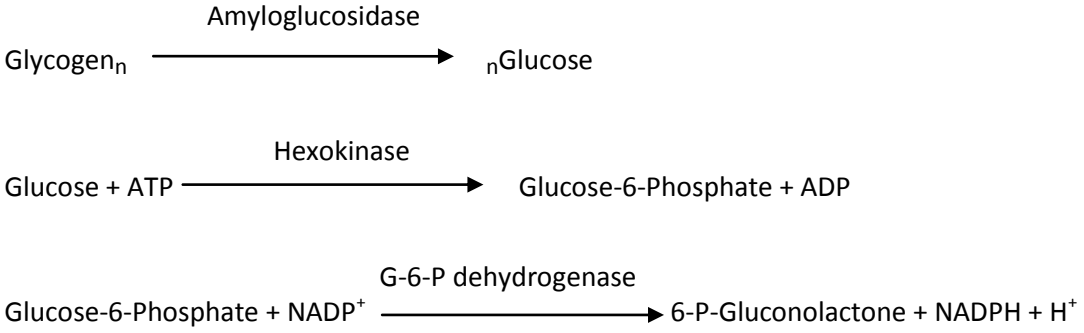

Amyloglucosidase first catalysed the conversion of glycogen into glucose. Glucose was then converted to G-6-P by hexokinase (in the presence of ATP), and subsequently G-6-P oxidation by G-6-P dehydrogenase (G-6-PDH) was coupled to the reduction of $NADP^+$ to NADPH. The appearance of NADPH was determined fluorimetrically (excitation 340nm/ emission 460nm). These reactions were carried out in two stages; the reaction governed by amyloglucosidase requires pH 4.7, however NADPH is unstable under pH 4.7. Glycogen was thus first converted to glucose at pH 4.7, and then the pH was changed to pH 8.8 for the remainder of the assay. The cellular glycogen was measured in cultured cells solubilised in 0.1M NaOH. Following treatment, the cells were washed 3 times in cold PBS, then scraped in a small volume of PBS and centrifuged lightly to pellet the cells. The supernatant was discarded and the pellet re-suspended in 300µl 0.1M NaOH, at which point they were vortexed and sonicated for 8s to help break up the cells and ensure complete solubilisation.

2.5.1 Conversion of Glycogen to Glucose

50µl of sample or standard in 0.1M NaOH was added to 7.3µl of 1M acetic acid in quadruplicate, giving a pH of approximately 4.7 (glycogen standards in 0.1M NaOH were prepared to give the equivalent of 0-9 nmoles of glucose). 6µl of 1.4U/ml amyloglucosidase was added to two of the tubes per sample or standard whereas 6µl of 0.9% NaCl (containing 1mg/ml BSA) was added to the other two. The tubes without amyloglucosidase were used to determine the glucose already in the sample, so that it could be subtracted from the total value of glucose, giving the actual glucose produced from the glycogen. The samples were mixed and incubated at 37°C for 1 hour.

2.5.2 Determination of Glucose produced from Glycogen Breakdown

50µl of the incubated samples or standards were added to 130µl of glucose reagent (146mM Tris-HCl (pH 8.8), 7.3mM MgCl2, 0.146mM DTT, 0.219 ATP, 0.0584mM NADP+, 0.44U/ml G-6-PDH) in a 96 well ELISA plate and an initial reading was made after 10 minutes. After this, the reaction was initiated by the addition of 10µl of hexokinase (final concentration 1.2U/ml). The mixture was mixed and left shaking gently at room temperature for 1 hour, before a secondary reading was taken. The primary reading was subtracted from the secondary one, and the value of glucose determined from the glycogen standard curve. A set of glucose standards (0-10 nmoles prepared in 100mM sodium acetate buffer pH 4.7) were assayed in parallel to determine the percentage conversion from glycogen to glucose by the amyloglucosidase.

2.6 [U-^{14}C] Glucose Incorporation into Glycogen

This method is based on that of Agius et. al. (Agius et al. 1990). The rate of glycogen synthesis in cells can be measured by the incorporation of [U-^{14}C] Glucose into glycogen over a given time. The amount of radioactive glycogen produced can be measured in a scintillation counter.

$$\text{Glycogen}_n + [\text{U-}^{14}\text{C}]\text{Glucose} \longrightarrow \text{Glycogen}_{n+1}\ (\text{containing one } [\text{U-}^{14}\text{C}]\ \text{Glucose molecule})$$

2.6.1 Perfection of the Method

The modified method was previously used in the laboratory for the study of hepatocyte glycogen metabolism under endotoxic shock (Wallington 2004). It was therefore used for this thesis but quickly caused problems with inconsistent results and bad recovery of radioactive glycogen. As a result the method was re-appraised in order to ensure consistency. The method used previously in our laboratory consisted first in washing the incubated cells with cold PBS thereby removing any non-incorporated [U-^{14}C] glucose. Subsequently solubilisation of the cells to release the glycogen, via 0.1M NaOH, followed by precipitation of the protein (via 40% (w/v) TCA containing 10mg/ml glycogen) to avoid non-specific radioactivity that may have been incorporated into protein during the culture period. The remaining solution was then mixed with ice-cold IMS to precipitate the glycogen for 10 minutes on ice, which was then pelleted and re-suspended in water before being assayed in the scintillation counter.

The initial experiments from this method yielded very low radioactivity from the scintillation counter, making it hard to distinguish between treatments. As a result a range of methods using criteria from different protocols were compared for linearity of the incorporation of [U-^{14}C] glucose into glycogen over time as well as taking into account the background reading which at the beginning proved to be high. The criteria addressed were the strength of base used to solubilise the cells, boiling the samples for 10 minutes following solubilisation, the concentration of glucose within the assay buffer and finally the use of Na_2SO_4 to help bring down the glycogen in the pellet. Stock glucose was added to bring up the concentration of glucose to 20mM (from 5.5mM which is the level present in MEM). This reduced the specific activity of glucose, so glucose levels were kept at the normal levels present in MEM, while the boiling of the samples improved recovery so was added to the protocol. The use of Na_2SO_4 was used to help precipitate the glycogen but at first seemed to increase the background as well. Finally, the precipitation of glycogen, which had normally been carried out on ice for 10 minutes was then tried at -80°C for 30 minutes, which showed better recovery. With this knowledge, 4 methods were focused on to compare the results with the aim of devising the suitable protocol for the C2C12 system.

The first and second method both used 0.1M NaOH, and differed only in the presence or absence of Na_2SO_4 during glycogen precipitation. The final two methods were the same except using 1M KOH, as well as differing in the presence or absence of Na_2SO_4. The use of 1M

KOH and Na_2SO_4 improved the % recovery, so was the chosen method to address glycogen synthesis.

2.6.2 Sample Preparation

The cells were grown in 6-well plates, and treated as described in Section 2.2. Following treatment the medium was removed and retained for determination of NOx levels, while the cells were incubated for 2 hours in 750µl of MEM containing 0.6 µCi/ml of [U-^{14}C] glucose. Subsequent to the 2h incubation, the medium was removed and the cells washed 3 times in 750µl of cold PBS. The cells were then solubilised in 500µl of 1M KOH for 1h at room temperature before being scraped into an eppendorf tube and boiled for 10 minutes. At this stage the samples could be left at -20°C until the day of the assay.

2.6.3 Procedure

350µl of the solubilised cell mixture was added to 50µl of Na_2SO_4 and 100µl of 40% TCA containing 10mg/ml carrier glycogen to precipitate the protein. The contents were mixed and then centrifuged at 10,000xg for 5 minutes in a cooled microcentrifuge. 400µl of the supernatant was then mixed with 800µl of ice cold IMS and left at -80°C for 30 minutes to precipitate the glycogen, and subsequently centrifuged at 10,000xg for 5 minutes in a cooled microcentrifuge. The supernatant was carefully decanted, and the pellet re-suspended in 400µl of pure water. Another 800µl of ice cold IMS was added to re-precipitate the glycogen at -80°C for 30 minutes before the mixture was re-centrifuged at 10,000xg for 5 minutes. The supernatant was carefully decanted, the final pellet re-suspended in 200µl of pure water and the dissolved contents transferred to a minivial for scintillation counting. An extra 200µl of pure water was added to the eppendorf tube to wash out any remaining contents followed by a brief centrifugation to ensure all the liquid was at the bottom of the tube, and then transferred to the minivial. 4ml of scintillation fluid was added to each sample and the minivials were then placed in a scintillation counter for 10 minutes to measure the amount of radioactivity incorporated into glycogen.

2.7 Determination of Glucose Transport

This method is based on that of Bedard et. al. (Bedard et al. 1997). The transport of glucose can be determined by the incorporation of 2-deoxy-D-[^{3}H]glucose ([^{3}H]-2DOG) into the cell over a given time. The radioactivity present inside the cell can be measured using a scintillation counter.

2.7.1 Sample preparation and Procedure

The cells were grown in 6-well plates, and treated as described in Section 2.2.5. Following treatment the medium was retained for measurement of NOx levels, while the cells were washed once in Hepes-buffered saline solution, pH 7.4 (130mM NaCl, 5mM KCl, 1.25mM $CaCl_2$, 0.8mM $MgSO_4$, 5.5mM Glucose, 20mM Hepes, containing 0.1% (w/v) BSA), and then incubated for 5 minutes in the same buffer in an atmosphere of 5% CO_2 at 37°C. Following these 5 minutes, 7.5μl of [^{3}H]-2DOG (1μCi/ml) was added and the cells were incubated for 15 minutes. After the radioactive incubation, the medium was removed and cells washed 3 times in 750μl of PBS, followed by the addition of 500μl of 1M KOH for 1h at room temperature, to solubilise the cells. 400μl of this cell extract was transferred to a minivial along with 4ml of scintillation fluid and the radioactivity determined in a scintillation counter.

2.8 Determination of Glycogen Phosphorylase Activity

This assay is based on the method of Halse et. al. (Halse et al. 2001). Glycogen phosphorylase (Phosphorylase) activity was measured in cell extracts in the reverse direction by the incorporation of [U-^{14}C] Glucose-1-Phosphate into glycogen in a 30 minute incubation. The radioactivity can then be measured using a scintillation counter.

$$\text{Glycogen}_n + \text{Pi} \xrightleftharpoons{\text{Glycogen Phosphorylase}} \text{Glucose-1-Phosphate} + \text{Glycogen}_{n-1}$$

2.8.1 Sample Preparation

The cells were grown in 10 cm diameter dishes, and treated as described in Section 2.2.5. Following treatment the medium was removed and retained for NOx determination, and 750µl of Buffer A (10mM Tris HCl pH 7.8, 150mM NaF, 60mM Sucrose, 15mM EDTA, 1mM Benzamidine, 10mg/ml Leupeptin, 1mM PMSF, 1mM BME) was added to the plate at which point the plate was frozen immediately by placing in liquid nitrogen to stop any reactions. The plates were thawed on ice, the cells scraped and transferred into eppendorf tubes. The cells were then broken up by sonication at a low amplitude for 8 seconds (4 seconds on, rest on ice followed by an extra 4 seconds on).

2.8.2 Procedure

Two buffers were used, Buffer B was used to measure the total Phosphorylase activity (a+b). AMP was included in this buffer to activate the Phosphorylase-b population by converting it from the T state to the R state. While Buffer C was used to measure Phosphorylase-a activity alone using caffeine to inhibit any Phosphorylase-b activity.

Duplicate 20µl aliquots of each sample was mixed with 40µl of Buffer B (33mM MES pH 6.3, 100mM NaF, 20mM EDTA, 1% (w/v) Glycogen, 50mM G-1-P, 2mM AMP, 0.0025µCi/µmol [U-^{14}C] G-1-P) or 40µl of Buffer C (33mM MES pH 6.3, 100mM NaF, 20mM EDTA, 1% (w/v) Glycogen, 50mM G-1-P, 5mM Caffeine, 10µM AMP, 0.0025µCi/µmol [U-^{14}C] G-1-P) for 30 minutes in a 30°C water bath. The reaction was stopped by pipetting 50µl of the reaction mix onto a 2cm square Whatman filter paper and dropping the filter paper into a beaker containing a guarded stirring bar with 6-8ml per paper of ice cold 66% (v/v) IMS to precipitate the glycogen. The filter papers were washed for 30 minutes, and subsequently washed two more times in fresh ice cold 66% (v/v) IMS to remove any remains of un incorporated [U-^{14}C] G-1-P. The filter papers were then briefly washed in acetone to remove any water and ethanol and then allowed to dry. After drying, the filter papers were placed in minivials with 2ml of scintillation fluid, and the radioactivity determined in a scintillation counter. Duplicate zero time samples (accounting for background binding to the filter) were included by adding the samples to Buffers B and C and immediately stopping the reaction by spotting 50µl onto a filter paper. The total activity in the buffer was determined by pipetting 5µl of Buffers B or C in duplicate onto filters, and allowed to dry before counting in minivials with 2ml of scintillation fluid.

2.9 Determination of Glycogen Synthase Activity

This assay is based on the method of Halse et. al. (Halse et al. 2001). Glycogen synthase (GS) activity was measured in cell extracts by the incorporation of [U-^{14}C] UDP-Glucose into glycogen in a 30 minute incubation. The radioactivity can then be measured using a scintillation counter.

$$\text{UDP-Glucose} + \text{Glycogen}_n \longrightarrow \text{UDP} + \text{Glycogen}_{n+1}$$

Samples were prepared as described for the method Phosphorylase activity assay in Section 2.8.1.

2.9.1 Procedure

Two buffers were used, Buffer X was used to measure the total GS activity (a+b). A high concentration of G-6-P was included in order to allosterically activate the GS-b population, while Buffer Y had a very low concentration of G-6-P, ensuring that only GS-a activity was assessed.

Duplicate 20µl aliquots of each sample was mixed with 40µl of Buffer X (50mM Tris-HCl pH 7.8, 20mM EDTA, 25mM NaF, 1% (w/v) Glycogen, 10mM G-6-P, 0.4mM [U-^{14}C] UDP-Glucose (specific activity 0.01µCi/µmol)) or 40µl of Buffer Y (50mM Tris-HCl pH 7.8, 20mM EDTA, 25mM NaF, 1% (w/v) Glycogen, 0.1mM G-6-P, 0.4mM [U-^{14}C] UDP-Glucose (specific activity 0.01µCi/µmol)) for 30 minutes in a 30°C water bath. The reaction was stopped by pipetting 50µl of the reaction mix onto a 2cm square Whatman filter paper and dropping the filter paper into a beaker containing a guarded stirring bar with 6-8ml per paper of ice cold 66% (v/v) IMS to precipitate the glycogen. The filter papers were washed for 30 minutes, and subsequently washed two more times in fresh ice cold 66% (v/v) IMS to remove any remains of un incorporated [U-^{14}C] UDP-Glucose. The filter papers were then briefly washed in acetone to remove any water and ethanol and then allowed to dry. After drying, the filter papers were placed in minivials with 2ml of scintillation fluid, and the radioactivity determined in a scintillation counter. Duplicate zero time samples (accounting for background binding to the filter) were included by adding the samples to Buffers X and Y and immediately stopping the

reaction by spotting 50µl onto a filter paper. The total activity in the buffer was determined by pipetting 5µl of Buffers X or Y in duplicate onto filters, and allowed to dry before counting in minivials with 2ml of scintillation fluid.

2.10 Determination of Glucose-6-Phosphate Concentration

This assay is based on the method of Passonneau and Lowry (Passonneau and Lowry 1993). The conversion of G-6-P into gluconolactone-6-P, which spontaneously converts into gluconate-6-P, is coupled to the conversion of $NADP^+$ into NADPH. The change in absorbance is measured at 340nm.

$$\text{G-6-P} + NADP^+ \xrightarrow{\text{G-6-P dehydrogenase}} \text{Gluconolactone-6-P} + NADPH + H^+$$

$$\text{Gluconolactone-6-P} + H_2O \xrightarrow{\text{Spontaneous}} \text{Gluconate-6-P}$$

2.10.1 Sample Preparation

Cells were grown in 10 cm plates, and treated as described in Section 2.2.5. Following treatment the medium was quickly removed and retained for determination of NOx levels, while the cells were left with 500µl of MEM at which point 50µl of 2.7M PCA was added and the cells scraped into an eppendorf before being flash frozen until the assay was carried out. On the day of the assay the samples were neutralised with neutralisation buffer (2M KOH, 0.4M KCl, 0.4M TEA) and centrifuged at 10,000xg for 1 minute to remove any debris. The supernatant was then used for the assay.

2.10.2 Procedure

100µl of the deproteinised/neutralised extract was added to 90µl of incubation buffer (222mM Imidazole, 22.2µM $NADP^+$, 0.111µM DTT) and the initial absorbance was measured at 340nm to account for any NADPH already in the solution. 10µl of G-6-PDH was added (to a final concentration of 0.02U/ml) to start the reaction. The plate was incubated at room

temperature for 30 minutes, when the second reading was taken. The initial reading was subtracted from the second, and the resulting absorbance was converted to concentration by comparison with a G-6-P standard curve made up in deproteinised/neutralised MEM, reproducing the same conditions as the samples.

2.11 Determination of UDP-Glucose Concentration

This assay is based on the method of Passonneau and Lowry (Passonneau and Lowry 1993). The conversion of UDP-glucose to UDP-glucuronate by UDP-glucose dehydrogenase is linked to the reduction of NAD^+ to NADH. The change in absorbance is measured 340nm.

$$\text{UDP-Glucose} + 2NAD^+ \xrightarrow{\text{UDP-Glucose Dehydrogenase}} \text{UDP-Glucuronate} + 2NADH + 2H^+$$

Samples were prepared as described in Section 2.10.1.

2.11.1 Procedure

100µl of the deproteinised neutralised extract was added to 90µl of incubation buffer (27.8mM Tris-HCl pH8.1, 2.22mM $MgCl_2$, 555.6µM NAD^+) and the initial absorbance measured at 340nm to account for any NADH already in the solution. 10µl of UDP-glucose dehydrogenase was added (to final concentration of 0.04U/ml) to start the reaction. The plate was incubated at room temperature for 60 minutes, when the second reading was taken. The initial reading was subtracted from the second, and the resulting absorbance was converted to concentration by comparison with a UDP-glucose standard curve made up in deproteinised/neutralised MEM, reproducing the same conditions as the samples.

2.12 [^{35}S] Methionine Incorporation into Protein

This method is based on the method of Fraser et. al. (Fraser et al. 1999). The rate of protein synthesis in cells can be measured by the incorporation of [^{35}S] Methionine into protein over a given time. The amount of radioactive protein produced can be measured in a scintillation counter.

2.12.1 Sample Preparation

The cells were grown in 6-well plates, and treated as described in Section 2.2.5. Following treatment the medium was removed and retained for determination of NOx levels, while the cells were incubated for 1 hour in 750µl of MEM containing 5µCi/µl [^{35}S] methionine. Subsequent to the 1 hour incubation, the media was removed and the cells washed 3 times in PBS. The cells were then solubilised in 500µl of 0.3M NaOH, the cell mixture scraped and transferred to an LP4 tube. A further 500µl was added to the well to wash out any remaining cells, and transferred to the same LP4 tube. The contents was vortexed and 100µl of the mixture was retained for measurement of protein.

2.12.2 Procedure

The protein was then precipitated with an equal volume (900µl) of 25% TCA. The tubes were vortexed for several seconds and then left for 10 minutes. Whatman GF/C filters were placed in a vacuum pump and 10% TCA was poured onto them. The contents of the tubes was then poured onto the filters while the vacuum was on, and washed out with an extra volume of 10% TCA. Following this, each filter had some IMS squirted on, to help drying. The filters were then placed in minivials with 2ml of scintillation fluid, and the radioactivity determined over 5 minutes.

2.13 SDS-PAGE and Western Blotting

Sodium dodecyl sulphate polyacrylamide gel electrophoresis (SDS-PAGE) is used for the separation of proteins according to their size. A polyacrylamide gel is prepared and an electrical current applied through it. SDS is an anionic detergent that disrupts the hydrogen bonds and Van der Waal's interactions in the proteins such that the proteins are rendered into their linear primary structure. The resulting denatured proteins are given a negative charge due to the binding of SDS, which is relative to their size since the number of SDS molecules that bind the protein is proportional to the number of amino acids in the polypeptide.

2.13.1 Sample Preparation

The cells were grown in 10 cm diameter dishes, and treated as described in Section 2.2.5. Following treatment the medium was removed and retained for NOx determination, while the cells were washed once in cold PBS, then scraped in 1ml of cold PBS and spun at 15,000xg for 1 minute in a cooled microcentrifuge to pellet the cells. The cell pellet was re-suspended in 200µl of lysis buffer (20mM MOPS pH 7.2, 25mM KCl, 2mM $MgCl_2$, 2mM Benzamidine, 1µm Microcysteine, 2mM EGTA, 20mM NaF, 1x Protease Inhibitors (Roche), 1% (v/v) Triton X) and the mixture quickly vortexed to break open the cells. The contents were then re-centrifuged in a cooled microcentrifuge at 15,000xg for 1 minute. The pellet was discarded and 2µl of the supernatant was aliquoted for the determination of protein as described in Section 2.4.2. The rest of the supernatant was flash frozen and kept at -80°C until required. Following protein determination, samples were thawed and the concentration of protein adjusted to 1mg/ml by the addition of sample buffer (5.4mM Tris-HCl pH 6.8, 0.2M DTT, 4% (w/v) SDS, 20% (v/v) glycerol, 0.02% bromophenol blue) before being boiled for 10 minutes to ensure complete protein denaturation.

2.13.2 Preparation of the Polyacrylamide Gel

All SDS-PAGE separations in this study were carried out using the mini-PROTEAN II gel electrophoresis system from Bio-Rad assembled according to the operation manual. A two-stage gel electrophoresis system was used to separate the proteins. This process uses a stacking gel (1.5cm) layered above an already set separating gel (4.5cm). The low acrylamide concentration of the stacking gel allows the proteins to move quickly and concentrate into a narrow band at the interface between the stacking and separating gel since the latter has a significantly higher concentration of acrylamide. The proteins then migrate down the separating gel and are separated according to their size, with the smallest proteins migrating further down, while the heavier proteins remaining at the top. 10% polyacrylamide separating gels were used for most of the SDS-PAGE experiments carried out in this study.

To prepare 2 polyacrylamide gels, 3.36ml of 30%:0.8% (w/v) acrylamide/N,N-methylene bisacrylamide solution was mixed with 2.49ml of 1.5M Tris-HCl (pH 8.8), 50µl of 20% (w/v) SDS, 50µl of 10% (w/v) APS and 4ml of distilled water. Polymerisation was initiated by the addition of 10µl of TEMED, at which point the solution was pipetted immediately into each gel sandwich to approximately 1.5cm from the top of the smaller plate. A thin layer of

water was added on top of the separating gel to eliminate the meniscus. After polymerisation (15-20 minutes) the water was removed by inverting the apparatus and the remaining water collected with paper tissue. A comb was slotted between the plates, and 2 volumes of stacking gel were prepared by mixing 835µl of 30%:0.8% (w/v) acrylamide/N,N-methylene bisacrylamide solution with 1.25ml of 1M Tris-HCl (pH 6.8), 25µl of 20% (w/v) SDS, 25µl of 10% (w/v) APS and 2.86ml of distilled water. The polymerisation was initiated by the addition of 10µl of TEMED at which point the solution was immediately pipetted through the gaps in the comb to fill up the chamber.

2.13.3 Loading of the Samples

The gel sandwiches were removed from the casting stand and the combs carefully removed so as not to disrupt the wells. Distilled water was sprayed into the well and any polymerised gel obstructing the wells was removed with a syringe. The gel sandwiches were then inserted into the inner cooling core, according the operation manual. The apparatus was then lowered into the buffer chamber of the mini-PROTEAN II cell and 4 cm of running buffer (0.1% (w/v) SDS) was added. The upper buffer chamber was completely filled with the same running buffer, at which point the samples were loaded into the wells at a concentration of 10µg and run alongside 7.5µl of a pre-stained SDS molecular weight markers. The gels were then run at 100v to ensure the maximum sample resolution and the straightest migration pattern. The dye front from the sample buffer in each well was allowed to migrate until it began to exude from the bottom of the gel sandwich.

2.13.4 Transfer of the Proteins

Once the proteins had been separated by gel electrophoresis, they were transferred to PVDF membrane (polyvinylidene fluoride) using the trans-blot semi-dry transfer Semi-Phor apparatus from Hoefer Scientific Instruments . The transfer of proteins from the gel to PVDF membrane was carried out using a 3 buffer system as follows: four pieces of Whatmann 3MM paper (6cm x 9cm) were soaked in anode buffer 1 (0.3M Tris-HCl and 20% (v/v) Methanol). This stack was taken out of anode buffer 1 and the excess buffer squeezed out. The paper was placed onto the anode of the Semi-Phor apparatus. Two more pieces of Whatmann 3MM paper were soaked in anode buffer 2 (25mM Tric-HCl and 20% (w/v) Methanol), the excess

buffer squeezed out and the pieces of paper placed on top of the anode buffer 1-soaked pieces. A piece of PVDF, pre-soaked in 100% methanol and rinsed in water was added to the stack. When this was complete, the separating gel which was removed from the gel sandwich and placed on to the PDVF membrane. Finally 4 more Whatmann 3MM papers were soaked in cathode buffer (25mM Tris-HCl, 20% (v/v) Methanol and 40mM 6-amino-n-caproic acid) and placed on top of the separating gel. A glass rod was then rolled over the stack in order to remove any bubbles which would interfere with the transfer process. The Semi-Phor apparatus was assembled and the proteins transferred from the gel to PVDF for 90 minutes at 80mA/cm² gel. The efficiency of the transfer of the proteins was determined by staining the gels overnight with a non-specific protein stain containing Coomassie blue (40% (v/v) methanol, 10% (v/v) acetic acid, 0.2% (w/v brilliant blue R-250) at room temperature. Excess stain was then removed and discarded and replaced with destaining solution (40% (v/v methanol, 10% (v/v) acetic acid). Appropriate transfer would leave the gel with virtually no protein. The PDVF membrane on the other hand can be incubated in Ponceau S stain (in 5% TCA) for approximately 5 minutes, showing the protein, indicating correct transfer. The PVDF was then washed several times in TBS-Tween (50mM Tris HC pH 7.5-8, 150mM NaCl, 0.5% (v/v) Tween 20) to remove any excess stain.

2.13.5 Immunodetection

Following transfer, the proteins on the PVDF were fixed by using 0.05% glutaraldehyde for 10 minutes at room temperature. Fixing minimised loss of protein during washes and allowed for re-probing without significant loss of the protein. The membrane was then washed 6 times for several minutes in TBS-Tween before being cut at specific points respective to the proteins of interest. With the help of the SDS molecular weight standards, the PVDF membrane was cut into strips containing a molecular weight range specific for a particular protein. Once this was done, the strips were incubated in 5% (w/v) non-fat dried milk powder for 1 hour at room temperature on a rocking table. This step was done to block the background of the PVDF membrane with protein so that non-specific binding of the antibodies was reduced. Following this blocking stage, the PDVF was briefly washed in TBS-Tween. Antibodies to the protein of interest were then incubated with the appropriate PVDF strips at the concentrations set out in Table 2.13.5a overnight at 4°C on a rocking table. Following primary antibody incubation, the PVDF strips were washed 3 times in TBS-Tween for 10 minutes at a time. The secondary antibody raised against the primary antibody was then

incubated with the membrane for 1 hour at room temperature on a rocking table, at the concentrations shown in the table below. Following this incubation, the PDVF strips were washed 5 times for 5-7 minutes at a time.

Table 2.13.5a. Table showing the 1° antibodies used, their size and the dilutions of 1° and 2° antibody used.

1° Antibody	Size kDa	1° Dilution	2° Antibody	2° Dilution
Caveolin	22	1:1000	Anti-Rabbit	1:2500
MHC	200	1:1000	Anti-Mouse	1:1500
iNOS	130	1:10,000	Anti-Rabbit	1:4000
GS	84	1:1000	Anti-Rabbit	1:1000
Phospho-GS	85-90	1:1000	Anti-Mouse	1:2000
AMPK	62	1:1500	Anti-Rabbit	1:2000
Phospho-AMPK	62	1:750	Anti-Rabbit	1:2000
Akt	60	1:1000	Anti-Rabbit	1:2000
Phospho-Akt	60	1:2000	Anti-Rabbit	1:2000
GSK3	51, 46	1:2500	Anti-Mouse	1:2000
Phospho-GSK3	51, 46	1:1500	Anti-Rabbit	1:2000
p38	38	1:1000	Anti-Rabbit	1:2000
Phospho-p38	38	1:750	Anti-Rabbit	1:1000
ERK	42,44	1:1000	Anti-Rabbit	1:2000
Phospho-ERK	42,44	1:500	Anti-Rabbit	1:2000
BP1	15-20	1:3000	Anti-Rabbit	1:2000
GLUT1	55	1:500	Anti-Rabbit	1:2000
GLUT4	50-63	1:750	Anti-Mouse	1:2000
PABP	80	1:5000	Anti-Rabbit	1:2000
Actin	40	1:5000	Anti-Mouse	1:5000

Determination of the antibody concentration was calculated by running a sample of C2C12 cells (10µg/well) on a 10% polyacrylamide gel against the SDS molecular weight standards. The PVDF was cut into strips and incubated with different combinations of primary and secondary antibody concentrations. The combination that gave the clearest signal was used for antibody incubations. In addition, it was important to ensure that the band density increased in a linear fashion relative to protein, to allow more accurate determination of small changes in the amount of protein. Protein samples were loaded on a gel in increasing amounts and subjected to the optimal antibody concentration. The density of the resulting bands was determined using ImageJ (described in Section 2.13.8); these results are displayed below.

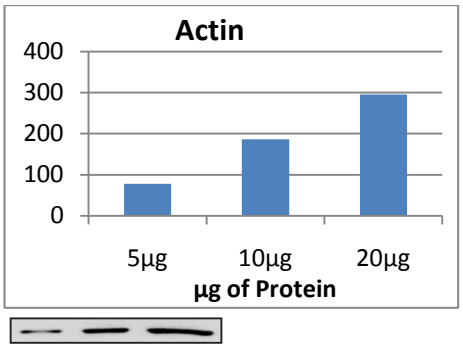

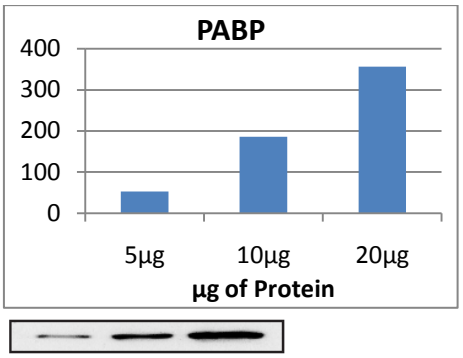

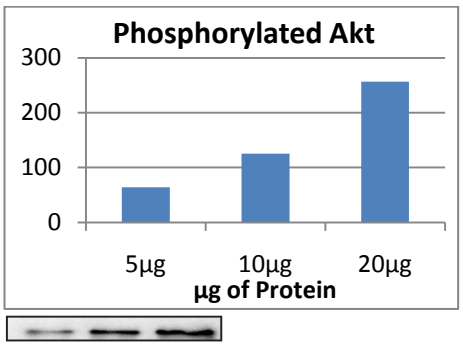

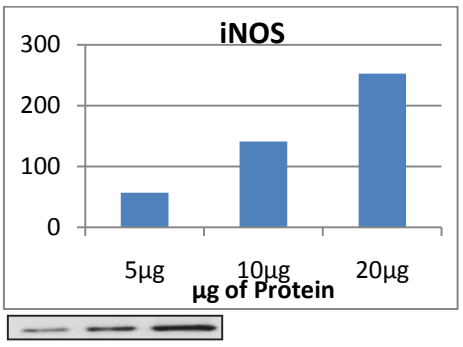

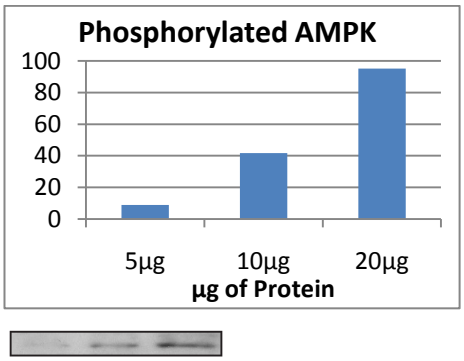

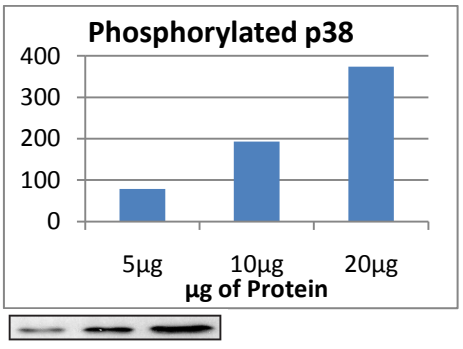

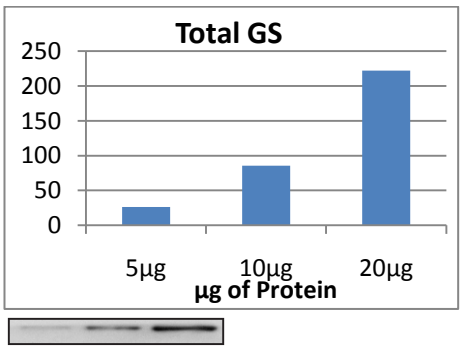

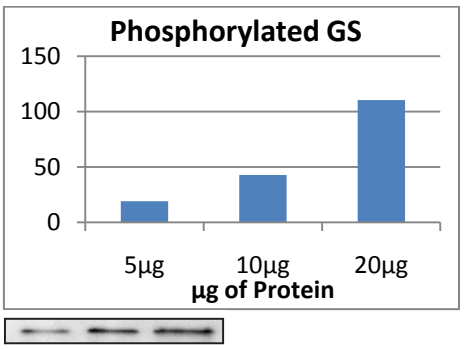

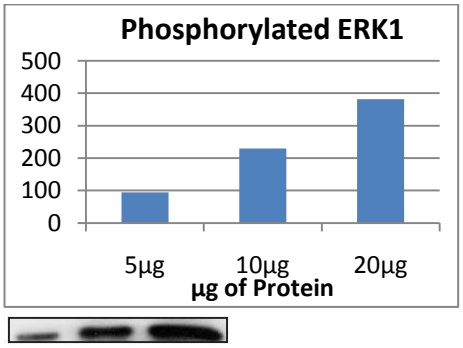

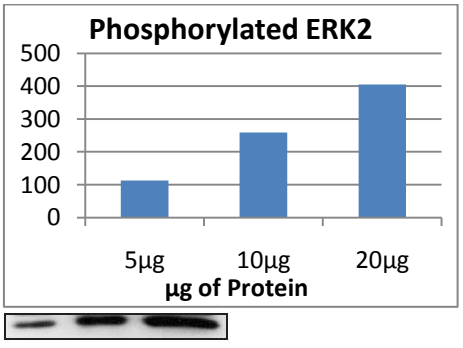

Table 2.13.5b. Bar charts showing the increase in optical density of the bands as protein levels increase (5, 10, and 20µg) along with the Western blot.

2.13.6 Western Blot Detection Using ECL

The ECL development solution was made up such that there was 1ml/PDVF membrane, the ratios of the components from the ECL solution were as follows: 1ml of Luminol (0.5mg/ml 5-amino-2,3-dihydro-1,4-phthalazinedione), 10µl of enhancer (11µg/ml parahydroxy-coumaric acid in 0.1M Tris-HCl pH6.8), and 3.1µl of 3% hydrogen peroxide. The PVDF membrane, incubated with the horseradish peroxidase-conjugated secondary antibody, was placed on a piece of Saran wrap and the ECL solution applied for 1 minute. Excess buffer was removed from the membrane on a piece of tissue and the membrane transferred to a second piece of Saran wrap. This second piece of Saran wrap was used to form an envelope around the membrane, taking care not to introduce creases, and it was placed in a cassette with the proteins facing up. In the dark room a sheet of X-ray film was placed on top of the membrane and the cassette closed. Following exposure the film was developed immediately.

2.13.7 Re-probing the Membrane

To eliminate differences in cell loading and transfer, the same membrane was used for detection of several different proteins by stripping and re-probing the membrane. Following detection using ECL, the membrane was incubated for 45 minutes in stripping buffer (2% SDS, 100mM mercaptoethanol, 62.5mM Tris-HCl pH 6.8) in a 50°C water bath, to remove both the primary and secondary antibodies. The PVDF membranes were then washed 6 times in TBS-Tween for 5 minutes on a rocking table before being blocked in non-fat dried milk powder and then re-probed with a different primary antibody.

2.13.8 Analysis of Western Blots

The developed X-ray film was scanned, and the densities of the band determined using ImageJ. An average density of each band was obtained by determining the density 3 times. The density was then expressed relative to the loading control (Actin or PABP) on the respective gel, and this ratio was then expressed relative to the control well.

2.14 Statistical Analysis

Statistical analysis was carried out using a Student's two tailed, paired t-test in Microsoft Excel. Significance is indicated throughout the results section as follows:

* = $p < 0.05$,

** = $p < 0.01$

*** = $p < 0.001$

Chapter Three – Effects of LPS plus Pro-Inflammatory Cytokines on Nitric Oxide Production and Glycogen Synthesis in C2C12 Myocytes

3.1 Introduction

As discussed in Section 1.6, skeletal muscle represents roughly 40% of total body weight, and it contains the largest store of glycogen in the body (Jensen 2009). This together with the fact that it stores much of the glucose ingested after a meal, makes skeletal muscle have a pivotal role in carbohydrate metabolism, and thus a necessary tissue to address if looking at the potential consequences LPS plus cytokines may have on carbohydrate metabolism. As a result there has been research into the effects of LPS, inflammatory mediators, or the combination of the two, on various aspects of glucose metabolism in skeletal muscle cells (Lee et al. 1987; Virkamaki and Ykijarvinen 1994; Vary et al. 1995; Begum and Ragolia 1996; Lang et al. 1996a; Bedard et al. 1997; Furnsinn et al. 1997; Ciaraldi et al. 1998; Halse et al. 2001; Crossland et al. 2008). Nevertheless there is a lack of studies specifically looking at skeletal muscle glycogen synthesis under endotoxic or pro-inflammatory conditions. One study of human primary myotubes reported that TNF-α treatment for 2 days failed to significantly affect basal glycogen synthesis, while after 5 days of treatment there was a small but significant downregulation (Halse et al. 2001). A lot of research is available regarding the insulin-resistant phenotypes expressed on glycogen metabolism during inflammatory disorders (Lang et al. 1990; Lang 1992; Hotamisligil et al. 1994; Virkamaki and Ykijarvinen 1994; Fan et al. 1996; Kroder et al. 1996; Ranganathan and Davidson 1996; Carlson 2004; Ueki et al. 2004; Plomgaard et al. 2005; Lorenzo 2008; Feve and Bastard 2009). Endotoxin treatment in rats for 300 minutes, or TNF-α treatment in L6 myotubes for 60 minutes was reported to inhibit insulin-stimulated glycogen synthesis (Virkamaki and Ykijarvinen 1994; Begum and Ragolia 1996), while TNF-α treatment (for 30 minutes, 6 hours and 24 hours) in isolated rat skeletal muscle failed to affect insulin signalling regarding glycogen synthesis (Furnsinn et al. 1997).

Due to these discrepancies and lack of studies regarding skeletal muscle glycogen synthesis under endotoxic conditions, the work presented in this chapter sought to elucidate whether or not LPS plus cytokines had an effect on basal and insulin stimulated skeletal muscle glycogen synthesis. With these results, the subsequent chapters follow on focusing on specific regulatory steps within the glycogen metabolic pathway. The method used in this chapter to determine glycogen synthesis involves the incorporation of [U-^{14}C]-glucose into glycogen. The cells were first treated for 18 hours as described in Section 2.2.5 (unless specified differently in the Section) before being solubilised and used for the determination of glycogen synthesis, as described in Section 2.6.

3.2 Effect of LPS plus Cytokine Treatment on Protein Content, Cell Viability and Nitric Oxide Levels in C2C12 Myocytes

3.2.1 Protein Content

Some cells grown on plates do not proliferate, such as hepatocytes, which tend to be seeded at a consistent density. C2C12 myoblasts on the other hand are immortal so keep growing. As a result it is imperative to measure protein levels in both myoblast and myotube experiments under different treatment conditions in order to ensure consistency amongst the metabolic determinations.

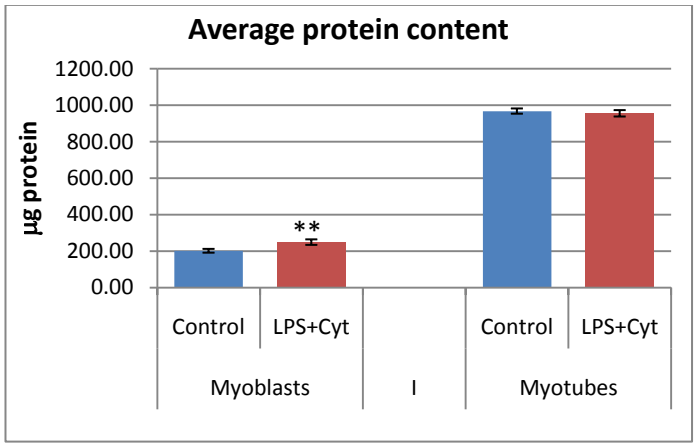

Fig. 3.2.1a. Average µg of protein present per plate in control and LPS plus cytokine treated myoblasts/myotubes. Cells were treated as described in 2.2.5. The results shown are the mean µg of protein ± SEM from 45 determinations from 7 independent experiments (myoblasts) and 36 determinations from 6 independent experiments (myotubes).
Statistical significance is as described in Section 2.14.
* = Significance from respective control

Figure 3.2.1a shows the average levels of protein per well in a 6-well plate from myoblast and myotube experiments. It is therefore not surprising that myotubes had over 4 fold more protein than myoblasts since they are seeded at a higher density in the first place as described in Section 2.2.1. In addition differentiation brings about the increased synthesis of mature muscle proteins as well as other metabolic proteins (Wahrmann et al. 1973; Halse et al. 2001; Al-Khalili et al. 2004; Frost et al. 2004). The difference in protein content between myoblasts and myotubes is in contrast with another study that also looked at protein content in C2C12 myoblasts and myotubes but reported that myotubes had just under 2 fold more protein than myoblasts (Langen et al. 2001). However, the myoblasts were left to grow for 72

hours instead of 48 hours (as done above), and in addition the study does not specify how many cells were plated out, making it difficult to compare data.

LPS plus cytokines had no effect on protein levels in myotubes, but induced a significant 24% increase in total protein in myoblasts. The myoblast results correlate with two in vitro studies using C2C12 myotubes where a 24 hour treatment with 10ng/ml (Plaisance et al. 2008) or 100ng/ml of TNF-α (Alvarez et al. 2001) significantly increased protein content. In contrast to the results shown above however, C2C12 cells and primary cultures from rat skeletal muscle were treated with TNF-α (6ng/ml) which directly induced skeletal muscle protein loss (Li et al. 1998). Indeed, TNF-α used to be known as cachectin, for its effects on muscle protein degradation (Cerami and Beutler 1988; Tracey et al. 1988). Despite this, in another study primary skeletal muscle cells taken from caecal ligation and puncture (CLP) treated rats, showed that the sepsis-mediated proteolysis symptom was regulated by glucocorticoids, which could explain why protein loss was not observed in the results presented above (Tiao et al. 1996).

Low levels of TNF-α (0.05 – 0.2ng/ml) are reported to promote myogenesis in C2C12 cells (Chen et al. 2007; Donati et al. 2007), suggesting an explanation for the increased protein content observed in the myoblasts above. However in contrast to this, another study using C2C12 cells noted that levels as low as 0.01ng/ml of TNF-α interfered with protein synthesis and muscle cell development (Broussard et al. 2003). The levels of TNF-α added in this study were 2ng/ml, which according to these studies is high enough to inhibit differentiation, making it unlikely that the LPS plus cytokine treatment induced myogenesis.

3.2.2 Ethidium Homodimer-1 Cell Viability Assay

NO and its derivatives are highly reactive. As a result, a notably important characteristic induced by sepsis is the potential damage to local host tissue. This is brought on by the excessive production of NO and reactive oxygen species (ROS) which has been shown to be produced by a variety of host tissues other than the macrophages (Titheradge 1999). In addition to this detrimental effect, it is well established that pro-inflammatory cytokines such as TNF-α can bring about apoptosis or necrosis (Camussi et al. 1991; MacEwan 2002). Due to this, when researching the effects of LPS or cytokines on any tissue, one must account for any cell death, in order to avoid spurious results. The Ethidium homodimer-1 (EthD-1) viability assay was performed (as described in Section 2.2.4) on cells after the 18 hours of LPS plus cytokine treatment and compared to the results from untreated cells (Markovits et al. 1979).

	Control (% viable cells)	LPS + Cytokine (% viable cells)
Myoblasts	80 ± 3%	82 ± 1%
Myotubes	78 ± 8%	79 ± 6%

Table 3.2.2a. Ethidium Homodimer cell viability assay results showing the amount of viable cells on the cell culture plates from control and LPS plus cytokine treated cells. Cells were treated as described in Section 2.2.5 and then the viability assay was carried out. The results shown are the mean viable cells ± SEM from 18 determinations from 3 independent experiments

The EthD-1 assay shows that the viability of the cells treated with LPS plus cytokines was not significantly different to the viability of control cells ($p = 0.22$ for myoblasts and $p = 0.45$ for myotubes). In accordance with this, despite using slightly different parameters, a study using 7-day old C2C12 myotubes found that a 48 hour incubation with TNF-α (1-40ng/ml) and IFN-γ (10-20ng/ml) did not induce apoptosis (Tolosa et al. 2005). What the results indicate is that any observed effects due to LPS plus cytokine treatment for 18 hours were not due to changes in cell viability.

3.2.3 Nitric Oxide Levels

Nitrite and nitrate are stable derivatives of NO and their determination together indicate the level of NO produced (the combination of the two is referred to as NOx). Due to the importance of NO in bringing about symptoms associated with sepsis, NO levels were measured in each experiment, both as a diagnostic method to determine the extent of the response following treatment and also to determine the correlation with changes in carbohydrate metabolism. The assessment of NO production is an important factor to consider, as not only does it display the extent of the response to the LPS plus cytokines, but it also justifies the model.

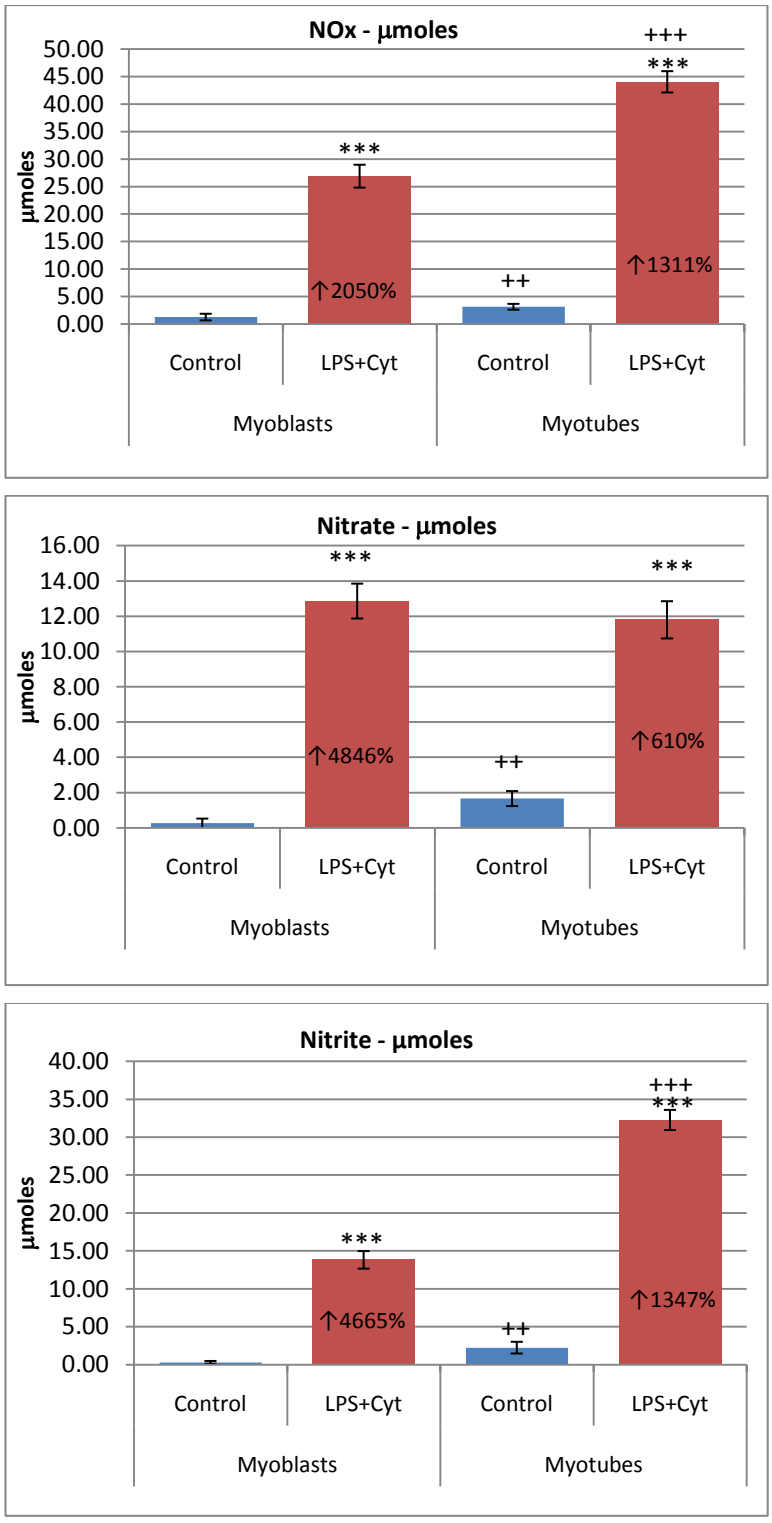

Fig 3.2.3a-c. The effect of LPS plus cytokine treatment on the level of NOx, Nitrite, Nitrate in µmoles. Cells were treated as described in Section 2.2.5. The results shown are the mean µmoles of product in the medium ± SEM from 29 determinations from 5 independent experiments (myoblasts and myotubes) Statistical significance is as described in Section 2.14
* = Significance from respective control
+ = Significance from corresponding treatment in myoblasts

Fig 3.2.3a-c displays the mean µmoles of NOx, nitrite and nitrate in the medium present in the cell culture plate. In myoblasts, the treatment caused a significant (2050%) increase in levels of NOx. In myotubes there was a significant (1311%) increase in NOx levels which were also significantly higher (65% more) than the levels produced in myoblasts. The

percentage stimulations induced by the LPS plus cytokine treatments were consistently and significantly higher in the myoblasts than in the myotubes despite the significantly higher levels of NOx and nitrite produced by the myotubes. However this is due to higher residual levels in the control wells of myotubes compared to the myoblast control wells. Nitrate levels between myoblasts and myotubes were not significantly different (p = 0.22). Nitrate production comprised only 27% of the total NOx in myotubes, the remaining 73% was in the form of nitrate. On the other hand myoblasts had equal amounts of nitrite (51%) and nitrate (48%). This indicates a difference in NO metabolism between both myocyte preparations, which signifies a difference in the micro-environmental redox states (Kelm 1999).

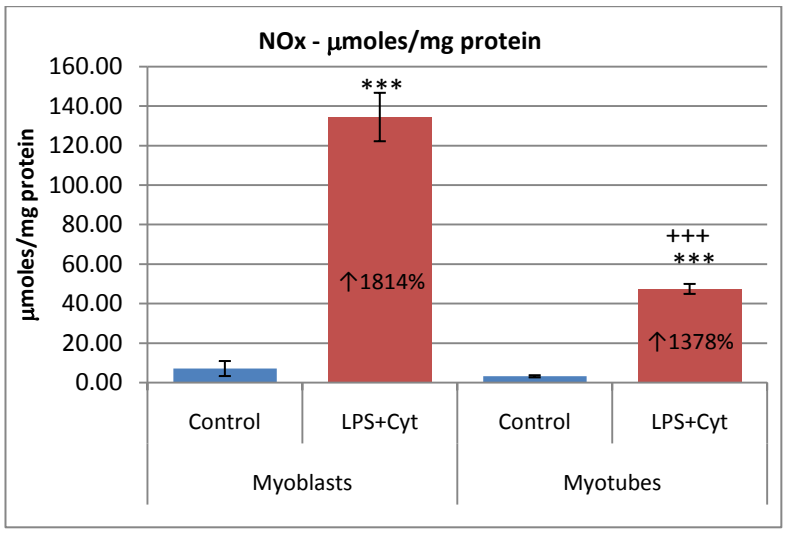

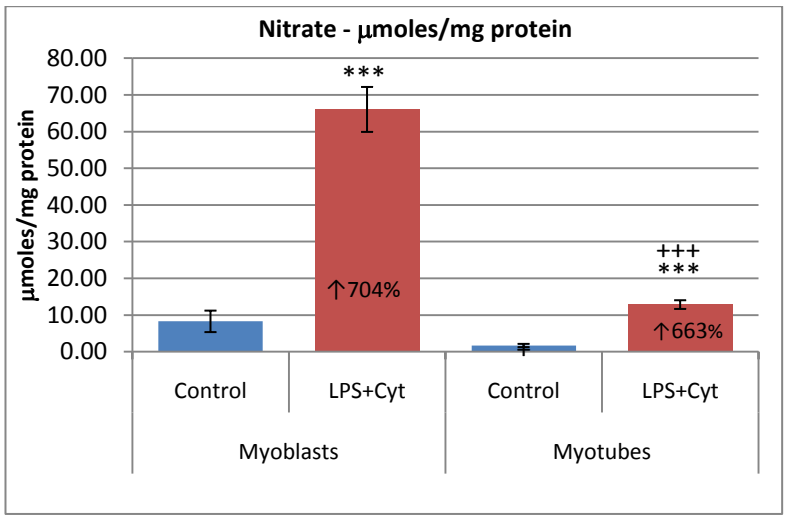

Fig 3.2.3d-f. The effect of LPS plus cytokine treatment on the level of NOx, Nitrate and Nitrite in µmoles/mg protein. Cells were treated as described in Section 2.2.5. The results shown are the mean µmoles of product in the medium/mg protein ± SEM from 29 determinations from 5 independent experiments (myoblasts and myotubes) Statistical significance is as described in Section 2.14
* = Significance from respective control
+ = Significance from corresponding treatment in myoblasts

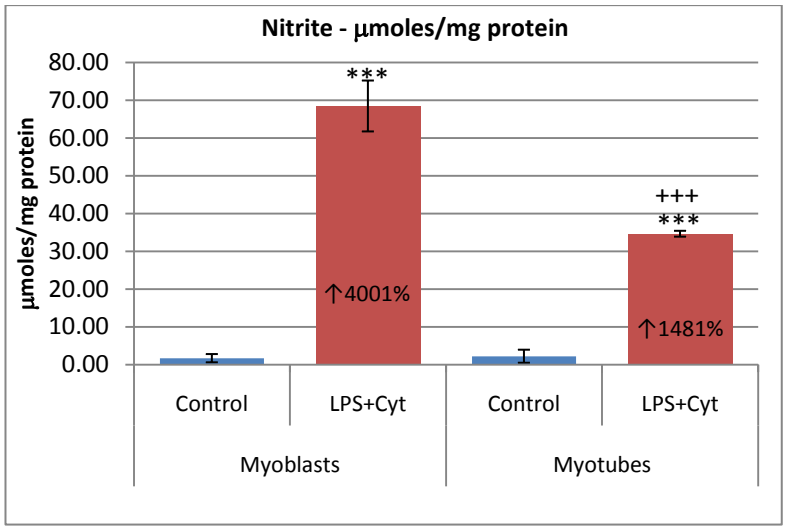

Figure 3.2.2d-f displays the levels of nitrite, nitrate and NOx produced by the cells relative to the amount of protein on the plate, a figure that is more appropriate for in vitro studies. The figure shows that myoblasts produced significantly more nitrite (100%), nitrate (415%) and NOx (183%) than myotubes, contrasting from the previous figure which showed almost the opposite relationship. The high level of protein present on the myotube plates was responsible for reversing these relationships. As described in Fig 3.2a, myotubes had over 4-fold more protein than myoblasts. Moreover, during differentiation, myocytes undergo drastic changes in protein expression, where increases in muscle fibre proteins occurs (Halse et al. 2001; Al-Khalili et al. 2004; Frost et al. 2004). This has the effect of under estimating the relative levels of NOx released in the myotubes compared to the myoblasts, therefore more NO was potentially produced in the myotubes. The myoblasts nitrite results displayed above (0.105μmol/mg) are in line with an in vitro study using L6 myoblasts treated with IL-1β (50ng/ml), IFN-γ (10ng/ml) and TNF-α(20ng/ml) for 24h which resulted in 0.125μmol/mg of nitrite (Adams et al. 2002). Interestingly Williams et. al. found that both myoblasts and myotubes produced equal amounts of nitrite (μmoles), and had equivalent percentage stimulations induced by the treatment (Williams et al. 1994), however the results displayed are in μmoles, without considering the differing amounts of cells on the plates between myoblasts and myotubes.

The measurement of NOx was carried out for each experiment presented in this thesis so as to consistently ensure a positive response as well as justifying the use of the results. In order to confirm the production of NO was indeed from the inducible form of the NOS enzyme, an antibody against iNOS was used to probe for the presence of the expressed

protein by SDS-PAGE and Western blotting (as described in Section 2.13). In addition this confirmed the difference in expression between both myocyte preparations.

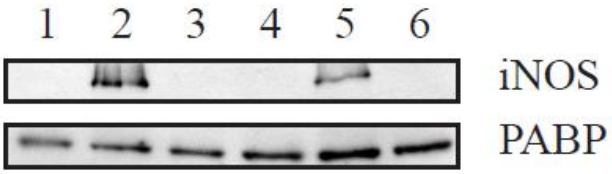

Fig. 3.2.3g. Western blot showing level of iNOS plus its loading control (PABP). Visualised using ECL, iNOS band runs at 130KDa. Myotubes 1-3, myoblasts 4-6.
1=Control, 2=LPS+Cytt, 3=Insulin, 4=Control, 5=LPS+Cyt, 6=Insulin

Figure 3.2.3g displays the level of iNOS expression in myotubes and myoblasts in control and insulin stimulated cells as well as after 18 hours of LPS plus cytokine treatment. It is clear that iNOS was only expressed in the cells treated with LPS plus cytokines. In addition, myotubes expressed a significantly higher amount of iNOS following the treatment compared to the myoblasts, suggesting that more NO was produced in the myotubes relative to the myoblast experiments, confirming the speculation that the significantly higher levels of protein in the myotubes caused an under estimation of NOx levels. These results are in contrast with the suggested claim that iNOS mRNA and protein expression in C2C12 myocytes was similar between myotubes and myoblasts between 0 and 6 hours following LPS treatment (Frost et al. 2004). The experimental conditions used by Frost et. al. were different however; the C2C12 myocytes from the experiments presented in this chapter were not only treated with LPS, but with 3 cytokines as well, and it has been well established that TNF-α, IFN-γ and IL-1β can also regulate iNOS expression (Kilbourn et al. 1997; Titheradge 1999; Schroder et al. 2004). In addition Frost et. al. simply observed the first 6 hours of stimulation, whereas the expression levels of iNOS displayed above were determined after 18 hours of LPS plus cytokine stimulation. Despite these discrepancies, the results presented in this section are in line with the general consensus that NO levels are significantly elevated in cells in response to LPS plus cytokines.

3.3 Effect of LPS plus Cytokine Treatment on Glycogen Synthesis in C2C12 Myocytes

Before using the assay to address the question of whether LPS plus cytokines affect glycogen synthesis, a time-course of glycogen synthesis was done in the presence and absence of LPS plus cytokines in order to ensure that synthesis was linear over the period at which the experiment would be carried out.

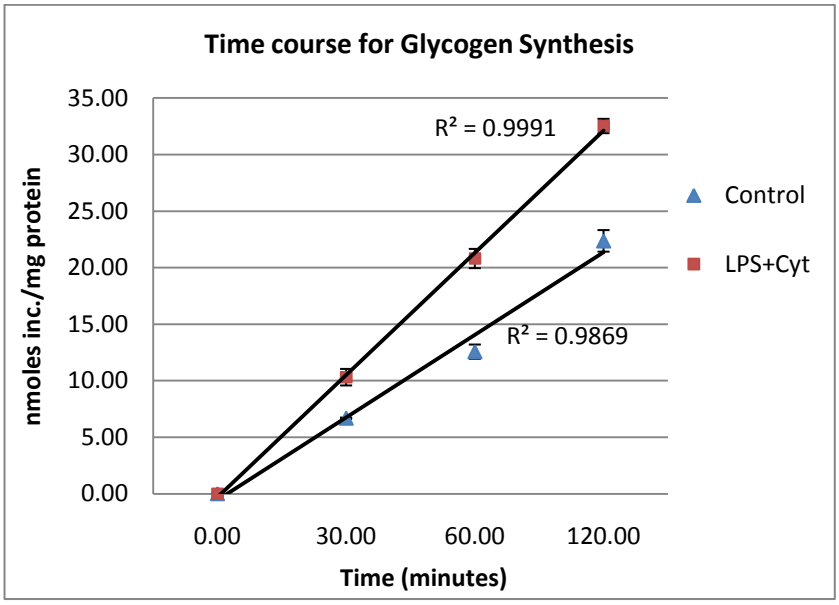

Fig 3.3a. Time-course for the incorporation of [U-^{14}C] glucose into glycogen under basal and LPS plus cytokine treated conditions. Cells were treated as described in Section 2.2.5, then incubated with [U-^{14}C] glucose for 30, 60 and 120 minutes (as described in Section 2.6). The results shown are the mean nmoles of glucose incorporated/mg protein ± SEM from 3 determinations.

The graph shows that the incorporation of glucose into glycogen was linear over the two hours as expressed by the R^2 values which are close to 1. The LPS plus cytokine treatment induced an upregulation in glycogen synthesis, which was present at all time points measured. The percentage stimulations brought on by the treatment were 55%, 65% and 47% for the 30, 60 and 120 minute time points, respectively. As the percentage stimulations were not significantly different from each other at any time point, and the two hour incubation time improved the sensitivity of the assay due to higher incorporation of radioactive glucose into glycogen, the remaining determinations of glycogen synthesis presented were done over two hours.

3.3.1 Effect of LPS plus Cytokine Treatment on Basal Glycogen Synthesis in C2C12 Myocytes

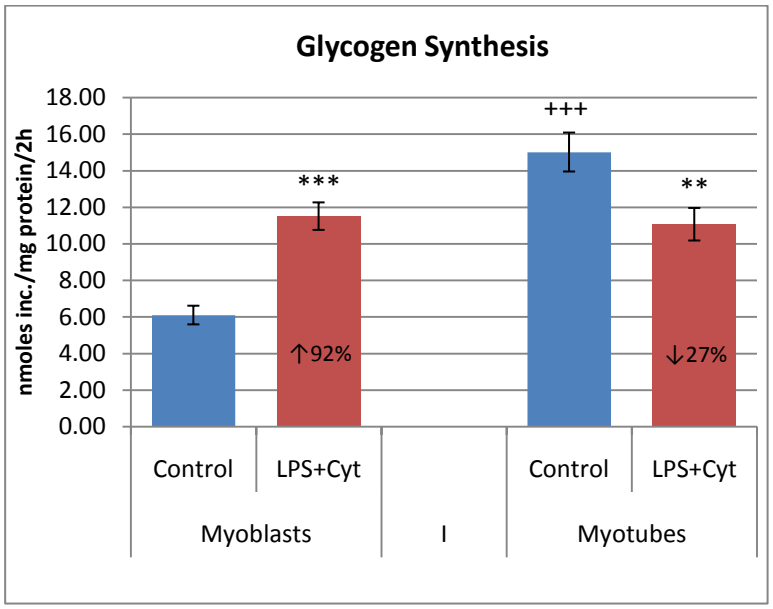

Fig 3.3.1a. The effect of LPS plus cytokine treatment on glycogen synthesis in myoblast and myotubes. Cells were treated as described in Section 2.2.5. The results shown are the mean nmoles of glucose incorporated into glycogen over two hours ± SEM from 18 determinations from 7 independent experiments (myoblasts), and 15 determinations from 5 independent experiments (myotubes).
Statistical significance is as described in Section 2.14.
* = Significance from respective control
+ = Significance from corresponding treatment in myoblasts

The data above demonstrate the effects of the LPS plus cytokine treatment on glycogen synthesis. Firstly, the basal glycogen synthetic rates were different between myoblasts and myotubes. Myotubes had a significantly higher rate of synthesis – 146% increase from that of myoblasts – despite the fact that the protein levels on the plate were significantly higher. It has been established that myocyte differentiation brings about an increase in glycogen synthase levels (Wahrmann et al. 1973; Halse et al. 2001). In addition to this, Wahrmann et. al. measured the activity of glycogen synthase in myotubes and observed it to be 2 to 5 fold higher than in undifferentiated myoblasts, while glycogen stores were 2.5 fold higher in myotubes compared to myoblasts (Wahrmann et al. 1973). This would help explain the difference in basal glycogen synthesis shown in Figure 3.3.1a. Another clear difference between both myocyte preparations is the effect induced by the treatment. Myoblast glycogen

synthesis was significantly upregulated, by 92% (or a net amount of 5.41nmoles/mg protein/2h), while in myotubes there was a significant downregulation of 27% (or 3.95nmoles/mg protein/2h) induced by LPS plus cytokine treatment. Interestingly however, glycogen synthetic rates for myoblasts and myotubes under LPS plus cytokine treatment were not significantly different ($p = 0.35$).

The basal glycogen synthetic rates presented in Fig 3.3.1a are not in accordance with rates observed in the literature, however the rates noted in the literature vary considerably. For example one in vitro study of C2C12 myotubes observed a basal rate of 22nmoles/mg/2h, which is 48% higher than the corresponding rate displayed above (Schmitz-Peiffer et al. 1999). Two groups using isolated rat soleus muscle in vitro observed basal rates of 3.5nmoles/mg/2h and 2.1nmoles/mg/2h (Furnsinn et al. 1997; Young et al. 1997). Similarly Halse et. al. measured a basal rate of 29.6nmoles/mg/2h in primary human lateral-quadricep myotubes (Halse et al. 2001), while resting human skeletal muscle (obtained from the vastus lateralis portion of the quadriceps) displayed a very low basal rate of 0.23nmoles/mg/2h (Glund et al. 2007). Azpiazu et. al. measured basal glycogen synthesis in vitro from 3 separate mouse primary muscle cells and found significant differences between muscle cell types. For example the extract from the diaphragm displayed a rate of 0.3nmoles/mg wet weight/2h, the extensor digitorum longus (EDL) extract a rate of 0.96nmoles/mg wet weight/2h; and the soleus extract showed one of 1.35nmoles/mg wet weight/2h (Azpiazu et al. 2000). Less literature is available regarding the effects of endotoxin or cytokines on the rate of glycogen synthesis. Halse et. al. treated human primary myotubes with TNF-α (5ng/ml) for 2 days but observed no change to basal glycogen synthesis, which is in contrast with either of the results presented in Fig 3.3.1a. In contrast, when TNF-α was added to differentiating myocytes for 5 days, there was a significant downregulation in glycogen synthesis – albeit small (7% decrease) (Halse et al. 2001).

3.3.2 Effects of LPS plus Cytokine Treatment on Insulin-Stimulated Glycogen Synthesis

Much attention has been focused on the impaired insulin response induced by sepsis, or certain cytokines (Shangraw et al. 1989; Virkamaki and Ykijarvinen 1994; Sugita et al. 2002; Ueki et al. 2004; Plomgaard et al. 2005). It has already been established that sepsis or inflammatory mediators impair insulin-stimulated glycogen synthesis in skeletal muscle, although the responsible factors are disputed (Virkamaki and Ykijarvinen 1995; Carlson 2004). The insulin response is a key factor regulating glucose homeostasis (Cohen 2006). In vivo

models of septic and endotoxic shock include glucoregulatory hormones which are known to fluctuate during sepsis as described in Section 1.7 (Titheradge 1999). For this reason and due to the dispute regarding the underlying causes of insulin-resistance observed in such models, in vitro models can be insightful in determining precise links between effectors and outcomes. Initially the insulin response was determined in untreated cells. The glycogen synthesis assay was carried out as normal, with or without 1µM insulin for the two hour radioactive incubation.

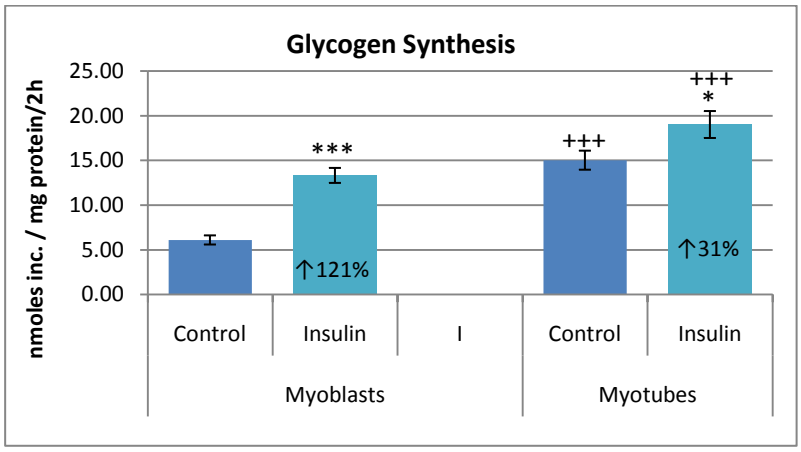

Fig3.3.2a. The effect of insulin (1µM) treatment on myoblast glycogen synthesis. The results shown are the mean nmoles of glucose incorporate into glycogen over two hours ± SEM from 18 determinations from 7 independent experiments (myoblasts), and 15 determinations from 5 independent experiments (myotubes).
Statistical significance is as described in Section 2.14.
* = Significance from respective control
+ = Significance from corresponding treatment in myoblasts

The data shows that there was a significant insulin response on glycogen synthesis in both myotubes and myoblasts. Insulin induced a significant 121% increase in the rate of glycogen synthesis in the myoblasts, while in the myotubes insulin induced a significant 31% increase from the basal rate. The insulin response in the myoblasts was significantly higher than in the myotubes. This difference may be due to the fact that myotubes are differentiated in medium containing insulin (as described in Section 2.2.1). Although during the last 18 hours of incubation with the LPS plus cytokines the insulin is removed, so they are exposed to insulin for 3 days straight before this treatment which may activate some negative feedback mechanisms. Negative feedback responses to stimulants such as insulin or growth factors is necessary to regulate the extent and duration of stimulations (Langlois et al. 1995), however involves short times rather than 3 days of constant stimulation as is the case here with the differentiation medium for the myotubes.

The net insulin-induced rate in the myotubes – 19nmoles/mg protein/2h - was significantly higher (43% more) than that of the myoblasts – 13nmoles/mg protein/2h. Similar to the observed published rates of muscle glycogen synthesis discussed above in section 3.3.1, there are varying insulin-dependent increases in the rate of glycogen synthesis within the literature. For example treating rat L6 myotubes with 100nM insulin resulted in a 40% increase, which is similar to the observed insulin response in the myotubes displayed above (D'Alessandris et al. 2007). Two further studies using 100nM insulin on C2C12 myotubes noted a significant (100%) upregulation of glycogen synthesis (Schmitz-Peiffer et al. 1999; Cazzolli et al. 2002). These results are more akin to the myoblast insulin-dependent response in Figure 3.3.2a rather than that of the myotubes despite the fact that both cited experiments also used C2C12 myotubes. Nevertheless, Cazzolli et. al., using the exact same conditions in independent experiments, reported an insulin-dependent 69 and 175% increase in glycogen synthesis (Cazzolli et al. 2002). This emphasises the potential variability when measuring metabolic rates, even when done under identical conditions.

One interesting study conducted by Azpiazu et. al. used 3 different skeletal muscle portions of mice, and showed 2 very different insulin responses with 1000μU/ml of insulin (Azpiazu et al. 2000). Isolated diaphragm displayed an insulin-dependent increase of 2166%, whereas isolated EDL and soleus responded to the same insulin concentration with a 300% increase in glycogen synthesis (Azpiazu et al. 2000). Therefore depending on the experimental conditions and the muscle type used, various degrees of insulin responses can be observed; even under the same conditions. Once the insulin response was determined within the conditions presented above, the effect of insulin on LPS plus cytokine treated myocytes was tested.

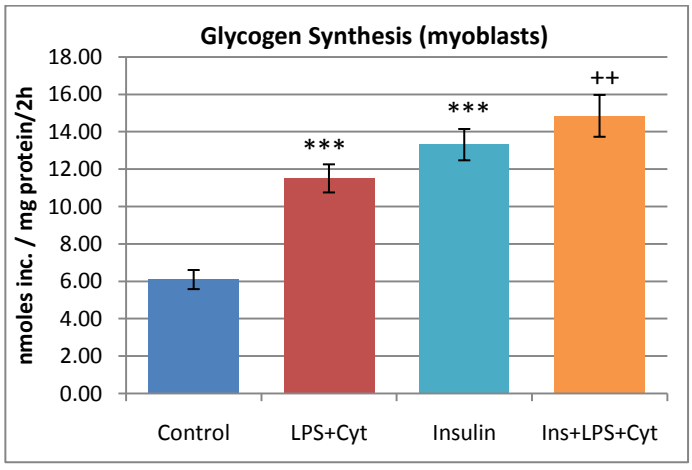

Fig3.3.2b+c. The effect of LPS plus cytokines on the insulin response on glycogen synthesis. Cells were treated as described in Section 2.2.5. The results shown are the mean nmoles of glucose incorporated into glycogen over two hours ± SEM from 18 determinations from 7 independent experiments (myoblasts), and 15 determinations from 5 independent experiments (myotubes).
Statistical significance is as described in Section 2.14
* = Significance from control
+ = Significance from LPS+Cyt
° = Significance from Insulin

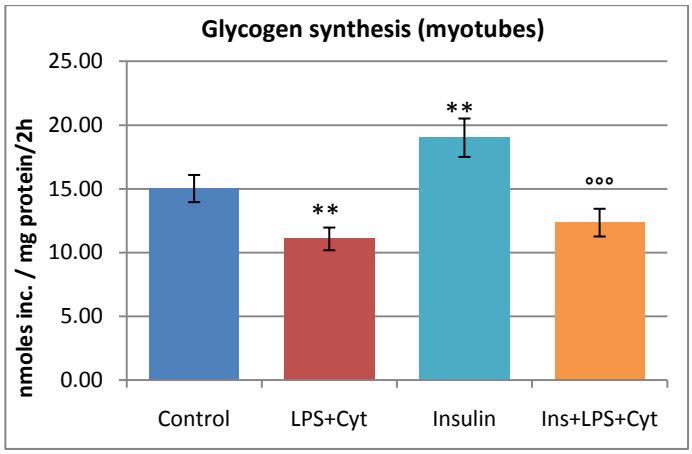

This Fig 3.3.2b+c shows the insulin stimulation of glycogen synthesis under LPS plus cytokine conditions in both myocyte types. It can be seen that there was a statistically significant increase in the insulin-stimulated glycogen synthetic rate in LPS plus cytokine treated myoblasts compared to LPS plus cytokine treated cell alone, which shows that treated cells were still responding to the insulin stimulation. However this rate was not significantly different ($p = 0.13$) from the rate induced by insulin on it's own. This was in contrast with the insulin stimulation of glycogen synthesis in LPS plus cytokine treated myotubes which was not significantly different to treated cells, but was significantly (35%) lower than the insulin-stimulated rate. The results from the myoblast experiments are interesting as they suggest that the insulin, and LPS plus cytokine stimulation of glucose storage were not additive, which could potentially imply that insulin stimulated glycogen synthesis in a manner similar to the LPS plus cytokine induced stimulation. It is known that LPS, TNF-α, IFN-γ, IL-1β, and insulin modulate common target proteins such as the MAPKs, PI-3K and Akt (Cohen 2006, Titheradge, 1999 #293; Marette 2002; Grzelkowska-Kowalczyk and Wieteska-Skrzeczynska 2009), which could explain an overlapping mechanism between the LPS plus cytokine induced effects and the insulin signalling pathway. These signalling proteins are discussed in Chapter 5. The table below analyses the figures further by displaying the average insulin effect on un-treated and treated cells. Taken together with the bar charts displayed above, a better idea of the actual effects can be elucidated.

	Control (% difference)	With LPS + Cytokines (% difference)
Myoblasts Insulin response	121 ± 16%	28 ± 3% ***
Myotubes Insulin response	31 ± 11% +++	12 ± 4% *,+++

Table3.3.2a . The average insulin effect on un-treated and LPS + cytokine treated myoblasts and myotubes. Cells were treated as described in Section 2.2.5. The results shown are the mean nmoles of glucose incorporated into glycogen over two hours ± SEM from 18 determinations from 7 independent experiments (myoblasts), and 15 determinations from 5 independent experiments.
Statistical significance is as described in Section 2.14
* = Significance from respective control
+ = Significance between myoblasts and myotubes

Table 3.3.2a emphasises further the difference in the responses to insulin between myoblasts and myotubes. The myoblasts responded to a greater extent to insulin, with a significantly higher stimulation under control conditions. Despite there being an insulin-induced increment of glycogen synthesis under LPS plus cytokine treatment in both cases, it was significantly smaller than the insulin response in untreated cells. LPS plus cytokine treatment significantly decreased the insulin response on glycogen synthesis by 77% in myoblasts and 61% in myotubes. The average increment induced by insulin in untreated cells was 7.22nmoles of glucose in myoblasts and 4nmoles in myotubes. In the presence of LPS plus cytokines this was significantly decreased to 3.35nmoles and 1.28nmoles in myoblasts and myotubes, respectively. This would indicate that the treatment impaired the insulin response on glycogen synthesis. What was interesting however, was that insulin still significantly upregulated myoblast glycogen synthesis following LPS plus cytokine treatment, which was not the case for myotubes. The results presented in this section would suggest that LPS plus cytokines impaired the myoblast insulin response due to a significantly different insulin-stimulated increase. Nevertheless since the LPS plus cytokine treatment alone upregulated glycogen synthesis, it is possible that a maximal rate may have been attained. The presence or lack of insulin resistance induced by LPS plus cytokines on glycogen synthesis in myoblasts will be further investigated in the subsequent chapters. For the myotubes however, insulin resistance was a clear result of the 18 hours LPS plus cytokine treatment.

Akin to the myotube results presented above, Begum et. al. observed a 56% decrease in insulin-stimulated glycogen synthesis after a 60 minute TNF-α (10ng/ml) treatment in cultured L6 myotubes (Begum and Ragolia 1996). Insulin resistance was observed to a slightly

lesser degree, than the results displayed above, during an in vivo treatment of rats with a bolus injection of LPS (1mg/kg). 105 – 300 minutes after LPS treatment there was a 37% decrease in insulin-stimulated glycogen synthesis (Virkamaki and Ykijarvinen 1994). However, a 30minute, 6 hour or 24 hour TNF-α treatment (up to 5nM) of isolated rat soleus muscle failed to affect insulin-stimulated glycogen storage (Furnsinn et al. 1997). Similarly, when 3-day old myotubes (obtained from lateral quadriceps in humans) were treated with TNF-α (5ng/ml) for 2 days, no change in the insulin-induced increment on glycogen synthesis was observed (Halse et al. 2001), although when TNF-α was added to the differentiating myocytes for 5 days, it impaired the insulin response to glycogen synthesis. This impairment was deduced to lie in TNF-α-dependent inhibition of a differentiation-induced upregulation of glycogen synthase, thus lowering the level of enzyme available to store glucose into glycogen (Halse et al. 2001). In contrast, Furnsinn et. al. implied that TNF-α-dependent insulin-resistance was governed by an in-direct mechanism, instead of a direct relationship between TNF-α and the skeletal muscles (Furnsinn et al. 1997). Despite the conflicting literature, the results presented in Table 3.3.2a show a clear impairment of the insulin response in myotubes which correlates with some available literature, however the situation in the myoblasts is not as clear, requiring further analysis. There are numerous suggestions for the underlying causes of LPS/cytokine-induced insulin resistance (Fan et al. 1996; Sugita et al. 2002; Ueki et al. 2004; Ghosh et al. 2007). Some of these issues will be dealt with in more detail in the next chapters, where key steps in the glycogen synthetic pathway are looked at. One other aspect to scrutinise from the data presented in Fig 3.3.2b+c is whether the cytokine effect on glycogen synthesis was altered in the presence of insulin. Myoblasts responded to LPS plus cytokines with a significantly upregulated rate of glycogen synthesis, whereas myotubes responded in the opposite way, with a significant downregulation.

	Control (% difference)	With Insulin (% difference)
Myoblasts LPS and Cytokine response	92 ± 15%	12 ± 4% ***
Myotubes LPS plus cytokine response	-27% ± 3% +++	-32 ± 7% +++

Table 3.3.2b. The average cytokine effect on basal and insulin glycogen synthetic rates. Cells were treated as described in Section 2.2.5. The results shown are the mean nmoles of glucose incorporated into glycogen over two hours ± SEM from 18 determinations from 7 independent experiments (myoblasts), and 15 determinations from 5 independent experiments.
Statistical significance is as described in Section 2.14
* = Significance from respective control
+ = Significance between myoblasts and myotubes

In the presence of insulin, LPS plus cytokine treatment still induced a significant upregulation in glycogen synthesis in myoblasts (Fig 3.3.2b+c), although the response was significantly decreased by 89%, when compared to the LPS plus cytokine stimulation induced in control myoblast cells. This table suggests that the apparent insulin-resistance could in fact be an impairment of the LPS plus cytokine-mediated stimulation of glycogen synthesis induced by insulin. Once again further analysis is required. For the myotubes LPS plus cytokines significantly downregulated glycogen synthesis (Fig 3.3.2b+c) and this was not affected by the presence of insulin as both figures displayed in the table above, -27 and -32%, were not significantly different from each other ($p = 0.22$). This could suggest that LPS plus cytokines targeted a step that was shared between myotube basal and insulin-stimulated glycogen synthesis or that the treatment targeted both pathways.

3.3.3 Role of Nitric Oxide on LPS plus Cytokine-Induced Changes in Basal Glycogen Synthesis

The NO levels released in the circulation during a systemic infection makes NO a very important potential mediator of any cellular changes observed under inflammatory conditions (Kilbourn et al. 1997; Titheradge 1999). Together with the research conducted by Young et. al. suggesting NO-dependent insulin-resistance in skeletal muscle, the effects of NO during a systemic infection has received much attention (Stadler et al. 1995; Borgs et al. 1996; Ceppi et al. 1996; Bedard et al. 1997; Smith et al. 1997; Sugita et al. 2002). Due to this, it is

indispensable to elucidate whether NO plays a role in the observations obtained. To establish this the effects of L-NAME (1mM), a competitive NOS inhibitor, was added to the medium at the beginning of the incubation period along with the LPS plus cytokines. The nitrate and nitrite levels were assayed in order to determine the efficiency of inhibition induced by L-NAME.

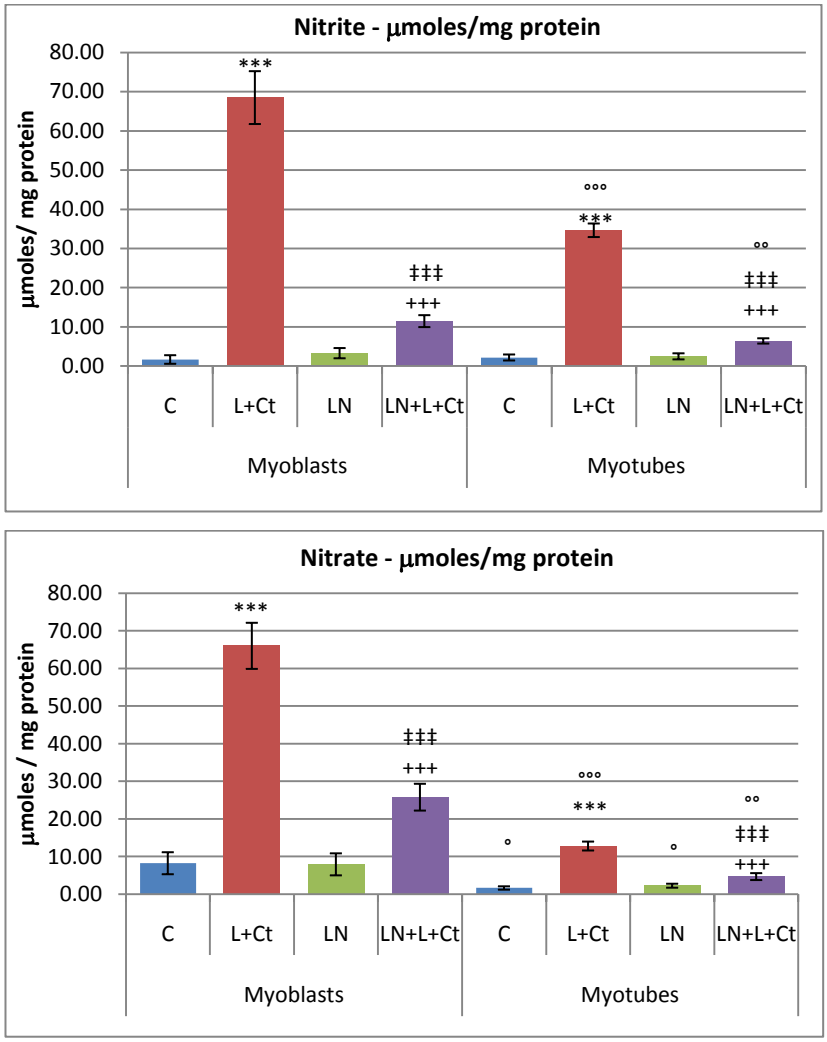

Fig 3.3.3a-c. The effect of L-NAME (1mM) on nitrite, nitrate and NOx levels. Fig: A - Nitrite; B – Nitrate; C – NOx. Cells were treated as described in Section 2.2.5. The results shown are the mean µmoles of product in the medium ± SEM from 29 determinations from 5 independent experiments (myoblasts and myotubes) Statistical significance is as described in Section 2.1
* = Significance from respective control
+ = Significance from respective LPS+Cytokine treatment.
‡ = Significance from respective L-Name treatment
° = Significance from corresponding treatment in myoblasts.
(C=Control, L+Ct=LPS+Cyt, LN=L-NAME,LN+L+Ct=L-Name+LPS+Cyt)

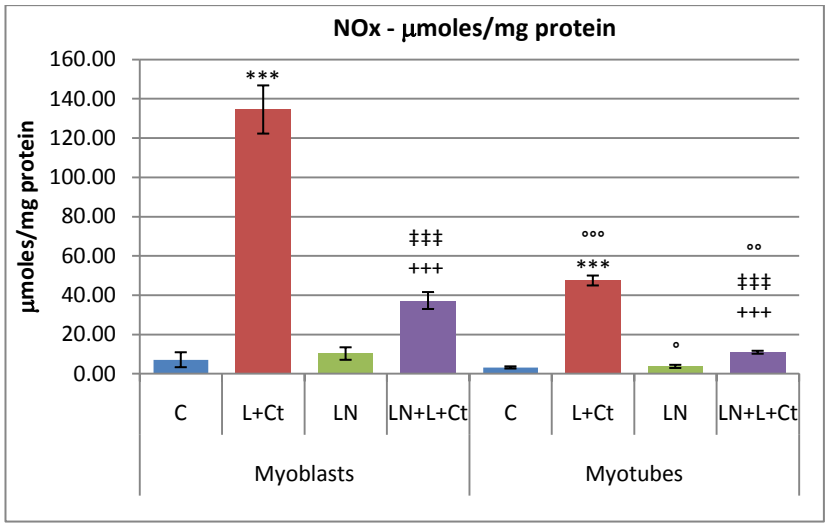

From Fig 3.3.3a-c it is clear that L-NAME significantly inhibited nitrate, nitrite and NOx production for both myocyte preparations. In myoblasts, LPS plus cytokines induced a 4000, 700 and 1800% increase in nitrite, nitrate and NOx levels, respectively. In the presence of L-NAME these figures dropped significantly to a 248, 224 and 263% increase for nitrite, nitrate and NOx levels, respectively. The same pattern was observed for myotubes where LPS plus cytokine treatment induced an increase in nitrite, nitrate and NOx levels of 1500, 664 and 1400%, respectively, whereas the presence of L-NAME significantly reduced the LPS plus cytokine-dependent induction of nitrite, nitrate and NOx to 159, 106 and 193%, respectively. L-NAME reduced nitrite levels by 57µmoles/mg protein (myoblasts) and 28µmoles/mg protein (myotubes), resulting in an 84 and 80% inhibition, respectively. Nitrate levels on the other hand were reduced by 40µmoles/mg protein in myoblasts (60% inhibition), and by 8µmoles/mg protein in myotubes (64% inhibition). Finally, total NOx production was reduced by 72% (97µM/mg protein) and 76% (36.5µM/mg protein) in myoblasts and myotubes, respectively. Interestingly the percentage inhibition induced by L-NAME was not significantly different between myoblasts and myotubes, showing that the effect of L-NAME was the same in both myocyte preparations, even if the actual concentrations of nitrite, nitrate and NOx were significantly different between myoblasts and myotubes. Despite the inhibition induced by L-NAME, it wasn't 100% effective since even in the presence of L-NAME, the LPS plus cytokine treatment significantly increased NOx, nitrite and nitrate levels compared to the control levels (with or without L-NAME). Nevertheless these results are in accordance with published data (Williams et al. 1994; Bedard et al. 1997; Khanna et al. 1999). Williams et. al. treated C2C12 myotubes with TNF-α (1ng/ml), IFN-γ (10ng/ml) and IL-1α (0.1ng/ml) for 18

hours in conjunction with L-NAME (5mM) which reduced nitrite levels by 78%. Similarly, L6 myotubes treated with TNF-α (50ng/ml), IFN-γ (500ng/ml) and LPS (10μg/ml) in the presence of 2mM L-NAME for 24 hours, resulted in a 75% decrease in NOx levels compared to treatment without L-NAME (Khanna et al. 1999). Finally, L-NAME (2mM) decreased nitrite levels by 90% in L6 myotubes treated with TNF-α (10ng/ml), IFN-γ (20ng/ml) and LPS (10μg/ml) for 24 hours (Bedard et al. 1997). Once the degree of inhibition on LPS plus cytokine-dependent NO levels induced by L-NAME was assessed, the role of NO in the treatment-induced effects on glucose incorporation into glycogen was determined.

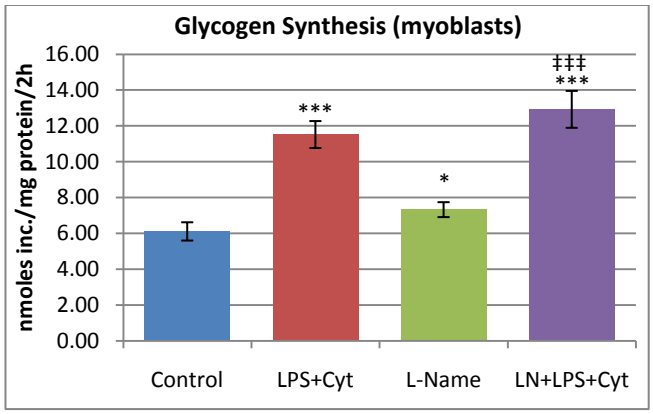

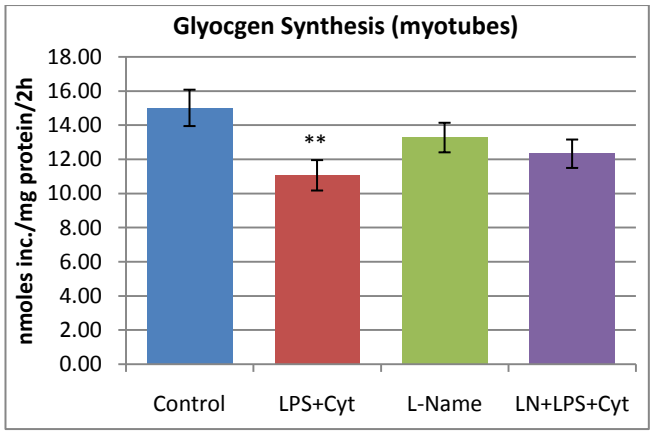

Fig 3.3.3d+e. The effect of 1mM L-NAME on LPS plus cytokine-induced changed in glycogen synthesis in myocytes. Cells were treated as described in Section 2.2.5. The results shown are the mean nmoles of glucose incorporated into glycogen over two hours ± SEM from 18 determinations from 7 independent experiments (myoblasts), and 15 determinations from 5 independent experiments (myotubes). Statistical significance is as described in Section 2.14
* = Significance from control
‡ = Significance from L-NAME

Fig 3.3.3d+e shows the effect L-NAME had on the LPS plus cytokine-induced effects on glycogen synthesis in myoblasts and myotubes. The significant 18 hour LPS plus cytokine-induced upregulation in myoblast glycogen synthesis was not altered by the presence of L-NAME, as both LPS plus cytokine-mediated increments were not significantly different ($p = 0.28$). LPS plus cytokines upregulated basal myoblast glycogen synthesis by 5.4nmoles/mg protein/2h, and by 4.9nmoles/mg protein/2h in the presence of L-NAME. The myoblast glycogen synthetic rate in the presence of L-NAME was significantly increased relative to the control basal rate, although this had no effect on the LPS plus cytokine treatment in the

presence of L-NAME as seen by the similar results obtained. In contrast, the significant downregulation of myotube glycogen synthesis induced by LPS plus cytokines was partially rescued by the presence of L-NAME. LPS plus cytokines reduced myotube glycogen synthesis by 27%, resulting in a rate of 11nmoles/mg protein/2h. In the presence of L-NAME however, LPS plus cytokines failed to significantly reduce glycogen synthesis. Although the average rate in treated cells in the presence of L-NAME was 6% lower, it was not significantly different to the rate of synthesis in the L-NAME treated myotubes ($p = 0.21$).

	Control (% difference)	With L-NAME (% difference)
Myoblasts LPS and Cytokine response	92 ± 15%	79 ± 17%
Myotubes LPS plus cytokine response	-27% ± 3% +++	-6 ± 4% ***, +++

Table 3.3.3a. The average percentage effect of LPS plus cytokines on glycogen metabolism in the presence and absence of L-NAME. Cells were treated as described in Section 2.2.5. The results shown are the means of nmoles of glucose incorporate into glycogen over two hours ± SEM from 18 determinations from 7 independent experiments (myoblasts), and 15 determinations from 5 independent experiments (myotubes). Statistical significance is as described in Section 2.14
* = Significance from control
+ = Significance from Myoblasts

Table 3.3.3a displays the average effects induced by LPS plus cytokines in the presence and absence of L-NAME, re-affirming the significant difference between the effect induced by L-NAME in myoblasts and in myotubes. In myoblasts, the LPS plus cytokine-dependent increment of 92% (or an increase of 5.4nmoles/mg protein/2h) was not significantly different from the increase induced by the same treatment in the presence of L-NAME which was 79% (or an increase of 4.99nmoles/mg protein/2h). This suggests that the LPS plus cytokine-dependent stimulation of myoblast glycogen synthesis was independent of NO. On the other hand, the LPS plus cytokine-dependent downregulation of myotube glycogen synthesis, -27% (or a reduction of 3.95nmoles/mg protein/2h), was significantly rescued (by 77%) due to the presence of L-NAME, which was then only a -6% decrease induced by the treatment (or a reduction of 0.95nmole/mg protein/2h). This latter result would suggest that the LPS plus cytokine induced downregulation of glycogen synthesis in myotubes was NO-dependent. Since

myotubes produced higher levels of NO compared to myoblasts (as discussed in Section 3.2.3), it could explain why glycogen synthesis was significantly inhibited by LPS plus cytokines in myotubes but not in myoblasts. A study that treated isolated rat soleus muscles with a NO-donor (SNP, 5 – 25mM) failed to show a NO-dependent effect on basal glycogen synthesis (Young et al. 1997), correlating with the myoblast results but contrasting with the myotube observations.

3.3.4 Role of Nitric Oxide on LPS plus Cytokine-Induced Impairment of Insulin-Stimulated Glycogen Synthesis

NO-induced insulin resistance has been suggested in the literature; two important findings suggested that: i) Akt is nitrosylated by increased NO levels, and ii) insulin receptor substrate-1 (IRS-1) is degraded by a proteasome-dependent mechanism in a NO-mediated manner (Sugita et al. 2005; Yasukawa et al. 2005). Young et. al. found that SNP (5 – 25mM) inhibited insulin-stimulated glycogen synthesis in a concentration dependent manner in isolated rat soleus muscle: 5 – 15mM inhibited the rate by 38%, whereas 20 and 25mM SNP decreased the response by 75% (Young et al. 1997). Myotubes, and possibly myoblasts, displayed an impairment of the insulin-stimulated glycogen synthetic rate, as presented in Figure 3.3.2b+c. As a result, the effect of L-NAME on insulin-resistance observed in LPS plus cytokine treated cells was addressed.

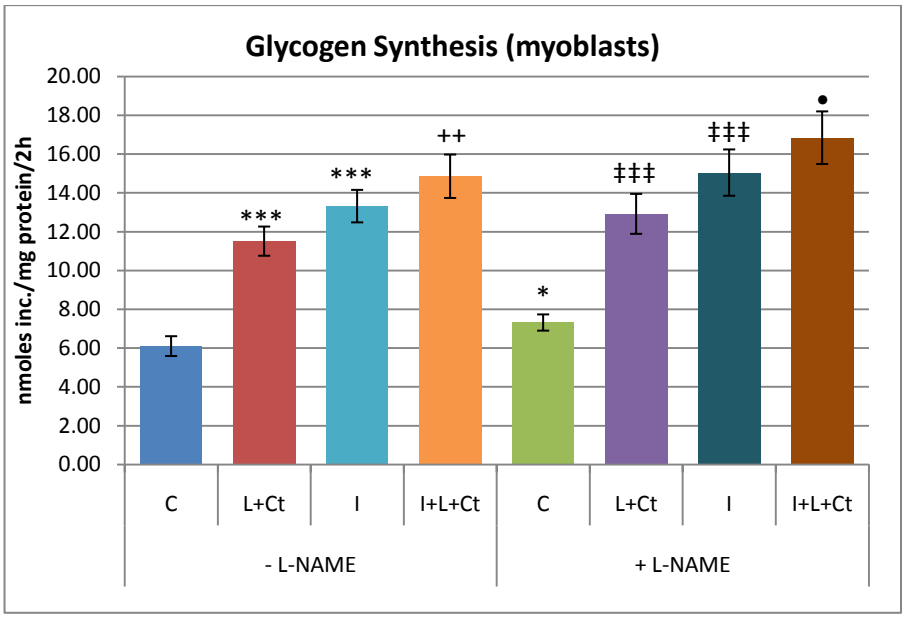

	Control (% difference)	With L-NAME (% difference)
LPS and Cytokine response	92 ± 15%	79 ± 17%
LPS plus cytokine response in the presence of Insulin	12 ± 4% <<<	13 ± 4% >>>
Insulin response	121 ± 16%	105 ± 18%
Insulin response in the presence of LPS plus cytokines	28 ± 3% ###	31 ± 3% §§§

Fig 3.3.4a and Table 3.3.4a. The effect of L-NAME on glycogen synthesis in the presence and absence of LPS plus cytokines and/or insulin in myoblasts. Cells were treated as described in Section 2.2.5. The results shown are the mean nmoles of glucose incorporated into glycogen over two hours ± SEM from 18 determinations from 7 independent experiments. (C=Control, L+Ct=LPS+Cyt, I=Insulin, I+L+Ct=Ins+LPS+Cyt)
Statistical significance is as described in Section 2.14
* = Significance from control
+ = Significance from LPS plus cytokines
‡ = Significance from L-NAME
• = Significance from LPS plus cytokines (+L-NAME)
< = Significance from LPS plus cytokine response (in the absence of insulin)
> = Significance from LPS plus cytokine response (+L-NAME, in the absence of insulin)
= Significance from insulin response
§ = Significance from insulin response (+ L-NAME)

The table and figure above shows that L-NAME had no substantial effect on any of the LPS plus cytokine-induced changes in myoblasts. The rate of glycogen synthesis induced by LPS

plus cytokines in the presence of both L-NAME and insulin (16.8nmoles/mg protein/2h) was not significantly different ($p = 0.16$) from the rate of synthesis induced by insulin in the presence of L-NAME (15nmoles/mg protein/2h). This is expressed differently in the table: the LPS plus cytokine-induced increment of glycogen synthesis in the presence of insulin, 12%, was not significantly different ($p = 0.38$) under the same conditions with L-NAME which was 13%. Both these results were significantly different to the LPS plus cytokine-induced increments in the absence of insulin, suggesting that the presence of insulin considerably impaired the treatment-induced upregulation of glycogen synthesis in myoblasts. L-NAME failed to significantly affect either the insulin response ($p = 0.24$) or the insulin response in the presence of LPS plus cytokines ($p = 0.27$). LPS plus cytokine treatment significantly lowered the insulin response from an increase of 7.2nmoles/mg protein/2h (a 121% increase), to an increase of 3.35nmoles/mg protein/2h (a 28% increase). In the presence of L-NAME this decrease was equally significant, 105% increase (7.12nmoles/mg protein/2h) in the presence of insulin down to a 31% (3.35nmoles/mg protein/2h) insulin-induced increase in the presence of LPS plus cytokines. This is in accordance with the initial results regarding the effects of L-NAME on myoblast glucose storage under LPS plus cytokine conditions presented in Fig 3.3.3d, the inhibition of iNOS had no effect on the observed insulin-induced rates presented in Fig 3.3.2b.

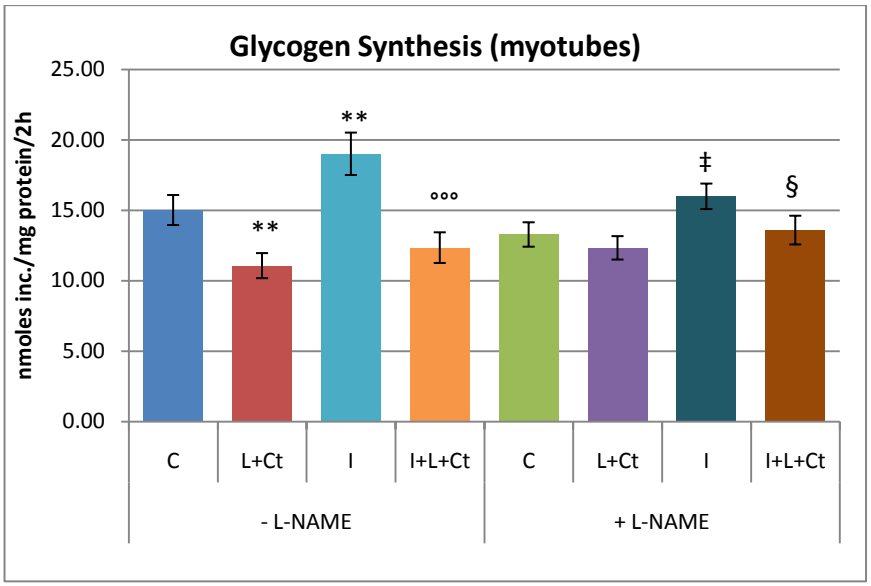

	Control (% difference)	With L-NAME (% difference)
LPS and Cytokine response	-27 ± 3%	-6 ± 4% <<<
LPS plus cytokine response in the presence of Insulin	-32 ± 7%	-15 ± 4% >, •
Insulin response	32 ± 12%	23 ± 5%
Insulin response in the presence of LPS plus cytokines	12 ± 4% #	10 ± 4% §

Fig 3.3.4b and Table 3.3.4b. The effect of L-NAME on glycogen synthesis in the presence and absence of LPS plus cytokines and/or insulin in myotubes. Cells were treated as described in Section 2.2.5. The results shown are the means of nmoles of glucose incorporate into glycogen over two hours ± SEM of 15 determinations from 5 independent experiments. (C=Control, L+Ct=LPS+Cyt, I=Insulin, I+L+Ct=Ins+LPS+Cyt) Statistical significance is as described in Section 2.14
* = Significance from control
° = Significance from Insulin
‡ = Significance from L-NAME
< = Significance from LPS plus cytokine response (in the absence of insulin)
> = Significance from LPS plus cytokine response (+L-NAME, in the absence of insulin)
• = Significance from LPS plus cytokine response in the presence of insulin
= Significance from insulin response
§ = Significance from insulin response (+L-NAME)

As described in Fig 3.3.3e, L-NAME significantly rescued the LPS plus cytokine-induced downregulation of glycogen synthesis in myotubes (rescued from -27 to -6% decrease). In the presence of insulin, the LPS plus cytokine-induced downregulation (-32%) was significantly diminished by 50% in the presence of L-NAME which was then at -15%. Interestingly however,

in the presence of L-NAME, the LPS plus cytokine-induced effect on the glycogen synthetic rate was significantly different between the presence and absence of insulin. In the absence of insulin it was -6%, whereas in the presence of insulin it was -15%. Both these results were in contrast with the myoblast data presented above in Figure 3.3.4a/Table 3.3.4a. The insulin response in the presence of L-NAME, 23% or 2.71nmoles/mg protein/2h increase, was lower but not significantly different ($p = 0.22$) than the control insulin response which was an increase of 32% or 3.99nmoles/mg protein/2h. As described in section 3.3.2, the insulin response was significantly impaired by LPS plus cytokine treatment; from a 32% increase down to a 12% increase (1.28nmoles/mg protein/2h). A similar impairment of the insulin response induced by LPS plus cytokines occurred in the presence of L-NAME as seen by the lack of significance ($p = 0.39$) between the two figures obtained: 12% in the absence of L-NAME and 10% in the presence of L-NAME. This latter result is also in line with the observations from the myoblasts presented above. Although the LPS plus cytokine-induced downregulation of the glycogen synthetic rate appeared to be NO-mediated in myotubes, the insulin-resistance induced by the treatment did not appear to be NO-mediated. This is in contrast with Young et. al.'s suggestion that NO impaired the insulin-stimulated glycogen synthetic rate (Young et al. 1997). However Young et. al. investigated this using the NO-donor SNP, which has been said to potentially create un-physiological conditions due to a rapid bolus release of NO which contrasts with the slow synthesis of NO induced by iNOS (Stamler and Meissner 2001). The results presented in this section emphasise once again the differing responses observed between myoblasts and myotubes in response to LPS plus cytokines.

3.3.5 Time-Dependent Changes in Glycogen Metabolism in Response to LPS plus Cytokines

As discussed within this chapter, the variability in the literature can often be related to the different experimental conditions, for example: cell types used; amount of LPS and/or cytokines used; the time of stimulation; as well as the common variability observed in metabolic experiments as noted by Cazzolli et. al. (Cazzolli et al. 2001). Although similar results have been shown using various amounts of these mediators, the time of incubation from one experimental design to the next can alter the level of stimulated mediators quite drastically. For example, as discussed in the introduction (Section 1.2), NFκB is an essential intracellular pro-inflammatory regulator: modulating the expression of key genes such as iNOS and pro- and anti-inflammatory cytokines (Guha and Mackman 2001; Palsson-McDermott and O'Neill

2004). Frost et. al. demonstrated using C2C12 myocytes treated with LPS that NFκB activity rose steeply after 4 hours of endotoxin stimulation and continued, albeit to a lesser degree, up until 24 hours (Frost et al. 2004). This suggests that the progression of potential responses induced by LPS and cytokines follow a cascade of events in a temporal fashion. As a result, in order to try and elucidate the times at which the observed changes in myoblast glycogen metabolism shown in this chapter occurred, C2C12 myoblasts were incubated with LPS plus cytokines for various times: 3, 6, 9, 12 and 18 hours.

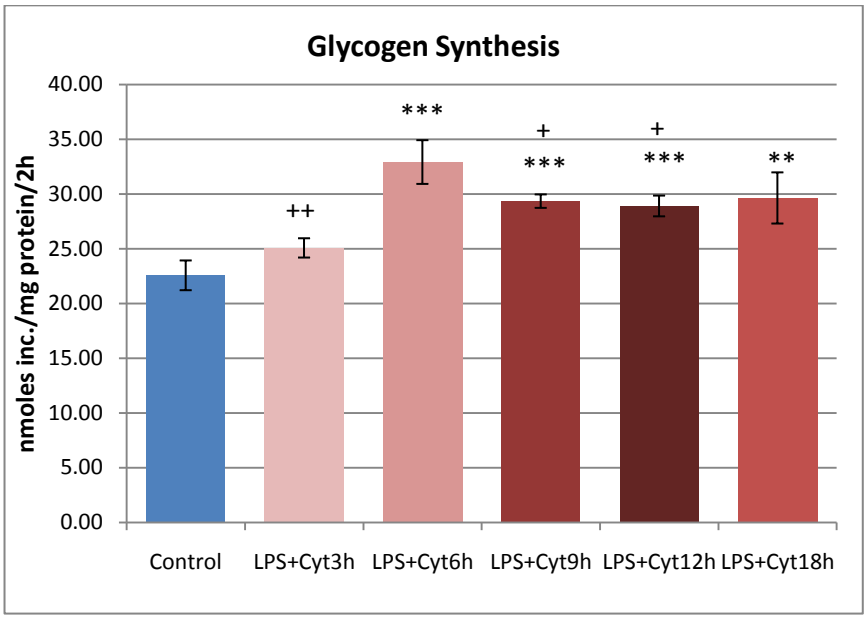

Fig 3.3.5a. The effect of varying the incubation period with LPS plus cytokine on glycogen synthesis in myoblasts. The results shown are the mean nmoles of glucose incorporated into glycogen over two hours ± SEM from 6 determinations from 2 independent experiments. Statistical significance is as described in Section 2.14
* = Significance from control
+ = Significance from LPS + Cyt 6h

Figure 3.3.5a shows the time course for the LPS plus cytokine-induced upregulation of glycogen synthesis. There was a small but insignificant (p=0.06) increase at 3 hours of treatment, while at 6 hours of treatment, the rate of glycogen synthesis was significantly increased. This increase then reduced slightly but was maintained at a significant level above the control rate. 6 hours after LPS plus cytokine treatment the rate of glucose storage rose to 49% above the control rate. This rate was significantly different to the 3, 9 and 12 hour rates as well. Despite this difference, the percentage stimulations induced at 9, 12 and 18 hours after treatment were 32%, 30% and 27% respectively, which were not significantly different from

the percentage stimulation induced by 6 hours of treatment. These results indicate that the upregulation observed in the myoblast experiments from section 3.3.1 appeared to occur with 3 hours of LPS plus cytokine incubation, was maximal by 6 hours, and stayed relatively consistent throughout the 18 hour incubation period. Varying the incubation time with LPS plus cytokines was also used to elucidate the effect on the insulin response.

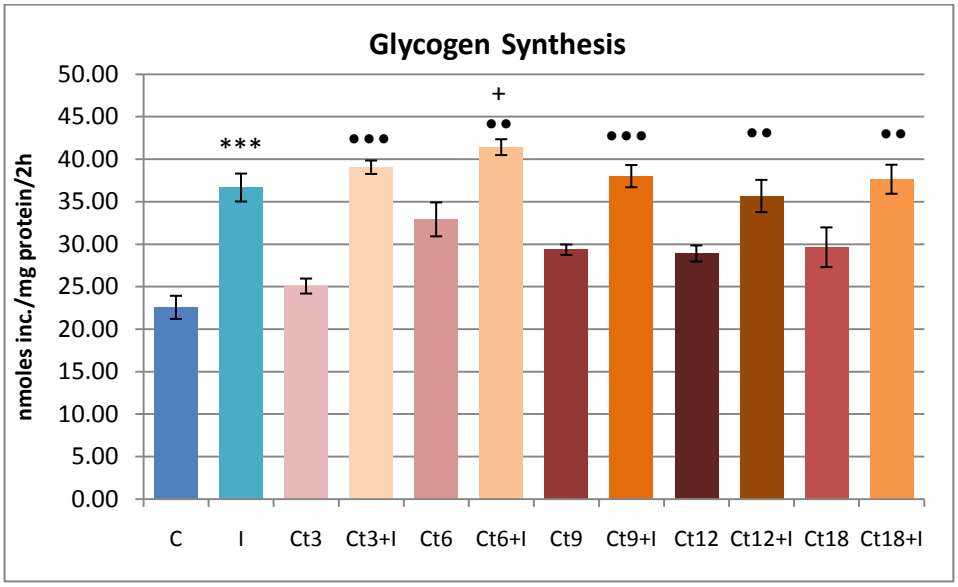

Fig 3.3.5b. The effect of varying the incubation period with stimulants on the LPS plus cytokine-induced impairment of the insulin-stimulated glycogen synthetic rate in myoblasts. The results shown are the mean nmoles of glucose incorporated into glycogen over two hours ± SEM from 6 determinations from 2 independent experiments.
(C=control;I=Insulin;Ct=LPS+Cytokine;Ct+I=LPS+Cyt+Insulin;3,6,9,12,18=hours of treatment)
Statistical significance is as described in Section 2.14
* = Significance from control
• = Significance from respective LPS + Cytokine treatment
+ = Significance from Insulin

What is noticeable is that insulin did indeed significantly stimulate glycogen synthesis regardless of the time of LPS plus cytokine treatment, in accordance with the initial 18 hour myoblast data presented in section 3.3.2. The net rate of glycogen synthesis under insulin stimulation in untreated cells was 36.7nmoles/mg protein/2h, which was not significantly different to the insulin-mediated rate in myoblasts treated with LPS plus cytokines for 3, 9, 12 and 18 hours. The rate of glycogen synthesis in myoblasts treated with LPS plus cytokines for 6 hours and then stimulated with insulin (41.4nmoles/mg/2h) was significantly different to the control insulin-mediated rate.

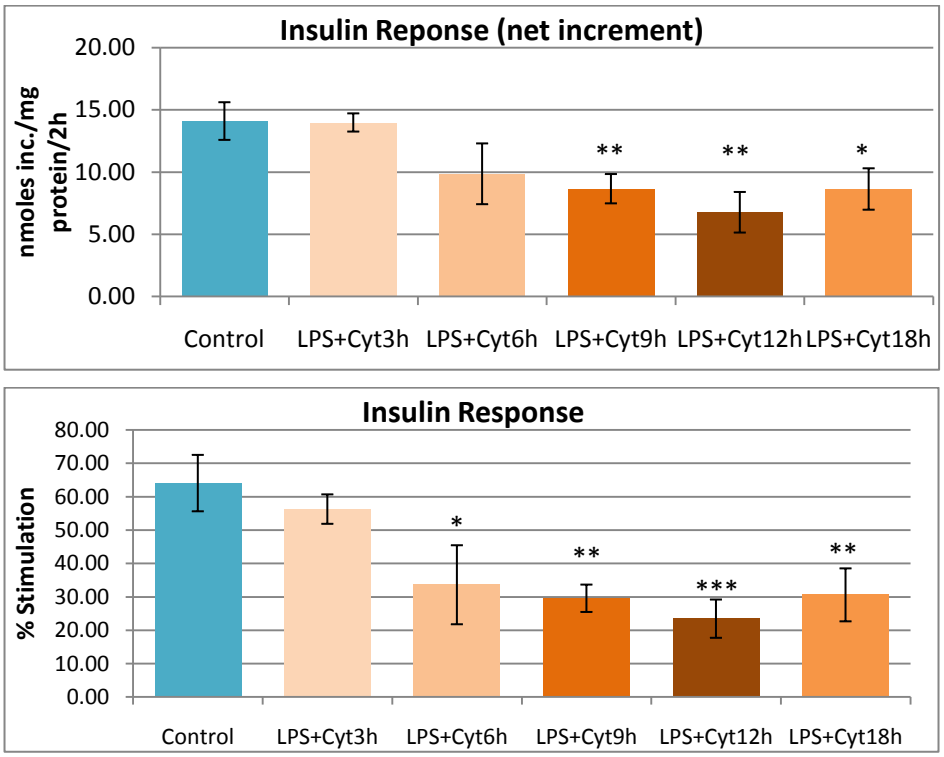

Fig 3.3.5c+d. c: Insulin response from the different LPS plus cytokine treatments measured in net increments induced by insulin in myoblasts. d: Same as c but measured as a % stimulation from the baseline. The results shown are the mean nmoles of glucose incorporate into glycogen over two hours ± SEM for 6 determinations from 2 independent experiments.
(C=control;I=Insulin;Ct=LPS+Cytokine;Ct+I=LPS+Cyt+Insulin;3,6,9,12,18=hours of treatment)
Statistical significance is as described in Section 2.14
* = Significance from control

Figure 3.3.5c+d shows the insulin response, represented as the net increment and the percentage stimulation. Both bar charts show approximately the same pattern. The insulin response following 3 hours of LPS plus cytokine treatment was not significantly different to the control insulin response, which also correlates with the pattern displayed in Figure 3.3.5a, where the rate of glycogen synthesis was comparable between untreated and 3 hour LPS plus cytokine treated myoblasts. After 6 hours of LPS plus cytokine treatment, the insulin-mediated increment (14nmoles/mg protein/2h) was not significantly different ($p=0.06$) to the control insulin-mediated increment (14.1nmoles/mg protein/2h), while interestingly the percentage stimulation induced by insulin in untreated cells (64%) was significantly different to the percentage stimulation induced in cells treated for 6 hours with LPS plus cytokines (56%)

(Figure 3.3.5d). Following 9, 12 and 18 hours of LPS plus cytokine treatment, the insulin-mediated increment was 8.7, 6.7 and 8.6nmoles/mg protein/2h, respectively. All three increments were significantly different to the control insulin increment. Similarly, the percentage stimulations induced by insulin after 9, 12 and 18 hours of treatment were 30, 24 and 31%, respectively, being significantly different to the control insulin percentage stimulation.

Insulin stimulated the basal rate of glycogen synthesis, as did the LPS plus cytokine treatment. If both these effects were going via the same mechanism, one would not anticipate the treatment to inhibit the insulin response. Once again it is difficult to assess whether this is in fact insulin resistance or not. Indeed, as discussed in Section 3.3.2, there may be no treatment-induced insulin-resistance in myoblasts because a maximal rate was reached. Since the LPS plus cytokines increased the basal rate of glycogen synthesis, insulin may have increased this rate up to the maximal point which was reached in each insulin-induced case following LPS plus cytokine treatment, which would mean that no significant degree of insulin resistance occurred. Furthermore, the onset of these two effects – treatment-induced increase and possible insulin-impairment of glycogen synthesis – coincided: being significantly different from their respective control rates following 6 hours of treatment. This could also suggest that there was no treatment-induced impairment in the insulin response, but in fact that the decrease of the insulin-induced rate (Figure 3.3.5c+d) occurred due to the rise of the control rate of glycogen synthesis induced by the LPS plus cytokines. This was further investigated in the next chapters.

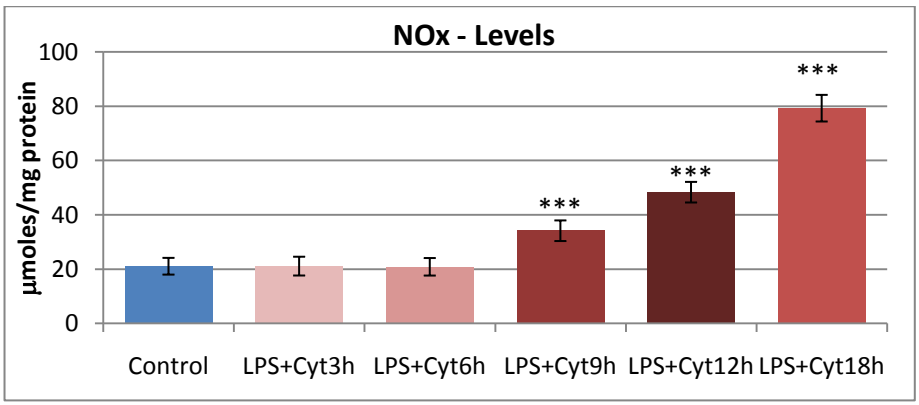

Fig 3.3.5e. The effect of varying the incubation period with LPS plus cytokine on NOx levels in myoblasts. The results shown are the mean µmoles of nitrite and nitrate in the medium ± SEM from 35 determinations from 6 independent experiments. Statistical significance is as described in Section 2.14
* = Significance from control

As discussed in sections 3.3.3 and 3.3.4, NOS inhibition by L-NAME made no difference to myoblast glycogen synthesis results observed under LPS plus cytokine treatment, insulin stimulation nor both in combination. Fig 3.3.5e shows that NOx levels were only significantly different to control levels after 9 hours of LPS plus cytokine incubation; where the levels of NOx were 62% higher than in the control. This represented an increase from 21μmoles to 34μmoles of NOx/mg protein. Following 12 and 18 hours of treatment the relative accumulated level of NOx was 128 and 276% higher than in the control cells, respectively. LPS plus cytokines significantly upregulated glycogen synthesis following 6 hours of LPS plus cytokine treatment and this increment was the same for the subsequent time-points (as shown in Figure 3.3.5a), which would imply that NO was unlikely to have had a role in the increase in myoblast glycogen synthesis induced by the treatment, correlating with the data discussed in Section 3.3.3.

3.4 Summary

Mouse C2C12 myocytes were treated with LPS, TNF-α, IFN-γ and IL-1β for 18 hours. The success, and indeed the extent, of the inflammatory insult was determined by the quantification of the NO levels, through the measurement of nitrite and nitrate concentrations. The induction of skeletal muscle iNOS in response to the LPS plus cytokines led to considerable NO production. This factor was used to distinguish between control (untreated) and treated cells, and confirm the LPS plus cytokine stimulation. The LPS plus cytokine treatment significantly increased NO production in both myocyte preparations, although the proportion of nitrite and nitrate compared between myoblasts and myotubes was different, suggesting a different redox environment within the cells. As shown in Figure 3.2.3g the level of expression of iNOS in myoblasts was significantly lower than in the myotubes following LPS plus cytokine treatment, indicating that NO production was higher in the myotubes. Despite the potential toxicity of elevated levels of NO, added to the possible apoptotic effects of cytokines (in particular TNF-α), the viability of the cells was not compromised for either myotubes or myoblasts, as seen in Table 3.2.2a

Myoblasts maintained a linear rate of glucose incorporation into glycogen over the 2 hours of measurement as displayed by Figure 3.3a. As a result, 2 hours of incubation with [U-^{14}C]-glucose was carried out for the glycogen synthesis method. The glycogen synthetic rate in myotubes was significantly higher than in the myoblasts, which can be explained by the higher

levels and activity of glycogen synthase present in myotubes (Wahrmann et al. 1973; Halse et al. 2001). Interestingly however, LPS plus cytokine treatment affected glycogen synthesis differently in myoblasts and myotubes. An 18 hour treatment significantly upregulated myoblasts glycogen synthesis – by 92% – whereas identical conditions significantly downregulated myotube glycogen synthesis – by 27%. The role played by NO in these observations also seemed to be different for both myocyte preparations. L-NAME was used to inhibit NOS activity, and it successfully prevented 76 and 72% of NO production in myoblasts and myotubes, respectively. This however had no effect on the treatment-induced increased rate of glucose storage seen in myoblasts, as the LPS plus cytokines still induced a comparably significant upregulation (by 79%) in the presence of L-NAME suggesting the effect was NO-independent.

In the myotubes on the other hand, NO appeared to play a role in the LPS plus cytokine induced downregulation of glycogen synthesis due to the fact that the presence of L-NAME rescued the phenotype: preventing the significant downregulation of glucose storage. This latter point, as mentioned in section 3.3.3, could be explained by NO-toxicity on the glycogen synthetic machinery, thereby decreasing the rate of synthesis. This is possible since NO production appeared higher in the myotubes, although LPS plus cytokines also significantly increased the level of NO produced in myoblasts, but had no such effect, making it questionable that NO-toxicity was the reason for the downregulation of myotube glycogen synthesis. In addition, NO-toxicity can induce cell death, however as observed with the EthD-1 cell viability assay results, the LPS plus cytokine treatment failed to induce any significant change in myotube viability relative to the untreated cells.

The insulin-stimulation of glycogen synthesis was different in both myocytes: myoblast glucose storage was upregulated by 121% in response to insulin, which was more pronounced than the 31% insulin-stimulation in myotubes (Figure 3.3.2a). Both these significant increases were impaired following treatment, although to differing degrees. There was a 77% impairment observed in the myoblasts, compared to a 61% impairment in the myotubes (Figure 3.3.2b+c). This result was expected, as observed in previous studies (Virkamaki and Ykijarvinen 1994; Begum and Ragolia 1996; Fan et al. 1996; Sugita et al. 2002; Ueki et al. 2004; Ghosh et al. 2007). Nevertheless the case of myoblast insulin-resistance was not clear. Despite the impairment of the myoblast insulin response observed, insulin was still able to significantly upregulate glycogen synthesis in the presence of the LPS plus cytokines – by 28% – implying the insulin response was not completely impaired. Since the LPS plus cytokine treatment increased the basal rate of glycogen synthesis it is possible that together with insulin a maximal rate of synthesis was reached, which would not imply a treatment-induced

impairment to the insulin response. On the other hand, myotubes displayed a completely impaired insulin response after treatment as the rate of glycogen synthesis was not statistically different to the rate in LPS plus cytokine treated cells ($p = 0.18$).

The LPS plus cytokine induced upregulation of myoblast glucose storage was different in the presence of insulin, as it failed to significantly increase the rate of storage, suggesting the two mechanisms were not additive, which could indicate that both increased glycogen synthesis in a similar fashion, correlating with the notion that a maximal rate of glycogen synthesis had been reached. In the myotubes on the other hand, the LPS plus cytokine induced downregulation occurred to a similar degree in the absence and presence of insulin. These two observations emphasise the difference between myoblasts and myotubes. As mentioned in section 3.3.2, LPS, IL-1β, TNF-α and insulin affect common target proteins such as the MAPKs, PI-3K and Akt (Titheradge 1999; Cohen 2006; Grzelkowska-Kowalczyk and Wieteska-Skrzeczynska 2009). These proteins will be looked at more closely in Chapter 5 in order to try and elucidate the mechanisms by which LPS plus cytokines altered glycogen metabolism, as well as the potential differences between the two myocyte preparations. The impairment of the insulin response was not NO-dependent for either myoblasts or myotubes. L-NAME failed to rescue the impairment as seen by the lack of significance between the insulin-stimulated rates of glucose storage in treated cells with or without L-NAME. L-NAME did however partially reduce the LPS plus cytokine-dependent downregulation of myotube glycogen synthesis in the presence of insulin. In the absence of L-NAME, myotube LPS plus cytokine treatment reduced the insulin rate by 32%. This value, in the presence of L-NAME, was reduced to 15%, thus dampening the LPS plus cytokine-induced downregulation.

Section 3.3.5 displayed the time of onset of LPS plus cytokine induced changes observed in myoblast glycogen synthesis. Interestingly, the LPS plus cytokine-dependent effects followed a similar time-dependent pattern. The upregulation of basal glucose storage induced by the treatment was significant after 6 hours of treatment, and the percentage increase induced after 6 hours of treatment (49%) was not significantly different to the percentage increases induced by 9, 12 and 18 hours – which were 32%, 30% and 27% respectively (Figure 3.3.5a). The possible insulin-impairment induced by the LPS plus cytokine treatment was significant after 6 hours of LPS plus cytokine incubation (with respect to the percentage stimulation), and similarly this degree of impairment was not significantly different to the impairments observed after 9, 12 and 18 hours of LPS plus cytokine treatment. However as described, this apparent impairment to the insulin response may well be due to the LPS plus cytokine treatment raising the control rate, explaining why the insulin-induced increase was

lower following 6, 9, 12 and 18 hours of LPS plus cytokine treatment. As a result whether there was insulin resistance in the myoblasts following LPS plus cytokine treatment is questionable.

Chapter Four – The Effects of LPS plus Pro-Inflammatory Cytokines on the Regulatory Steps Governing Glycogen Synthesis in C2C12 Myocytes

4.1 Introduction

Skeletal muscle glycogen serves to store glucose and sustain muscle contraction during periods of intense exercise which would otherwise lag if the energy consumed came solely from glucose uptake (Azpiazu et al. 2000; Roach et al. 2004). Skeletal muscle also plays a fundamental role in glucose homeostasis in the sense that it is responsible for approximately 80% of insulin-stimulated glucose disposal after a meal (Jensen et al. 2006; Nedachi and Kanzaki 2006). As described in Section 1.6, the main regulatory sites governing glycogen synthesis are glucose uptake, the activity ratio of glycogen synthase and the level of glycogen stores in the cell, however the rate limiting steps in glycogen synthesis regulation are glucose entering the cell and the reaction catalysed by glycogen synthase (Azpiazu et al. 2000; Jensen et al. 2006; Jensen 2009; Lai et al. 2010).

As presented in the previous chapter, the effects of LPS plus cytokine treatment on myoblast and myotube glycogen synthesis gave contrasting results. The myoblasts responded to the treatment with a significant increased rate of glycogen synthesis, compared to the significant decrease observed in the myotubes. In order to try and elucidate which components of the glycogen synthetic pathway may have been responsible for these observations, it was necessary to investigate the key regulatory steps outlined above and in Section 1.6. Some of these steps have already been studied under similar inflammatory, septic or endotoxic conditions. For example much attention has been focused on the role LPS, inflammatory cytokines or nitric oxide have on skeletal muscle glucose transport, and similar to the literature presented in Chapter 3 on glycogen synthesis, there are conflicting results. (Vary et al. 1995; Begum and Ragolia 1996; Bedard et al. 1997; Etgen et al. 1997; Del Aguila et al. 1999; Khanna et al. 1999; Higaki et al. 2001; Lira et al. 2007; Nishiki et al. 2008; Grzelkowska-Kowalczyk and Wieteska-Skrzeczynska 2009). Several studies observed a significant upregulation of glucose transport under inflammatory conditions, even though the experimental conditions differed, for example TNF-α alone in primary human skeletal muscle cells (Ciaraldi et al. 1998); LPS, TNF-α and IFN-γ treatment of L6 myotubes (Bedard et al. 1997; Khanna et al. 1999); and L6 myotubes treated with monokines obtained from LPS-treated RAW 264.7 macrophages (Lee et al. 1987). However in contrast to this, TNF-α treatment of L6 myotubes was shown to significantly inhibit glucose transport (Begum and Ragolia 1996).

NO is an appropriate potential mediator of these observed effects due to its suggested role in regulating skeletal muscle glucose transport (Roberts 1997; Roy et al. 1998; Li et al. 2004; Lira et al. 2007). Studies using the NO-donor SNP on isolated rat skeletal muscle cells

displayed a significant dose-dependent upregulation of basal glucose transport (Balon and Nadler 1997; Etgen et al. 1997; Young et al. 1997). Reactive oxygen species have also been implicated in glucose transport, as described by Khanna et. al. who found that PDTC (an antioxidant/inhibitor of NFκB) significantly suppressed the stimulatory effect on glucose transport induced by IFN-γ or LPS on their own (Khanna et al. 1999).

The effect of LPS and/or cytokines on glycogen stores has also been documented due to the important role played by skeletal muscle in glucose disposal after a meal (Virkamaki and Ykijarvinen 1994; Vary et al. 1995; Furnsinn et al. 1997; Crossland et al. 2008; Lee et al. 1987; Ciaraldi et al. 1998). Assessing the glycogen stores takes into account the rate of glycogen synthesis minus the rate of glycogen breakdown. Levels of glycogen affect the rate of glucose storage (via GS and glucose transport), making it an important measurement to take. Two in vivo studies observed significant glycogen store depletion as a result of 24 hours (Crossland et al. 2008) and 105 minutes (Virkamaki and Ykijarvinen 1994) of endotoxic insult. Similarly, L6 myotubes subjected to 3 hours of treatment with monokines resulted in depletion of glycogen reserves, which increased between 6 and 24 hours after monokine exposure, yet never reached basal levels (Lee et al. 1987). On the other hand, two other studies found no differences in skeletal muscle glycogen stores after LPS treatment in rats (Vary et al. 1995) or TNF-α treatment in isolated human cells (Ciaraldi et al. 1998).

Glycogen synthase has also been investigated under inflammatory conditions, and here the various pieces of literature appear to correlate with each other. Both L6 myotubes and in vitro analysis of isolated human muscle cells displayed an inhibition of glycogen synthase fractional activity in response to TNF-α (Begum and Ragolia 1996; Ciaraldi et al. 1998). Similarly, glycogen synthase fractional activity was inhibited in rats treated with LPS (Virkamaki and Ykijarvinen 1995). In addition to this, insulin-stimulated glycogen synthase fractional activity was also hindered by TNF-α treatment (Begum and Ragolia 1996; Ciaraldi et al. 1998). In the liver, Wallington et. al. observed similar results where the glycogen synthase activity ratio was lowered in response to LPS plus cytokines (Wallington et al. 2008). Glycogen phosphorylase (Phosphorylase) catalyses the first step of glycogenolysis, and as a result will also be looked at, since changes in its activation can affect both the net synthesis and storage of glycogen. Unfortunately, less literature is available concerning this enzyme during inflammatory conditions with regards to skeletal muscle. Wallington et. al. nevertheless observed no changes to Phosphorylase activity in hepatocytes in response to the endotoxic model (Wallington et al. 2008). In addition to this, the levels of G-6-P and UDP-glucose will be determined since G-6-P is a potent allosteric activator of GS, while UDP-glucose is the

substrate for GS (Jensen 2009). Vary et. al. noted a 2-fold increase in skeletal muscle G-6-P levels after a chronic, intra-abdominal septic abscess in rats (Vary et al. 1995). The endotoxic shock model in the liver however, caused a significant decrease in G-6-P levels, as well as UDP-glucose (Wallington et al. 2008). Due to the importance of these various steps in the glycogen synthetic process, they were investigated under LPS plus cytokine treated myoblasts and myotubes, the methods of which are described in Chapter 2.

4.2 Effect Of LPS plus Cytokine Treatment on Glucose Uptake in C2C12 Myocytes

Glucose uptake is a fundamental process for any cell in the body as it provides the particular tissue with a source of energy. Skeletal muscle express GLUT1 (constitutive transporters) that are present at the membrane and the insulin-dependent GLUT4 transporters (Holloszy 2003; Huang and Czech 2007). The glucose uptake assay was carried out as described in Section 2.7. Before trying to elucidate any effects LPS plus cytokines were having on basal glucose transport, a time-course was carried out in order to ensure the transport of glucose was linear over time.

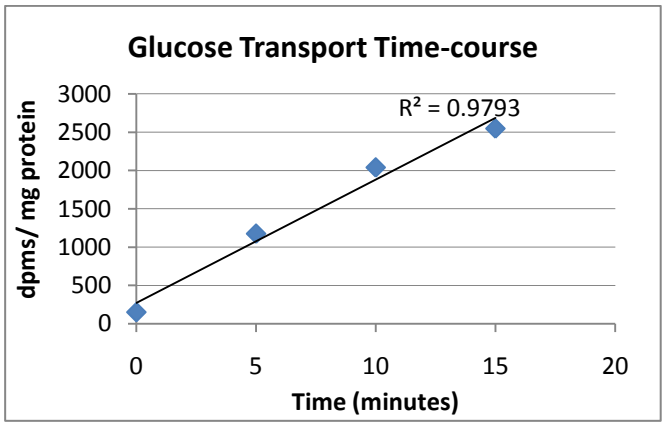

Fig 4.2.a. Time-course for the transport of [^{3}H] 2-deoxyglucose (2DOG) into myoblasts over 15 minutes. The results shown are the mean dpms of [^{3}H]-2DOG incorporated/mg protein ± SEM from 6 determinations from 2 independent experiments.

As shown by the R^2 value in Figure 4.2.2a, glucose uptake was linear over the 15 minutes of experiment. In order to maximise the incorporation of radioactive 2-deoxyglucose ([^{3}H]-2DOG), 15 minutes was the chosen time-point for the subsequent glucose transport assays. Once the linearity of glucose transport was determined, a comparison was made between glucose transport rates in both myoblasts and myotubes.

4.2.1 Effects of LPS plus Cytokine Treatment on Basal Glucose Uptake in C2C12 Myocytes

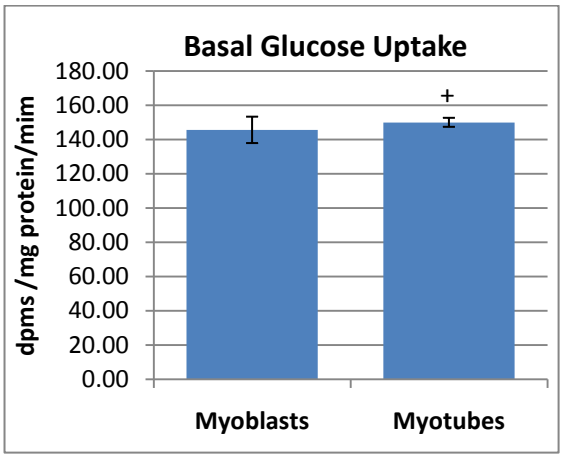

Fig 4.2.1a. A comparison of basal glucose uptake in myoblasts and myotubes. The results shown are the mean dpms of [^{3}H]-2DOG incorporated/mg protein/min ± SEM from 8 determinations from 3 independent experiments (myoblasts) and 11 determinations from 2 independent experiments (myotubes).
Statistical significance is as described in Section 2.14.
+ = Significance from myoblasts

Figure 4.2.1a shows that basal glucose uptake was comparable between both myoblasts and myotubes, despite a small yet significant 19% difference between the two ($p = 0.03$). This is in contrast with the clear difference observed in Section 3.3.1 between the myoblast and myotube basal glycogen synthetic rate which showed that myotubes had a rate 146% higher than the rate in myoblasts. A study using C2C12 cells noted comparable basal rates of glucose uptake in myoblasts and myotubes, which is akin to the relationship displayed in the figure above (Tortorella and Pilch 2002). In contrast to this study and the results above, Palmer et. al. observed a rate of glucose transport 8 fold lower in myotubes compared to myoblasts (Palmer et al. 1997).

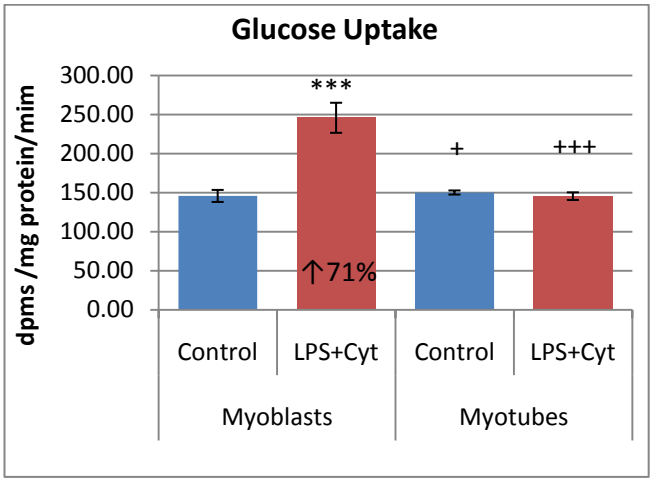

Fig 4.2.1b. Effect of LPS plus cytokines on basal glucose uptake in myocytes. Cells were treated as described in Section 2.2.5. The results shown are the mean dpms of [^{3}H]-2DOG incorporated/mg protein/min ± SEM from 8 determinations from 3 independent experiments (myoblasts) and 11 determinations from 2 independent experiments (myotubes).
Statistical significance is as described in Section 2.14.
* = Significance from respective control
+ = Significance from myoblasts

The figure above shows the effect of treating C2C12 myocytes with LPS plus cytokines on glucose transport. As clearly displayed, the treatment significantly upregulated glucose transport in the myoblasts, from 145 dpms/mg protein/min to 245 dpms/mg protein/min. This 71% increase did not occur under the same experimental conditions in myotubes, where the rate of glucose uptake in treated cells was not significantly different from the basal rate ($p = 0.19$). The LPS plus cytokine-induced percentage increase in myoblast glucose transport correlates with the same treatment-induced percentage increase in myoblast glycogen synthesis which was 92% (as shown in Figure 3.3.1a). This would support the concept suggested by previous studies which indicated that the rate of glucose uptake strongly influences the rate of glycogen synthesis (Ren et al. 1993; Hansen et al. 1995). In contrast the significant downregulation of glycogen synthesis observed in treated myotubes (Figure 3.3.1a) cannot be explained by a reduced rate of glucose uptake as LPS plus cytokines had no effect on this process as indicated in Figure 4.2.1b.

In agreement with the myoblast but in contrast to the myotube results presented above, similar studies using L6 myotubes also noted an increase in glucose transport, although the magnitude of the response was variable (Lee et al. 1987; Bedard et al. 1997; Khanna et al. 1999). L6 myotubes treated with TNF-α (50 ng/ml), IFN-γ (500ng/ml), and LPS (10 μg/ml) for 24 hours induced a 50% upregulation in glucose transport (Khanna et al. 1999), whereas a 124% upregulation of glucose uptake was observed by Bedard et. al. following a 24 hour treatment with TNF-α (10ng/ml), IFN-γ (200U/ml) and LPS (10ug/ml) (Bedard et al. 1997). Similarly, L6 myotubes treated with a crude monokine preparation, obtained from LPS-treated RAW 264.7 macrophages, for 24 hours showed an even higher upregulation, 180% of the control rate of glucose uptake (Lee et al. 1987). Unfortunately the basal rates measured by these studies are not given in two of the studies, however Bedard et. al. noted one much lower (31pmol/mg/min) than the basal rates displayed above, which could be a reason for the higher stimulation induced by TNF-α, IFN-γ and LPS (Bedard et al. 1997). One study that used C2C12 myocytes, in a considerably different experimental design, deduced the effects of the individual cytokines TNF-α, IFN-γ and IL-1β, all added at 10ng/ml for 5 days on glucose transport (Grzelkowska-Kowalczyk and Wieteska-Skrzeczynska 2009). Under these conditions TNF-α or IL-1β treatment had no effect on basal glucose transport, but IFN-γ alone upregulated glucose transport by 75%, similar to the myoblast results presented above (Grzelkowska-Kowalczyk and Wieteska-Skrzeczynska 2009). In contrast to these studies and the results presented in Figure 4.2.1b, a 12 hour exposure to TNF-α induced a 100% decrease in glucose uptake in L6 myotubes (Begum and Ragolia 1996).

4.2.2 Effects of LPS Plus Cytokine Treatment on Insulin-Stimulated Glucose Uptake in C2C12 Myocytes

Research suggests that insulin-stimulated glucose transport is impaired by LPS and/or cytokines (Begum and Ragolia 1996; Fan et al. 1996; Bedard et al. 1997; Ciaraldi et al. 1998; Del Aguila et al. 1999). As such, prior to measuring glucose uptake, myoblasts and myotubes were treated with 1μM insulin for a total of 35 minutes; the insulin was added 15 minutes prior to the beginning of the 2DOG procedure and then added again during the 20 minute assay (as described in Section 2.7)

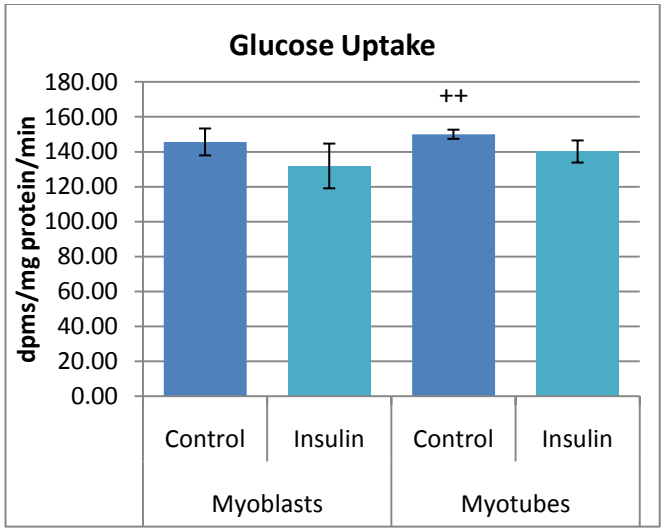

Fig 4.2.2a. Effect of insulin (1μM) on glucose uptake in myoblasts and myotube. The results shown are the mean dpms of [^{3}H]-2DOG incorporated/mg protein/min ± SEM from 8 determinations from 3 independent experiments (myoblasts) and 11 determinations from 2 independent experiments (myotubes). Statistical significance is as described in 2.14
+ = Significance from myoblasts

What is initially noticeable in Figure 4.2.2a is the lack of insulin response in both myocyte preparations, despite the fact that skeletal muscle is responsible for roughly 80% of glucose disposal after a meal due to the insulin-stimulated translocation of GLUT4 transporters to the membrane (Jensen et al. 2006; Nedachi and Kanzaki 2006). There is evidence that the insulin-dependent glucose uptake in C2C12 cells is difficult to measure, even after differentiation (Schmitz-Peiffer et al. 1999; Tortorella and Pilch 2002; Nedachi and Kanzaki 2006; Lorenzo 2008). In order to investigate the apparent lack of insulin-induced glucose uptake in C2C12 myotubes, Tortorella et. al. significantly upregulated GLUT4 expression via dexamethasone treatment, however despite this upregulation, the cells did not take up more glucose compared to non-dexamethasone treated cells in response to 100nM insulin (Tortorella and Pilch 2002). Two further studies also failed to observe an insulin-stimulated glucose uptake rate in C2C12 myotubes, also using 100nM insulin (Schmitz-Peiffer et al. 1999;

Chavez and Summers 2003). Nedachi et. al. assessed the insulin-dependent translocation of GLUT4 in C2C12 cells and observed a ~3-fold increase in GLUT4 presence at the plasma membrane, which significantly increased glucose uptake but only by 34% (Nedachi and Kanzaki 2006). In another study using C2C12 myoblasts and myotubes, insulin significantly increased glucose transport by 50% in both myocyte preparations (Palmer et al. 1997). In contrast to the negative studies using C2C12 cells, experiments using L6 myotubes have shown consistent increases in insulin-dependent glucose transport, although the magnitude of the response differs: increases of 38% (100nM insulin), 94% (10nM insulin) and 68% (0.6mM insulin) were noted (Begum and Ragolia 1996; Bedard et al. 1997; D'Alessandris et al. 2007).

Due to the lack of a noticeable insulin response on glucose transport, it was not possible to address whether or not LPS plus cytokine treatment impaired insulin-dependent glucose uptake. Nevertheless, assessing the rate of glucose transport in treated cells under insulin stimulation could provide insight into explaining the glycogen synthetic results presented in Chapter 3.

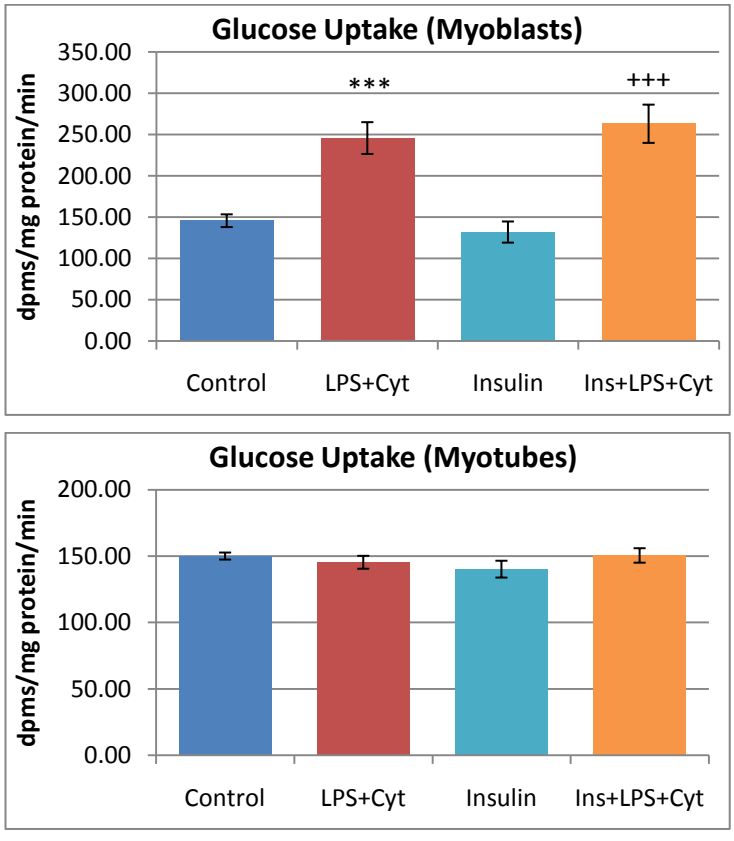

Fig 4.2.2b+c. Insulin (1μM) response on LPS plus cytokines treated cells on glucose uptake in myocytes. The cells were treated as described in Section 2.2.5. The results shown are the mean dpms of [^{3}H]-2DOG incorporated/mg protein/min ± SEM from 8 determinations from 3 independent experiments (myoblasts) and 11 determinations from 2 independent experiments (myotubes). Statistical significance is as described in Chapter Section 2.14
* = Significance from control
+ = Significance from insulin

As observed in the previous two figures (4.2.1a+b), myotubes did not appear to respond at all to LPS plus cytokine treatment, insulin, nor both together (Figure 4.2.2c). For myoblasts on the other hand, the same significant upregulation in response to LPS plus

cytokines occurred in the absence or presence of insulin. The treatment upregulated glucose transport by an average of 86% in the presence of insulin, which was not statistically different ($p=0.45$) to the average increment induced by the treatment over the basal rate, 83%. The general consensus is that LPS and/or cytokines impair insulin-dependent glucose uptake (Begum and Ragolia 1996; Fan et al. 1996; Bedard et al. 1997; Ciaraldi et al. 1998). Using L6 myotubes, two groups noted an approximate 75% decrease in the insulin-dependent glucose uptake response under slightly different conditions: 12 hours with 10ng/ml TNF-α (Begum and Ragolia 1996); and 24 hours with 10ng/ml TNF-α, 20ng/ml IFN-γ and 10μg/ml LPS (Bedard et al. 1997). A similar impairment of 70% was observed in cultured human muscle cells treated with TNF-α for 24 hours (Ciaraldi et al. 1998). In vivo, a 50% impairment was measured after 24 hours treatment with LPS (100μg/100g of body weight) (Fan et al. 1996). Finally, one study using C2C12 myotubes suggested a similar impairment of the insulin-response after a 1h treatment with TNF-α (10ng/ml), however closer scrutiny of the results presented suggest the opposite (Del Aguila et al. 1999). The apparent impairment of the insulin response was based on the grounds that TNF-α treated cells incubated with insulin had a lower rate of glucose uptake compared to insulin treated cells. However, a more appropriate way of determining the insulin response is to differentiate between control cells and insulin treated ones, and similarly to compare TNF-α treated with TNF-α and insulin treated cells. When the latter analysis is applied to the results, insulin stimulated basal glucose uptake by 33% (from 45 to 60pmoles/mg/min), which compares to the 75% insulin-induced increase in TNF-α treated cells (from 24 to 42pmoles/mg/min), thus suggesting that TNF-α treatment actually increased the response to insulin despite significantly lowering the basal rate of glucose uptake (Del Aguila et al. 1999).

Despite a lack of insulin-sensitivity, conclusions can be drawn from the results presented in Figure 4.2.2b+c with regards to the glycogen synthesis results presented in Chapter 3 of this thesis. In the myoblasts the observed upregulation of glucose transport induced by the LPS plus cytokine treatment with or without insulin was comparable. In addition to this, the experimental conditions failed to elicit an insulin-stimulated increase in glucose uptake, although the rates of glycogen synthesis in insulin-treated cells, and LPS plus cytokine treated cells stimulated with insulin were not significantly different ($p = 0.13$). The LPS plus cytokine treated cells stimulated with insulin had a much higher level of glucose entering the cell compared to insulin-induced cells, as shown in Figure 4.2.2b, yet did not result in higher levels of glycogen synthesis. As already discussed, GLUT4 translocation is not readily distinguished in a glucose uptake assay (Nedachi and Kanzaki 2006; Lorenzo 2008). This

together with the fact that insulin increased myoblast glycogen synthesis implies that LPS plus cytokine stimulated myoblast glucose transport via a mechanism that is independent of the insulin-dependent cascade. This treatment-mediated increase in glucose transport would have strongly favoured an increase in glycogen synthesis, as discussed by Azpiazu et. al and Holloszy et. al. (Azpiazu et al. 2000; Holloszy 2003). For the myotubes on the other hand, the observed increase in glycogen synthesis in response to insulin (Figure 3.3.2c) cannot be accounted for by an increase in glucose uptake under the same conditions. Moreover these glucose transport data suggests that the observed decrease in myotube glycogen deposition noted in response to LPS plus cytokines (Figure 3.3.1a), was not due to a decrease in glucose uptake, as seen by Figure 4.2.2, suggesting another means of inhibition occurred.

4.2.3 Role of Nitric Oxide on LPS plus Cytokine-Induced Changes in Glucose Uptake

Much evidence suggest that NO is involved in the regulation of carbohydrate metabolism in skeletal muscle cells, especially glucose transport (Balon and Nadler 1997; Bedard et al. 1997; Roberts 1997; Young et al. 1997; Roy et al. 1998; Higaki et al. 2001; Nishiki et al. 2008). These cited papers all agree that NO is involved in upregulating glucose transport, but the conflict regards which pathway NO is involved in, contraction or insulin mediated, or indeed if NO-dependent glucose transport is distinct from the contraction and insulin-stimulated pathways. Due to this fact, the NOS inhibitor L-NAME was used to study the role played by NO in the observations presented in this chapter, by incubating the cells with 1mM L-NAME during the 18 hour incubation. L-NAME significantly reduced NOx levels by 84% and by 86% in myoblasts and myotubes, respectively (data not shown), similarly to the results presented in Section 3.3.3.

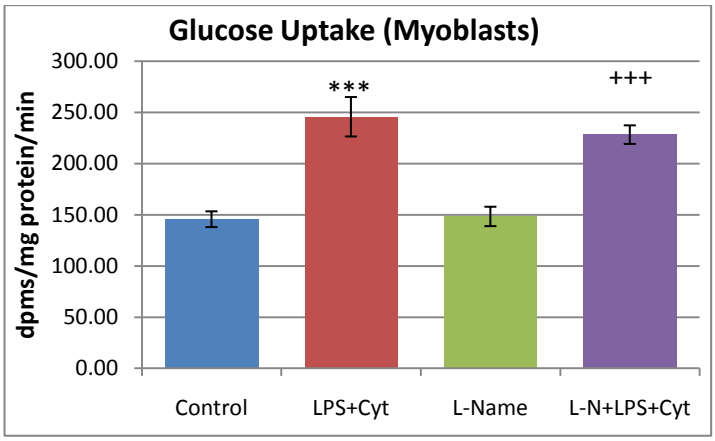

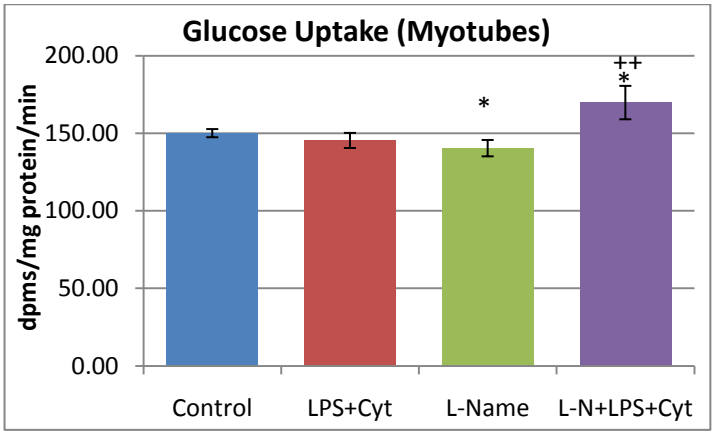

Fig 4.2.3a+b. Effect of L-NAME (1mM) on glucose uptake in LPS plus cytokine treated cells myocytes. The cells were treated as described in Section 2.2.5. The results shown are the mean dpms of [^{3}H]-2DOG incorporated/mg protein/min ± SEM from 8 determinations from 3 independent experiments (myoblasts) and 9-11 determinations from 2 independent experiments (myotubes).
Statistical significance is as described in Chapter Section 2.14.
* = Significance from control
+ = Significance from L-NAME

The figure above displays the effects of adding L-NAME to LPS plus cytokine treated cells on glucose transport. Figure 4.2.3a indicates that inclusion of L-NAME had no effect on the basal rate of myoblast glucose transport nor the LPS plus cytokine-induced upregulation of myoblast glucose transport, since the respective rates were not statistically different; $p = 0.41$ for the untreated and $p = 0.23$ for the LPS plus cytokine treated myoblasts. This was in spite of an 84% reduction in NO production induced by L-NAME in LPS plus cytokine treated myoblasts. The net increase in glucose incorporated into the cells following LPS plus cytokine treatment in the presence of L-NAME was 80 dpms/mg/min, compared with the basal increase induced by the treatment which was 100 dpms/mg/min. L-NAME significantly, albeit minimally, reduced the basal rate of myotube glucose uptake (Figure 4.2.3b). In addition, LPS plus cytokine treated myotubes co-treated with L-NAME had a significantly (21%) increased rate of glucose uptake compared to the L-NAME treated myotubes. This upregulation in the presence of L-NAME was also significantly different to the control rate, yet considerably lower than the treatment-induced increment observed in myoblasts.

The myoblast and myotube results presented above correlate with the glycogen storage results presented in the previous chapter. Both the LPS plus cytokine-mediated stimulation of myoblast glycogen synthesis and glucose transport were unaffected by L-NAME

treatment, suggesting NO was not responsible for the observations. In myotubes, L-NAME prevented the LPS plus cytokine-induced inhibition of glycogen synthesis, while in addition there was a small but significant increase in glucose uptake in L-NAME and LPS plus cytokine treated myotubes (Figure 4.2.3b). The latter may partly explain why L-NAME rescued the myotube glycogen synthesis downregulation mediated by the LPS plus cytokine treatment.

	Control (% difference)	With L-NAME (% difference)
Myoblasts LPS plus cytokine response	83 ± 24%	58 ± 11%
Myotubes LPS plus cytokine response	-3% ± 4% +++	21 ± 7% **, ++

Table 4.2.3a. The average percentage effect of LPS plus cytokines on glucose uptake in the presence and absence of L-NAME. Cells were treated as described in Section 2.2.5. The results shown are the mean percentages differences ± SEM from 8 determinations from 3 independent experiments (myoblasts) and 9-11 determinations from 2 independent experiments (myotubes). Statistical significance is as described in Section 2.14.
* = Significance from respective control
+ = Significance from myoblasts

In this table, it clearly shows the differing effects L-NAME had in the myoblasts and myotubes on the LPS plus cytokine induced effects on glucose uptake. In the myoblasts L-NAME had no significant effect on the average increment induced by the treatment on glucose uptake, suggesting that NO had no role in upregulating basal glucose transport. In the myotubes on the other hand, first of all the LPS plus cytokine treatment had no significant effect on glucose uptake, while the addition of L-NAME significantly increased the rate. The inhibition of NO production allowed the LPS plus cytokines to significantly upregulate glucose transport by an average of 21%, which was significantly lower than the same experiment in myoblasts. This latter result suggests that the presence of NO during the treatment of myotubes prevented an upregulation of glucose transport, in contrast to the myoblasts. This favours the proposal that NO was not responsible for an upregulation in glucose uptake in either myoblasts or myotubes.

These results are in contrast with some published data that suggest NO is responsible for upregulating glucose uptake (Bedard et al. 1997; Young et al. 1997; Higaki et al. 2001; Nishiki et al. 2008). In a study using L6 cells, a significant increase in glucose uptake – in

response to LPS (10μg/ml), TNF-α (50ng/ml) and IFN-γ (500ng/ml) for 24 hours – was unaltered by the presence of L-NAME, confirming the results presented above (Khanna et al. 1999). In a similar study, Bedard et. al. reported that a 124% upregulation in glucose uptake after a 24 hour treatment with 10ng/ml TNF-α, 20ng/ml IFN-γ and 10μg/ml LPS in L6 myotubes, was completely reversed by the addition of L-NAME (2mM), contrasting with the data displayed in Table 4.2.3a and those of Khanna et. al. (Bedard et al. 1997). The inhibition of NO production induced by L-NAME observed by Bedard et. al. was comparable to the results presented in Section 3.3.3, excluding any possible variations in the effectiveness of the inhibitor. Other research using the NO donor SNP – which brings about a large increase in NO – strongly suggests NO to be an important mediator of glucose uptake, as observed by a dose-dependent increase in glucose transport in response to SNP in rat skeletal muscle cells (Balon and Nadler 1997; Young et al. 1997; Higaki et al. 2001). However, SNP results in a quick release of large amounts of NO, which is different to the prolonged consistent release of NO during endotoxic shock, which may explain these discrepancies.

During muscle contraction small increases in NO occur, mainly via the constitutive calcium-dependent NOS enzymes, which has been suggested to mediate the contraction-induced increase in glucose uptake (Balon and Nadler 1997; Roberts 1997). Both cited groups treated isolated rat skeletal muscle, extensor digitorum longus (EDL) (Balon and Nadler 1997) and sarcolemmal membranes (Roberts 1997), with L-NAME during electrical stimulation to assess the effects of NO in contraction-mediated glucose uptake. In both cases L-NAME impaired the contraction-induced increase in glucose uptake, suggesting a role for NO in exercise-mediated glucose transport. In contrast with this however, Higaki et. al. treated rat EDL cells with SNP and electrical stimulation (mimicking contraction) and observed an additive effect, suggesting that NO regulated glucose transport via a mechanism other than the contraction-mediated pathway (Higaki et al. 2001). It must be noted however that the levels of NO induced during exercise are significantly lower than the NO production indicative of an inflammatory insult. Nevertheless, the results presented in this section clearly imply that NO was not involved in upregulating glucose transport in C2C12 cells in response to LPS plus cytokines.

4.2.4 Role of Reactive Oxygen Species on LPS plus Cytokine-Induced Changes in Myoblast Glucose Uptake

Another potential mediator of skeletal muscle glucose uptake, suggested by some research, are reactive oxygen species (ROS) (Khanna et al. 1999; Kim et al. 2006; Katz 2007). During inflammatory conditions such as sepsis or endotoxic shock, the level of ROS and RNS increases (Lydyard 2000). As a result the rate of glucose transport in LPS plus cytokine treated myoblasts was assessed in the presence or absence of two antioxidants: Euk8 (a free-radical scavenger) at a concentration of 30μM and pyrolidine dithiocarbamate (PDTC – an inhibitor of NFκB) at 0.2mM. Both antioxidants were added 2 hours prior to the 18 hour LPS plus cytokine incubation.

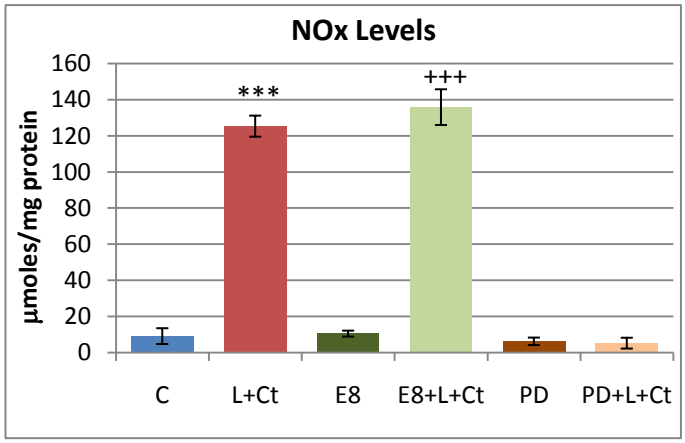

Fig 4.2.4a. The effect of Euk8 (30μM) or PDTC (0.2mM) on the LPS plus cytokine induced increase in NOx levels in myoblasts. The cells were treated as described in Section 2.2.5, with or without Euk8/PDTC. The results shown are the mean μmoles/mg protein ± SEM from 6 determinations from 2 independent experiments
Statistical significance is as described in Section 2.14.
* = Significance from control
+ = Significance from Euk8
(C=control, L+Ct=LPS+Cyt, E8=Euk8, E8+L+Ct=Euk8+LPS+Cyt, PD=PDTC, PD+L+Ct=PDTC+LPS+Cyt)

Figure 4.2.4a shows the levels of NOx in μmoles/mg protein measured from the various treatments. As shown, LPS plus cytokines significantly increased NOx levels in the presence or absence of Euk8, but failed to do so when myoblasts were co-treated with PDTC as it is an inhibitor of NFκB – which brings about the induction of iNOS following LPS and/or cytokine stimulation (Kleinert et al. 2004).

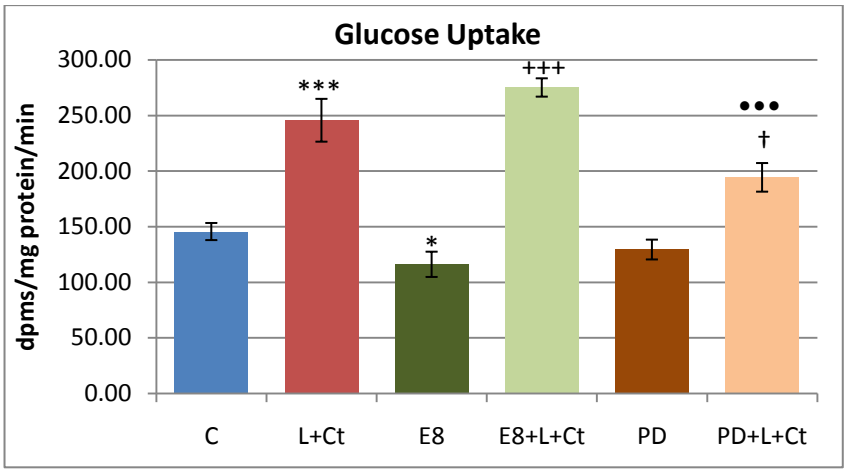

Fig 4.2.4b. Effect of Euk8 (30μM) or PDTC (0.2mM) on glucose uptake in LPS plus cytokine treated myoblasts. The cells were treated as described in Section 2.2.5, with or without Euk8/PDTC. The results shown are the mean dpms of [^{3}H]-2DOG incorporated/mg protein/min ± SEM from 8 determinations from 3 independent experiments. Statistical significance is as described in Section 2.14
* = Significance from control
+ = Significance from Euk8
• = Significance from PDTC
† = Significance from LPS plus cytokine
(C=control, L+Ct=LPS+Cyt, E8=Euk8, E8+L+Ct=Euk8+LPS+Cyt, PD=PDTC, PD+L+Ct=PDTC+LPS+Cyt)

Figure 4.2.4b displays the effect of LPS plus cytokines in combination with the antioxidants Euk8 or PDTC on glucose transport. What is initially noticeable is that the treatment induced a significant upregulation of glucose transport in the presence of either antioxidant. The basal rate in Euk8-treated cells was marginally but significantly lower than the control rate, but in the presence of LPS plus cytokines, Euk8 did not significantly alter the rate compared to the rate in LPS plus cytokine treated cells alone ($p = 0.12$). This suggests that the antioxidant properties of Euk8 failed to alter the LPS plus cytokine-induced upregulation of glucose transport, implying that ROS were not responsible for the upregulation observed. PDTC is an antioxidant in the sense that it inhibits the NFκB pathway, and thus prevents the NFκB-dependent generation of NO and ROS/RNS (Cvek and Dvorak 2007). In the presence of PDTC, the basal rate remained the same, but the LPS plus cytokine treated cells had a significantly lower rate compared to the LPS plus cytokine treated myoblasts with PDTC, suggesting that the inhibition of NFκB impaired the treatment-induced upregulation of glucose uptake.

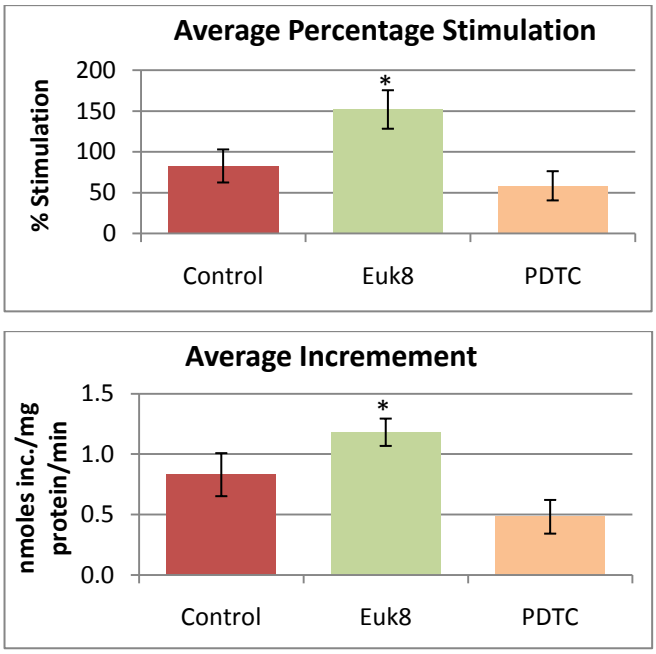

Fig 4.2.4c+d. Effect of Euk8 (30µM) or PDTC (0.2mM) on the percentage stimulation as well as the increment induced by LPS plus cytokines on glucose uptake in myoblasts. The cells were treated as described in Section 2.2.5, with or without Euk8/PDTC. The results shown are the mean stimulations induced by LPS plus cytokines ± SEM from 8 determinations from 3 independent experiments.
Statistical significance is as described in Section 2.14
* = Significance from control

In figure 4.2.4c, the average percentage stimulation as well as the average increment induced (Figure 4.2.4d) by the LPS plus cytokine treatment in the presence or absence of Euk8 and PDTC are given, allowing for a better analysis of the effect the antioxidants had on the LPS plus cytokine response. Although the rate of glucose uptake in cells treated with PDTC and LPS plus cytokines was statistically different to the rate from cells treated with LPS plus cytokines alone (Figure 4.2.4b), the average percentage increase induced by the LPS plus cytokine treatment was not significantly different to the average percentage increase induced over the basal rate ($p = 0.29$). This was also the case with regards to the average increment induced by the LPS plus cytokines with or without PDTC treatment. These results suggest that the activation of NFκB induced by LPS plus cytokines was not necessary for the treatment-dependent upregulation of glucose uptake, and in addition this re-enforces the conclusion made in Section 4.2.3 that the process is NO-independent. In Figure 4.2.4b, Euk8 did not significantly alter the net LPS plus cytokine-induced rate of glucose uptake, suggesting that the scavenging of free radicals performed by Euk8 had no effect on the treatment-induced increase in glucose transport. However Figure 4.2.4c+d above suggests that the antioxidant properties of Euk8 enabled a significantly higher upregulation of glucose uptake induced by the LPS plus cytokines: from the 70% increase induced by the treatment on its own, to a 150% increase induced by the treatment and Euk8. This latter result implies that the oxidative stress induced by the LPS plus cytokines appeared to impair glucose transport slightly. This could be

due to a slight effect on cell viability, however as discussed in Section 3.2.2, LPS plus cytokine treatment had no significant effect on cell viability.

This result is in contrast to studies made by Kim et. al., which noted that oxidative stress – induced by H_2O_2 release from glucose oxidase treatment – stimulated glucose uptake in two different primary rat skeletal muscle cells (Kim et al. 2006). Another contrasting study treated L6 myotubes with IFN-γ (500ng/ml) or LPS (10μg)/ml) for 24 hours, and observed a 30% increase in glucose uptake for both treatments, which was then significantly reduced to a 15% increase by co-treatment with PDTC (0.2mM) that was no longer statistically different to the basal rate (Khanna et al. 1999). Although co-treatment with PDTC in the C2C12 results presented above, reduced the rate of glucose uptake in LPS plus cytokine treated cells (Figure 4.2.4b), the percentage stimulation and increment induced by the treatment was not significantly different, suggesting PDTC failed to inhibit or impair the upregulation. Despite these two contrasting studies, neither Euk8 nor PDTC inhibited the LPS plus cytokine induced upregulation, implying that the rise in ROS that occurs during an inflammatory response was not responsible for the observed increment induced by the treatment.

4.2.5. Effects of LPS plus Cytokines on GLUT1 and GLUT4 Transporters

Basal glucose uptake in skeletal muscle cells is mediated by GLUT1, while GLUT4 is responsible for the insulin-stimulation of glucose transport (Holloszy 2003; Huang and Czech 2007). Determining the levels of these proteins could help explain why insulin failed to increase basal glucose transport or why LPS plus cytokines significantly upregulated myoblast glucose uptake. Indeed, some literature has suggested that sepsis in vivo or in vitro treatment with LPS and cytokines can modulate the expression levels of GLUT1 (Vary et al. 1995; Bedard et al. 1997; Ciaraldi et al. 1998; Wiernan et al. 2007). Antibodies recognising the glucose transporters were used to assess the cellular levels of GLUT1 and GLUT4 via SDS-PAGE and Western blotting however the specificity of each antibody was poor making it difficult to assess the results. This was despite the fact that several different combinations of primary and secondary concentrations were tried out in order to perfect the recognition of the appropriate band. As a result the comparison of GLUT1 and GLUT4 levels in either myoblasts or myotubes under the different treatments was not able to be addressed in this study.

In L6 myotubes, TNF-α, IFN-γ and LPS treatment for 24 hours significantly increased GLUT1 expression (Bedard et al. 1997), while the same occurred in human muscle cells

following a 24 hour treatment with TNF-α (Ciaraldi et al. 1998). Induction of sepsis in vivo in rats also resulted in a significant increase in GLUT1 levels (Vary et al. 1995). These studies, especially the one performed by Bedard et. al. would suggest that LPS plus cytokine treatment in the myoblasts may well have increased GLUT1 levels, which could help explain the significant increase in glucose uptake. Moreover the lack of a significant insulin-stimulation of glucose transport would suggest that GLUT4 machinery was unlikely to be the mechanism of action induced by the LPS plus cytokine treatment.

4.3 Effects of LPS plus Cytokines Treatment on Total Glycogen Stores in C2C12 Myocytes

The level of glycogen stores present in skeletal muscle will affect the rate of glucose transport and the activity of glycogen synthase, which are the two rate limiting steps in glycogen synthesis regulation (Azpiazu et al. 2000; Jensen et al. 2006; Jensen 2009; Lai et al. 2010). As a result determining the level of glycogen stores in myocytes with or without LPS plus cytokine treatment may aid in deducing the underlying causes for the glycogen synthetic results presented in Chapter 3. Cells were treated as described in Section 2.2.5, then total cell glycogen was assayed (as described in Section 2.5).

When the assay was performed on myoblasts the values were below the lowest standard, giving negative results, thus failing to be within the range of sensitivity of the assay. As a result larger plates were harvested but the values were still too low. Even when two plates of the same treatment were combined within one sample, the values failed to approach a range high enough for the sensitivity of the assay. This was the same case for the myotubes as well which was surprising since as mature C2C12 cells form, more glycogen synthase is expressed and thus the capacity for glycogen synthesis increases (Wahrmann et al. 1973). To ensure that the assay was working, it was tested with some mouse skeletal muscle tissue extracted from the hind limbs of 3 day post-natal mice. With this extract, 3 linear dilutions were prepared and the total glycogen content was tested.

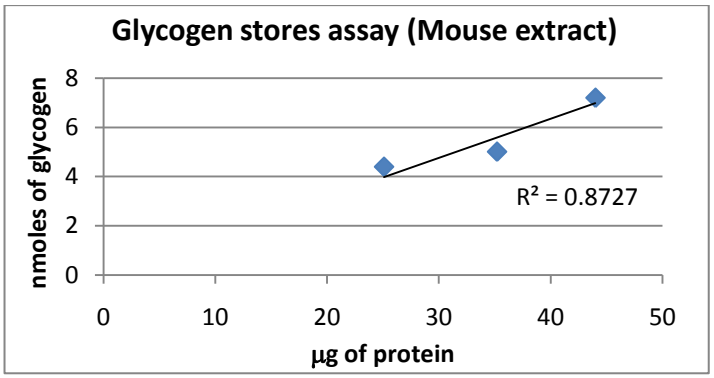

Fig 4.3a. Graph showing the levels of glycogen in nmoles from three separate dilutions of mouse skeletal muscle extract.

As the graph above shows, the glycogen stores assay worked fine, giving a linear relationship of glycogen content with the three separate dilutions made from the mouse skeletal muscle extract. The average nmoles/µg protein obtained from the mouse extract was approximately 0.15nmoles/µg protein. This value coincides with three studies that noted rat skeletal muscle glycogen content to be approximately 0.19 nmoles/µg protein (Virkamaki and Ykijarvinen 1995; Jensen et al. 2006; Crossland et al. 2008). In vitro studies using L6 myotubes measured total glycogen levels ranging from 0.023 – 0.06nmoles/µg protein (Pardridge et al. 1978; Huang and Tao 1980; Elsner et al. 1998). When the same cells were incubated with higher concentrations of glucose, glycogen content rose to 0.25nmoles/mg protein (Wahrmann et al. 1973). However this latter study used glucose concentrations 5 fold higher (25mM) than those used during the LPS plus cytokine experiments carried out in this thesis, which were 5mM, which as described by Elsner et. al. would have resulted in an increase in glycogen content (Elsner et al. 1998). The results presented in Figure 4.3a and these studies cited suggest that primary cells express higher levels of glycogen, potentially explaining the difficulty of measuring glycogen stores in the C2C12 cell line.

Glycogen store depletion was reported after 3-6 hours of treatment in L6 myotubes with a crude monokine preparation – obtained from LPS treated RAW 264.7 macrophage cells (Lee et al. 1987). Then between 6 and 24 hours of exposure the glycogen stores increased, although did not surpass 1/3 of the original level of glycogen present in the control cells (Lee et al. 1987). In response to LPS in vivo it has also been reported that glycogen stores were depleted; continuous intravenous infusion of LPS (15 µg/kg/h) in rats (Crossland et al. 2008), or a bolus LPS injection (1mg/kg) for 105 minutes (Virkamaki and Ykijarvinen 1994) significantly reduced skeletal muscle glycogen content.

4.4 Effects of LPS plus Cytokines Treatment on Glycogen Synthase and Glycogen Phosphorylase in C2C12 Myocytes

The second rate limiting step in glycogen synthesis is governed by glycogen synthase (GS) while the reverse reaction, glycogen breakdown, is governed by Phosphorylase as described in Section 1.6 (Roach et al. 2004; Lai et al. 2010). The assessment of GS or Phosphorylase activity involves measuring the activity of the entire enzyme population (total activity), the determination of the level of active enzyme and the activity ratio which is the ratio of the latter determination over the total activity. For GS this activity ratio is termed the fractional activity. The methods are described in Sections 2.8 (Phosphorylase assay) and 2.9 (GS assay).

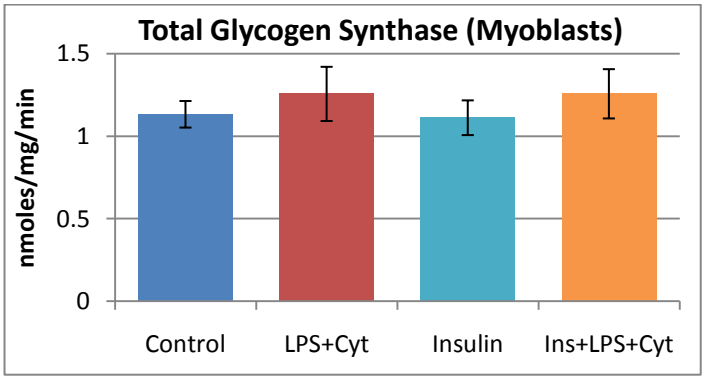

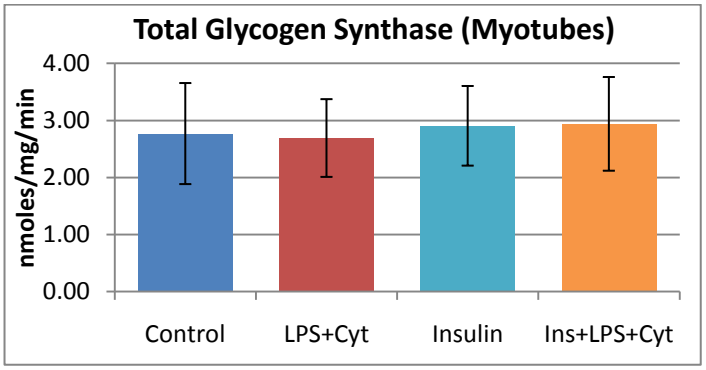

Fig 4.4a. Graphs showing the total activity of glycogen synthase in myoblasts and myotubes. Cells were treated as described in Section 2.2.5. Results are the mean fractional activity ± SEM from 6 independent experiments for myoblasts and from 4 independent experiments for myotubes.

The figure above shows the total activity of GS in both myocyte preparations under the different treatments. No significant difference in total activity was induced by either treatment in both myocyte preparations. However myotubes did show a significantly higher GS total activity of 2.8 compared to 1.2 nmoles/mg/min in myoblasts. This is likely due to the increased levels of GS present in myotubes (Wahrmann et al. 1973; Halse et al. 2001). Indeed Wahrmann

et. al. determined that GS expression was higher in L6 myotubes compared to L6 myoblasts (Wahrmann et al. 1973). What this figure suggests is that neither LPS plus cytokines, insulin treatment nor both together significantly altered total levels of GS. In both the myoblasts and myotubes these activities would be able to sustain the rates of glycogen synthesis discussed in Chapter 3. Total levels of GS in myoblasts would have been able to incorporate approximately 100nmoles/mg protein over the 2 hour incubation done for the glycogen synthesis experiment, while in myotubes this would have been approximately 250nmoles/mg protein over the 2 hour period.

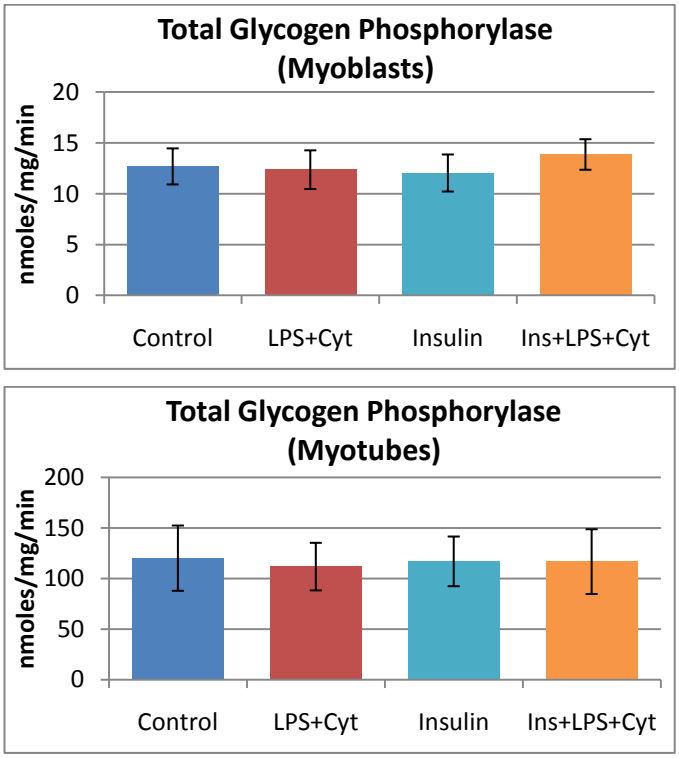

Fig 4.4b. Graphs showing the total activity of Phosphorylase in myoblasts and myotubes. Cells were treated as described in Section 2.2.5. Results are the mean fractional activity ± SEM from 6 independent experiments for myoblasts and from 4 independent experiments for myotubes.

Similar to the total GS results, there was no significant change in total Phosphorylase activity in either myoblasts or myotubes under the treatments, suggesting that total levels of Phosphorylase remained the same regardless of the treatment. The total activity present in myotubes was once again significantly higher than that in the myoblasts, approximately 10 fold higher (from 12 in the myoblasts to 120 nmoles/mg/min in the myotubes). This increase can be explained by the fact that differentiation brings about an increase in Phosphorylase expression, as discussed in (Wahrmann et al. 1973).

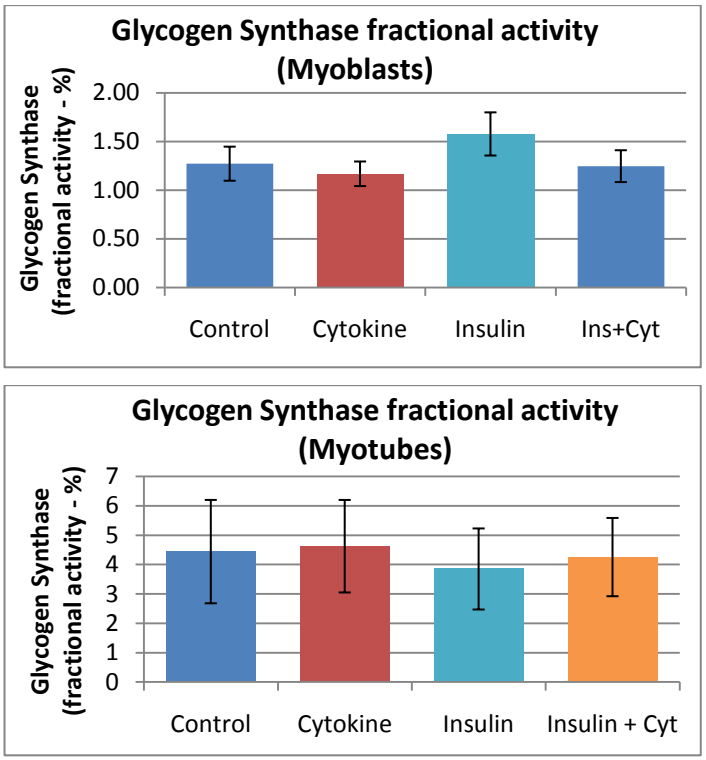

Fig 4.4c. Graphs showing the fractional activity of glycogen synthase in myoblasts and myotubes. Cells were treated as described in Section 2.2.5. Results are the mean fractional activity ± SEM from 6 independent experiments for myoblasts and from 4 independent experiments for myotubes.

Figure 4.4c above shows the mean fractional activity of GS in both myocyte preparations following LPS plus cytokine treatment, insulin stimulation and both together. In both cases neither the treatment nor insulin stimulation affected the activity ratio of GS. In the myoblasts there was approximately 1.3% active GS relative to total GS under basal conditions, whereas in the myotubes this ratio was significantly higher at about 4%. Differentiated L6 myotubes displayed a 2 to 5 fold increase in GS fractional activity relative to undifferentiated L6 myoblasts, which correlates with the results presented above (Wahrmann et al. 1973). Nevertheless these fractional activities seemed low, as a result the assay was tested on a skeletal muscle extract from the hind limb of a 3 day post-natal mouse, which gave a fractional activity of 40%, suggesting the assay conditions were not responsible for the low fractional activity. Indeed, two studies in L6 myotubes noted a similar low activity ratio of GS (5%) (Huang and Tao 1980; Begum and Ragolia 1996). Studies using extracted skeletal muscle had slightly varying fractional activities for GS as well, ranging from 15 to 88% in rat skeletal muscle (Virkamaki and Ykijarvinen 1995; Jensen et al. 2006; Kim et al. 2006). The LPS plus cytokines did not affect the fractional activity of GS in either myoblasts or myotubes. This contrasts with experiments using L6 myotubes treated with TNF-α (10ng/ml) for 60 minutes, or in vivo studies treating rats for 300 minutes with LPS (1mg/kg), where a significant reduction in fractional activity was apparent (Virkamaki and Ykijarvinen 1995; Begum and Ragolia 1996). The latter two studies were however quite different to the experimental conditions used to

obtain the results presented in Figure 4.4c, since the timing was considerably shorter. More akin to the conditions used in this thesis, despite taking place in the liver, a 24 hour treatment of rat hepatocytes with LPS (10μg/ml), IFN-γ (10ng/ml), TNF-α (20ng/ml) and IL-1β (20U/ml) significantly reduced GS fractional activity by 40% (Wallington et al. 2008).

In contrast to the literature, insulin failed to stimulate GS activity in both myocyte preparations, despite significantly stimulating glycogen synthesis as described in Section 3.3.2. The failure of insulin to stimulate GS activity was surprising as insulin has been reported to do so by 46 and 80% in rat epitrochlearis and L6 myotubes, respectively (Begum and Ragolia 1996; Jensen et al. 2006). As shown in Figure 4.4a, total levels of GS did not alter between one treatment and the next, and now in addition to this the GS fractional activities presented above imply that the alterations to myocyte glycogen metabolism discussed in Chapter 3 are not likely to be due to alterations in GS total levels or fractional activity.

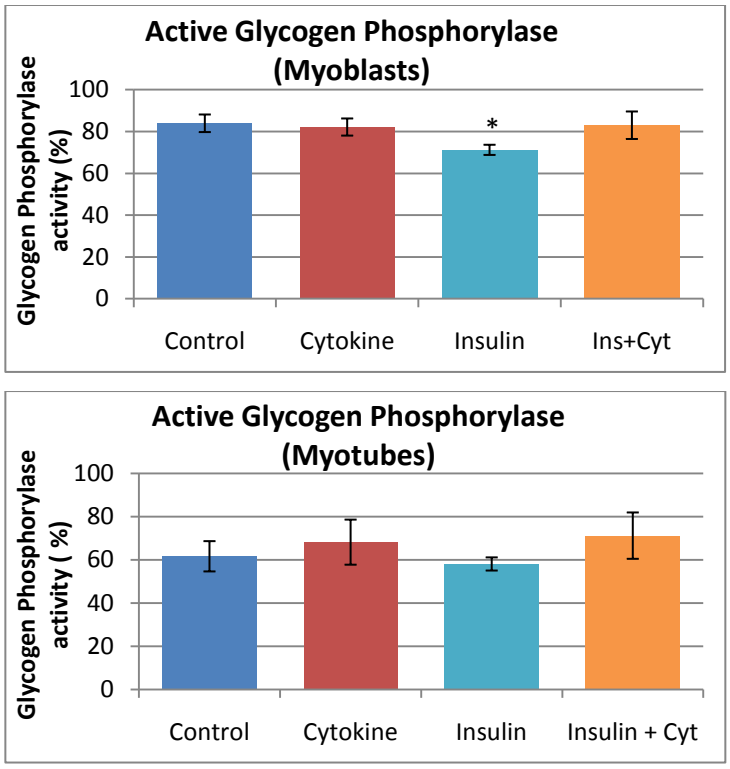

Fig 4.4d. Graphs showing the activity ratio of Phosphorylase in myoblasts and myotubes. Cells were treated as described in Section 2.2.5. Results are the mean fractional activity ± SEM from 6 independent experiments for myoblasts and from 4 independent experiments for myotubes. Statistical significance is as described in Section 2.14.
* = Significance from Control

Figure 4.4d shows the activity ratio of Phosphorylase in both myocyte preparations. Once again, the basal activity ratio was significantly different between both myocytes, although in this instance myoblasts displayed a higher ratio than in the myotubes. In two studies using L6 myotubes two significantly different activity ratios of Phosphorylase were

noted: 28% (Huang and Tao 1980) and 90% (Elsner et al. 1998). Both these observations are in contrast to those presented above, although myoblast Phosphorylase activity (80%) is akin to the 90% figure noted by Elsner et. al. The skeletal muscle obtained from the hind limb of 3 day post-natal mouse gave an activity ratio of 55%, which is more in line with the myotube result shown above. These activity ratios correlate with the low GS fractional activities presented in Figure 4.4c, since GS and Phosphorylase are reciprocally regulated, suggesting both enzymes are in their phosphorylated form (Huang and Tao 1980; Syed and Khandelwal 2000). The LPS plus cytokine treatment had no effect on the activity ratio of Phosphorylase in either myocyte preparation. Insulin stimulation significantly reduced the activity ratio of Phosphorylase in the myoblasts – by 16% – however failed to significantly do so in myotubes. This is surprising as insulin has been reported to reduced Phosphorylase activity in skeletal muscle (Ykijarvinen et al. 1987; Zhang et al. 1989; Dent et al. 1990), while similar to the myotube results shown above, no insulin-mediated response on Phosphorylase was noted in a study using rat epitrochlearis (Bouskila et al. 2008).

Taken together with the GS rates presented in Figure 4.4c it is surprising that insulin failed to induce a significant change in the activity ratio of myotube Phosphorylase, since as shown in Section 3.3.2, insulin significantly upregulated myotube glycogen synthesis. This implies that another mechanism must have induced the stimulation. Indeed it has been shown that knockin mice expressing constitutively active GSK3α/β isoforms in skeletal muscle still enabled an insulin-mediated increase in glycogen synthesis (Bouskila et al. 2008). This study also noted no insulin-mediated decrease in Phosphorylase activity, which suggested that insulin-stimulated glucose transport was enough to upregulate glycogen synthesis despite the lack of GSK3 insulin-mediated inhibition. Nevertheless, as observed in Figure 4.2.2a 4.4c and 4.4d, insulin failed to increase myotube glucose transport. Indicating that the increase in myotube glycogen synthesis induced by insulin was not due to an upregulation of glucose transport, GS fractional activity nor an inactivation of Phosphorylase. Similarly in myoblasts, insulin failed to upregulate glucose transport, GS fractional activity however increased glycogen synthesis (as observed in Figure 4.2.2a). The Phosphorylase activity ratio in myoblasts was significantly decreased in response to insulin, albeit small, which would have brought on a decrease in glycogen breakdown and thus the net rate of incorporation of glucose would have increased as GS fractional activity remained the same with or without insulin treatment (Figure 4.4c). In addition to this, LPS plus cytokine treatment inhibited the insulin-mediated decrease in Phosphorylase activity ratio, suggesting a slight impairment to the insulin response. This is interesting because as discussed in Section 3.3.2, the insulin resistance induced by LPS plus cytokines on myoblast glycogen synthesis was not clear, however Figure 4.4d shows that the

18 hour treatment impaired the insulin-mediated inactivation of Phosphorylase, suggesting a degree of resistance.

Another way of assessing GS levels and activity is by probing for the protein with the use of SDS-PAGE and Western blotting (as described in Section 2.13). In this case total levels of GS were assessed as well as the level of phosphorylated GS. In these experiments the antibody recognised the Serine^{641} phosphorylation site, the state of which is indicative of GS activity, being the site phosphorylated by GSK3, where increased phosphorylation indicates a less active GS (Jensen 2009).

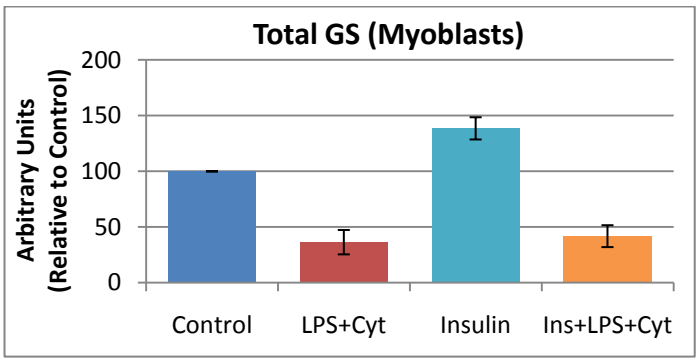

Fig. 4.4e. Sum of the optical densities of total GS protein in myoblasts. Cells were treated as described in Section 2.2.5. Results shown are the mean units ± SEM from 4 independent experiments

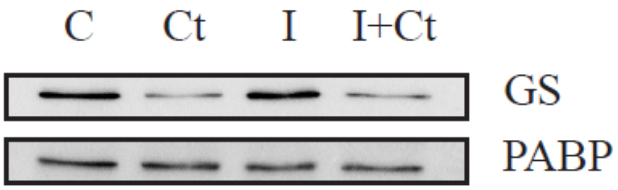

Fig. 4.4f. Example of a Western blot for total GS alongside loading control (PABP). Visualised using ECL, GS band runs between 85 and 90 KDa. C=Control, Ct=LPS+Cyt, I=Insulin, I+Ct=Ins+LPS+Cyt

Figure 4.4e shows the total levels of GS present in myoblasts under the various treatments. LPS plus cytokine treatment clearly downregulated total levels of GS regardless of insulin treatment (by roughly 60%), while insulin alone partially increased the levels (by about 40%). This result is intriguing because LPS plus cytokines significantly

upregulated myoblast glycogen synthesis, suggesting that the considerably lower levels of GS in the treated myoblasts must have been significantly more active than in the untreated cells. Moreover, these Western blot data would suggest a very different situation than that portrayed by measurement of the total GS activity data displayed in Figure 4.4a, which clearly implied there to be no change in total levels of GS. This discrepancy between the

total enzyme activity and the total levels assessed by SDS-PAGE and Western blotting suggested that the lower levels of GS noted in LPS plus cytokine myoblasts shown in Figure 4.4e may be due to the harvesting protocol since the harvesting technique for the enzyme assay obtains a full cell extract, different to the one used to prepare samples for SDS-PAGE and Western blotting which excludes the nuclear fraction. Indeed skeletal muscle GS is known to translocate from the nucleus to the cytoplasm in response to glucose (Ferrer et al. 1997). Due to this, it was speculated whether the GS levels extracted for the Western blot in LPS plus cytokine treated myoblasts was failing to recover the whole population of GS as any GS associated with the nucleus would have been lost thus causing the underestimation of total GS levels. As a result a complete cell extract of myoblasts was obtained and GS levels were assessed.

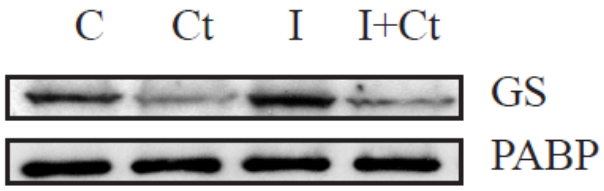

Fig. 4.4g. Example of a Western blot for total GS alongside loading control (PABP) in total myoblast cell extract. Visualised using ECL, GS band runs between 85 and 90 KDa. C=Control, Ct=LPS+Cyt, I=Insulin, I+Ct=Ins+LPS+Cyt

As the blot in Figure 4.4g shows, LPS plus cytokines still reduced total GS levels, suggesting that the data presented in Figure 4.4e was not due to an underestimation of total GS protein, and confirms that GS levels are reduced in response to LPS plus cytokine treatment. However, this still contrasts with the data presented in Figure 4.4a, which implied there was no change to total GS activity in myoblasts following LPS plus cytokine treatment.

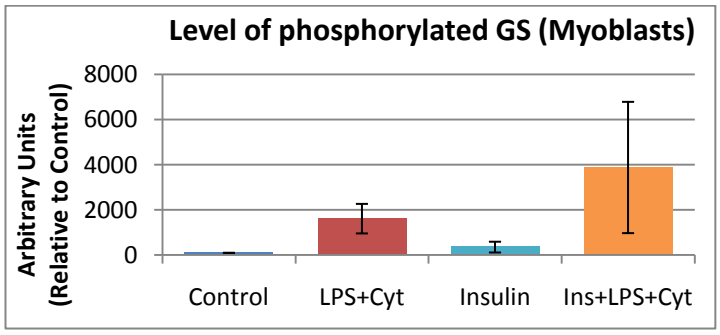

Fig. 4.4h hours. Sum of the optical densities of phosphorylated GS in myoblasts. Cells were treated as described in Section 2.2.5. Results shown are the mean units ± SEM from 4 independent experiments

Fig. 4.4i. Example of a Western blot for phosphorylated GS alongside the loading control (PABP). Visualised using ECL, GS band runs between 85 and 90 KDa. C=Control, Ct=LPS+Cyt, I=Insulin, I+Ct=Ins+LPS+Cyt

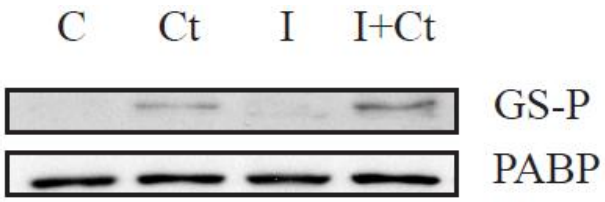

Figure 4.4h shows that phosphorylated GS levels were higher in LPS plus cytokine treated cells, suggesting an inhibition of GS activity. However since total GS levels were not the same between treatments, it is necessary to calculate the ratio of phosphorylated GS relative to total GS.

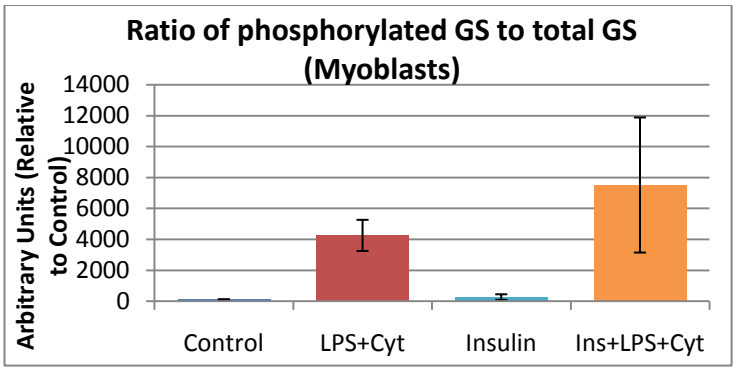

Fig. 4.4j. Proportion of phosphorylated GS relative to total GS in myoblasts. Cells were treated as described in Section 2.2.5. Results shown are the mean units ± SEM from 4 independent experiments

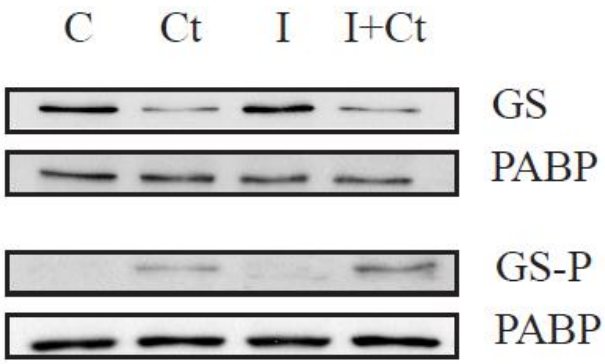

Fig. 4.4k. Example of a Western blot for phosphorylated GS and total GS alongside their respective loading controls (PABP). Visualised using ECL, GS band runs between 85 and 90 KDa. C=Control, Ct=LPS+Cyt, I=Insulin, I+Ct=Ins+LPS+Cyt

The graphs above show the ratio of phosphorylated GS to total GS in myoblasts. As introduced in Section 1.6.3, GS can be covalently and allosterically regulated. The former refers to its phosphorylation state, which includes numerous other phosphorylation sites besides Ser^{641} shown above (Jensen 2009). In this instance the LPS plus cytokines increased the ratio of phosphorylated to total GS relative to the untreated cells, thus indicating that GS was switched off as this phosphorylation site represents the site phosphorylated by GSK3, PASK or DYRK,

which is known to inhibit GS activity (Skurat and Dietrich 2004; Jensen 2009). Insulin had no significant effect on GS phosphorylation. Insulin should promote the dephosphorylation of GS at Site 3, however as seen in Figure 4.4k, there was no significant phosphorylated GS in the basal state, which would explain why insulin had no significant effect on the phosphorylation state of GS. This correlates with the lack of change in GS fractional activity (presented in Figure 4.4c) even after insulin stimulation. Myoblast GS appeared to be heavily phosphorylated in the basal state however, since the majority of the population was in the inactive b-form. As the results shown above indicate that GS was not basally phosphorylated at Site 3, this suggests that the low fractional activity of basal GS observed was probably due to the other inactivation site (Site 2).

As displayed in the Western blot in Figure 4.4j, regardless of taking into account the total levels of GS, LPS plus cytokine considerably increased the levels of phosphorylated GS, suggesting GS was considerably inactivated by covalent modification. This could be due to an LPS plus cytokine-mediated activation of GSK3, since basal GSK3 activity was likely very low, or also PASK and DYRK-mediated phosphorylation. Myoblast GSK3 activity is discussed in Section 5.3.1. These Western blot data contrast with results presented in Figure 4.4c since the fractional activity of myoblast GS was unchanged by LPS plus cytokine treatment, which suggested the phosphorylation state of GS remained the same. Nevertheless, as discussed above, Site 2 is likely phosphorylated – explaining the low basal fractional activity – which means that if LPS plus cytokine treatment increased Site 3 phosphorylation, fractional activity would not change significantly relative to control. Linking these results with those presented in Section 3.3.2 regarding glycogen synthesis would suggest that the increase in myoblast glycogen synthesis induced by the LPS plus cytokines is unlikely to involve an increase in GS activity or levels. This would correlate with the suggestion put forward by Bouskila et. al. regarding an increase in glycogen synthesis that did not require the activation of GS via inhibition of GSK3α/β (Bouskila et al. 2008). Indeed, LPS plus cytokines significantly increased glucose transport, which would be enough to increase glycogen synthesis, as discussed by Ren et. al. (Ren et al. 1993). In addition, Elsner et. al. noted an increase in glycogen synthesis over a 4 hour period in L6 myotubes which correlated with an increase in G-6-P levels and intracellular glucose but surprisingly the GS-a population significantly decreased throughout the incubation, which could help explain the myoblast results (Elsner et al. 1998).

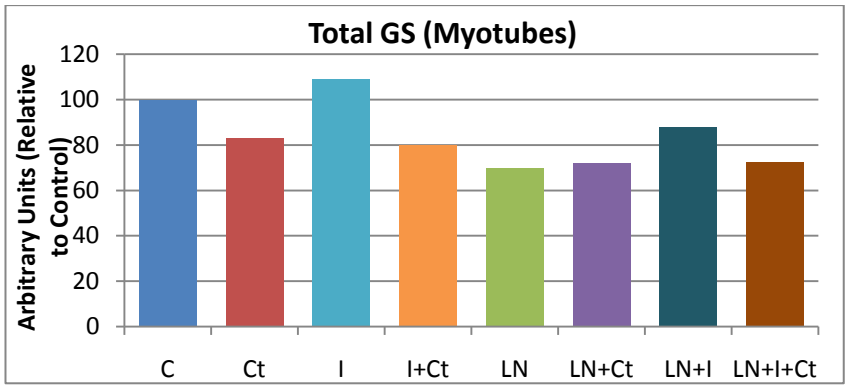

Fig. 4.4l. Sum of the optical densities of total GS protein in myotubes. Cells were treated as described in Section 2.2.5. Results shown are the mean units from 2 independent experiments (C=Control, Ct=LPS+Cyt, I=Insulin, I+Ct=Ins+LPS+Cyt, LN=L-NAME)

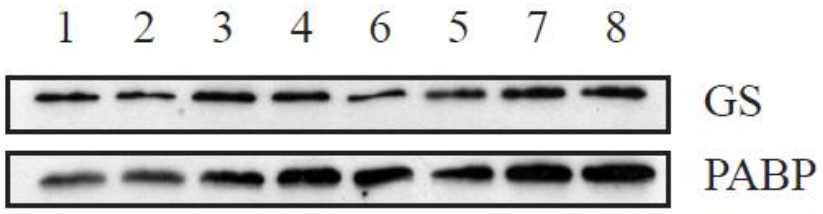

Fig. 4.4m. Example of a Western blot for total GS alongside the loading control (PABP). Visualised using ECL, GS band runs between 85 and 90 KDa. 1=C, 2=Ct, 3=I, 4=I+Ct, 5=LN, 6=LN+Ct, 7=LN+I, 8=LN+I+Ct.

Figure 4.4j shows the total levels of GS present in the myotubes under the various different treatments. No large significant change in total GS was observable among the treatments as noted in the myoblast data. This data correlates with the results presented in Figure 4.4a, where no change to total GS activity was observed in the myotubes treated with LPS plus cytokines, insulin or both. However L-NAME treated myotubes did appear to express lower levels of GS.

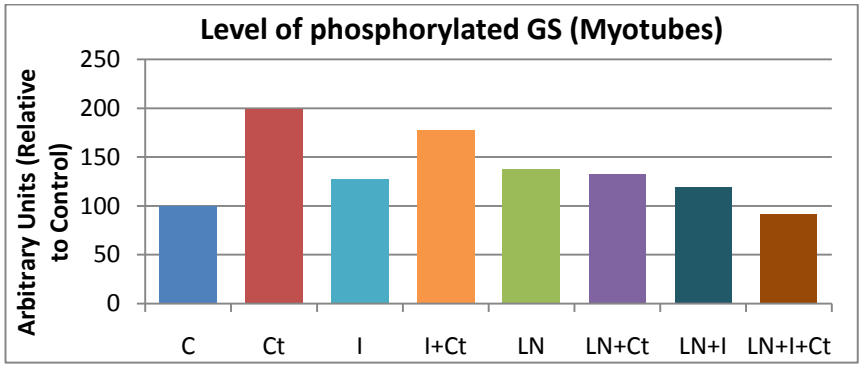

Fig. 4.4n. Sum of the optical densities of phosphorylated GS protein in myotubes. Cells were treated as described in Section 2.2.5. Results shown are the mean units from 2 independent experiments (C=Control, Ct=LPS+Cyt, I=Insulin, I+Ct=Ins+LPS+Cyt, LN=L-NAME)

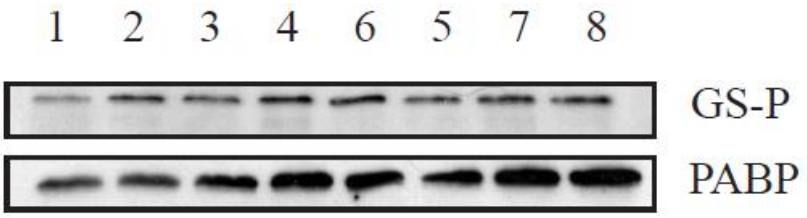

Fig. 4.4o. Example of a Western blot for phosphorylated GS alongside the loading control (PABP). Visualised using ECL, GS band runs between 85 and 90 KDa. 1=C, 2=Ct, 3=I, 4=I+Ct, 5=LN, 6=LN+Ct, 7=LN+I, 8=LN+I+Ct.

Figure 4.4n shows the levels of phosphorylated GS in the various treatments in myotubes. LPS plus cytokines inhibited GS activity, as seen by the increase in GS phosphorylation. This appeared to be a NO-dependent process, as when LPS plus cytokine treated myotubes were incubated with L-NAME, the increase in GS phosphorylation was prevented. This would coincide with the myotube glycogen synthesis results discussed in Section 3.3.3, where L-NAME prevented the LPS plus cytokine induced downregulation in glycogen synthesis. The ratio of phosphorylated GS relative to total GS is presented below.

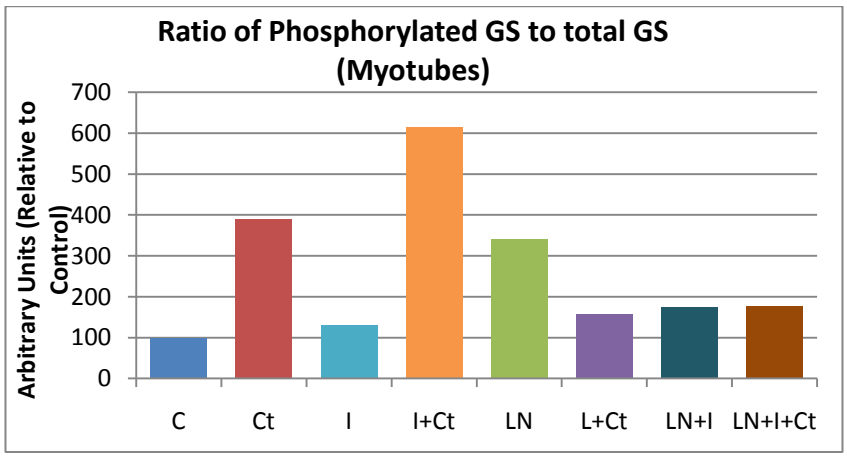

Fig. 4.4p. Proportion of phosphorylated GS relative to total GS in myotubes. Cells were treated as described in Section2.2.5. Results shown are the mean units ± SEM from 2 independent experiments

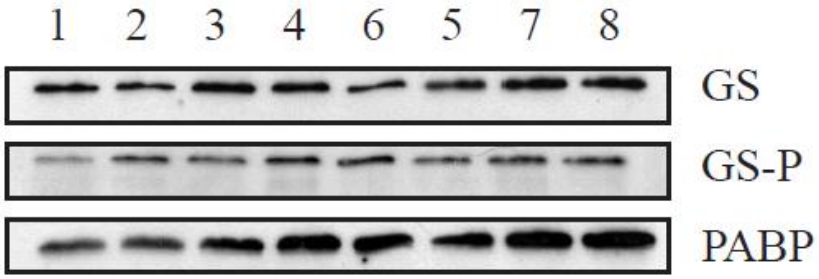

Fig. 4.4q. Example of a Western blot for phosphorylated and total GS alongside the loading control (PABP) in myotubes. Visualised using ECL, GS band runs between 85 and 90 KDa. 1=C, 2=Ct, 3=I, 4=I+Ct, 5=LN, 6=LN+Ct, 7=LN+I, 8=LN+I+Ct.

Figure 4.4p shows the ratio of phosphorylated GS relative to total GS in myotubes following the various treatments. As shown, LPS plus cytokines increased the ratio, regardless of insulin stimulation, as seen in Figure 4.4n and much like the myoblast GS-Ser^{641} results presented in Figure 4.4h. The other treatments failed to considerably increase the ratio of phosphorylated GS relative to total GS levels except an apparent increase in myotubes incubated with L-NAME only. As shown in Figure 4.4c, myotube GS fractional activity was low, indicating the majority of the GS population to be phosphorylated. The figure above shows that GS was basally phosphorylated at Site 3, correlating with the fractional activity results, however LPS plus cytokines increased GS phosphorylation which was not apparent in Figure 4.4c. This appeared to be NO-dependent, since L-NAME and LPS plus cytokine treated myotubes failed to stimulate GS phosphorylation. These results would therefore coincide with the myotube glycogen synthesis data presented in Section 3.3.4 as L-NAME prevented the LPS plus cytokine-induced downregulation in glycogen synthesis. As a result it is likely that this increase in GS phosphorylation at Ser^{641} contributed to the LPS plus cytokine-mediated decrease in myotube glycogen synthesis. Despite the basal level of phosphorylated GS, insulin failed to reduce it, which correlates with the apparent lack of insulin response observed in the myotubes throughout this chapter. In addition this suggests that the insulin resistant phenotype observed in myotubes regarding glycogen synthesis (Section 3.3.2) cannot be explained by an impairment to an insulin-stimulation of GS, but must be due to another mechanism.

4.5 Effect of LPS plus Cytokine Treatment on Levels of Glucose-6-Phosphate and UDP-Glucose in C2C12 Myocytes

As described in Section 1.6, glucose is converted to G-6-P as soon as it enters skeletal muscle, and is then channelled to glycogen synthesis or glycolysis depending on the metabolic state of the cell (Ferrer et al. 2003). G-6-P is a potent allosteric activator of GS, promoting glycogen synthesis (VillarPalasi and Guinovart 1997). Therefore determining G-6-P levels can indicate the state of glucose transport as well as the potential for glycogen synthesis. UDP-glucose on the other hand is the substrate of GS, so determining its levels under the various treatments can indicate the flux of glucose into glycogen, shedding light on the results already discussed in Chapter 3 and above. The cells were harvested and samples prepared before

assessing total cellular G-6-P or UDP-glucose as described in Sections 2.10 (G-6-P assay) and 2.11 (UDP-glucose assay).

The results from both myoblast and myotube samples gave values that were below the lowest standard, failing to be within the range of sensitivity of the assay, thus making it difficult to compare the levels of either metabolite from one treatment to the next. This was not a case of a problem with the assay since the standard curves for both assays were linear with increasing concentration of G-6-P and UDP-glucose, indicating that the activities of the enzymes used within the assay and the conditions enabled the appropriate reactions, as seen by the standard curves in the figure below.

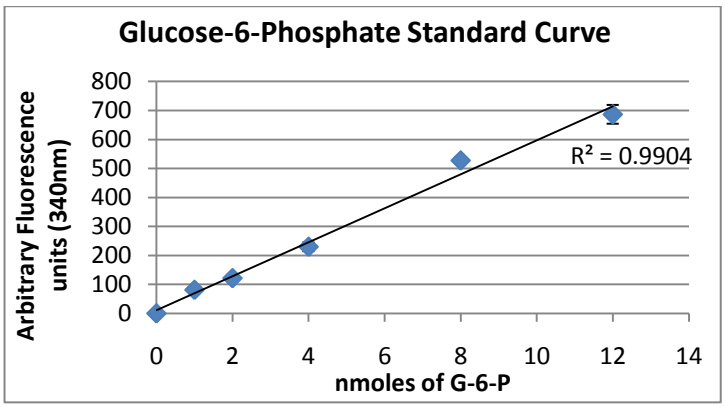

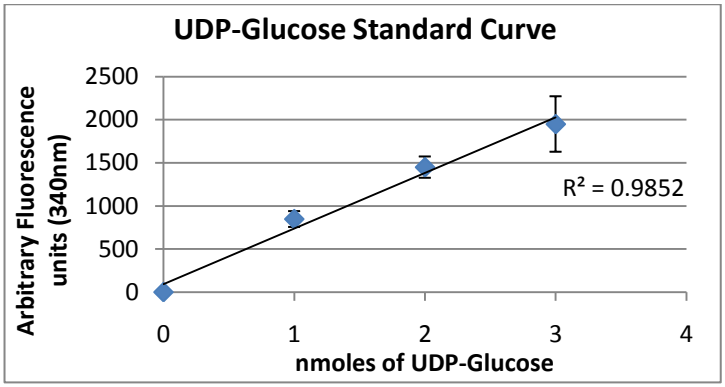

Fig. 4.5a. Graphs showing the standard curves obtained for the G-6-P and UDP-glucose assays. Results shown are the mean nmoles ± SEM from 3 independent experiments

Giving a value of 0.1nmoles as the lowest level possible within both these standards, added to the fact that roughly 200µg of myotube protein were present in the assay well would give a value of 0.5nmoles/mg of protein. This would be the maximum amount of G-6-P and UDP-glucose present in the myotubes. Similar to this value, a study using L6 myotubes grown in medium containing 5mM glucose reported basal G-6-P levels of 0.5nmoles/mg of protein (Elsner et al. 1998). The studies performed by Elsner et. al. looked at optimum conditions for myoblast differentiation: glucose concentration and the use of factors such as creatine and dexamethasone (Elsner et al. 1998). The study reported that an increase in glucose

concentration within the medium upregulated glucose levels in the cell, which correlated with a significant increase in G-6-P levels, and glycogen deposition over 4 hours but no increase in GS fractional activity, if not a surprising decrease in the levels of GS-a (Elsner et al. 1998). These results would confirm the suggestion that the increase in glucose uptake observed in the myoblasts treated with LPS plus cytokines would have contributed to an increase in glycogen synthesis.

4.6 Summary

The basal rates of glucose uptake between the myoblasts and myotubes were comparable, although the myotubes did express a marginally significant 19% increased rate. The incubation of myoblasts with LPS plus cytokines for 18 hours significantly increased glucose uptake, by 71%, which contrasted with the same measurement in myotubes where there was no change. This significant increase in myoblast glucose transport in response to LPS plus cytokines was comparable to the significant upregulation induced by the same treatment on myoblast glycogen synthesis, since the average percentage stimulations induced in both cases were not statistically different ($p=0.35$). Correlating with this, studies have put much emphasis on glucose transport modulating glycogen synthesis (Ren et al. 1993; Hansen et al. 1995), indicating that this increase in myoblast glucose transport is likely to explain the increase in myoblast glycogen synthesis under the same treatment. In contrast, the significant LPS plus cytokine induced downregulation in myotube glycogen synthesis (Figure 3.3.1a) cannot be explained by an alteration to the rate of myotube glucose transport, suggesting the role of other underlying mechanisms.

Insulin stimulated myotube and myoblast glycogen synthesis, as described in Section 3.3.2, however failed to increase glucose transport in either myocyte preparation, implying that the former stimulation cannot be explained by an increase in glucose transport. Correlating with this however, there is considerable evidence in the literature that describes the difficulty of measuring the insulin-stimulated glucose uptake rate in C2C12 cells (Schmitz-Peiffer et al. 1999; Tortorella and Pilch 2002; Nedachi and Kanzaki 2006; Lorenzo 2008). The rate of glycogen synthesis in insulin and LPS plus cytokine treated myoblasts was significantly higher than the rate of glycogen synthesis in myoblasts treated with LPS plus cytokines alone, however the rate of glucose transport in both was not significantly different. Since insulin treatment on its own failed to significantly increase glucose transport the results imply that insulin stimulated glycogen synthesis via a route independent of glucose transport. Equally this

would suggest that LPS plus cytokines and insulin did not upregulate myoblast glycogen synthesis via a similar mechanism, which could imply that there had been insulin resistance on myoblast glycogen synthesis following LPS plus cytokine treatment, although this cannot be confirmed. In addition, the lack of a significant insulin-mediated increase in glucose transport could suggest that LPS plus cytokines may have increased glucose uptake via GLUT1 expression as described in previous studies (Vary et al. 1995; Bedard et al. 1997; Ciaraldi et al. 1998), or a stimulation of GLUT1 intrinsic activity (Bedard et al. 1997).

LPS plus cytokine treatment had no effect on myotube glucose uptake, however did significantly increase the rate when co-treated with L-NAME (Figure 4.2.3b). This would imply that NO production prevented an LPS plus cytokine-mediated increase in glucose uptake. This result may help explain why L-NAME treatment prevented the LPS plus cytokine induced downregulation of myotube glycogen synthesis (Figure 3.3.3d**).** In contrast, in the myoblasts L-NAME failed to significantly affect the LPS plus cytokines mediated upregulation in glucose uptake, as seen by comparable increments induced by the treatment. This suggests that glucose uptake was stimulated in an NO-independent manner, correlating with the myoblast glycogen synthetic results presented in Section 3.3.3 where L-NAME also failed to significantly alter the LPS plus cytokine induced increase in glycogen synthesis.

In addition to testing the role of NO in the LPS plus cytokine mediated upregulation of glucose uptake, oxidative stress was addressed. A free-radical scavenger (Euk8), and an inhibitor of NFκB (PDTC) were used in conjunction with the LPS plus cytokine treatment. LPS plus cytokines significantly increased glucose uptake in cells treated with Euk8 or PDTC, suggesting that the antioxidant properties of both Euk8 and PDTC failed to significantly affect the increase in glucose uptake. The rate of uptake from myoblasts treated with PDTC and LPS plus cytokines was significantly lower than the rate of uptake from LPS plus cytokine treated myoblasts, suggesting a slight impairment occurred. However the average percentage increase induced by LPS plus cytokines with or without PDTC (when compared on a paired basis) was not statistically different ($p=0.17$), indicating that there was no significant change to the LPS plus cytokine mediated increase in glucose uptake. In addition to this PDTC completely prevented the accumulation of NOx, which would re-affirm the fact that NO did not appear to play an important role in the increase in glucose uptake following LPS plus cytokine treatment. Although the increased rates of glucose uptake in LPS plus cytokine treated myoblasts incubated with or without Euk8 were not significantly different ($p=0.12$) (Figure 4.4.2b), the average increments and average percentage stimulations from both treatments were significantly different (Figure 4.2.4c+d). This indicated that the scavenging of free radicals allowed for a more pronounced increase in glucose uptake, perhaps due to oxidant toxicity but

not cell viability since the EthD-1 results presented in Section 3.2.2 showed that LPS plus cytokines failed to affect cell viability. Moreover it clearly suggests that oxidant stress is an unlikely mechanism bringing about the LPS plus cytokine stimulated glucose uptake.

The total levels of GS and Phosphorylase in myotubes were considerably higher than in the myoblasts, as shown by the total enzyme assays (Figure 4.4a+b). Neither LPS plus cytokines, insulin stimulation nor both in combination significantly affected total levels of GS or Phosphorylase in myoblasts or myotubes. However, Western blot analysis of myoblast GS showed that LPS plus cytokines greatly reduced total GS levels (Figure 4.4e), contrasting with the myoblast GS enzyme assay. The basal activity ratios of GS and Phosphorylase in myoblasts suggested that the majority of both protein populations were phosphorylated; myoblast GS had a low fractional activity of 1.2% while myoblast Phosphorylase had a high activity ratio of 80%. The same was apparent for the myotubes, where GS had a fractional activity of 5% and Phosphorylase one of 60%.

The GS fractional activity and the Phosphorylase activity ratio in myoblasts was also unchanged following LPS plus cytokine treatment. In contrast to this though, the ratio of phosphorylated GS (Site 3) relative to total GS was increased, suggesting an inhibition of glycogen synthase activity. This LPS plus cytokine-induced phosphorylation of GS would not correlate with the fact that LPS plus cytokines increased myoblast glycogen synthesis, however as discussed, studies performed by Ren et. al. (Ren et al. 1993) observed an increased glucose transport rate due to raising the GLUT1 levels, which upregulated glycogen synthesis without increasing the activity ratio of GS. The mechanism of LPS plus cytokine induced upregulation of glycogen synthesis is more likely due to an increase in allosteric activation of glycogen synthase – resulting from a rise in G-6-P levels due to the increased flux of glucose into the cell. Insulin failed to stimulate myoblast GS activity however basal GS phosphorylation levels were low, which may explain the lack of insulin-response on GS, and may indicate that since myoblast GS fractional activities in control cells were low, that Site 2 may be heavily phosphorylated. Insulin significantly reduced myoblast Phosphorylase activity which would have contributed to the insulin-mediated increase in glycogen synthesis. This was impaired by LPS plus cytokine treatment however, suggesting a degree of insulin resistance, confirming the suggestion that LPS plus cytokines increased glycogen synthesis via a distinct mechanism than did insulin.

In the myotubes, both the GS fractional activity and Phosphorylase activity ratio were unchanged following LPS plus cytokine treatment, suggesting another mechanism was responsible for the treatment-induced downregulation in glycogen synthesis. However, Western blot analysis of GS levels and phosphorylation state (Site 3) revealed that the levels of

phosphorylated GS in LPS plus cytokine treated myotubes were considerably higher than in the control cells, correlating with the LPS plus cytokine induced downregulation of glycogen synthesis (Figure 3.3.1a). In addition, this increase in phosphorylation of GS appeared to be NO-mediated, since co-treatment with L-NAME ablated the effect. This latter observation also correlates with the myotube glycogen synthesis results presented in Section 3.3.3, as L-NAME prevented the LPS plus cytokine induced downregulation of glycogen synthesis. Insulin failed to stimulate myotube GS activity, as well as not reducing Phosphorylase activity. This together with the lack of insulin-stimulated glucose transport suggests the increase in myotube glycogen synthesis induced by insulin must be due to another mechanism.

Chapter Five – The State of the Signalling Machinery Following LPS plus Pro-Inflammatory Cytokine Treatment in C2C12 Myocytes

5.1 – Introduction

The previous two results chapters established the overall effects of LPS plus cytokine treatment on glycogen metabolism, specifically looking at the synthesis of glycogen, the uptake of glucose into the cell and the level of activity of GS and Phosphorylase. The next step was to attempt to elucidate how such effects occurred. As discussed in chapter 1, the stimulation of muscle cells with LPS, TNF-α, IL-1β, and IFN-γ brings about intracellular changes, such that a multitude of signalling cascades are initiated resulting in a wide range of activated or inhibited factors. In order to try and shed light on the possible factors contributing to the results presented in chapters 3 and 4 SDS-PAGE and Western blotting was used to look at the signalling molecules post treatment (as described in Section 2.13). Of the numerous signalling molecules affected by LPS plus cytokines, some have a role in glycogen metabolism under basal conditions and/or are stimulated by insulin. These signalling molecules were the initial ones looked at since they are more likely to contribute to the LPS plus cytokine induced effects observed on carbohydrate metabolism. In addition to this, insulin resistance can also be addressed.

AMPK (5' AMP-activated protein kinase) is an important energy sensor of the cell that becomes active when the AMP:ATP ratio is high (indicative of a low energy state in the cell). Once active, it subsequently switches off energy consuming processes like protein and glycogen synthesis while stimulating glucose uptake, glycolysis and fatty acid oxidation in order to restore the energy state of the cell (Fujii et al. 2006; Niesler et al. 2007; Towler and Hardie 2007; Jorgensen and Rose 2008). Although this is the most common route of AMPK activation, it is also physiologically activated by adipokines (cytokines released by adipose tissue such as TNF-α), as well as being modulated by NO (Fantuzzi 2005; Lira et al. 2007; Zhang et al. 2008). When active, AMPK phosphorylates GS at Site 2 (which is moderately inactivating), and stimulates the entry of glucose into the cell by modulating the intrinsic activity of GLUT1, increasing GLUT4 translocation and stimulating GLUT4 gene expression (Barnes et al. 2002; Jorgensen et al. 2004; Fujii et al. 2006; Hardie et al. 2006; Towler and Hardie 2007).

The MAPKs may also be important since they are activated by LPS plus cytokines (MacEwan 2002; Palsson-McDermott and O'Neill 2004; Subramaniam et al. 2004; Dauphinee and Karsan 2006; Kramer and Goodyear 2007; Lu et al. 2008). Indeed it has been noted that TNF-α alone or in combination with IFN-γ, can activate ERK and p38 in both in vitro and in vivo experiments (Del Aguila et al. 1999; Frost et al. 2003b; Tolosa et al. 2005; Chen et al. 2007; Austin et al. 2008; Plaisance et al. 2008). ERK is also a known target of the insulin-stimulated

cascade (Ragolia and Begum 1998; Toole and Cohen 2007), whereas it has been shown that p38 phosphorylates GS (promoting GSK3-mediated phosphorylation) and increases GLUT4 gene expression (Kuma et al. 2004; Kramer and Goodyear 2007). For these reasons it is necessary to address the potential roles played by AMPK, p38 and ERK within the C2C12 myocyte system under LPS plus cytokine treatment as it may help determine which signalling molecules were responsible for the effects the treatment had on glycogen metabolism.

Finally, Akt and GSK3 are both activated by LPS, and it is thought that GSK3 plays a key role in the modulation of the inflammatory response by regulating NFκB (Woodgett and Ohashi 2005; Jope et al. 2007). In the unstimulated state, GSK3 is active and maintains GS in a phosphorylated inactive form, until GSK3 itself is phosphorylated and rendered inactive by Akt, resulting in the induction of glycogen synthesis (Frame and Cohen 2001; Grimes and Jope 2001). Previous studies indicate that insulin regulates the synthesis of glycogen and glucose transport by transducing the signal through Akt and GSK3 (Cohen 2006). However as shown in the previous chapter, the GS enzyme assay failed to corroborate with the degree of phosphorylation of GS as measured by Western blotting, therefore assessing GSK3 and Akt activities, which lie upstream of GS, may help to shed light on the matter. An NO-dependent phosphorylation of GSK3β and inhibition of Akt has been demonstrated in C2C12 myotubes, suggesting that the LPS plus cytokine treatment may well modulate both in an NO-dependent manner (Yasukawa et al. 2005; Drenning et al. 2008). In addition to this it is known that LPS activates PI3K which lies upstream of the Akt-GSK3 cascade (Guha and Mackman 2001), while recent studies using C2C12 myotubes indicate that TNF-α alone (or in combination with IFN-γ) stimulated Akt and GSK3 phosphorylation (Tolosa et al. 2005; Austin et al. 2008; Plaisance et al. 2008). In contrast to this however, one study found that LPS and IFN-γ treatment on C2C12 myotubes inhibited the phosphorylation of Akt substrates (Frost et al. 2009), while another study noted a reduction in GSK3 phosphorylation after a septic abscess in rats (Vary et al. 2002). It is important to note that the timing of stimulation induced in these experiments is a possible explanation for the conflicting results; since signalling molecules can change their state very quickly in response to stimuli such as LPS, cytokines and insulin, as depicted in experiments carried out by Williamson et. al. and Tolosa et. al. using TNF-α and IFN-γ on C2C12 myotubes (Tolosa et al. 2005; Williamson et al. 2005). This point must be considered when discussing any literature in this chapter as experimental conditions vary considerably and the activation state of signalling molecules is regulated in a temporal manner. In addition to this, it must be noted that due to the semi-quantitative nature of Western blotting, results presented

in this chapter are indications as opposed to the precise values. As a result the Western blots results were used in parallel with other results previously presented in the thesis.

The myotube signalling experiments presented in this chapter included the presence of L-NAME since NO appeared to play a role in the LPS plus cytokine-induced downregulation of myotube glycogen synthesis, as seen in Section 3.3.3. Each bar chart presented in this chapter presents the optical density of a particular protein band (determined using ImageJ as described in Section 2.13.8), corrected for the loading control using PABP or Actin. In all the experiments discussed below, insulin stimulation was assessed by a 45 minute incubation with 1µM insulin following the 18 hours incubation with or without LPS plus cytokines. Following this, the cells were harvested and prepared for SDS-PAGE and Western blotting as described in Section 2.13.

5.2 Effects of LPS plus Cytokine Treatment on AMPK Levels and Activity in C2C12 Cells

5.2.1 Effects of LPS plus Cytokine Treatment on AMPK Levels and Activity in Myoblasts

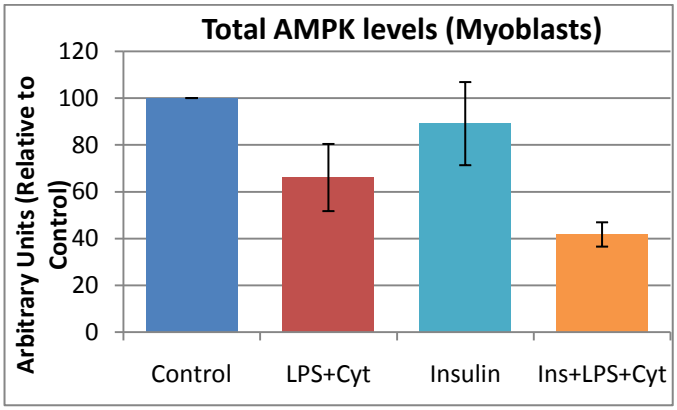

Fig. 5.2.1a. Sum of the optical densities of total AMPK protein in myoblasts. Cells were treated as described in Section 2.2.5. Results shown are the mean units ± SEM from 3 independent experiments

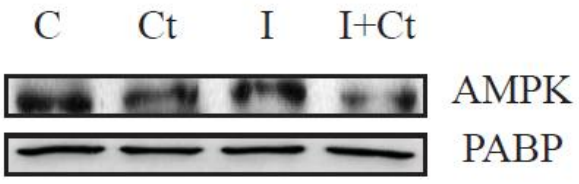

Fig. 5.2.1b. Example of a Western blot for total-AMPK with loading control (PABP) visualised using ECL, bands run at 62kDa. C=Control, Ct=LPS+Cyt, I=Insulin, I+Ct=Ins+LPS+Cyt

As displayed in the figures above, it appears as though the 18 hour LPS plus cytokine treatment reduced total levels of AMPK in myoblasts by roughly 35%. In the presence of insulin this reduction was more pronounced (roughly 60%). Insulin treatment on its own however did not appear to alter levels significantly. In contrast to this, a 24 hour incubation of isolated hepatocytes with LPS, TNF-α, INF-γ and IL-1β failed to alter total AMPK levels (Wallington et al. 2008), while Lira et. al. noted that the NO-donor (SNAP) failed to alter total levels of AMPK in L6 myotubes, suggesting that the results observed above are NO-independent (Lira et al. 2007).

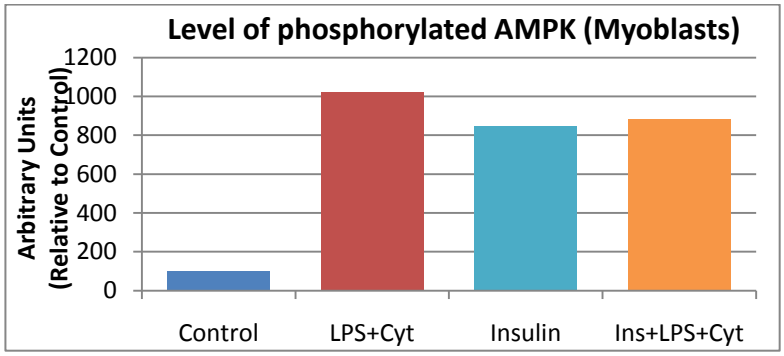

Fig. 5.2.1c. Sum of the optical densities of phosphorylated AMPK in myoblasts. Cells were treated as described in Section 2.2.5.
Results shown are the mean units from 2 independent experiments.

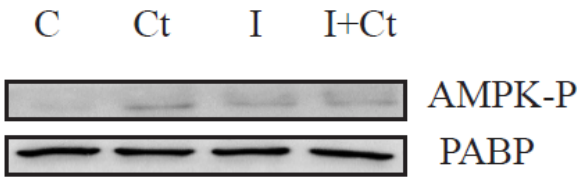

Fig. 5.2.1d. Example of a Western blot for phosphorylated AMPK alongside loading control (PABP). Visualised using ECL, AMPK band runs at 62kDa. C=Control, Ct=LPS+Cyt, I=Insulin, I+Ct=Ins+LPS+Cyt

As seen by the two figures above, AMPK was phosphorylated under LPS plus cytokine treatment, with or without insulin and also in the presence of insulin alone, suggesting it was more active. Since the total levels of AMPK altered between one treatment and the next, the levels of phosphorylated AMPK relative to total AMPK are presented in Figure 5.2.1e.

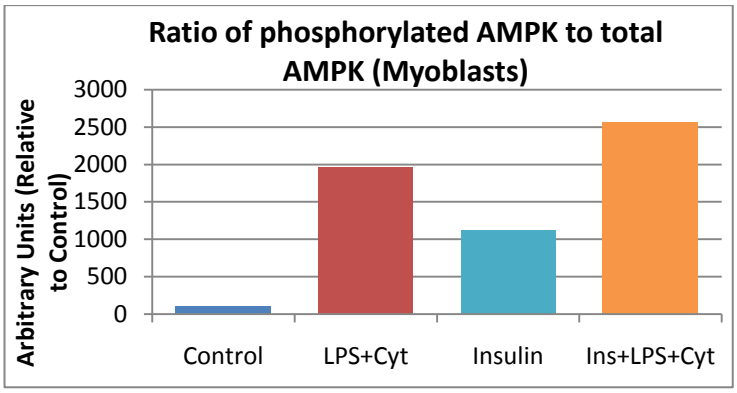

Fig. 5.2.1e. Proportion of phosphorylated AMPK relative to total AMPK in myoblasts. Cells were treated as described in Section 2.2.5. Results shown are the mean units from 2 independent experiments.

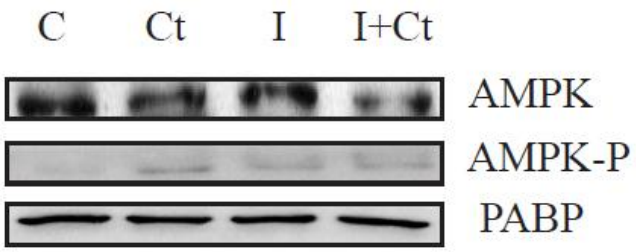

Fig. 5.2.1f. Example of a Western blot for phosphorylated AMPK alongside loading control and total AMPK plus its loading control. Visualised using ECL, AMPK band runs at 62kDa. C=Control, Ct=LPS+Cyt, I=Insulin, I+Ct=Ins+LPS+Cyt

Figure 5.2.1c displays the proportion of phosphorylated AMPK relative to the total AMPK levels in myoblasts. It is evident that the LPS plus cytokine treatment increased the proportion of phosphorylated AMPK to total AMPK, in the presence and absence of insulin. The insulin treatment also considerably increased the level of phosphorylated AMPK compared to the control value. This was surprising as AMPK stimulation by insulin is not an established mechanism in skeletal muscle cells, rather AMPK has been implicated in an insulin-sensitizing mechanism; via the phosphorylation of insulin receptor substrate-1 (IRS-1, which lies at the top of the insulin cascade) where it enhances the cascade (Towler and Hardie 2007). Insulin stimulation primarily occurs when nutrients are abundant, resulting in the promotion of anabolic processes such as glycogen synthesis and fat deposition (Cohen 2006). AMPK activity on the other hand, is associated with situations of energy stress, resulting in the promotion of ATP generation, which would oppose most of the insulin-mediated effects (Towler and Hardie 2007; Jorgensen and Rose 2008).

AMPK has been implicated in the regulation of glucose transport during contraction/exercise, in particular skeletal muscle GLUT4 translocation as well as GLUT1 intrinsic activity (Fujii et al. 2006; Lira et al. 2007; Towler and Hardie 2007; Deshmukh et al. 2010). As a result, it is possible that the stimulation of AMPK phosphorylation by the LPS plus cytokine treatment may have increased the capacity and rate of glucose transport in myoblasts. AMPK also regulates the synthesis of glycogen, by phosphorylating GS it partially

inhibits the process, thereby allowing the cell to regain a positive energy balance (Jorgensen et al. 2004; Fujii et al. 2006; Towler and Hardie 2007). The antibody used to probe for phosphorylated GS in Section 4.4 recognised the site phosphorylated by GSK3 (Site 3) whereas AMPK phosphorylates GS on Site 2 (Jensen 2009). This means that the level of phosphorylated GS in response to AMPK activation could not be assessed by this antibody. Nevertheless the results presented above would imply that LPS plus cytokines, and indeed insulin stimulation could have brought about the phosphorylation of GS. In contrast to this, the glycogen synthesis results presented in Chapter 3 would not suggest an inhibition of glycogen synthesis in response to LPS plus cytokines or insulin stimulation. On the one hand, increased activity of AMPK in response to LPS plus cytokines could potentially contribute to the increase in myoblast glucose transport observed (Figure 4.2.1b), however activated AMPK would also moderately inhibit GS. The GS enzyme assay presented in Section 4.4 showed that neither LPS plus cytokine nor insulin stimulation affected the activity ratio of the enzyme, implying that the state of GS phosphorylation was not altered by the treatments. In contrast, the ratio of phosphorylated GS relative to total GS determined by SDS-PAGE and Western blotting was indeed higher in LPS plus cytokine treated myoblasts (Figure 4.4j), indicating the enzyme was covalently modified yet glycogen synthesis was still significantly upregulated following LPS plus cytokine treatment (Figure 3.3.1a).

Despite these contrasting results, it is well established that the entrance of glucose into the cell is enough to stimulate glycogen synthesis due to the allosteric activation of GS by G-6-P (Ren et al. 1993; Hansen et al. 1995). So it cannot be excluded that the LPS plus cytokine-induced activation of AMPK in myoblast may have contributed to the increase in glucose transport observed in Section 4.2.1. Although if this was the case, Figure 5.2.1c shows that insulin treatment also increased the level of phosphorylated AMPK compared to the control, which would imply that glucose transport would have also been upregulated via the same mechanism, though it was not evident (as seen in Figure 4.2.2a). This would imply that AMPK is either not responsible, or not the sole contributing factor to the LPS plus cytokine induced upregulation of myoblast glucose transport. It has been shown that NO brings about the phosphorylation and activation of AMPK (Lira et al. 2007; Zhang et al. 2008; Deshmukh et al. 2010), and this could be the mechanism of activation in the myoblasts in response to LPS plus cytokines. If this was the case however, then it would imply that the NO-mediated phosphorylation and activation of AMPK had no real contributing role to the glucose transport and indeed glycogen synthesis observations, since L-NAME failed to alter any of the LPS plus cytokine induced effects in myoblasts as seen in Figures 3.3.3d and 4.2.3a.

5.2.2 Effects of LPS plus Cytokine Treatment on AMPK Levels and Activity in Myotubes

Myotubes were grown and treated as described in Section 2.2, followed by harvesting and preparation for SDS-PAGE and Western blotting as indicated in Section 2.13. 1mM L-NAME was added to the medium during the 18 hour LPS plus cytokine incubation.

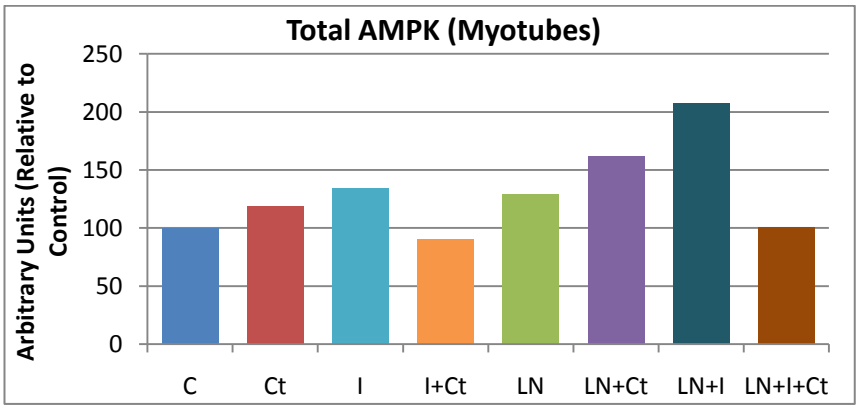

Fig. 5.2.2a. Sum of the optical densities of total AMPK protein in myotubes. Cells were treated as described in Section 2.2.5. Results shown are the mean units from 2 independent experiments. C=Control, Ct=LPS+Cyt, I=Insulin, I+Ct=Ins+LPS+Cyt, with or without LN=L-NAME

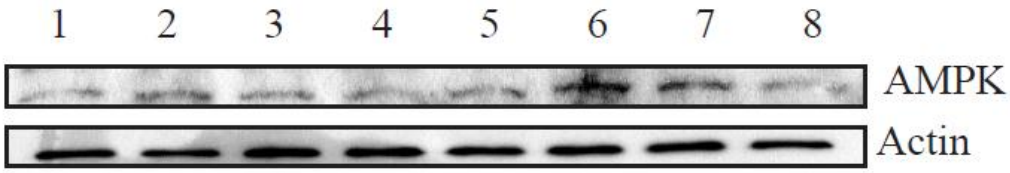

Fig. 5.2.b. Example of a Western blot for total AMPK along with the loading control (Actin) visualised using ECL, AMPK band runs at 62kDa. 1=C, 2=Ct, 3=I, 4=I+Ct, 5=LN, 6=LN+Ct, 7=LN+I, 8=LN+I+Ct.

Figure 5.2.2a displays the total levels of AMPK in myotubes after LPS plus cytokine treatment, with or without insulin stimulation. The LPS plus cytokine treatment did not have much effect on total levels of AMPK with or without insulin stimulation. Despite the slight differences, it appears as though neither LPS plus cytokines nor insulin significantly altered the levels of total AMPK in the cells. This is in contrast to the myoblast results from Figure 5.2.1a. In the presence of L-NAME, myotubes also treated with LPS plus cytokines or stimulated with insulin appeared to increase the total levels.

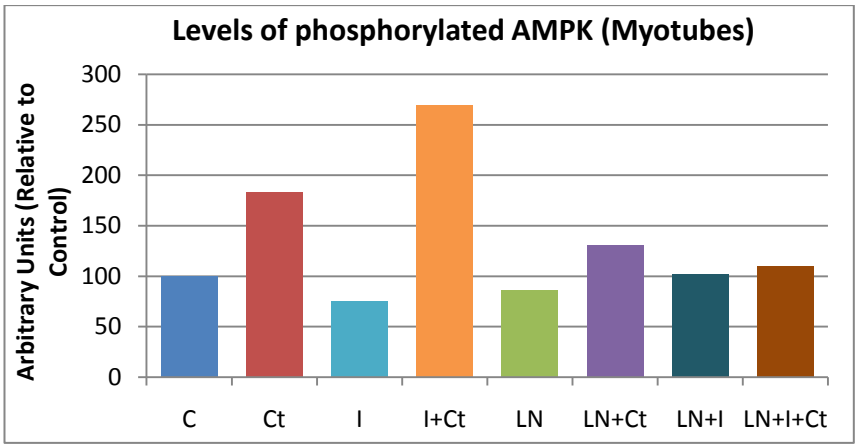

Fig. 5.2.2c. Sum of the optical densities of phosphorylated AMPK in myotubes. Cells were treated as described in Section 2.2.5. Results shown are the mean units from 2 independent experiments. C=Control, Ct=LPS+Cyt, I=Insulin, I+Ct=Ins+LPS+Cyt, with or without LN=L-NAME

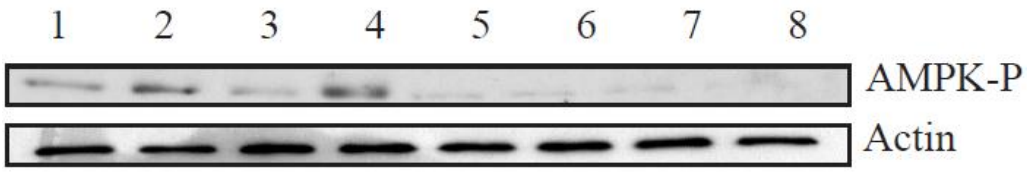

Fig. 5.2.2d. Example of a Western blot for phosphorylated-AMPK alongside loading control and total AMPK plus its loading control. Visualised using ECL, AMPK band runs at 62kDa. 1=C, 2=Ct, 3=I, 4=I+Ct, 5=LN, 6=LN+Ct, 7=LN+I, 8=LN+I+Ct.

As shown by the figures above, AMPK was phosphorylated by the LPS plus cytokine treatment, regardless of insulin stimulation, correlating with the myoblast results in Figure 5.2.1c where the same effect was observed. Nevertheless these myotube results contrast with the insulin-induced activation of AMPK observed in myoblasts, since insulin had no effect on the level of AMPK phosphorylation in myotubes. The LPS plus cytokine-mediated response was almost completely abrogated by L-NAME treatment, suggesting the activation of AMPK was NO-dependent. This would coincide with a study that showed that inhibition of NOS diminished AMPK activity in endothelial cells (Zhang et al. 2008) or that the NO-donor spermine NONOate increased AMPK activity in L6 cells (Deshmukh et al. 2010). As discussed above in Section 5.2.1, upon AMPK activation, glucose transport should be increased and glycogen synthesis partially inhibited – among other processes – yet as seen in Figure 4.2.1b, myotube glucose transport remained the same with or without LPS plus cytokine treatment. Taken together with the fact that the figures above suggest L-NAME reduced the LPS plus cytokine induced activation of AMPK, contradicts the idea that activated AMPK may have stimulated myotube glucose transport (Fujii et al. 2006; Lira et al. 2007; Towler and Hardie 2007; Deshmukh et al. 2010). The myotube results discussed in Section 3.3.3 showed that LPS

plus cytokine treatment significantly inhibited glycogen synthesis via a NO-dependent mechanism since the effect was rescued by L-NAME. This would correlate with the phosphorylation and activation of AMPK as AMPK phosphorylates and partially inhibits GS, hence it is possible that the NO-dependent activation of AMPK following LPS plus cytokine stimulation contributed to the downregulation in glycogen synthesis observed in the myotubes.

5.3 Effects of LPS plus Cytokine Treatment On Akt And GSK3 Levels and Activity in C2C12 Cells

5.3.1 Effects of LPS plus Cytokine Treatment on Akt and GSK3 Levels and Activity in Myoblasts

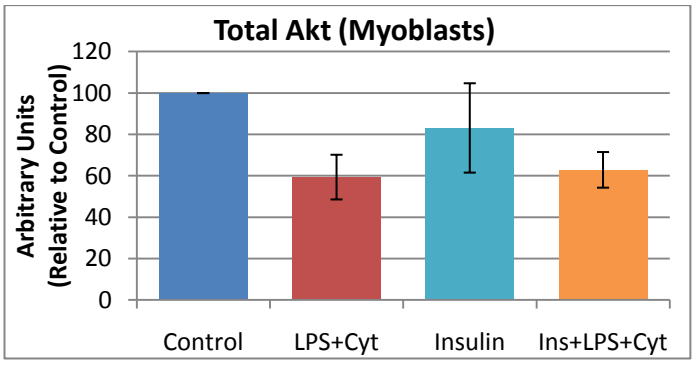

Fig. 5.3.1a. Sum of the optical densities of total Akt in myoblasts. Cells were treated as described in Section 2.2.5. Results shown are the mean units ± SEM from 3 independent experiments

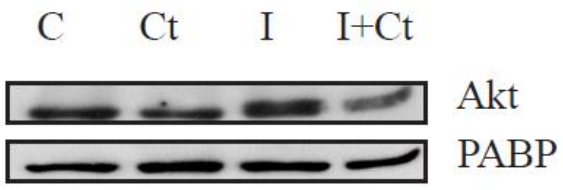

Fig. 5.3.1b. Example of a Western blot for total Akt the loading control (PABP). Visualised using ECL, Aktband runs at 60KDa. C=Control, Ct=LPS+Cyt, I=Insulin, I+Ct=Ins+LPS+Cyt,

Figure 5.3.1a shows the quantified levels of total Akt present in myoblast cells under each treatment. As shown, LPS plus cytokines decreased total levels of Akt compared to the control cells. The presence of insulin lowered the average, but failed to do so significantly. This pattern is similar to the one observed in Figure 5.2.1a for total AMPK levels in myoblasts.

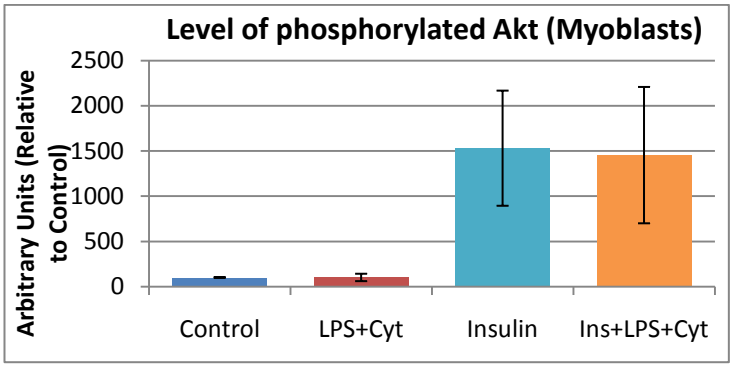

Fig. 5.3.1c. Sum of the optical densities of phosphorylated Akt (Thr308) in myoblasts. Cells were treated as described in Section 2.2.5. Results shown are the mean units ± SEM from 3 independent experiments

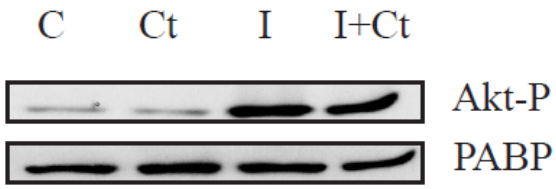

Fig. 5.3.1d. Example of a Western blot for phosphorylated Akt (Thr308) alongside the loading control (PABP). Visualised using ECL, Aktband runs at 60KDa. C=Control, Ct=LPS+Cyt, I=Insulin, I+Ct=Ins+LPS+Cyt,

The blot in Figure 5.3.1d shows that there was a low level of phosphorylated Akt in the untreated cells which was not altered by the LPS plus cytokine treatment. On the other hand, insulin increased the level of phosphorylated Akt (Thr308) in myoblasts, and the presence of LPS plus cytokines did not affect this stimulation, suggesting that the insulin response was not impaired. The ratio of phosphorylated Akt relative to total Akt is shown below, Figure 5.3.1e.

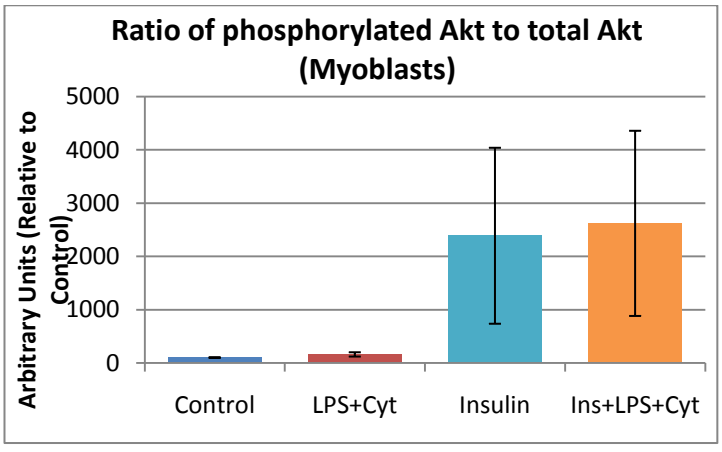

Fig. 5.3.1e. Proportion of phosphorylated Akt(Thr308) relative to total Akt levels in myoblasts. Cells were treated as described in Section 2.2.5. Results shown are the mean units ± SEM from 3 independent experiments.

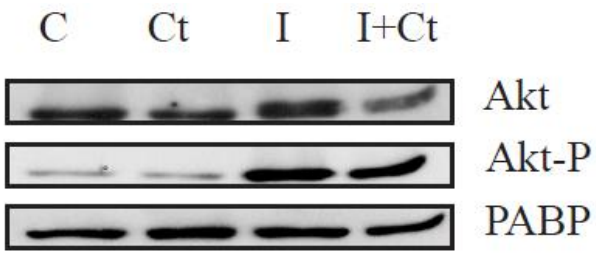

Fig. 5.3.1f. Example of a Western blot for phosphorylated Akt (Thr308) and total Akt alongside the loading control (PABP). Visualised using ECL, Aktband runs at 60KDa. C=Control, Ct=LPS+Cyt, I=Insulin, I+Ct=Ins+LPS+Cyt,

The results are very much the same as those presented in Figure 5.3.1c, showing the clear insulin-mediated stimulation of Akt phosphorylation, regardless of LPS plus cytokine treatment. Although the treatment alone increased the average ratio by approximately 60%, it was a very minimal change compared to the clear increase induced by insulin, suggesting LPS plus cytokines failed to induce Akt phosphorylation and activation. Activation of Akt is critical for the insulin response, and the fact that insulin-mediated Akt phosphorylation was not hindered by the presence of LPS plus cytokines would correlate with the proposal that the potential insulin-resistance observed in myoblasts in Section 3.3.2 was more likely due to glycogen synthesis reaching a maximal rate. In contrast, this would not correlate with the LPS plus cytokine-induced impairment to the insulin-mediated inhibition of Phosphorylase, as discussed in Section 4.4. The result shown in Figure 5.3.1e is in contrast to the suggestion that inflammatory cytokines induce skeletal muscle insulin resistance via steps upstream of Akt, resulting in an impaired activation of Akt (Hotamisligil et al. 1994; Hotamisligil et al. 1996; Rui et al. 2001; Austin et al. 2008). Other evidence suggests that NO impairs the insulin response, by nitrosylation of Akt, resulting in diminished activation but unaltered phosphorylation (Marette 2002; Yasukawa et al. 2005). Therefore it is possible that despite the unimpaired insulin-mediated phosphorylation of Akt after LPS plus cytokine treatment, that the activity of Akt was hindered by NO production. Despite not having co-treated myoblasts with L-NAME and performed Western blots, the glycogen synthetic results observed in Section 3.3.2 were unchanged by the presence of L-NAME, suggesting NO was not responsible.

The data dealing with total Akt levels coincides with two studies which also noted a reduction in total Akt levels; the in vitro study used differentiating C1C12 myocytes which were treated for 5 days with TNF-α (Grzelkowska-Kowalczyk and Wieteska-Skrzeczynska 2009) while the in vivo study treated rats with LPS for 24 hours (1.5mg/100mg/h) (Crossland et al. 2008). In accordance with the results presented in Figure 5.3.1e, studies in C2C12 myotubes also noted no change to the ratio of phosphorylated Akt (Thr308) to total Akt after a 24 hour treatment with TNF-α and IFN-γ (5ng/ml each) (Dehoux et al. 2007), or a 14h treatment with LPS (1ug/ml)

and IFN-γ (3ng/ml) (Frost et al. 2009). On the other hand, Akt activation was observed in C2C12 myotubes in response to a 10 and 60 minute treatment with TNF-α and IFN-γ (each at 10ng/ml) (Tolosa et al. 2005; Plaisance et al. 2008). It must be said however that this latter study treated the cells for a considerably shorter time compared with the 18 hour treatment induced in the experiments presented in this thesis, as a result it is possible that this effect was no longer visible after the 18 hours treatment.

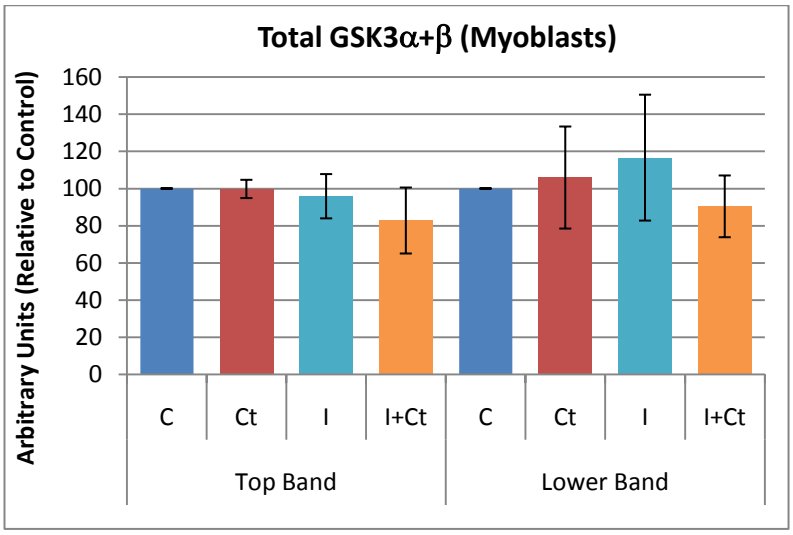

Fig. 5.3.1e. Sum of the optical densities of total GSK3α+β levels in myoblasts. Cells were treated as described in Section 2.2.5. Results shown are the mean units ± SEM of 4 independent experiments
C=Control, Ct=LPS+Cyt, I=Insulin, I+Ct=Ins+LPS+Cyt.

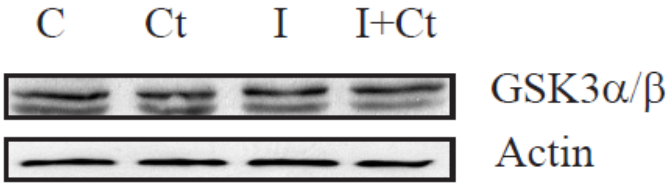

Fig. 5.3.1f. Example of a Western blot for total GSK3α+β plus its loading control (Actin). Visualised using ECL, GSK3α and GSK3β bands run at 51 and 46KDa, respectively. C=Control, Ct=LPS+Cyt, I=Insulin, I+Ct=Ins+LPS+Cyt,

GSK3 comes in two isoforms, GSK3α and GSK3β, they are very closely related with 97% sequence identity, and are ubiquitously expressed in mammalian tissue (Frame and Cohen 2001). GSK3α represents the top band (51KDa) and GSK3β the lower band (46KDa). Figure 5.3.2e displays the average levels of GSK3α and GSK3β present in myoblasts after LPS plus cytokine treatment, with or without the stimulation of insulin. As seen in these figures, neither the LPS plus cytokine treatment, the insulin stimulation nor both together significantly affected the levels of GSK3 in myoblasts. In accordance with these results, Dehoux et. al. treated C2C12 myotubes with TNF-α and IFN-γ (5ng/ml each) for 24 hours and noted no change in total levels of GSK3α/β (Dehoux et al. 2007).

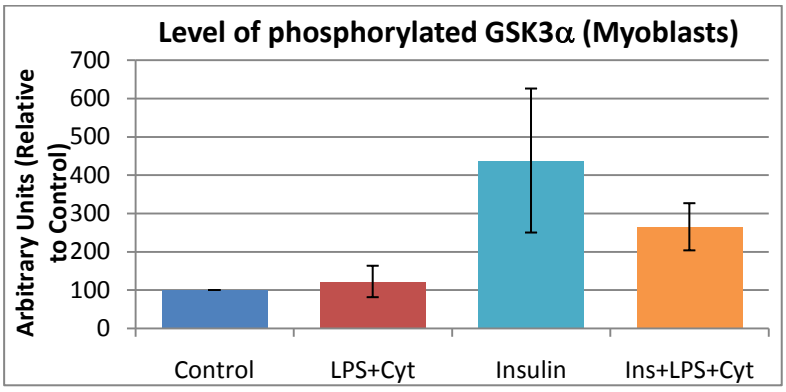

Fig. 5.3.1g. Sum of the optical densities of phosphorylated GSK3α in myoblasts. Cells were treated as described in Section 2.2.5. Results shown are the mean units ± SEM of 3 independent experiments

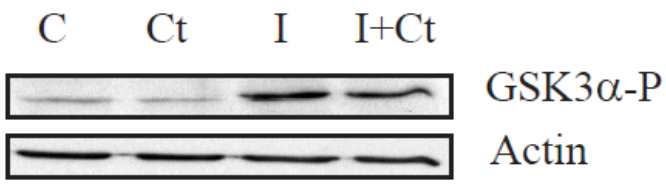

Fig. 5.3.2h. Example of a Western blot for phosphorylated GSK3α+β plus the loading control. Visualised using ECL, GSK3α and GSK3β bands run at 51 and 46KDa, respectively. C=Control, Ct=LPS+Cyt, I=Insulin, I+Ct=Ins+LPS+Cyt,

Figure 5.3.2g shows the level of phosphorylated GSK3α under the various treatments in myoblasts. The levels of phosphorylated GSK3β were not included because no change was apparent between the treatments. 18 hours of LPS plus cytokine treatment failed to significantly increase GSK3α phosphorylation, while the insulin response was clear, inducing a significant increase in the level of phosphorylated GSK3α. This result correlates with the insulin-stimulation of myoblast Akt since phosphorylated and activated Akt leads to GSK3 phosphorylation. In Chapter 3, it was shown that myoblast glycogen synthesis was upregulated by LPS plus cytokine treatment. With regards to GSK3 activity, the figures above suggest that GSK3 was still active and thus able to inhibit GS. This coincides with the Western blot data presented in Section 4.4 since GS was phosphorylated under LPS plus cytokine conditions, contrasting with the control results. Yet the data above suggests GSK3 activity remained roughly the same between control and LPS plus cytokine treated cells, which would imply that the GSK3-mediated phosphorylation of GS would also have been fairly consistent between control and LPS plus cytokine treated cells, which was not the case (Figure 4.4h). In addition insulin-stimulated myoblasts treated with LPS plus cytokines also displayed increased GS phosphorylation while in contrast, as shown above, GSK3 was inhibited under the same treatment, albeit to a lesser extent than untreated cells stimulated with insulin, indicating that

GS phosphorylation at Site 3 should have been decreased. These latter points may suggest that other Site 3 kinases were responsible for the increased phosphorylation of GS. Nevertheless, insulin increased GSK3α phosphorylation regardless of the presence of LPS plus cytokines – despite the lower average relative to untreated cells – correlating with the Akt data presented in Figure 5.3.1e which also showed no LPS plus cytokine-induced effect on the insulin-mediated phosphorylation of Akt. Both these results confirm the fact that LPS plus cytokines did not significantly impair the Akt-mediated insulin response in myoblasts.

5.3.2 Effects of LPS plus Cytokine Treatment on Akt and GSK3 Levels and Activity in Myotubes

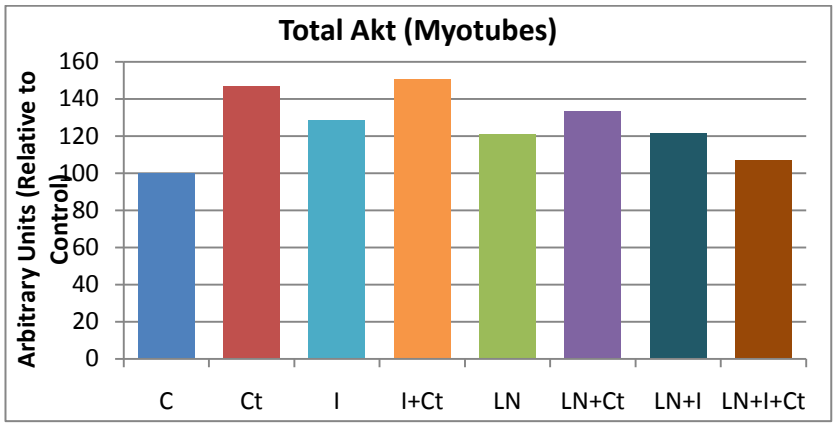

Fig. 5.3.2a. Sum of the optical densities of total Akt levels in myotubes. Cells were treated as described in Section 2.2.5. Results shown are the mean units from 2 independent experiments
C=Control, Ct=LPS+Cyt, I=Insulin, I+Ct=Ins+LPS+Cyt, with or without LN=L-NAME

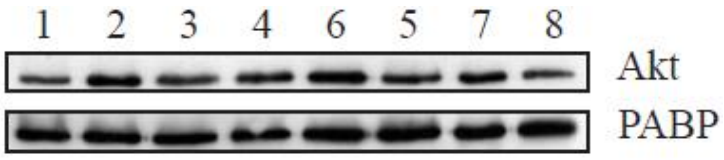

Fig. 5.3.2b. Example of a Western blot for total Akt plus its loading control (PABP). Visualised using ECL, Akt band runs at 60KDa
1=C, 2=Ct, 3=I, 4=I+Ct, 5=LN, 6=LN+Ct, 7=LN+I, 8=LN+I+Ct.

Figure 5.3.2a displays the total Akt levels in myotubes treated with or without insulin, L-NAME, and LPS plus cytokine. The figure shows that LPS plus cytokines increased total Akt levels regardless of the presence of insulin. This contrasts with the myoblast data in Figure 5.3.1a, where LPS plus cytokines reduced total Akt levels. The levels of Akt in L-NAME treated

myotubes were slightly higher than the levels in control cells, however this was unlikely to be significant.

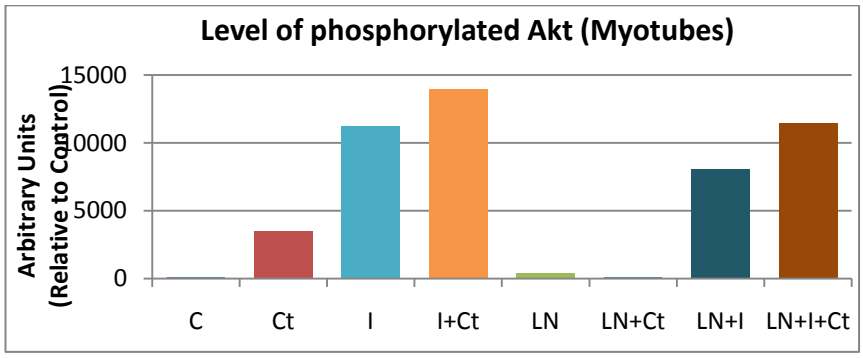

Fig. 5.3.2c. Sum of the optical densities of phosphorylated Akt (Thr308) in myotubes. Cells were treated as described in Section 2.2.5. Results shown are the mean units from 2 independent experiments ± variation from the mean
C=Control, Ct=LPS+Cyt, I=Insulin, I+Ct=Ins+LPS+Cyt, then same treatments with or without LN=L-NAME

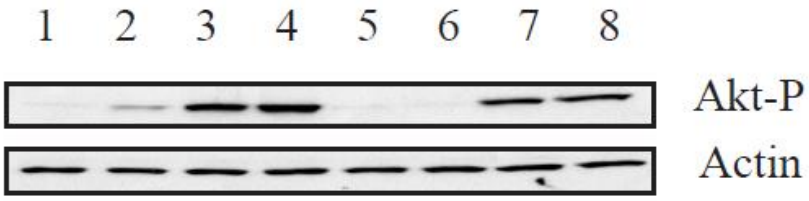

Fig. 5.3.2d. Example of a Western blot for phosphorylated Akt (Thr308) alongside the loading control (Actin). Visualised using ECL, Akt band runs at 60KDa
1=C, 2=Ct, 3=I, 4=I+Ct, 5=LN, 6=LN+Ct, 7=LN+I, 8=LN+I+Ct.

Figure 5.3.2c displays the amount of phosphorylated Akt (Thr308) present in the myotubes after the various treatments. The 18 hour LPS plus cytokine treatment increased Akt phosphorylation relative to the control, which contrasts with the corresponding myoblast experiments (Figure 5.3.1c). Insulin stimulation greatly increased the amount of phosphorylated Akt, and the response was not impaired by LPS plus cytokines, correlating with the myoblast data presented in Section 5.3.1. The addition of L-NAME failed to affect the results except the LPS plus cytokine-mediated phosphorylation of Akt, suggesting that this effect may be NO-dependent.

Once activated, Akt stimulates glucose transport, especially in an insulin-dependent manner (Tremblay et al. 2003; Cohen 2006). According to this, it could be suggested that since LPS plus cytokines activated Akt, an increase in glucose transport may have occurred, however as displayed in Section 4.2.2, myotube glucose transport was un-altered by LPS plus cytokine treatment. The only change in myotube glucose uptake observed in Chapter 4 was when cells were treated with L-NAME and LPS plus cytokines, yet as presented above, the level of phosphorylated Akt was not increased, suggesting Akt is an unlikely mediator of this increase

in glucose uptake. In addition, Figure 5.3.2c shows an insulin-mediated increase in Akt phosphorylation, yet glucose transport was un-affected by insulin in myotubes, further emphasising the difficulty of measuring an insulin-stimulated glucose uptake rate in in vitro models of skeletal muscle, as discussed in Section 4.2.2 (Tortorella and Pilch 2002; Nedachi and Kanzaki 2006; Lorenzo 2008). Tortorella et. al. induced GLUT4 expression via dexamethasone treatment, yet still failed to observe an insulin-dependent increase in glucose transport despite also noting an apparent normal signalling cascade through Akt, correlating with the results presented here (Tortorella and Pilch 2002). Similar to the myoblast results shown in the previous section, insulin stimulation of Akt was unchanged by LPS plus cytokine treatment, contrasting with some lines of evidence that suggest an impairment to the insulin-mediated activation of Akt (Hotamisligil et al. 1994; Hotamisligil et al. 1996; Rui et al. 2001). In addition, some literature suggests NO-mediated insulin resistance caused by nitrosylation of Akt, which lowers its activity but not its phosphorylation (Marette 2002; Yasukawa et al. 2005). As a result insulin-resistance due to this mechanism cannot be deduced from the results presented in Figure 5.3.2c, however as discussed in Section 3.3.4, L-NAME failed to reverse the LPS plus cytokine-mediated insulin-resistance with regards to glycogen synthesis, implying that NO is unlikely to be impairing Akt activity. What the data above indicates is that the insulin-resistance on glycogen synthesis noted in myotubes in Section 3.3.2 is unlikely due to an impairment to the insulin cascade leading to Akt.

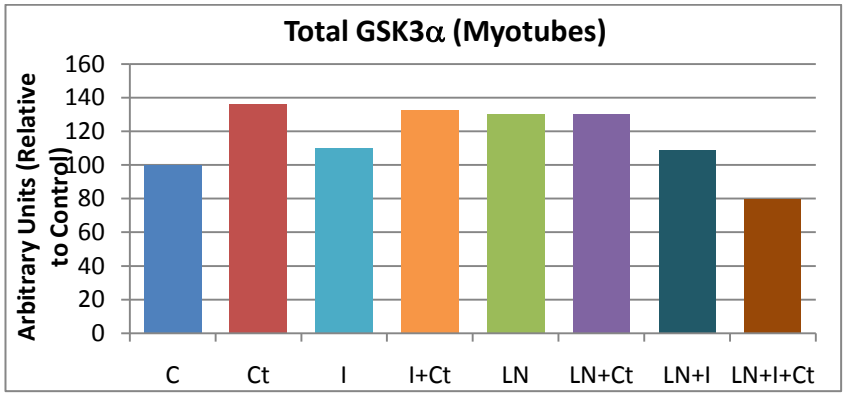

Fig. 5.3.2e. Sum of the optical densities of total GSK3α and GSK3β levels in myotubes. Cells were treated as described in Section 2.2.5. Results shown are from 2 independent experiments. C=Control, Ct=LPS+Cyt, I=Insulin, I+Ct=Ins+LPS+Cyt, then same treatments with or without LN=L-NAME

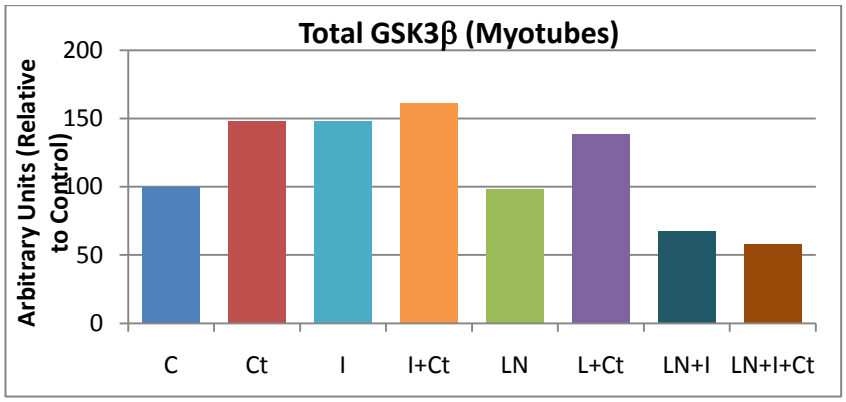

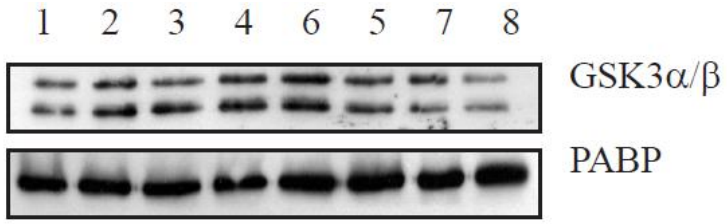

Fig. 5.3.2f. Example of a Western blot for total GSK3α/β along with the loading control (PABP). Visualised using ECL, GSK3α and GSK3β bands run at 51 and 46KDa, respectively. 1=C, 2=Ct, 3=I, 4=I+Ct, 5=LN, 6=LN+Ct, 7=LN+I, 8=LN+I+Ct. Note

Figure 5.3.2e shows the total levels of GSK3α and those of GSK3β present in the myotubes after the various treatments. LPS plus cytokines slightly increased total levels of GSK3α, except when co-treated with L-NAME and the cells stimulated with insulin. L-NAME treatment on its own also slightly increased total levels. This contrasts with the myoblast results presented in Figure 5.3.1e, where total levels of GSK3α remained stable despite the treatments. For GSK3β, LPS plus cytokines increased total levels regardless of the presence of insulin or L-NAME. L-NAME, LPS plus cytokine treatment followed by insulin stimulation decreased total GSK3β levels however, as did L-NAME treated myotubes stimulated with insulin. Dissimilar from the GSK3α results, insulin on its own also increased total levels of GSK3β. This is in contrast to the myoblast data, where the levels of GSK3β remained the same regardless of insulin or LPS plus cytokine treatment. These results are contradictory to those published by Dehoux et. al., where total GSK3α/β levels failed to changed after C2C12 myotubes were treated for 24 hours with TNF-α and INF-γ (5ng/ml each) (Dehoux et al. 2007).

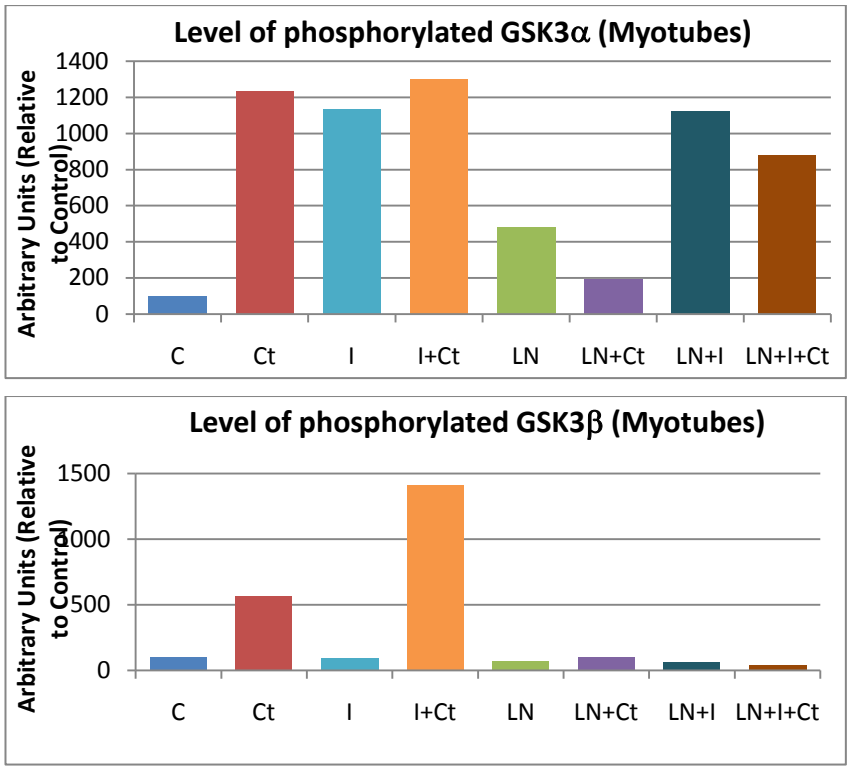

Fig. 5.3.2g. Sum of the optical densities of phosphorylated GSK3α and phosphorylated GSK3β in myotubes. Cells were treated as described in Section 2.2.5. Results shown are from 2 independent experiments. C=Control, Ct=LPS+Cyt, I=Insulin, I+Ct=Ins+LPS+Cyt, then same treatments with or without LN=L-NAME

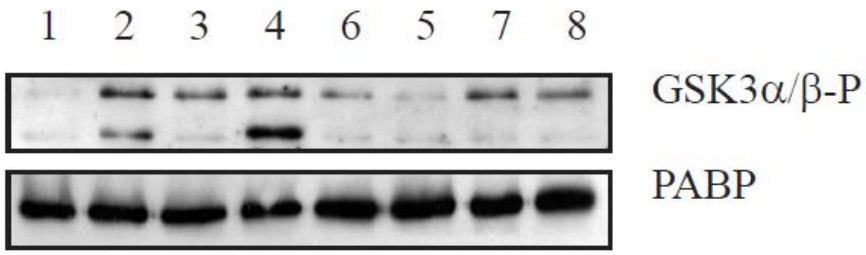

Fig. 5.3.2h. Example of a Western blot for phosphorylated GSK3 α/β, with loading control (PABP. Visualised using ECL, GSK3α and GSK3β bands run at 51 and 46KDa, respectively. 1=C, 2=Ct, 3=I, 4=I+Ct, 5=LN, 6=LN+Ct, 7=LN+I, 8=LN+I+Ct.

Figure 5.3.2g shows the level of phosphorylated GSK3α and GSK3β. LPS plus cytokines considerably increased the level of phosphorylated GSK3α, contrasting with the myoblast results where LPS plus cytokines failed to affect the phosphorylation state of either GSK3 isoform. Co-treatment with L-NAME noticeably prevented the LPS plus cytokine mediated inhibition of GSK3α, suggesting that this was brought on in an NO-dependent manner. Importantly, this result coincides with the myotube Akt blots presented above (Figure 5.3.2c). Also in accordance with the Akt results, insulin stimulated the phosphorylation of GSK3α, with or without the presence of L-NAME. In addition the insulin-stimulated inactivation of GSK3α was not impaired by the LPS plus cytokine treatment. This LPS plus cytokine induced increase in GSK3α phosphorylation contrasts with a study performed on C2C12 myotubes where a 24

hours treatment with TNF-α and IFN-γ (5ng/ml each) reduced GSK3α phosphorylation (Dehoux et al. 2007). Despite using C2C12 myotubes and two of the cytokines also used in the experiments performed here, the experimental conditions used by Dehoux et. al. were considerably different. As mentioned previously, much evidence suggests an impairment of the insulin signalling cascade affecting Akt and GSK3 in reponse to inflammatory stimuli (Hotamisligil et al. 1994; Hotamisligil et al. 1996; Rui et al. 2001; Ghosh et al. 2007; Austin et al. 2008). Nevertheless as seen above and in the figures presented above, this was not the case for Akt, nor GSK3α signalling in myotubes.

The activity of GSK3β on the other hand was quite different. The only treatments in which it was inactivated were LPS plus cytokines and LPS plus cytokines treated cells stimulated with insulin. The latter treatment had a much more pronounced increase in the phosphorylation of GSK3β than LPS plus cytokines alone. The co-treatment with L-NAME completely ablated this effect, suggesting that the LPS plus cytokines phosphorylated GSK3β in a NO-dependent manner. Indeed, Drenning et. al. noted similar observations in C2C12 myotubes, as L-NAME or an sGC inhibitor prevented an NO-donor-dependent increase in GSK3β phosphorylation (Drenning et al. 2008).

It is interesting that the results presented above suggest both isoforms of GSK3 are differently regulated in myotubes, especially with regards to insulin stimulation. LPS plus cytokines increased the phosphorylation state of both isoforms, in a NO-dependent manner, however insulin only stimulated GSK3α. As a result both isoforms must be appropriately distinguished in order to attempt to deduce whether either one could be an important contributing factor with regards to the myotube results presented in Chapters 3 and 4. Unfortunately information regarding the role of each isoform is conflicting. It was noted in human skeletal muscle that insulin infusion brought on a greater increase in phosphorylated GSK3α compared to GSK3β (Nikoulina et al. 2000), and GSK3α overexpression in human skeletal muscle impaired insulin responsiveness while reducing its expression improved the insulin response (Ciaraldi et al. 2007). In spite of this, another study using knock-in mice lacking either the GSK3α or GSK3β phosphorylation site, found that GSK3β was the more important isoform in insulin signalling (McManus et al. 2005). The results presented in Figure 5.3.2g, and indeed those of Figure 5.3.1g suggest that GSK3α is the more prominent insulin sensitive GSK3 isoform in these C2C12 myocytes, correlating with the human skeletal muscle results but interestingly contrasting with the mouse studies. It must be added however, that GSK3β failed to be phosphorylated under insulin stimulation in either myocyte preparation, which contrasts with both the human and mouse skeletal muscle studies cited here.

As shown in Chapter 3, LPS plus cytokines significantly inhibited myotube glycogen synthesis. This result does not fit in with the apparent activation state of myotube GSK3. The treatment phosphorylated GSK3 which would have relieved GS from GSK3-dependent inhibition, allowing glycogen synthesis to occur, however this was not the case as seen in Figure 3.3.1a where LPS plus cytokines inhibited glycogen synthesis. In addition, the results presented in Section 4.4 showed that LPS plus cytokines increased the ratio of phosphorylated GS relative to total GS in a NO-dependent fashion, which does not correlate with the results presented above. The GS phosphorylation site recognised by the antibody used in Section 4.4 recognises the site phosphorylated by GSK3 (Site 3), so the results shown in Figure 5.3.2g and 4.4p should correlate, which is not the case. It is possible that despite the LPS plus cytokine-mediated inhibition of GSK3 activity, that GS remained phosphorylated at Site 3 due to either an impairment to protein phosphatase-1 (PP-1) activity, which is responsible for dephosphorylating GS (Halse et al. 2003), or a PASK/DYRK-dependent phosphorylation at the same site (Skurat and Dietrich 2004; Wilson et al. 2005). What these results do suggest however, is that the inhibition of myotube glycogen synthesis seen after an 18 hour treatment with LPS plus cytokines was not due to a change in GSK3 activity. In addition to this, the insulin-stimulated response on GSK3α was not impaired by the presence of LPS plus cytokines, further demonstrating that the insulin impairment with regards to myotube glycogen synthesis observed in Chapter 3 was not due to an impaired Akt-GSK3 signal cascade, and must have been due to another mechanism.

5.3.3 Comparison of the Akt and GSK3 Activity Between Myoblasts and Myotubes

As already discussed, both Akt and GSK3 responded differently to LPS plus cytokines between myoblasts and myotubes. Akt and GSK3 phosphorylation increased under insulin stimulation only in both myocytes, but also after LPS plus cytokine treatment in myotubes. The Western blot analysis presented so far has kept both myocyte preparations separate, as a result a control, LPS plus cytokine, and insulin stimulated set of myoblasts and myotubes were run on a gel in order to better assess these differences.

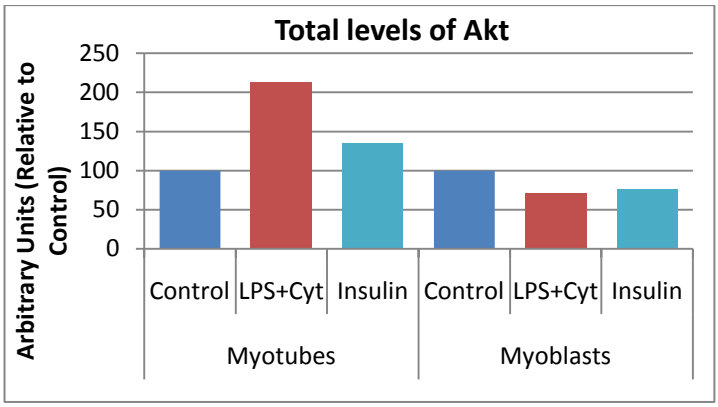

Fig. 5.3.3a. Sum of the optical densities of total Akt in myoblasts and myotubes. Cells were treated as described in Section 2.2.5. Results shown are average units from 1 experiment

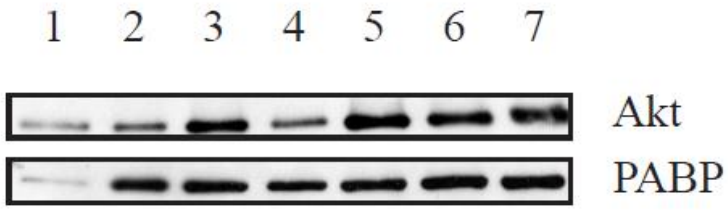

Fig. 5.3.3b. Example of a Western blot for total Akt along with loading control (PABP). Visualised using ECL, Akt band runs at 60KDa. 1=Mouse extract, 2=Control (myotube), 3=LPS+Cyt (myotube), 4=Insulin (myotube), 5=Control (myoblast), 6=LPS+Cyt (myoblast), 7=Insulin (myoblast).

The two figures above show the total levels of Akt in a mouse skeletal muscle extract (Lane 1), myotubes (Lanes 2-4) and myoblasts (Lanes 5-7). What is first noticeable from the blot in Figure 5.3.3b is the fact that Akt levels appear higher in myoblasts than in myotubes. This is most probably due to the fact that as mature skeletal muscle cells, myotubes express a multitude of other proteins which are actively transcribed during differentiation. As a result, the proportion of Akt relative to the total protein content in myotubes will be lower than the ratio in myoblasts. In this instance, LPS plus cytokines increased total levels of Akt in myotubes, as observed in the Figure 5.3.2a, while Akt levels in myoblasts were lower in the LPS plus cytokine treated and insulin stimulated cells, similar to the results observed in Section 5.3.1a. The level of Akt present in the mouse skeletal muscle extract (Lane 1) was higher when taking into account the loading control (PABP) which itself was lower than the levels of PABP in the myoblasts and myotubes.

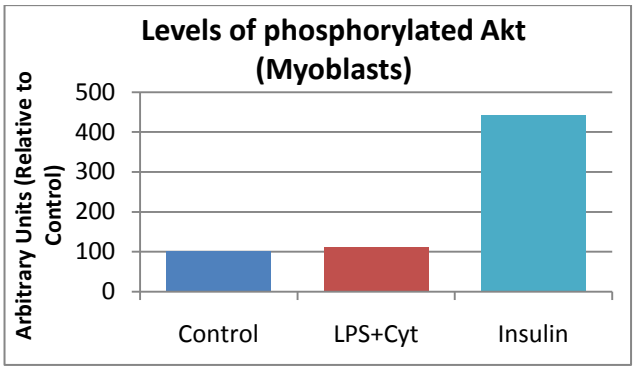

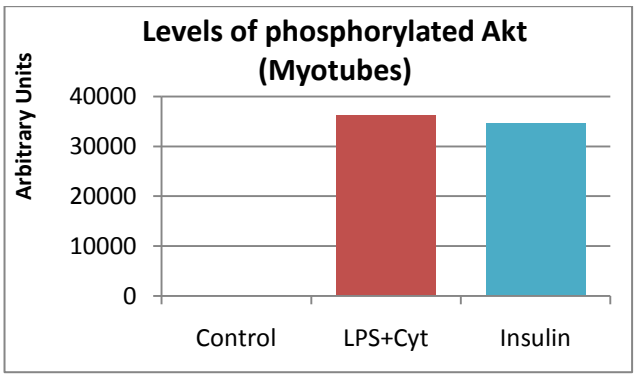

Fig. 5.3.3c. Sum of the optical densities of phosphorylated Akt in myoblasts and myotubes. Cells were treated as described in Section 2.2.5. Results shown are average units from 1 experiment

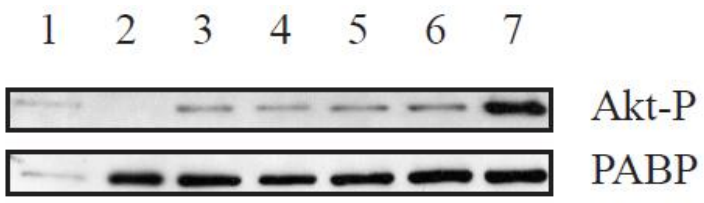

Fig. 5.3.3d. Example of a Western blot for phosphorylated Akt along with loading control (PABP). Visualised using ECL, Akt band runs at 60KDa. 1=Mouse extract, 2=Control (myotube), 3=LPS+Cyt (myotube), 4=Insulin (myotube), 5=Control (myoblast), 6=LPS+Cyt (myoblast), 7=Insulin (myoblast).

Figure 5.3.3c shows the level of phosphorylated Akt in myoblasts and myotubes, following LPS plus cytokine treatment, and insulin stimulation. The reason for putting them on separate graphs is that the magnitude of the response was different. In both cases, insulin notably increased the phosphorylation of Akt (as observed in the previously shown Akt data in Sections 5.3.1 and 5.3.2), and the magnitude of the response appeared much higher in the myotubes. However, by looking at Figure 5.3.3d, it can be seen that myotubes had no basal phosphorylated Akt, whereas myoblasts did. For this reason the magnitude of the response appeared higher in myotubes. In addition the level of phosphorylated Akt following insulin stimulation in the myoblasts as seen by the blot (Figure 5.3d) was higher than that seen in myotubes. The other clear difference between both

myocytes is that the 18 hour LPS plus cytokine treatment induced activation of Akt in myotubes, which did not occur in myoblasts. The actual level of phosphorylated Akt in LPS plus cytokine treated myotubes (Lane 3) was similar to the corresponding treatment in myoblasts (Lane 6), suggesting a similar situation. However relative to the untreated sample (Lanes 2 and 5), it is clear that LPS plus cytokines failed to increase the population of basally phosphorylated Akt in myoblasts. As discussed in the previous two sections, the glucose transport and glycogen synthesis data presented in Chapters 3 and 4 cannot adequately be explained by the activity of Akt for either myotubes or myoblasts. Activation of Akt leads to the translocation of GLUT4 transporters to the plasma membrane, and glucose uptake is consequently increased (Tremblay et al. 2003). However Akt activation failed to correlate with an increase in glucose uptake in either myoblasts or myotubes, suggesting the LPS plus cytokine induced increase in myoblast glucose transport was not due to Akt activity.

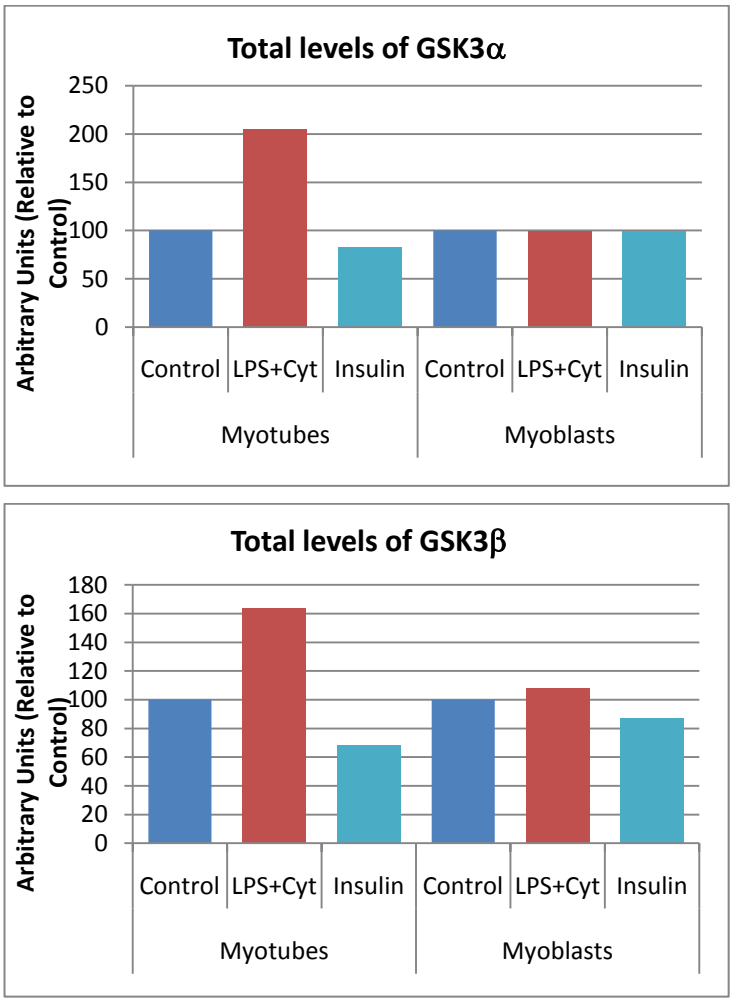

Fig. 5.3.3e. Sum of the optical densities of total GSK3α/β in myoblasts and myotubes. Cells were treated as described in Section 2.2.5. Results shown are average units from 1 experiment

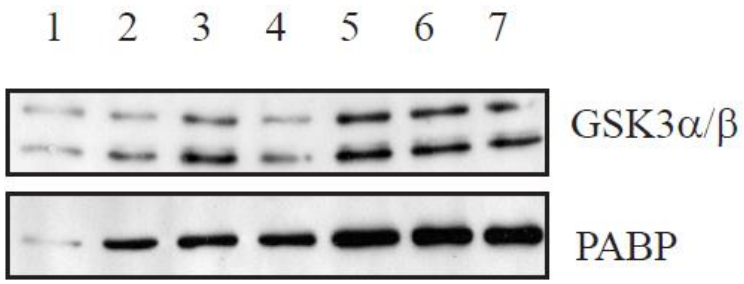

Fig. 5.3.3f. Example of a Western blot for total GSK3α/β along with loading control. Visualised using ECL, GSK3α and GSK3β run at 51 and 46KDa, respectively. 1=Mouse extract, 2=Control (myotube), 3=LPS+Cyt (myotube), 4=Insulin (myotube), 5=Control (myoblast), 6=LPS+Cyt (myoblast), 7=Insulin (myoblast).

The figures above show the total levels of GSK3α/β in myoblasts and myotubes. Myoblasts appeared to express a higher proportion of GSK3 relative to cellular protein compared to myotubes but when the loading control is considered it brings the levels back down to a more similar level. From the blot it is noticeable that GSK3 levels were higher in the mouse extract, once the loading control is taken into account. Myoblasts had slightly higher levels of PABP relative to total protein, probably due to the increased level of mature muscle fibre protein present in differentiated myotubes which lowers the relative proportion of PABP to total protein. The levels of GSK3 in the myoblasts did not change under either treatment, although in the myotubes LPS plus cytokines increased total levels of GSK3α/β. These results are virtually the same as those presented in Sections 5.3.1 and 5.3.2, although the only difference was that in the figures above insulin slightly decreased total GSK3β levels in myotubes whereas in Figure 5.3.2e insulin treatment had slightly increased total GSK3β levels.

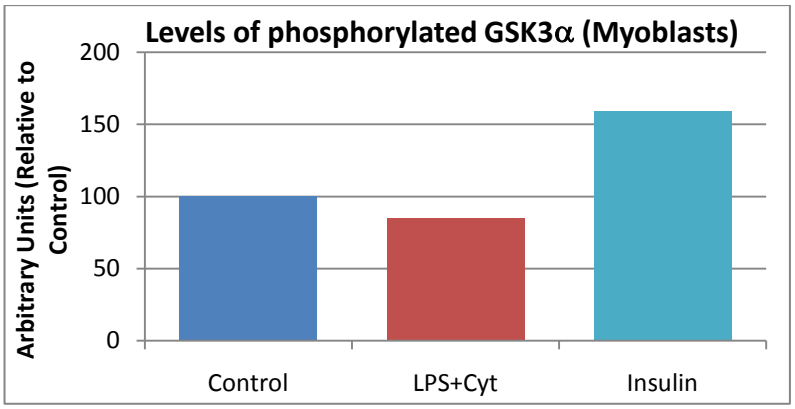

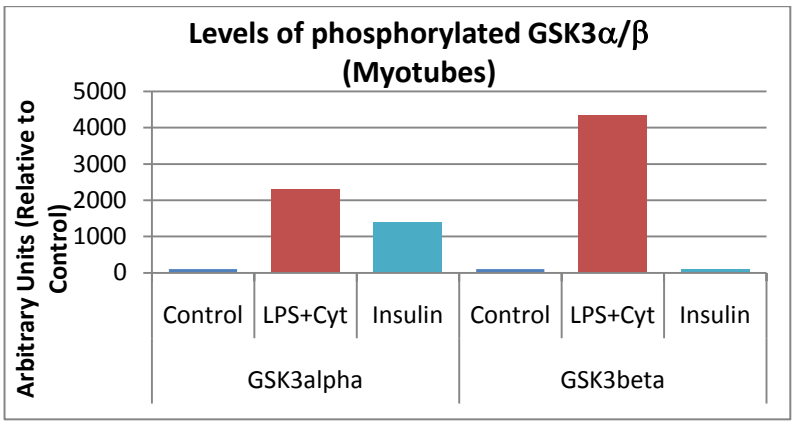

Fig. 5.3.3g. Sum of the optical densities of phosphorylated GSK3α/β in myoblasts and myotubes. Cells were treated as described in Section 2.2.5. Results shown are average units from 1 experiment

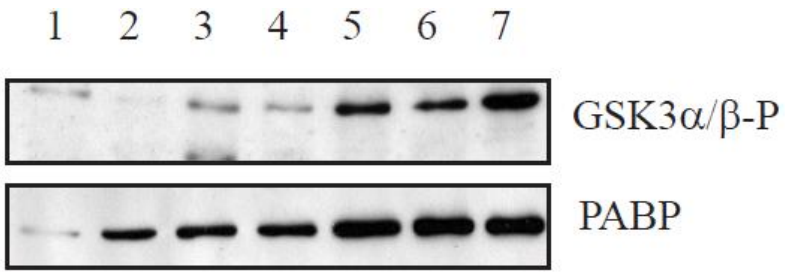

Fig. 5.3.3h. Example of a Western blot for phosphorylated GSK3α/β along with loading control (PABP). Visualised using ECL, GSK3α and GSK3β run at 51 and 46KDa, respectively. 1=Mouse extract, 2=Control (myotube), 3=LPS+Cyt (myotube), 4=Insulin (myotube), 5=Control (myoblast), 6=LPS+Cyt (myoblast), 7=Insulin (myoblast).

The figures above present the levels of phosphorylated GSK3α/β in myoblasts and myotubes following LPS plus cytokine treatment and insulin stimulation. In the myoblasts, LPS plus cytokine treatment failed to affect GSK3 phosphorylation, insulin increased the phosphorylation of GSK3α, while no activity was visible with regards to GSK3β after insulin stimulation. These results coincide with the same myoblast experiments presented in Figure 5.3.1g. In myotubes, as observed previously in Figure 5.3.2g, GSK3α phosphorylation was increased after insulin stimulation, while LPS plus cytokines increased the phosphorylation of both GSK3α and GSK3β. There is a clear difference in GSK3α/β regulation between myoblasts

and myotubes; although GSK3α is activated by insulin in both cases, LPS plus cytokines have no effect on either isoform in myoblasts but brought about the phosphorylation of both α and β isoforms in myotubes. In addition GSK3α is phosphorylated under basal conditions in myoblasts but not at all in myotubes. As for the mouse extract, there was a visible basal level of phosphorylated GSK3α, however no basal phosphorylated GSK3β was visible.

As discussed in the previous two sub-sections, the literature available regarding the precise roles of both GSK3 isoforms is slightly contradictory, and in addition the mouse C2C12 cells used in this thesis appear to correlate with human skeletal muscle studies but not mouse skeletal muscle studies. Two studies have tried to establish more information on the role played by GSK3α and β in basal and insulin stimulated glucose metabolism in human skeletal muscle by knocking down the expression of the isoform via siRNA treatment (small interfering RNA) (Ciaraldi et al. 2007; Ciaraldi et al. 2010). What they noted was that reducing or over-expressing GSK3α levels failed to affect basal activity of GS, whereas the same procedures done with GSK3β did affect the basal regulation of GS (Ciaraldi et al. 2007; Ciaraldi et al. 2010). As shown above, GSK3β was only inactivated by LPS plus cytokines in myotubes, in a NO-dependent fashion (as seen from Figure 5.3.2g). This suggests that after the LPS plus cytokine treatment, GS basal activity would have increased, potentially upregulating glycogen synthesis in a NO-dependent manner. However as discussed in Section 3.3.3, LPS plus cytokines significantly downregulated myotube glycogen synthesis in a NO-dependent manner, which would not correlate with the GSK3β data above. In addition, the GS enzyme data and Western blot analysis presented in Section 4.4 failed to correlate with the results presented in this Section (5.3); as discussed in Section 5.3.1 (myoblasts) and 5.3.2 (myotubes).

5.4 Effects of LPS plus Cytokine Treatment on p38 and ERK Levels and Activity in C2C12 Cells

5.4.1 Effects of LPS plus Cytokine Treatment on p38 and ERK Levels and Activity in Myoblasts

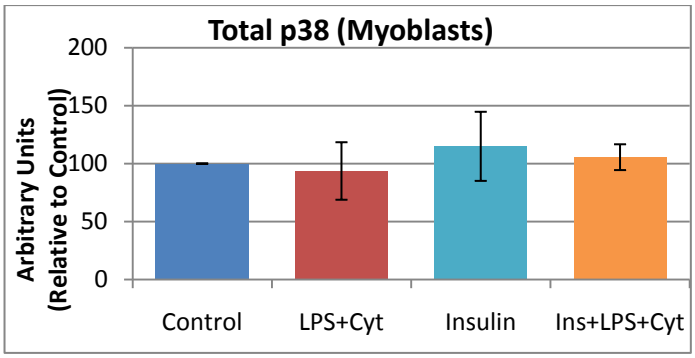

Fig. 5.4.1a. Sum of the optical densities of total p38 in myoblasts. Cells were treated as described in Section 2.2.5. Results shown are average units ± SEM from 3 independent experiments

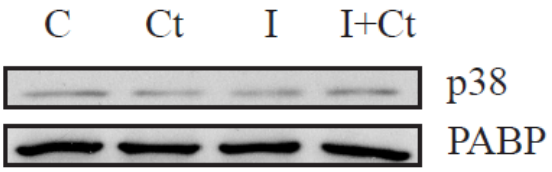

Fig. 5.4.1b. Western blot for total p38 in myoblasts along with loading control (PABP). Visualised using ECL, p38 band runs at 38KDa. C=Control, Ct=LPS+Cyt, I=Insulin, I+Ct=Ins+LPS+Cyt,

The two figures above display the total level of p38 present in myoblasts under the various different treatments. As shown, the overall level of p38 was the same in myoblasts with or without LPS plus cytokines, and in the presence or absence of insulin stimulation. This agrees with previous studies: TNF-α and IFN-γ (10ng/ml each) treatment of C2C12 myotubes (from 5 – 60 minutes) and a TNF-α (10ng/ml) treatment in L6 myoblasts (from 5 minutes to 18 hours) failed to alter total levels of p38 (Tolosa et al. 2005; Roher et al. 2008).

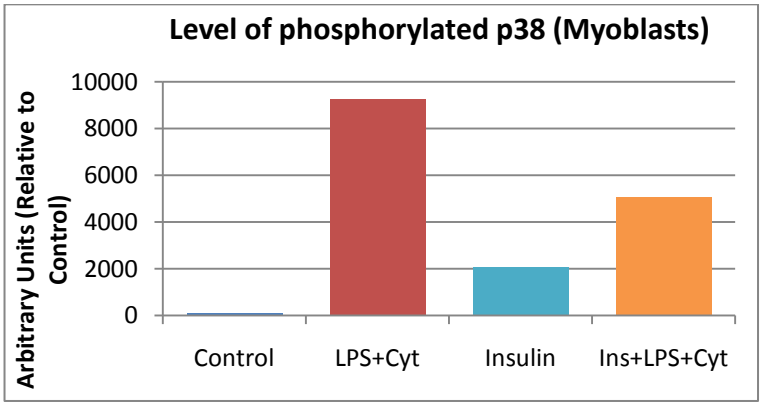

Fig. 5.4.1c. Sum of the optical densities of phosphorylated p38 in myoblasts. Cells were treated as described in Section 2.2.5. Results shown are average units from 2 experiments

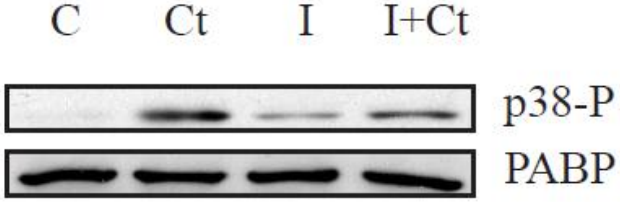

Fig. 5.4.1d. Example of a Western blot for phosphorylated p38 with the loading control (PABP). Visualised using ECL, p38 band runs at 38KDa. C=Control, Ct=LPS+Cyt, I=Insulin, I+Ct=Ins+LPS+Cyt,

Figure 5.4.1c above shows the level of phosphorylated p38 in myoblasts. What is clear is that LPS plus cytokines greatly increased the level of phosphorylated p38. Insulin also increased p38 phosphorylation, but to a lower degree than LPS plus cytokines (roughly 80% less). The combination of both treatments also increased the level of phosphorylated p38, however the level was roughly 45% lower than the LPS plus cytokine treatment alone, yet over 50% higher than the insulin stimulation alone. Cytokine induced activation of p38 is well established, with studies noting an induction of p38 phosphorylation using a range of different cytokine models (Tolosa et al. 2005; Chen et al. 2007; Roher et al. 2008). In C2C12 myocytes, p38 was phosphorylated subsequent to a treatment with TNF-α alone (10/ml) from 180 minutes up to 18 hours (Roher et al. 2008), or in combination with IFN-γ (10ng/ml) for 5-60 minutes (Tolosa et al. 2005). One contrasting study however, found that 5 days of septic abscess in rats decreased p38 activity (Vary et al. 2004), although this conflicting data could be due to the considerably different parameters used as well the fact that it took place in vivo. In accordance with this insulin stimulation noted above, an insulin-induced activation of p38 was noted in L6 myotubes (Tsakiridis et al. 1996) and rat EDL extracts (Somwar et al. 2000).

There is a large amount of conflicting evidence regarding the role of p38 in skeletal muscle carbohydrate metabolism. First of all, as discussed above, some data suggest p38 is insulin-stimulated (Tsakiridis et al. 1996; Somwar et al. 2000), although this is not universally accepted (Turban et al. 2005); and secondly there is evidence implicating p38 in stimulating glucose transport (Sweeney et al. 1999; Kim et al. 2006; Somwar et al. 2000), which Turban et. al. also refute (Turban et al. 2005). P38 has been implicated in the regulation of glucose transport because the use of a p38 inhibitor (SB203580) impaired insulin-stimulated glucose transport in L6 myotubes (Sweeney et al. 1999), and the same inhibitor impaired insulin – as well as contraction – stimulated glucose transport (Somwar et al. 2000). Moreover, hydrogen peroxide-enhanced glucose transport in rat skeletal muscle was completely ablated by the use of another p38 inhibitor (A304000) (Kim et al. 2006). Interestingly, studies performed by Turban et. al. found that insulin failed to activate p38, but that SB203580 impaired insulin stimulated glucose transport, which they claim implies that SB203580 inhibited the process via a mechanism other than p38-inhibition (Turban et al. 2005). The activation of p38 leads to the activation of the transcription factor MEF2 which is known to stimulate GLUT4 expression, although overexpression of dominant-negative variants of p38α and β in L6 cells failed to affect insulin-stimulated glucose transport (Antonescu et al. 2005), while overexpression of

p38-γ (the abundant isoform in skeletal muscle) decreased GLUT4 expression and impaired contraction-stimulated glucose uptake in L6 cells (Ho et al. 2004). SB203580 has been shown to consistently inhibit insulin-stimulated glucose transport despite any noticeable insulin-mediated p38 activation in rat adipocytes; although this is attributed to SB203580 acting as a competitive inhibitor at the endofacial surface of GLUT4, explaining why Turban et. al. also noted similar results (Ribe et al. 2005).

These studies suggest p38 is unlikely to have a stimulatory role on glucose transport. Nevertheless, if p38 were to be considered as a potential contributing factor to an increase in glucose transport it would make sense to implicate it in the LPS plus cytokine mediated increase in myoblast glucose uptake as presented in Section 4.2.2. However, insulin also increased p38 activity, albeit to a lesser extent, yet had no effect on glucose uptake. Moreover LPS plus cytokine treated cells stimulated with insulin increased myoblast glucose transport to a similar extent as LPS plus cytokines on their own, but both treatments failed to activate p38 to a similar extent, as shown above. These facts taken together along with the cited papers discussed above suggest that p38 is unlikely to be an important factor governing skeletal muscle glucose transport in C2C12 myoblasts.

The phosphorylation of GS by p38 is a novel concept but has been shown to be important with regards to promoting GSK3-mediated phosphorylation of GS (Kuma et al. 2004). P38 phosphorylates GS on five sites, two of which are also phosphorylated by GSK3 (3b and 4), the other 3 were previously unknown to be phosphorylated (Kuma et al. 2004). The study reported that p38-mediated phosphorylation at sites 3b and 4 did not inhibit GS activity as expected, but encouraged GSK3-mediated phosphorylation of GS, resulting in decreased activity. This may well explain why despite the lack of difference in GSK3 activity between control and LPS plus cytokine-treated myoblasts (Figure 5.3.1g), there was still an increase in GS phosphorylation at Site 3 following treatment as discussed in Section 4.4. There was no evident basal p38 activity in myoblasts, but LPS plus cytokines phosphorylated and activated it, which according to these studies would have led to GS phosphorylation, resulting in further phosphorylation carried out by GSK3.

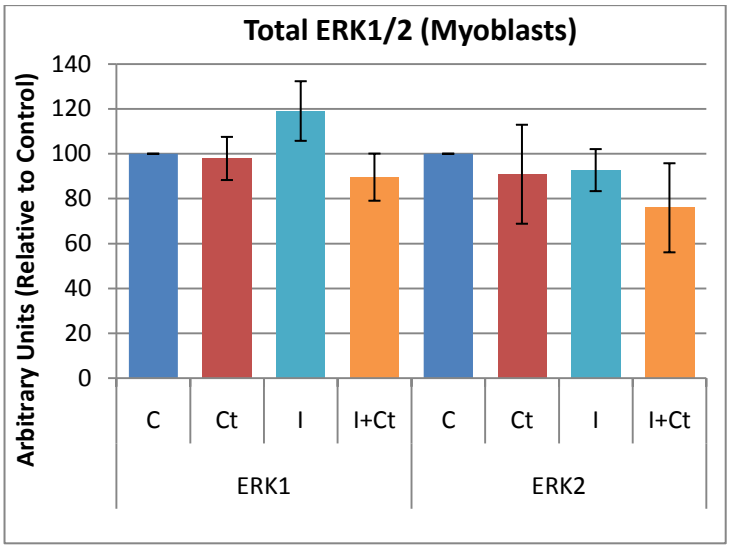

Fig. 5.4.1e. Sum of the optical densities of total ERK1/2 in myoblasts. Cells were treated as described in Section 2.2.5. Results shown are mean units ± SEM from 4 independent experiments. C=Control, Ct=LPS+Cyt, I=Insulin, I+Ct=Ins+LPS+Cyt

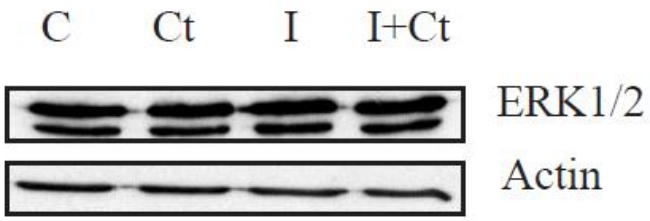

Fig. 5.4.1f. Example of a Western blot for total ERK1/2 along with the loading control (PABP). Visualised using ECL, ERK1 and ERK2 bands run at 44 and 42 KDa, respectively. C=Control, Ct=LPS+Cyt, I=Insulin, I+Ct=Ins+LPS+Cyt,

The two figures above display the levels of ERK1/2 in myoblasts. As shown, the levels of either isoform remained roughly the same despite LPS plus cytokine treatment, and insulin stimulation. In accordance with this a 3 hour treatment of C2C12 myoblasts with LPS (1mg/ml) failed to alter total levels of ERK1/2 (Frost et al. 2004). Interestingly, despite using the same cell type, the myoblasts used by Frost et. al. expressed considerably more ERK2 than ERK1 contrasting with the blot in Figure 5.4.1f which shows that ERK1 was slightly more abundant (Frost et al. 2004). The growth conditions used by Frost et. al. were quite different, since they used 10% bovine calf serum as opposed to 20% foetal calf serum used in the experiments presented in this thesis, in addition a slightly different medium was employed.

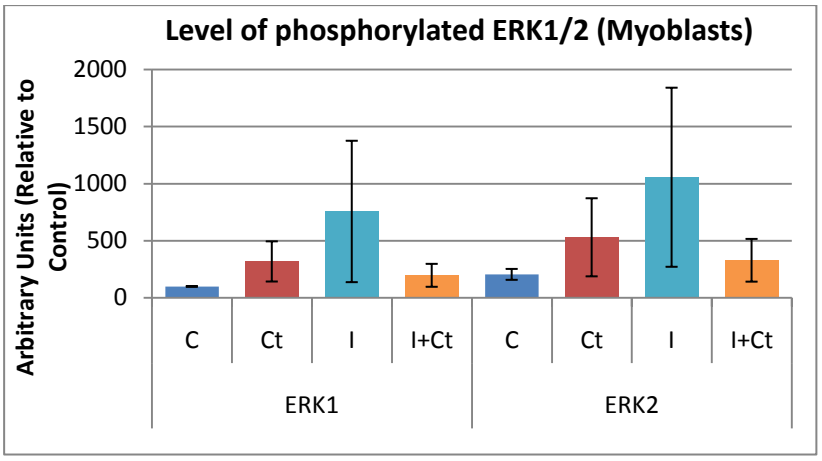

Fig. 5.4.1g. Sum of the optical densities of phosphorylated ERK1/2 in myoblasts. Cells were treated as described in Section 2.2.5. Results shown are mean units ± SEM from 4 independent experiments. C=Control, Ct=LPS+Cyt, I=Insulin, I+Ct=Ins+LPS+Cyt

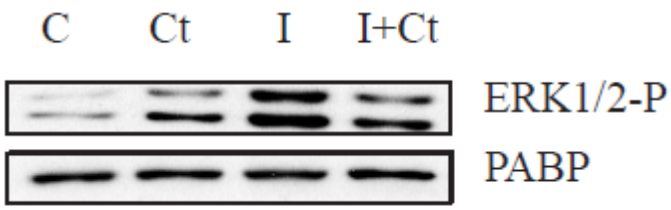

Fig. 5.4.1h. Example of a Western blot for phosphorylated ERK1/2 along with the loading control (PABP). Visualised using ECL, ERK1 and ERK2 bands run at 44 and 42 KDa, respectively. C=Control, Ct=LPS+Cyt, I=Insulin, I+Ct=Ins+LPS+Cyt,

Figure 5.4.1g above displays the level of phosphorylated ERK1/2 . As seen from the bar chart and the example Western blot, LPS plus cytokines, insulin, and insulin-stimulation of LPS plus cytokine treated cells increased the activity of ERK1/2. The four independent experiments consistently gave the same trend with regards to the level of ERK1/2 activation although the degree of stimulation varied, hence the large error bars. The 18 hour LPS plus cytokine treatment considerably lowered the insulin-mediated activation of ERK1/2, suggesting insulin resistance. In accordance with these results, insulin-stimulation of ERK1/2 was also observed in C2C12 cells and primary human skeletal muscle cells (Del Aguila et al. 1999; Williamson et al. 2005; Austin et al. 2008). The stimulatory effect of LPS or cytokines on ERK1/2 activity has also been observed in the literature (Frost et al. 2004; Tolosa et al. 2005; Austin et al. 2008; Plaisance et al. 2008), albeit under considerably different models. Correlating with the results presented above, studies performed on C2C12 myoblasts noted an increase in ERK1/2 activity after a 3 hour treatment with LPS (1mg/ml) (Frost et al. 2004). Despite utilising shorter time frames of treatment, C2C12 cells treated with TNF-α or TNF-α plus IFN-γ (10ng/ml each) for 10 – 60 minutes also noted activation of ERK1/2 (Tolosa et al. 2005; Plaisance et al. 2008).

ERK1/2 is activated by insulin, and as a result is a potential target for LPS and/or cytokine induced insulin-resistance. The results displayed above suggest that LPS plus cytokine

treatment impaired the insulin-stimulated activation of ERK1/2. Indeed Austin et. al. also noted an impairment to the insulin-stimulated activation of ERK isoforms in response to a 2 hour treatment with TNF-α in primary human skeletal muscle cells (Austin et al. 2008). As discussed in Section 1.6.5, the insulin-mediated activation of ERK1/2 leads to the activation of PP-1 (Ragolia and Begum 1998). The data presented in Figure 5.4.1g indicated an LPS plus cytokine-dependent increase in ERK1/2 activity. This may have brought about the activation of PP-1, which would have dephosphorylated GS thereby activating glycogen synthesis. This would coincide with the myoblast data presented in Section 3.3.1, since LPS plus cytokines upregulated glycogen synthesis.

In Section 5.3.1, myoblast GSK3 activity was not inhibited following LPS plus cytokine treatment, suggesting GS phosphorylation at Site 3 was maintained. This phosphorylated site is dephosphorylated by PP-1, which would contradict the idea that LPS plus cytokine-mediated activation of ERK1/2 may have brought about PP-1 activation. However the state of phosphorylation of a residue is down to the balance between the phosphatase and kinase activities. As discussed, p38 may have promoted GSK3-mediated phosphorylation of GS, which would push the equilibrium of GS phosphorylation towards the phosphorylated state, suggesting that PP-1 may have been activated but failed to considerably reduce GS phosphorylation. With regards to the impairment of the insulin-mediated activation of ERK1/2 following LPS plus cytokine treatment, PP-1 activity would have also been hindered, correlating with a study in L6 myotubes that reported an inhibition of insulin-stimulation of PP-1 activity following 60 minutes of TNF-α treatment (Begum and Ragolia 1996). This result may explain why insulin-mediated inactivation of Phosphorylase was impaired by LPS plus cytokines (as shown in Figure 4.4d), since PP-1 is responsible for dephosphorylating and thus inactivating Phosphorylase.

5.4.2 Effects of LPS plus Cytokine Treatment on p38 and ERK Levels and Activity in Myotubes

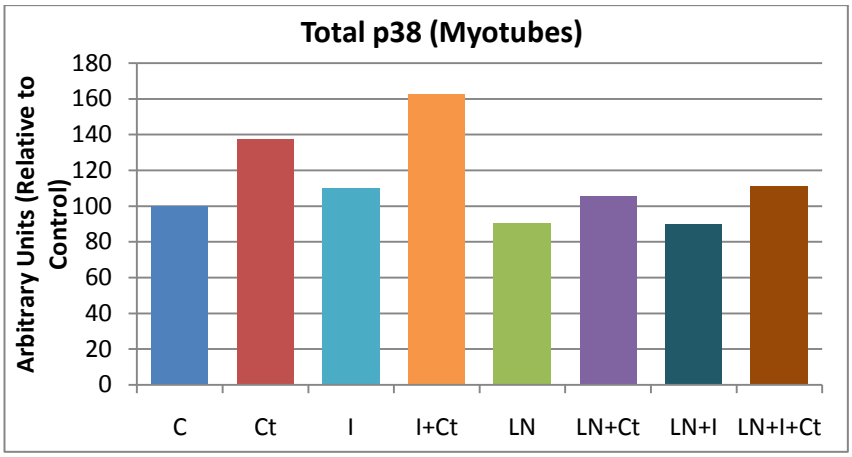

Fig. 5.4.2a. Sum of the optical densities of total p38 in myotubes. Cells were treated as described in Section 2.2.5. Results shown are mean units from 2 independent experiments. C=Control, Ct=LPS+Cyt, I=Insulin, I+Ct=Ins+LPS+Cyt, then same with L-NAME

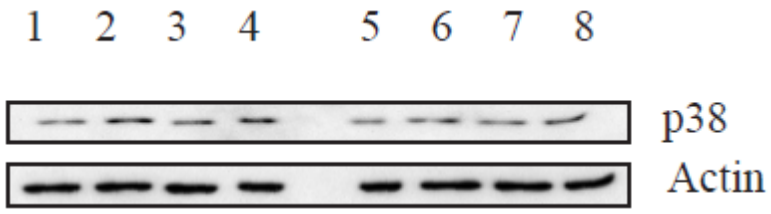

Fig. 5.4.2b. Example of a Western blot for total p38 with the loading control for myotubes. Visualised using ECL, p38 band runs at 38 KDa. 1=C, 2=Ct, 3=I, 4=I+Ct, 5=LN, 6=LN+Ct, 7=LN+I, 8=LN+I+Ct.

Figure 5.4.2a displays the average total level of p38 in myotubes after the various treatments. None of the treatments affected total p38 levels except the LPS plus cytokine treatment, which increased p38 levels in an NO-dependent fashion since L-NAME prevented this.

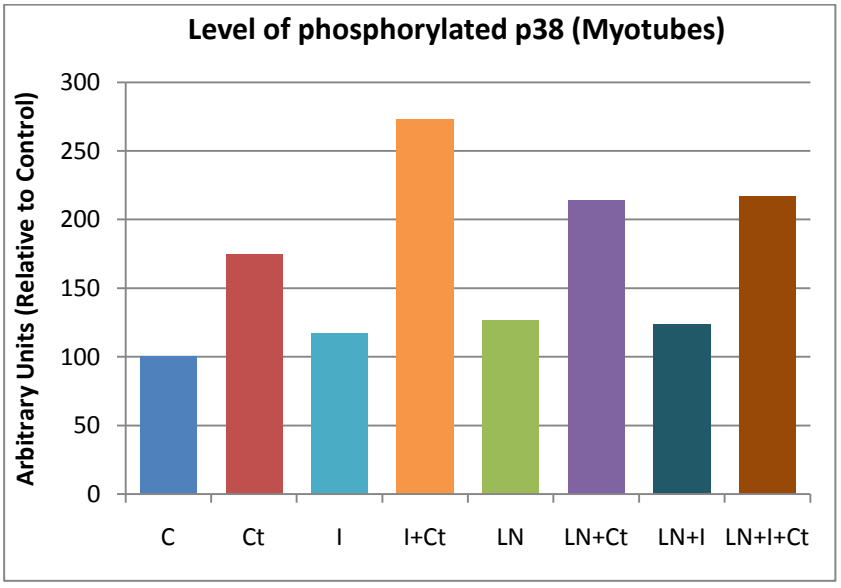

Fig. 5.4.2c. Sum of the optical densities of phosphorylated p38 in myotubes. Cells were treated as described in Section 2.2.5. Results shown are mean units from 2 independent experiments. C=Control, Ct=LPS+Cyt, I=Insulin, I+Ct=Ins+LPS+Cyt, then same with L-NAME

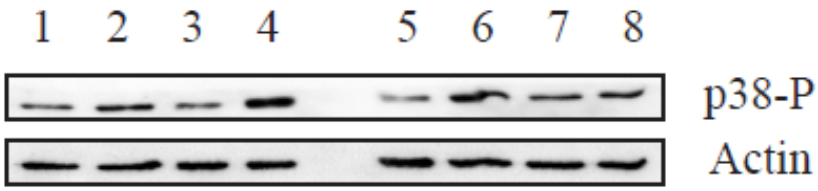

Fig. 5.4.2d. Example of a Western blot for phosphorylated p38 along with the loading control for myotubes. Visualised using ECL, p38 band runs at 38 KDa. 1=C, 2=Ct, 3=I, 4=I+Ct, 5=LN, 6=LN+Ct, 7=LN+I, 8=LN+I+Ct.

Figure 5.4.2c shows the level of phosphorylated p38 in myotubes following the various treatments. LPS plus cytokines increased the level of p38 phosphorylation, the pattern was the same for each LPS plus cytokine treatment (with or without insulin/L-NAME) suggesting that LPS plus cytokines consistently activated p38. The results shown above correlate with the myoblasts p38 results presented in Figure 5.4.1c, where LPS plus cytokines also activated p38, although there was no basal phosphorylated p38 in the myoblasts. One clear difference between the activation state of p38 in myoblasts and myotubes was the insulin-stimulated phosphorylation of p38 in myoblasts, which was not evident in myotubes – as shown above. Correlating with this, extracted mouse skeletal muscle cells failed to show an activated p38 in response to insulin (Turban et al. 2005), and L6 myotubes (Tsakiridis et al. 1996). The LPS plus cytokine-induced activation of p38 on the other hand is a well established process, as discussed in Section 5.4.1 (Tolosa et al. 2005; Chen et al. 2007; Roher et al. 2008). As discussed in Section in 5.4.1, there are conflicting data regarding the precise function of p38 with regards to glucose metabolism. Apart from one study that noted a decrease in GLUT4 expression following overexpression of p38-γ (Ho et al. 2004), the conflicting arguments lie in that some claim p38 plays an important role in insulin or contraction mediated glucose transport whereas other studies have refuted this. Neither insulin, nor LPS plus cytokine treatment affected glucose transport in myotubes (as seen and discussed in Section 4.2.1 and 4.2.2). This together with the data displayed in Figure 5.4.2c suggest that p38 is unlikely to have played any role in stimulating myotube glucose transport. The ratio of phosphorylated p38 relative to total p38 in myotubes is given below.

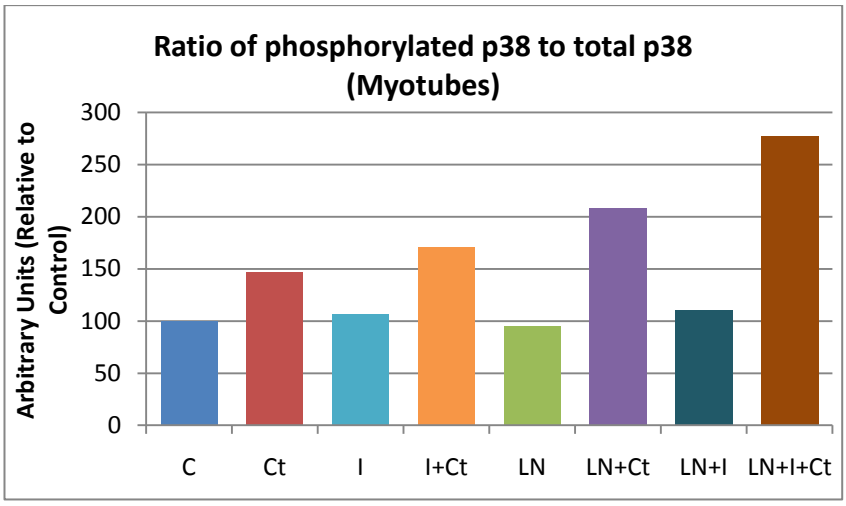

Fig. 5.4.2e. Sum of the optical densities of phosphorylated p38 in myotubes. Cells were treated as described in Section 2.2.5, and with or without L-NAME at 1mM. Results shown are mean units from 2 independent experiments. C=Control, Ct=LPS+Cyt, I=Insulin, I+Ct=Ins+LPS+Cyt, then same with L-NAME

Figure 5.4.2e shows the levels of phosphorylated p38 relative to total levels of p38 in myotubes. As observed, LPS plus cytokines still increased the ratio of phosphorylated p38 to total p38. Interestingly, L-NAME and LPS plus cytokine treated myotubes stimulated with insulin appeared to have a higher ratio of phosphorylated p38 relative to total then did the other LPS plus cytokine treatments. Nonetheless the overall response was the same as discussed below Figure 5.4.2c: LPS plus cytokines increased the activity of p38.

As discussed in Section 5.4.1, p38-mediated phosphorylation of myoblasts GS following LPS plus cytokine treatment may have explained the increase in GS phosphorylation despite there being no change in GSK3 relative to the control. Although myotube GS phosphorylation at Site 3 was increased following LPS plus cytokine treatment, the treatment also increased GSK3 phosphorylation (hence inhibited GSK3). In addition GS phosphorylation at Site 3 occurred in a NO-dependent manner following treatment whereas L-NAME had no effect on the LPS plus cytokine-mediated p38 phosphorylation.

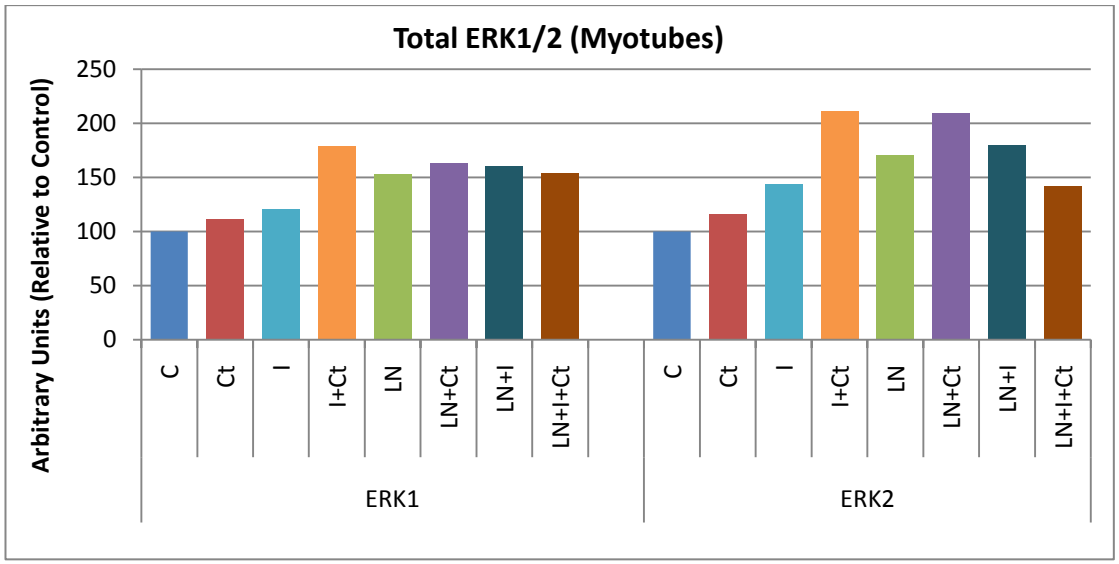

Fig. 5.4.2f. Sum of the optical densities of total ERK1/2 in myotubes. Cells were treated as described in Section 2.2.5. Results shown are mean units from 2 independent experiments. C=Control, Ct=LPS+Cyt, I=Insulin, I+Ct=Ins+LPS+Cyt, then same with L-NAME

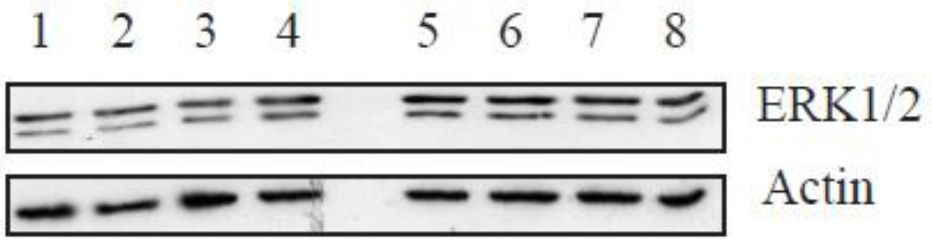

Fig. 5.4.2g. Example of a Western blot for total ERK1/2 along with the loading control. Visualised using ECL, ERK1 and ERK2 bands run at 44 and 42 KDa, respectively. 1=C, 2=Ct, 3=I, 4=I+Ct, 5=LN, 6=LN+Ct, 7=LN+I, 8=LN+I+Ct.

Figure 5.4.2f displays the total levels of ERK1/2 present in the myotubes following the various treatments. The ERK1/2 levels appeared to consistently increase following L-NAME treatment. In addition, LPS plus cytokine treated myotubes stimulated with insulin also appeared to increase total levels slightly. As displayed in Figure 5.4.1e, ERK1/2 levels did not change under any treatment in myoblasts, which contrasts with some of the changes displayed above.

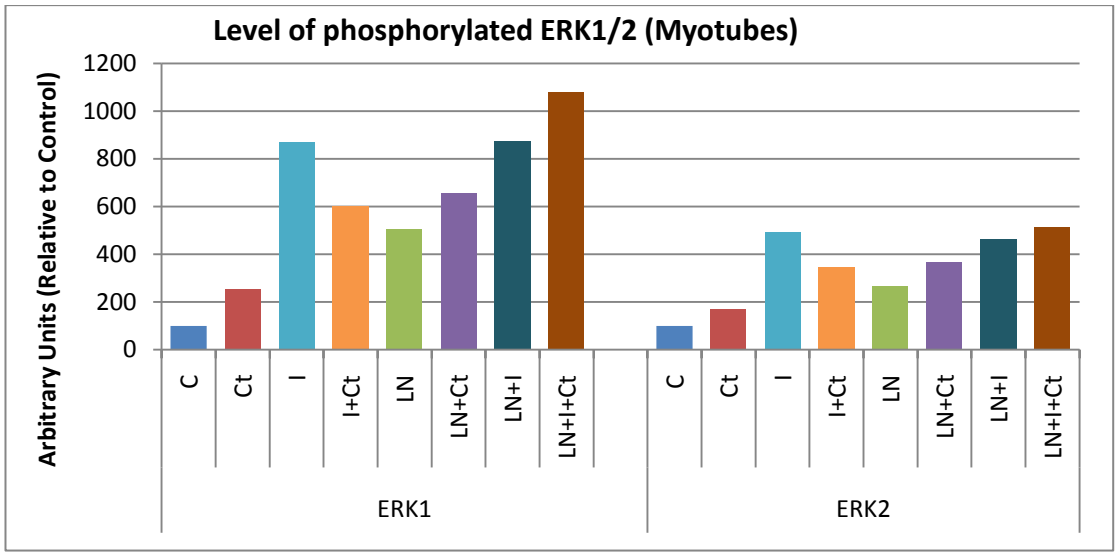

Fig. 5.4.2h. Sum of the optical densities of phosphorylated ERK1/2 in myotubes. Cells were treated as described in Section 2.2.5. Results shown are mean units from 2 independent experiments. C=Control, Ct=LPS+Cyt, I=Insulin, I+Ct=Ins+LPS+Cyt, then same with L-NAME

Fig. 5.4.2i. Example of a Western blot for phosphorylated ERK1/2 along with the loading control in myotubes. Visualised using ECL, ERK1 and ERK2 bands run at 44 and 42 KDa, respectively. 1=C, 2=Ct, 3=I, 4=I+Ct, 5=LN, 6=LN+Ct, 7=LN+I, 8=LN+I+Ct.

Figure 5.4.2h shows the level of phosphorylated ERK1/2 in myotubes following the treatments shown. The relationships between the various treatments were roughly the same for both ERK1 and ERK2. The only difference worth noting between ERK1 and ERK2 was that the control cells expressed a considerable basal activation of ERK2, as seen from the blot in Figure 5.4.2i, which explains why the relative activation of ERK2 was lower than that of ERK1. LPS plus cytokines partially increased the phosphorylation state, correlating with the myoblast results shown in Section 5.4.1. In the presence of L-NAME, LPS plus cytokines also increased ERK1/2 phosphorylation relative to control, to a higher degree than LPS plus cytokines on their own, but the relative difference between L-NAME, and L-NAME and LPS plus cytokine treatment was not that noticeable due to L-NAME increasing basal ERK1/2 activity, as can be seen by the blot in Figure 5.4.2g. Experiments using C2C12 cells treated with TNF-α or TNF-α

plus IFN-γ (10ng/ml each) for 10 – 60 minutes also noted activation of ERK1/2 (Tolosa et al. 2005; Plaisance et al. 2008).

Similar to the ERK1/2 myoblast data already discussed, insulin stimulation on its own notably increased ERK1/2 phosphorylation, which remained the same in the presence of L-NAME, correlating with previous studies (Del Aguila et al. 1999; Williamson et al. 2005; Austin et al. 2008). The insulin response was lower in the LPS plus cytokine treated myotubes – albeit higher than the ERK1/2 activation seen in LPS plus cytokine treated myotubes alone – suggesting there was an impairment to the insulin response. This impairment would coincide with the insulin-resistance observed in the myoblast results presented in Figure 5.4.1g as well as correlating with a previous study treating primary human skeletal muscle cells with TNF-a for 2 hours (Austin et al. 2008). In the presence of L-NAME, this insulin-resistance was no longer evident, implying that the impairment to ERK1/2 stimulation under insulin treatment was NO-dependent. One study has implicated NO in insulin-resistance because it promoted the downregulation of insulin-receptor substrate 1 (IRS-1) (Sugita et al. 2005). This effect would inhibit insulin signalling to ERK1/2, and as a result could be a potential mechanism for this impairment of the myotube insulin response. If this were the case though, the other route of insulin signalling involving PI3K, Akt and GSK3 would also be affected, however as seen in the previous sections within this chapter, neither Akt nor GSK3 signalling was significantly affected by LPS plus cytokines in myotubes.

This indicates that the NO-dependent impairment to the insulin-mediated activation of ERK1/2 must be due to another mechanism, only affecting the Raf/ERK route of insulin signalling. As discussed in Section 5.4.1, an impairment to the insulin-mediated phosphorylation of ERK1/2 would also impair the insulin-mediated activation of PP-1. In Section 5.3.2 the level of myotube GSK3 activity was discussed and it was proposed that the lack of correlation between the myotube GSK3 data and the myotube GS phosphorylation at Site 3 data presented in Section 4.4 could have been due to either an impairment to the activity of PP-1 or due to sustained phosphorylation at Site 3 of GS by other proteins such as PASK or DYRK. There was no apparent insulin-resistance induced by the LPS plus cytokines on GSK3 phosphorylation, however the LPS plus cytokines increased GS phosphorylation following insulin stimulation relative to the insulin only stimulated myotubes, which could be considered resistance to insulin signalling (as shown in Figures 4.4n and 4.4p). The NO-dependent impairment of the insulin response following LPS plus cytokine treatment would lead to the subsequent impairment of PP-1 activation. This could explain the NO-dependent sustained phosphorylation of GS at Site 3 despite inactivation of GSK3. This being said, the myotube glycogen synthetic data presented in Section 3.3.4 showed that LPS plus cytokine-induced

insulin resistance was not NO-dependent, since L-NAME failed to reverse the impairment, suggesting that if a NO-dependent inhibition of PP-1 activity was occurring, then another mechanism was also contributing to the insulin-resistance observed in Section 3.3.4.

5.5 Summary

Myoblasts

Protein	LPS plus Cyt	Insulin	Ins+LPS plus Cyt
AMPK	↑↑	↑	↑↑
Akt	—	↑↑	↑↑
GSK3α	—	↑↑	↑↑
GSK3β	—	—	—
p38	↑↑↑	↑	↑↑
ERK1	↑	↑↑	↑ Δ
ERK2	↑	↑↑	↑ Δ

Table 5.5 a+b. These tables summarise the phosphorylation states of each protein investigated under each treatment. (note: an increase in the phosphorylation state for each protein suggests a higher activity, except for GSK3 where phosphorylation implies a loss of activity). Increased arrows indicates more phosphorylated.
Δ = Insulin resistance × = Rescued by L-NAME.
C=Control, Ct=LPS+Cyt, I=Insulin, I+Ct=Ins+LPS+Cyt, then the same with L-NAME

Myotubes

Protein	Without L-NAME			With L-NAME			
	Ct	I	I+Ct	LN	LN+Ct	LN+I	LN+I+Ct
AMPK	↑↑	—	↑↑	—	× —	—	× —
Akt	↑	↑↑↑	↑↑↑	—	× —	↑↑	↑↑
GSK3α	↑↑	↑↑	↑↑	↑	× —	↑↑	↑↑
GSK3β	↑	—	↑↑	—	× —	—	× —
p38	↑↑	—	↑↑	—	↑↑	—	↑↑
ERK1	↑	↑↑↑	↑↑ Δ	↑	↑↑	↑↑↑	× ↑↑↑
ERK2	↑	↑↑↑	↑↑ Δ	↑	↑↑	↑↑↑	× ↑↑↑

In the myoblasts, total AMPK levels were decreased under LPS plus cytokine conditions, with or without the subsequent insulin stimulation (Figure 5.2.1a). Within the myotube results, total levels of AMPK appeared relatively consistent, although L-NAME treated myotubes stimulated with insulin expressed more AMPK (Figure 5.2.2a). In both myocyte preparations AMPK was phosphorylated (activated) after the 18 hour LPS plus cytokine treatment, with or without the subsequent insulin stimulation (Figure 5.2.1e and Figure 5.2.2c). This stimulation appeared to be NO-dependent in the myotubes, as observed by the lack of AMPK activation in L-NAME and LPS plus cytokine treated cells. AMPK activation results in an upregulation of skeletal muscle glucose transport (Fujii et al. 2006), which suggests that AMPK may well have contributed to the increase in myoblast glucose uptake observed after LPS plus cytokine treatment discussed in Section 4.2.1, however insulin failed to stimulate glucose uptake yet considerably activated AMPK, making AMPK an unlikely candidate for the LPS plus cytokine mediated increase in myoblast glucose uptake. Despite the LPS plus cytokine induced activation of AMPK in myotubes, no increase was observed in glucose uptake. The only difference in glucose uptake observed relative to control was in L-NAME and LPS plus cytokine treated myotubes (Figure 4.2.3b), yet this treatment failed to considerably activate AMPK.

AMPK is known to partially inhibit glycogen synthesis upon activation via direct phosphorylation of GS (Halse et al. 2003; Hardie et al. 2006). This would not correlate with the myoblast glycogen synthetic results presented in Section 3.3.1 since there was a significant increase in the rate of synthesis. The latter may however be a consequence of a significant increase in glucose uptake, leading to increased levels of G-6-P which can upregulate glycogen synthesis despite GS phosphorylation. As a result it is possible that AMPK phosphorylated GS at Site 2, partially inhibiting it, but that the influx of glucose overrode this mechanism. Concerning the myotubes, AMPK is a potential contributing factor to the LPS plus cytokine mediated downregulation of glycogen synthesis observed in Section 3.3.1, especially since L-NAME prevented the myotube AMPK activation and downregulation in glycogen synthesis brought on by the LPS plus cytokine treatment (Figures 3.3.3e and 4.4l). In addition this NO-dependent effect would correlate with the concept that NO stimulates AMPK activity (Lira et al. 2007; Zhang et al. 2008), which would then lead to GS phosphorylation, and hence partial inhibition of glycogen synthesis. However, the myotube GS fractional activity results in Figure 4.4c failed to show any significant change in GS phosphorylation state.

Emphasising the differences between myoblasts and myotubes yet again, the regulation of Akt and GSK3α/β between both myocyte preparations under the same treatments also differed. The total levels of Akt in the myoblasts were reduced post LPS plus cytokine treatment, whereas stayed relatively consistent under the various treatments in the myotubes apart from an increase induced by LPS plus cytokines (in the absence of L-NAME). With regards to Akt activity, insulin increased the phosphorylation of the protein in both myocyte preparations, even after LPS plus cytokine treatment. LPS plus cytokines failed to activate Akt in myoblasts but did so in myotubes in an NO-dependent manner. Akt is involved in promoting glucose uptake via GLUT4 translocation in response to insulin, however despite adequate insulin stimulation of the protein in both myocyte preparations, insulin failed to increase glucose uptake (as seen in Figure 4.2.2a and discussed in Section 4.2.2). LPS plus cytokines significantly upregulated myoblast glucose uptake, yet failed to activate Akt, implying it was an unlikely mediator of the effect. In myotubes, L-NAME and LPS plus cytokine treatment brought about a small but significant increase in glucose uptake, yet this treatment also prevented the LPS plus cytokine-mediated activation of Akt, indicating that Akt is unlikely to be responsible for this observation.

Total GSK3α/β levels remained consistent throughout the various treatments in myoblasts, and similarly GSK3α levels remained unchanged in the myotube experimental treatments. For GSK3β in myotubes however, LPS plus cytokines increased total levels regardless of the presence of insulin or L-NAME, although L-NAME and LPS plus cytokine treatment followed by insulin stimulation decreased total GSK3β levels, as did L-NAME treated myotubes stimulated with insulin. With regards to GSK3α/β phosphorylation, insulin increased the phosphorylation of GSK3α in both myocyte preparations, as expected from the Akt results; while LPS plus cytokines had no effect on this insulin-induced response. LPS plus cytokines also considerably increased GSK3α/β phosphorylation in myotubes in an NO-dependent fashion, but failed to affect either GSK3 isoform in myoblasts. Both these observations correlate with the Akt data from their respective myocyte preparations.

GSK3 directly phosphorylates GS, which inhibits its activity. By bringing about the phosphorylation and thus inhibition of GSK3, insulin relieves the GSK3-mediated inhibition on GS, thus allowing glycogen synthesis to occur. In Section 3.3.2, insulin upregulated glycogen synthesis in both myoblasts and myotubes, which correlated with the GSK3 data presented in this chapter, but failed to correlate with the GS enzyme assay data, or the GS Western blot data presented in Section 4.4. The myoblasts also had an increased rate of glycogen synthesis after LPS plus cytokine treatment, however this did not coincide with an effect on GSK3α/β

activity, implying that this treatment-induced upregulation was not due to the release of GS from GSK3-mediated inhibition, as seen by the higher ratio of phosphorylated GS relative to total GS in myoblasts (Figure 4.4j). In myotubes, L-NAME prevented GSK3α/β phosphorylation, GS-Site 3 phosphorylation and the downregulation of glycogen synthesis, all of which were induced by LPS plus cytokine treatment. These observations do not correlate however, since the treatment-induced phosphorylation of GSK3α/β would have increased glycogen synthesis rather than decrease it. This suggests there must be another mechanism causing the inhibition of glycogen synthesis in LPS plus cytokine treated myotubes such as increased GS-Site 3 phosphorylation by either PASK or DYRK or inhibition of PP-1 activity. In addition to this, the treatment impaired the myotube insulin response on glycogen synthesis, however insulin-mediated GSK3α phosphorylation was unchanged by LPS plus cytokine treatment, implying that the insulin resistance observed in Section 3.2.2 is unlikely due to impaired signalling to GSK3α.

The total levels of p38 in myoblasts remained constant regardless of the treatments, however in contrast, in myotubes LPS plus cytokines appeared to increase total levels in a NO-dependent fashion. LPS plus cytokines increased p38 phosphorylation in both myocyte preparations, and did so regardless of insulin treatment. No basal p38 phosphorylation was visible in myoblasts but in the myotubes p38 was basally phosphorylated. In addition, another stark difference between myoblasts and myotubes was that insulin activated myoblast p38 but had no such effect in myotubes. P38 has been suggested to be implicated in upregulating glucose transport (Sweeney et al. 1999; Somwar et al. 2000), although this has also been disputed by other studies (Turban et al. 2005). As presented in Chapter 4, glucose transport was upregulated by LPS plus cytokines, suggesting p38 may have contributed, however insulin also activated p38 but failed to increase myoblast glucose uptake. Myotube glucose uptake was unaltered by LPS plus cytokines except when co-treated with L-NAME, yet all LPS plus cytokine treatments in myotubes increased p38 phosphorylation regardless of the presence of insulin or L-NAME, indicating that p38 is unlikely to have a stimulatory role in glucose transport in C2C12 myocytes.

Phosphorylation of GS can also be mediated by p38 (as discussed in Section 5.4.1). Phosphorylation of GS mediated by p38 promotes GSK3-mediated phosphorylation of GS, thus inhibiting it (Kuma et al. 2004). This mechanism may explain the increase in phosphorylation of myoblast GS following LPS plus cytokine treatment. GSK3 activity did not differ between treated and untreated myoblasts, yet GS Site 3 phosphorylation did. This could implicate an inhibition of basal PP-1 activity or phosphorylation by PASK and DYRK. However a more active

p38 in LPS plus cytokine treated myoblasts would lead to increased GS phosphorylation which would then promote GSK3-mediated phosphorylation.

ERK1/2 levels remained constant in myoblast experiments. In myotubes the same was apparent however levels increased with L-NAME treatment as well as insulin stimulation of LPS plus cytokine treated cells, once again highlighting the potential variability of responses between both myocyte preparations. All treatments – LPS plus cytokines, insulin, and insulin stimulation of LPS plus cytokine treated myoblasts – upregulated ERK1/2 phosphorylation. Despite the upregulation, LPS plus cytokines impaired the insulin-mediated activation of ERK1/2 (Figure 5.4.1g). This myoblast result may explain why the LPS plus cytokine treatment impaired the insulin-mediated inactivation of Phosphorylase observed in Figure 4.4d. ERK1/2 activation following insulin-stimulation activates PP-1, which contributes to inactivating Phosphorylase. Insulin failed to causes GS dephosphorylation (as seen in Section 4.4), which should have occurred with an activated PP-1, however as discussed, other kinases may be responsible for maintaining GS phosphorylation.

In myotubes, LPS plus cytokines increased ERK1/2 phosphorylation, regardless of insulin treatment. Insulin too, augmented ERK1/2 activity to a considerably higher degree than LPS plus cytokines alone, and there was also an impairment to the insulin response induced by LPS plus cytokines, correlating with the myoblast data. This insulin-resistance noted in myotubes was NO-dependent since L-NAME reversed the impairment. This would not correlate with the fact that the LPS plus cytokine-induced insulin-resistance concerning myotube glycogen synthesis was NO-independent. However it is possible that there is another factor contributing to the LPS plus cytokine induced insulin-impairment.

Chapter Six – Effects of LPS plus Pro-Inflammatory Cytokines on Protein Synthesis in C2C12 Myocytes

6.1 Introduction

Myoblasts treated with LPS plus cytokines consistently had significantly more protein on the plate compared to control cells (Figure 3.2.1a), indicating that protein synthesis was upregulated during the 18 hour treatment. In contrast to this, myotubes failed to show any significant difference in protein content following treatment. Some upstream regulators of protein synthesis (Akt, MAPKs and AMPK) are also implicated in the signalling pathways discussed in this thesis, in particular in Chapter 5. Due to these facts and that protein synthesis is a process that lies at the centre of metabolic regulation (Proud 2007), it was important to address as it may shed light onto other contributing factors regarding the results presented in this study.

Much regulation of cap-dependent protein synthesis governs translation initiation (reviewed in (Proud 2007)). Of this process there are two important mechanisms: the binding of the eIF4F (eukaryotic initiation factor 4 F) complex to the 5' cap structure of the mRNA strand, and the formation of the ternary complex (Pain 1996; Sonenberg and Dever 2003; Proud 2007; Jackson et al. 2010). The ternary complex is composed of the GTPase eIF2 factor and Met-tRNA (Methionine-transfer RNA), and is only active when bound to GTP (Pain 1996; Jackson et al. 2010). Another initiation factor termed eIF2B is the guanine nucleotide exchange factor for eIF2, being responsible for replacing GDP for GTP in eIF2, leading to its activation (Pain 1996; Jackson et al. 2010). The active ternary complex leads to the formation of the 43S preinitiation complex which is composed of the 40S ribosomal subunit and other initiation factors (Jackson et al. 2010). This complex then associates with the an 'active' mRNA strand which is complexed with the 5' cap binding complex (eIF4F) and PABP (Jackson et al. 2010). The eIF4F complex consists of three initiation factors, eIF4E which binds the 5' terminal cap structure of mRNA, eIF4A (ATP-dependent RNA helicase) that aids in mRNA processing and eIF4G which is a scaffold protein that binds eIF4E, eIF4A, PABP (poly-A-binding protein) and the mRNA strand, as well as enhancing eIF4A activity (Pain 1996; Sonenberg and Dever 2003; Jackson et al. 2010). The association of the 43S complex and the activated mRNA leads to 5' to 3' scanning of the strand until the initiation codon is reached, at which point translation of the particular protein can start (Jackson et al. 2010). As a result, the regulation of the activation of eIF2 or the formation of the eIF4F complex is tightly regulated (Sonenberg and Dever 2003; Proud 2007; Goodfellow and Roberts 2008; Jackson et al. 2010). Some of these important regulatory mechanisms are outlined in the figure below.

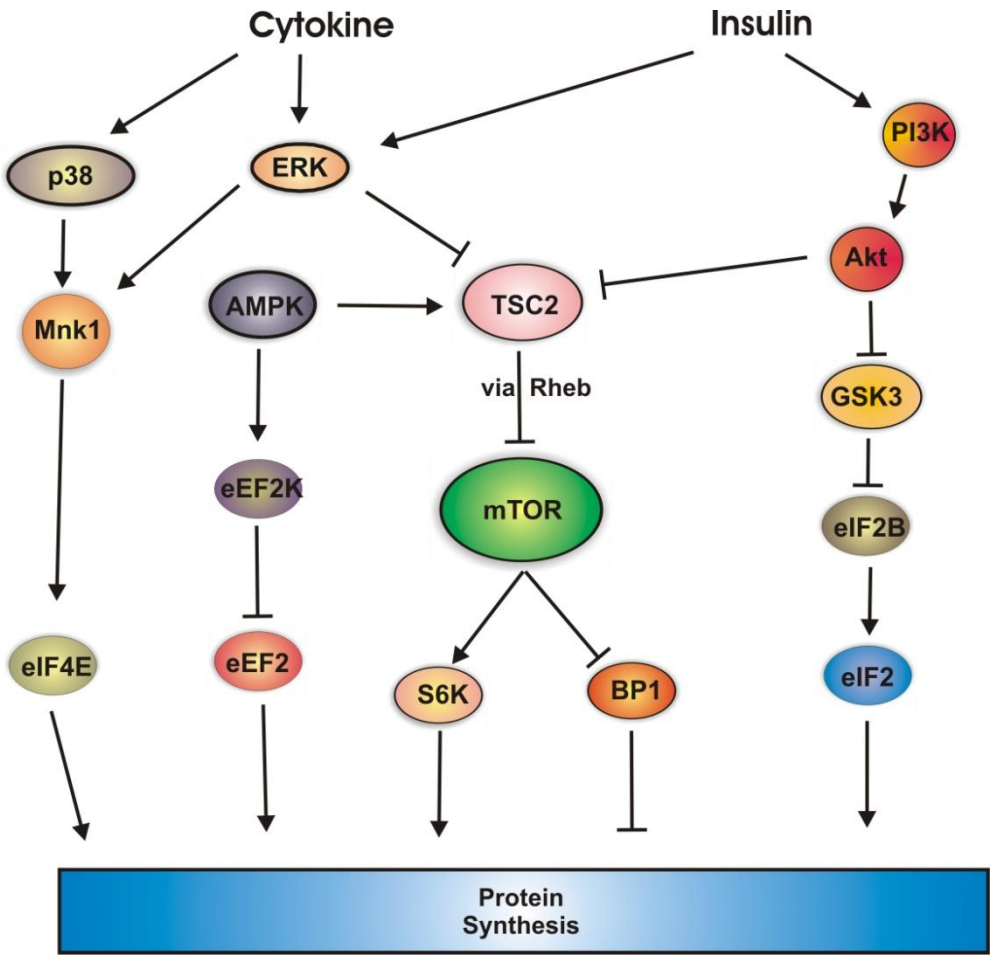

Table 6.1a. Schematic diagram describing some of major regulatory mechanisms governing protein synthesis.

Much like the GSK3-mediated inhibition of GS, eIF2B regulation involves GSK3-induced phosphorylation and inhibition (Cohen and Frame 2001; Sonenberg and Dever 2003; Proud 2007). The eIF4E factor on the other hand is sequestered by a family of 4E-binding proteins (4E-BPs), of which 4E-BP1 (BP1) is the most widely studied, which compete for eIF4E binding with eIF4G, thus preventing the formation of the eIF4F complex and hence initiation of translation (Inoki et al. 2005; Goodfellow and Roberts 2008). BP1 is regulated by phosphorylation via the mTOR pathway (mammalian target of rapamycin – mTOR), whereby hypophosphorylated BP1 sequesters eIF4E thus impinging translation, whereas the hyperphosphorylated form releases eIF4E, allowing protein translation to occur (Inoki et al. 2005; Goodfellow and Roberts 2008). In addition to BP1, mTOR regulates protein synthesis by the activation of another kinase: S6K (Shaw 2008). As shown in Figure 6.1a, numerous proteins associated with glycogen synthesis and the pathways activated by LPS and cytokines also regulate protein synthesis. Activation of the MAPKs ERK1/2 and p38 leads to the activation of Mnk1 (MAPK signal-integrating kinase-1) which stimulates eIF4E phosphorylation and in turn

activates protein synthesis (Proud 2007; Plaisance et al. 2008). In addition, ERK1/2 activates mTOR by releasing it from TSC2-mediated (tuberous sclerosis complex) inhibition (Proud 2007). Insulin stimulation of Akt leads to the same mechanism of mTOR activation as with ERK1/2, as well as leading to the inhibition of GSK3 which releases eIF2B (Proud 2007). Finally, AMPK also regulates protein synthesis, on the one hand it promotes TSC2-mediated inhibition of mTOR, while also causes the phosphorylation of eEF2 (eukaryotic elongation factor 2) by activating eEF2 kinase which impairs translation elongation (Proud 2007).

It is well established that the induction of sepsis and endotoxic shock induce the loss of skeletal muscle protein (Vary and Kimball 1992; Lang et al. 2000; Vary et al. 2002; Lang and Frost 2007; Eley et al. 2008), due to this there has been much research regarding the underlying causes of this process (Lang et al. 1996b; Llovera et al. 1997; Li et al. 1998; Lang et al. 2000; Alvarez et al. 2001; Vary et al. 2001; Williamson et al. 2005; Crossland et al. 2008; Lang et al. 2008; Plaisance et al. 2008; Frost et al. 2009). Much research has focused on the possible role of TNF-α in generating this catabolic mechanism (Llovera et al. 1997; Ji et al. 1998; Li et al. 1998; Alvarez et al. 2001; Lang and Frost 2007). TNF-α alone, or in combination with LPS, IFN-γ or IL-1, has been shown to significantly reduce skeletal muscle protein in vivo as well as in vitro (Li et al. 1998; Llovera et al. 1998; Eley et al. 2008). In contrast to this however, some studies observed a significant increase in skeletal muscle protein synthesis in vitro in response to TNF-α (Plaisance et al. 2008) or TNF-α and IL-1α (Ji et al. 1998). Experimental conditions often differ, such as the timing or concentration of stimulant used, which may explain these differences. A study looking at the bimodal effects of TNF-α found that a 48 hour incubation on differentiating C2C12 cells with 0.05ng/ml of TNF-α brought about tissue regenerative properties and myogenesis, whereas 48 hours of 0.5-5ng/ml of TNF-α inhibited differentiation (Chen et al. 2007). Chen et. al. made the same observations in rat primary skeletal muscle cells, reinforcing the argument. Like in previous chapters, NO is another potential contributing factor to the results observed in the literature regarding protein synthesis. Indeed a NO-dependent inhibition of protein synthesis in response to LPS and IFN-γ was shown in C2C12 myotubes as L-NAME completely reversed the inhibition (Frost et al. 2009). Some insights into the mechanism of this inhibition have also been suggested by Yasukawa et. al. who claim that NO nitrosylates Akt, impairing its function and hence affecting the correct signalling between Akt, mTOR and GSK3 (Yasukawa et al. 2005).

Protein synthesis was measured by the incorporation of [35S] Methionine into protein. The cells were treated as described in Section 2.2.5 unless otherwise stated, then harvested and protein synthesis determined as described in Section 2.12.

6.2 Effects of LPS plus Cytokines on Protein Synthesis in C2C12 Myocytes

LPS plus cytokine treatment increased myoblast protein content on the plate compared to control cells, which suggests an upregulation of protein synthesis must have occurred during the 18 hours treatment. This was not seen in the myotubes, where protein levels remained the same regardless of the treatment (Fig 6.2a, already discussed in Section 3.2.1).

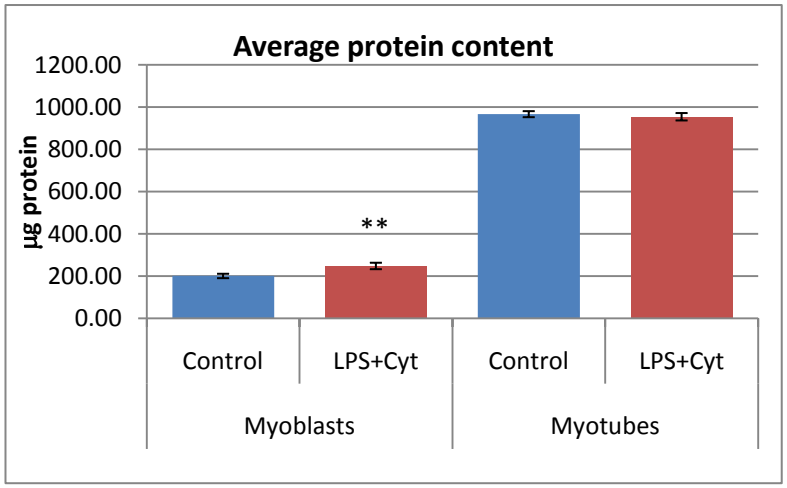

Fig. 6.2a. Average µg of protein present per plate. The results shown are the mean µg of protein ± SEM from 45 determinations from 7 independent experiments (myoblasts) and 36 determinations from 6 independent experiments (myotubes).
Statistical significance is as described in Section 2.14.
* = Significance from respective control

The treatment caused a significant (24%) increase in protein content in the myoblast experiments. Protein synthesis is a key function within cells which requires considerable amounts of energy and affects general cellular metabolism (Proud 2007). Correlating with the myoblast but not with the myotube data shown above, C2C12 myotubes treated for 24 hours with 10ng/ml (Plaisance et al. 2008) or 100ng/ml of TNF-α (Alvarez et al. 2001) caused a significant increase in protein content. In contrast, 24 hours of TNF-α (6ng/ml) treatment in C2C12 myotubes significantly reduced cellular protein levels (Li et al. 1998). As discussed in Section 3.2.1, some literature have reported that low levels of TNF-α (0.05-0.2ng/ml) promoted differentiation in C2C12 cells (Chen et al. 2007; Donati et al. 2007), however similarly low levels (0.01ng/ml) inhibited C2C12 differentiation (Broussard et al. 2003), suggesting that it is unlikely that the LPS plus cytokine treatment upregulated myoblast protein content for this reason. In addition, the levels of TNF-α added in this study are above the levels used by two of these studies, which found that differentiation was inhibited (Broussard et al.

2003; Chen et al. 2007). In order to establish whether protein synthesis was linear with time, a time-course was performed where protein synthesis was determined following 15, 30 and 60 minutes of incubation with [^{35}S] Methionine in control and LPS plus cytokine treated myoblasts, as shown in Figure 6.2b.

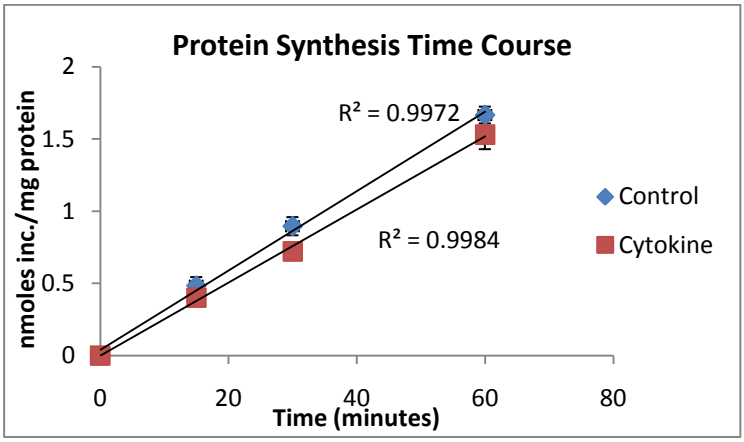

Fig. 6.2b. Time-course of protein synthesis over one hour in control and LPS plus cytokine treated cells. Cells were treated as described in Section 2.2.5. The results shown are the mean nmoles of methionine incorporated / mg protein ± SEM from 6 determinations from 2 independent experiments.

The rate of protein synthesis was linear over an hour for both treated and untreated myoblasts as displayed by their R^2 values which were close to 1. All of the following protein synthetic experiments were performed over one hour.

6.2.1 Effects of LPS plus Cytokines on Basal Protein Synthesis in C2C12 Myocytes

In spite of not showing any difference in protein content in response to treatment, myotube protein synthesis was also determined alongside the myoblast in order to compare both myocyte preparations.

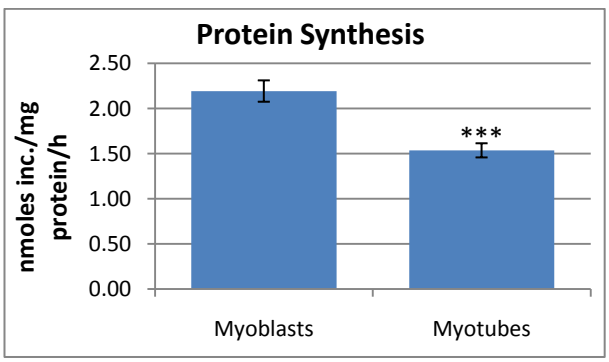

Fig. 6.2.1a. Basal protein synthetic rate in myoblasts and myotubes. Cells were treated as described in Section 2.2.5. The results shown are the mean nmoles of methionine incorporated into protein over one hour ± SEM from 19 determinations from 8 independent experiments (myoblasts), and 13 determinations from 3 independent experiments (myotubes) Statistical significance is as described in Section 2.14
* = Significance from myoblasts

As displayed above, the rate of protein synthesis in myotubes was significantly lower (by 30%) than the rate in myoblasts. The net rates were 2.19 nmoles inc./mg protein/h for the myoblasts and 1.56 nmoles inc./mg protein/h for the myotubes. These rates were considerably higher than in vivo rates observed in the literature. However four separate studies looking at protein synthesis in rat gastrocnemius muscle, each gave slightly differing rates: 0.095, 0.12, 0.26 and 0.42 nmoles/mg protein/h (Vary and Kimball 1992; Cooney et al. 1999; Lang et al. 2000; Vary et al. 2001). One study using C2C12 cells noted that myotubes expressed a rate 10% higher than in myoblast, contrasting with the data above (Palmer et al. 1997). It is not surprising to obtain a different rate of synthesis compared with the in vivo examples discussed, as protein synthesis is affected by many external circulating factors that are present during in vivo experiments but are lacking during in vitro work. Unfortunately most in vitro studies discussed in this chapter do not provide a net rate of protein synthesis, instead expressing all treatments relative to a control value of 100%, making it difficult to compare the exact rates of protein synthesis.

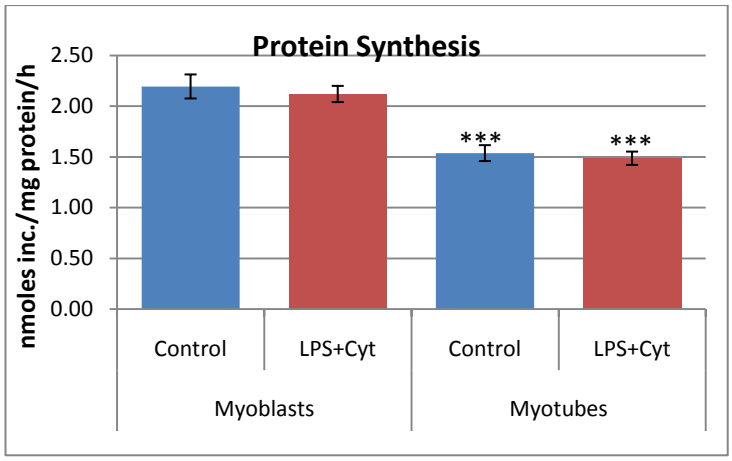

Fig. 6.2.1b. The effect of LPS plus cytokine treatment on myocyte protein synthesis. Cells were treated as described in Section 2.2.5. The results shown are the mean nmoles of methionine incorporated into protein over one hour ± SEM from 19 determinations from 8 independent experiments (myoblasts), and 13 determinations from 3 independent experiments (myotubes)
Statistical significance is as described in Section 2.2.5
* = Significance from corresponding treatment in myoblasts

Figure 6.2.1b shows that protein synthesis after 18 hours of LPS plus cytokine treatment had no effect on basal protein synthesis in either myoblasts or myotubes. As discussed in Section 5.3.1, neither Akt nor GSK3 activity was altered in LPS plus cytokine treated myoblasts as measured by phosphorylation, while in the myotubes the same treatment increased the level of phosphorylated Akt and GSK3. Increasing Akt activity and decreasing GSK3 activity would relieve the inhibitory effect on protein synthesis brought on by GSK3 (as described in Section 6.1), suggesting that protein synthesis might have been increased, yet this was not apparent. The LPS plus cytokine treatment phosphorylated AMPK in both myoblasts (Figure 5.2.1e) and myotubes (Figure 5.2.2c); when active, AMPK can inhibit

protein synthesis, which would suggest that protein synthesis may have been inhibited by the treatment. Yet as shown in the figure above, protein synthesis was unchanged by the treatment. Finally, ERK1/2 and p38 were phosphorylated following LPS plus cytokine treatment which would have promoted protein synthesis, however this mechanism is not apparent in the data above. Protein synthesis is highly regulated and as such is influenced by many different signalling molecules (Proud 2007; Jackson et al. 2010). In vitro studies using C2C12 myotubes displayed varying results. A 24 hour incubation with LPS (100ng/1ml), a 2 hour incubation with TNF-α (50ng/ml) alone or in combination with IFN-γ (10ng/ml) decreased C2C12 myotube protein synthesis by 40, 30, and 50%, respectively (Eley et al. 2008). However in contrast, a 24 hour incubation with increasing doses of TNF-α (1-100ng/ml) significantly increased myotube protein synthesis in a dose dependent manner (Plaisance et al. 2008). Both these studies differ in their experimental conditions, as well as contrasting with the conditions used for the results shown above, which highlights the possible variability between studies.

6.2.2 Effects of LPS plus Cytokines on Insulin-Stimulated Protein Synthesis in C2C12 Myocytes

Much like the impairment to the insulin-stimulated glucose transport and glycogen synthesis processes induced by sepsis, several lines of evidence show that the insulin-stimulated protein synthetic system is impaired by sepsis and inflammatory cytokines (Alvarez et al. 2001; Vary et al. 2001; Williamson et al. 2005; Orellana et al. 2007). As a result, the insulin response was assessed by adding 1µM insulin to the cells 1 hour prior to the assay, and then again during the hour incubation with the radio-labelled methionine.

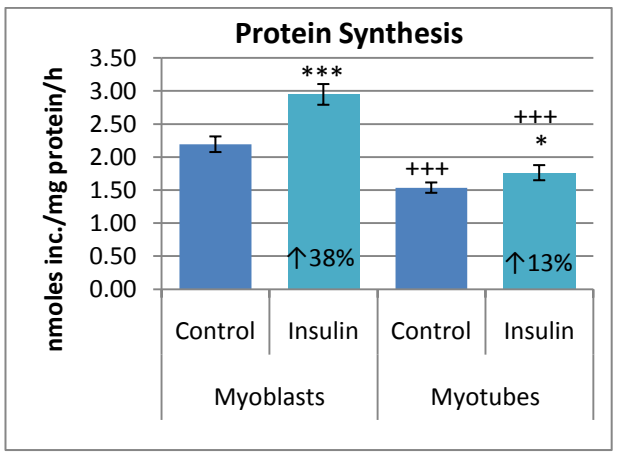

Fig. 6.2.2a. Effect of insulin (1µM) on protein synthesis in myoblasts and myotubes. Cells were treated as described in Section 2.2.5. The results shown are the mean nmoles of methionine incorporated into protein over one hour ± SEM from 19 determinations from 8 independent experiments (myoblasts), and 10-13 determinations from 3 independent experiments (myotubes)
Statistical significance is as described in Section 2.2.5
* = Significance from respective control
+ = Significance from myoblasts

Insulin treatment significantly upregulated protein synthesis; it induced a 38% increase in protein synthesis in the myoblasts (or a net increase of 0.76 nmoles inc./mg protein/h) which was considerably higher than the significant 13% increase observed in the myotubes – representing a net increase of 0.22 nmols inc./mg protein/h. This data would correlate with the insulin-induced phosphorylation of Akt, GSK3 and ERK1/2 presented in Chapter 5, Sections 5.3.1 and 5.3.2. The insulin-induced increments displayed above are lower than some found in the literature. Palmer et. al. treated myoblasts and myotubes with 1μM insulin for 6 hours which induced a 58% increase in myoblast protein synthesis but failed to significantly upregulated the myotube rate (Palmer et al. 1997), which contrasts with both the insulin-induced rates presented in Figure6.2.2a. Nevertheless the insulin-induced rate in the myotubes above is very small. In contrast to this myotube result, and that noted by Palmer et. al., a 40 minute treatment with 20nM insulin was reported to induce a 50% increase in myotube protein synthesis (Williamson et al. 2005). Once the insulin response was determined, the possible insulin-resistance induced by LPS plus cytokine treatment was addressed.

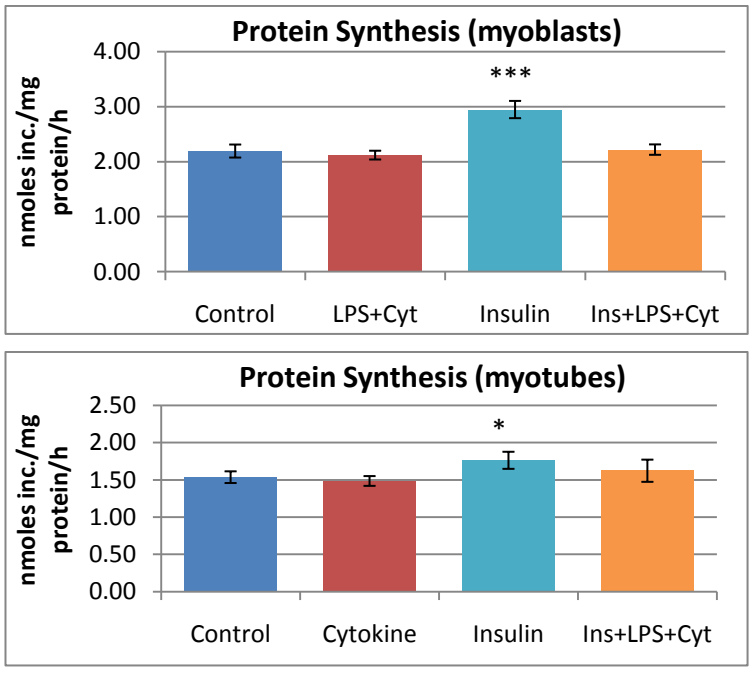

Fig. 6.2.2b+c. Effect of LPS plus cytokines on insulin stimulated protein synthesis in myoblasts and myotubes. Cells were treated as described in Section 2.2.5. The results shown are the mean nmoles of methionine incorporated into protein over one hour ± SEM from 19 determinations from 8 independent experiments (myoblasts), and 10-13 determinations from 3 independent experiments (myotubes)
Statistical significance is as described in Section 2.14
* = Significance from control

Figure 6.2.2b+c shows the effect of an 18 hour LPS plus cytokine treatment on the insulin response in myoblasts and myotubes. In both cases, the treatment impaired the insulin response. The rate of insulin-stimulated protein synthesis in LPS plus cytokine treated

myoblasts and myotubes was not significantly different to the LPS plus cytokine treatment alone; p = 0.21 and p = 0.17, respectively. In the myoblasts, LPS plus cytokines decreased the insulin response from a significant 38% increase, to a non-significant 5% increase, suggesting insulin resistance. In the myotubes the treatment lowered the insulin response from a significant 13% increase to a non-significant 7% increase. Although the impairment in the myotube result was statistically significant, it was difficult to address a change from 13 to 7% since the error from the mean was 5%. Correlating with the results shown above, the use of TNF-α in vitro on C2C12 myotubes has been reported to induce insulin resistance (Alvarez et al. 2001; Williamson et al. 2005).

	Control (% difference)	With LPS + Cytokines (% difference)
Myoblasts Insulin response	38 ± 7%	5 ± 3% ***
Myotubes Insulin response	13 ± 5% +	7 ± 5%

Table6.2.2a . The average insulin effect on un-treated and LPS + cytokine treated myoblasts and myotubes. Cells were treated as described in Section 2.2.5. The results shown are the mean nmoles of methionine incorporated into protein over one hour ± SEM from 19 determinations from 8 independent experiments (myoblasts), and 10-13 determinations from 3 independent experiments (myotubes)
Statistical significance is as described in Section 2.14.
* = Significance from respective control
+ = Significance between myoblasts and myotubes

Table 6.2.2a provides the average increment induced by insulin in myoblasts or myotubes, with or without LPS plus cytokine treatment. Reaffirming what was shown in the Figure 6.2.2b, the myoblast insulin response was significantly impaired by the LPS plus cytokine treatment. LPS plus cytokine treatment had no significant effect (p = 0.16) on the already low insulin response noted in myotubes. The insulin response in untreated myotubes was significantly different from that of the myoblasts, while the two insulin responses in LPS plus cytokine treated myoblasts and myotubes were not significantly different (p = 0.37). The difference in magnitudes of the insulin responses in the myoblasts compared to the myotubes coincides with the relationship observed between the insulin stimulated glycogen synthetic rate in both myocyte preparations (Table 3.3.2a); insulin stimulated myoblast glycogen synthesis to a significantly higher degree relative to the insulin response in myotubes. Indeed the insulin stimulation on glycogen synthesis was 74% lower in myotubes relative to myoblasts

which is similar to the 66% lower insulin response on myotube protein synthesis. LPS plus cytokines significantly impaired the insulin stimulation on myotube glycogen synthesis, which cannot be appropriately determined above since the insulin response in myotubes was minimal. In the myoblasts however, the impairment is clear, yet this contrasts with some of the signalling data presented in Chapter 5 since insulin stimulated phosphorylation of myoblast Akt and GSK3 were not hindered by LPS plus cytokine treatment (Figure 5.3.1e and 5.3.1g), suggesting the impairment must be due to another mechanism. However, insulin-induced ERK1/2 activation in myoblasts was significantly hindered by the LPS plus cytokine treatment (Figure 5.4.1g), which could be responsible for this insulin-resistance since ERK1/2 activity promotes protein synthesis via Mnk1 activation as well as TSC2 inhibition (as shown in Figure 6.1a) (Proud 2007; Plaisance et al. 2008).

6.2.3 Role of Nitric Oxide on LPS plus Cytokine Induced Effects on Basal and Insulin-Stimulated Protein Synthesis

To confirm NO had no role in the regulation of protein synthesis in the presence of LPS plus cytokines or the impairment to the insulin response observed in Section 6.2.4, L-NAME was used to inhibit NO production. As discussed in section 6.1, mTOR plays an important role with regards to protein synthesis regulation, and it is itself regulated by Akt, which has been shown to be directly inhibited by nitrosylation (Yasukawa et al. 2005). In other evidence, IRS-1 is degraded in a NO-dependent manner by a proteasome mechanism (Sugita et al. 2005).

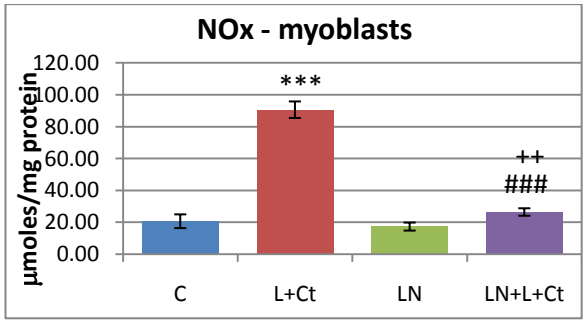

Fig 6.2.3a. The effect of L-NAME on total NO levels (NOx) induced by LPS plus cytokine treatment in myoblasts. Cells were treated as described in Section 2.2.5.. The results shown are the mean µmoles NOx in the medium ± SEM from 12 determinations from 2 independent experiments. Statistical significance is as described in Section 2.14.
* = Significance from control
+ = Significance from L-NAME
# = Significant from LPS + Cytokine
(C=Control, L+Ct=LPS+Cyt, LN=L-NAME, LN+L+Ct=L-NAME+LPS+Cyt)

As Figure 6.2.3a displays, L-NAME inhibited NO production by 72%, which was to a similar degree as observed in Section 3.3.3, as well as correlating with the literature discussed in the same section (Williams et al. 1994; Bedard et al. 1997; Khanna et al. 1999).

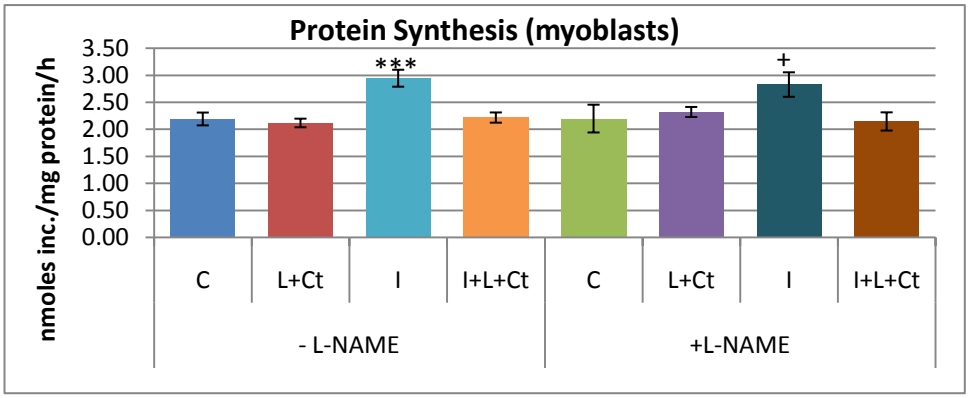

	Control (% difference)	With L-NAME (% difference)
Insulin response	38 ± 7%	26 ± 9%
Insulin response in the presence of LPS plus cytokines	5 ± 4% ###	-7 ± 6% ••, >

Fig 6.2.3b and Table 6.2.3a. The effect of L-NAME on protein synthesis in the presence and absence of LPS plus cytokines and/or insulin in myoblasts. Cells were treated as described in Section 2.2.5. The results shown are the mean nmoles of methionine incorporated into protein over one hour ± SEM from 19 determinations from 8 independent experiments (without L-NAME) and 6 determinations from 2 independent experiments (with L-NAME). Statistical significance is as described in Section 2.14.
* = Significance from control
+ = Significance from L-NAME
# = Significance from insulin response
• = Significance from insulin response (+ L-NAME)
> = Significance from Insulin response (+LPS plus cytokines)
(C=Control, L+Ct=LPS+Cyt, I=Insulin,

The figure above shows that L-NAME had no effect on the basal nor the LPS plus cytokine-induced rate of protein synthesis in myoblasts. Confirming that LPS plus cytokines, and indeed NO, had no effect on protein synthesis. Insulin induced an average 26% increase in protein synthesis in the presence of L-NAME, which was not statistically different to the insulin response of untreated myoblasts – 38% ($p = 0.21$). Similarly, the average rate of protein synthesis induced by insulin without L-NAME – 2.95 nmoles inc./mg protein/h – was not statistically different to that with L-NAME – 2.83 nmoles inc./mg protein/h ($p = 0.35$). The LPS plus cytokine-induced impairment discussed in Section 6.2.2 was still apparent when

myoblasts were co-treated with L-NAME; the insulin-induced increment in the presence of LPS plus cytokines was 5% – down from 38% in untreated cells – while in the presence of L-NAME the insulin response was significantly decreased from 26% in untreated myoblasts to -7% in treated cells. These results indicate that the impairment to the insulin response was not NO-dependent, correlating with the glycogen synthetic data from Section 3.3.2 where L-NAME had no effect on the LPS plus cytokine-induced impairment of the insulin response. This is in contrast to the suggestion that NO nitrosylates Akt, impairing protein synthesis, and similarly impairing the insulin-induced increase in protein synthesis (Yasukawa et al. 2005; Frost et al. 2009). Frost et. al. only treated C2C12 myotubes with LPS (1μg/ml) and IFN-γ (3ng/ml) for 10 hours, but this inhibited basal protein synthesis by 80% and was reversed by the co-treatment with L-NAME.

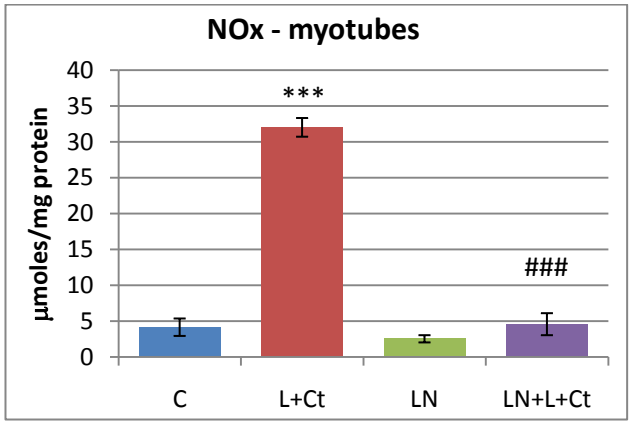

Fig 6.2.3c. The effect of L-NAME on total NO levels (NOx) induced by LPS plus cytokine treatment in myotubes. Cells were treated as described in Section 2.2.5. The results shown are the mean μmoles NOx in the medium ± SEM from 10-13 determinations from 3 independent experiments (without L-NAME) and 3 determinations from 1 experiment (with L-NAME).
Statistical significance is as described in Section 2.14.
* = Significance from control
# = Significant from LPS + Cytokine
(C=Control, L+Ct=LPS+Cyt, LN=L-NAME, LN+L+Ct=L-NAME+LPS+Cyt)

Figure 6.2.3c shows the effects of L-NAME on the production of NO in myotubes. L-NAME effectively and significantly inhibited the production of NO in LPS plus cytokine treated myotubes by 86%.

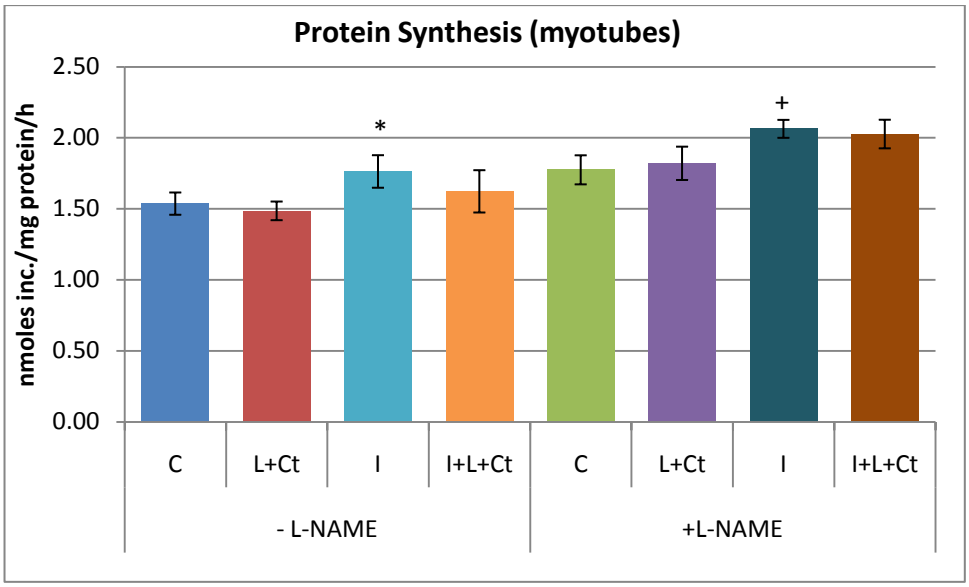

	Control (% difference)	With L-NAME (% difference)
Insulin response	13 ± 5%	17 ± 9%
Insulin response in the presence of LPS plus cytokines	7 ± 5%	12 ± 6%

Fig 6.2.3d and Table 6.2.3b. The effect of L-NAME on protein synthesis in the presence and absence of LPS plus cytokines and/or insulin in myotubes. Cells were treated as described in Section 2.2.5. The results shown are the mean nmoles of methionine incorporated into protein over one hour ± SEM from 10-13 determinations from 3 independent experiments (without L-NAME) and 3 determinations from 1 experiment (with L-NAME).
Statistical significance is as described in Section 2.14.
* = Significance from control
+ = Significance from L-NAME
(C=Control, L+Ct=LPS+Cyt, I=Insulin, I+L+Ct=Ins+LPS+Cyt)

As seen with the myoblast results presented in Figure 6.2.3b, L-NAME did not alter the basal or LPS plus cytokine induced rate of myotube protein synthesis. Equally, the insulin response in the presence of L-NAME (17%) was not statistically different to the control insulin response (13%) ($p = 0.35$). L-NAME did not appear to reverse the LPS plus cytokine induced impairment of the insulin response, since the insulin response in LPS plus cytokine treated cells with or without L-NAME co-treatment were not statistically different ($p = 0.31$). However as described in Section 6.2.2, it was difficult to address insulin resistance in the myotubes since the percentage increase induced by insulin was so minimal. In Section 5.3.2, the levels of

phosphorylated myotube Akt and GSK3 were discussed, and it was shown that LPS plus cytokines increased the phosphorylation of Akt and GSK3 in a NO-dependent fashion. This would suggest that LPS plus cytokines may have increased protein synthesis relative to LPS plus cytokine treated myotubes co-treated with L-NAME. However as seen in the figure above, this was not the case. The literature discussed under Figure/Table 6.2.3a suggested a NO mediated nitrosylation of Akt, impairing protein synthesis, which would as well inhibit insulin-induced protein synthesis (Yasukawa et al. 2005). Both these situations contrast with the myotube results presented in the figure above.

6.3 Effects of LPS plus Cytokine Treatment on 4E-BP1 Phosphorylation

As described in Section 6.1, BP1 is an important protein involved in the regulation of cap-dependent protein synthesis. Its role is to sequester eIF4E from the cap structure eIF4F, thus inhibiting protein synthesis. When protein translation is favoured, BP1 becomes hyperphosphorylated which releases it from eIF4E, allowing the eIF4F complex to form and thus protein translation to commence. In the Western blots described below, BP1 is present in three phosphorylated forms: α, β and γ-BP1, where γ represents the hyperphosphorylated form (top band), which can no longer bind eIF4E and therefore is no longer able to inhibit protein translation initiation (Bodine 2006). β-BP1 is the middle band, and finally α-BP1 is the lower band which is the least phosphorylated form and hence is able to bind and sequester eIF4E more prominently (Bodine 2006).

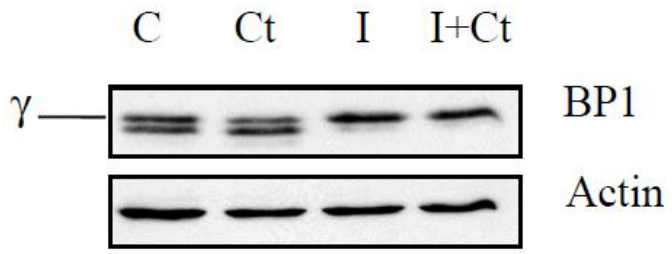

Fig. 6.3a. Example of a western blot for myoblast BP1 along with the loading control (Actin). Visualised using ECL, BP1 bands run between 15-20 KDa. . C=Control, Ct=LPS+Cyt, I=Insulin, I+Ct=Ins+LPS+Cyt

Figure 6.3a shows the different levels of α, β and γ BP1. The 18 hour LPS plus cytokine treatment slightly decreased the population of γ-BP1, partially increased the level of β-BP1 relative to the control and although faint, brought about the appearance of the α-BP1 band. This could suggests that there may have been a slight increase in protein synthesis relative to

the control, however as seen in Figure 6.2.1b, protein synthesis did not differ between control and treated cells. Insulin increased the appearance of the hyperphosphorylated form of BP1, regardless of LPS plus cytokine treatment, implying that translation was uninhibited by BP1 binding to eIF4E. These insulin-induced results correlated with the myoblast Akt/GSK3 data presented in Section 5.3.1 where insulin stimulated the phosphorylation of both proteins regardless of LPS plus cytokine treatment. In contrast, the actual protein synthetic results presented in Section 6.2.2 showed an impairment of the insulin response induced by LPS plus cytokines, reinforcing once again that the underlying mechanism of this impairment was not related to Akt/GSK3 signalling nor the downstream event of BP1 phosphorylation (Proud 2007; Plaisance et al. 2008). Interestingly however, insulin-mediated ERK1/2 phosphorylation was impaired by LPS plus cytokines. As discussed in Section 6.1, ERK1/2, together with Akt, inhibit TSC2 upon insulin stimulation which releases the TSC2-mediated inhibition of mTOR, thus allowing BP1 phosphorylation. These results would therefore imply that despite the impairment of insulin-mediated ERK1/2 activation by the LPS plus cytokine treatment, insulin-induced BP1 phosphorylation occurred unimpaired due to unaltered insulin signalling through Akt, even in the presence of LPS plus cytokines.

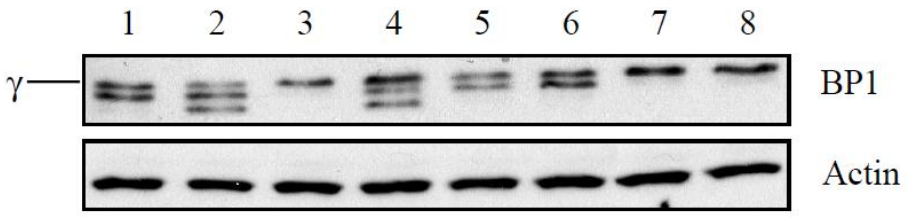

Fig. 6.3b. Example of a western blot for myotube BP1 along with the loading control (Actin). Visualised using ECL, BP1 bands run between 15-20 KDa. 1=Control, 2=LPS+Cyt, 3=Insulin, 4=Ins+LPS+Cyt, 5=L-NAME, 6=L-NAME+LPS+Cyt, 7=L-NAME+Ins, 8=L-NAME+Ins+LPS+Cyt.

Figure 6.3b shows the levels of α, β and γ-BP1 present in the myotubes following the various treatments. LPS plus cytokines increased the level of α-BP1 (hypophosphorylated form) which would suggest sequestration of a larger proportion of eIF4E relative to control. This should result in a potential inhibition of protein synthesis, however this was not the case as seen in Figure 6.2.1b where the rates of protein synthesis were unchanged. The fact that LPS plus cytokines brought about the dephosphorylation of BP1 relative to control correlates with the myoblast data shown in Figure 6.2.1a, although this was more pronounced in the myotubes. This LPS plus cytokine-mediated effect was NO-dependent, as seen by the lack of

the α-BP1 band when the myotubes were co-treated with L-NAME. Insulin increased the phosphorylation of BP1, as seen by the prominent γ-BP1 band relative to the control. This response was impaired by LPS plus cytokines, since the treatment prevented that total shift of BP1 to the hyperphosphorylated form, which is in contrast to the myoblast data. Interestingly this impairment was completely inhibited by the presence of L-NAME, whereby insulin was able to shift the BP1 population to the γ-BP1 band even after LPS plus cytokine treatment, indicating the insulin-resistance induced by the LPS plus cytokines was NO-dependent.

These results might imply that the insulin signalling cascades transduced via Akt and ERK1/2 were impaired following LPS plus cytokine treatment, yet as shown by the Western blot data in Section 5.3.2, insulin-stimulated phosphorylation of Akt was unimpaired following treatment. Insulin-mediated activation of ERK1/2 on the other hand was hindered by LPS plus cytokine treatment (Figure 5.4.2g), which could be a reason for the impaired phosphorylation of BP1, as described above regarding the BP1 results for myoblasts. The LPS plus cytokine-mediated effects presented in both figures within this section are in accordance with a study that induced sepsis in rats via a caecal ligation and puncture for 20-24 hours which noted a decreased phosphorylation of BP1 (Lang and Frost 2007). However, in contrast to the myoblast and myotube results, Plaisance et. al. observed an increase in BP1 phosphorylation after treating C2C12 myotubes with TNF-α (10ng/ml) for 24 and 48h (Plaisance et al. 2008). Despite also using C2C12 cells, the latter study did not include LPS, IFN-γ and IL-1β for the treatment of the cells, which could explain the differing results.

6.4 LPS plus Cytokine-Induced Time-Dependent Changes on Basal and Insulin-Stimulated Protein Synthesis in Myoblasts

The 18 hour LPS plus cytokine treatment consistently raised total protein in myoblasts. However in contrast to this, the measurements of protein synthesis discussed in Section 6.2.1 failed to show any sign of increased protein synthesis. It is possible that the 18 hour treatment failed to show a change in protein synthesis because the increase occurred earlier in the treatment. Consequently myoblasts were treated with LPS plus cytokines for varying times so as to address this: the times chosen were 3, 6, 9, 12 and 18 hours.

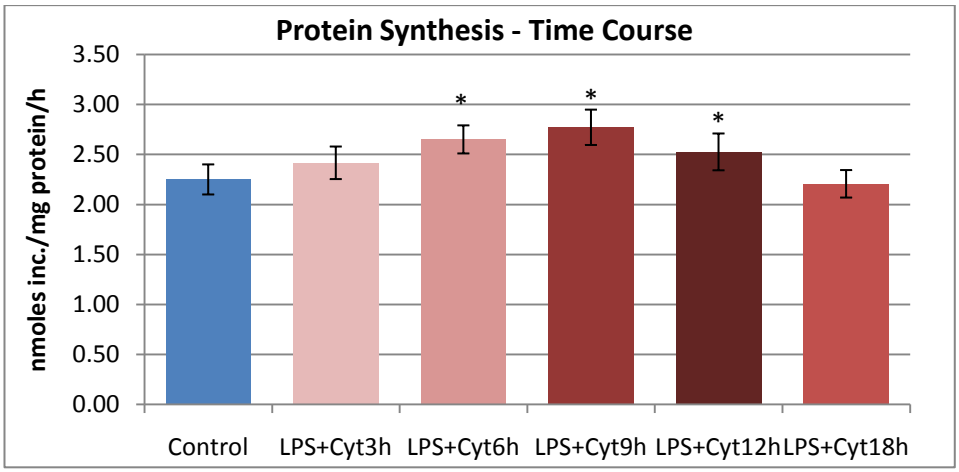

Fig. 6.4a. Effect of varying the time of LPS plus cytokine treatment on basal protein synthesis in myoblasts. Cells were treated with LPS plus cytokines for the times displayed. The results shown are the mean nmoles of methionine incorporated into protein over one hour ± SEM from 10-12 determinations from 4 independent experiments. Statistical significance is as described in Section 2.14.
* = Significance from control

Figure 6.4a displays the rate of protein synthesis after 3, 6, 9, 12 and 18 hours of LPS plus cytokine treatment. Protein synthesis after 3 and 18 hours of treatment was 2.42 and 2.21 nmoles inc./mg protein/h, respectively. These rates were not significantly different to the control rate which was 2.25 nmoles inc./mg protein/h. Between 6 and 12 hours of LPS plus cytokine treatment however, protein synthesis was significantly upregulated compared to the control rate. 6 hours of treatment increased protein synthesis by 18%, from 2.25 to 2.65 nmoles inc./mg protein/h, while 9 and 12 hours of treatment increased the rate by 23% and 12%, respectively, or up to 2.77 and 2.53 nmoles inc./mg protein/h, respectively. Similarly, LPS plus cytokines increased myoblast glycogen synthesis following 6 hours of treatment (as discussed in Section 3.3.5), which could suggest that the mechanism of action was similar to the effect observed in the figure above. However 18 hours of treatment still upregulated myoblast glycogen synthesis, in contrast to the data presented above, indicating that if both stimulations occurred due to a common mechanism, that the stimulation of protein synthesis was switched off due to a mechanism that was not shared by the glycogen synthesis increase induced by the LPS plus cytokine treatment.

The significant increase in protein synthesis shown above correlates with a study performed on C2C12 myotubes where 6 hours of TNF-α treatment (100ng/ml) upregulated protein synthesis, however the extent of the upregulation, 70%, does not coincide with the result above (Alvarez et al. 2001). Nevertheless the conditions were different; LPS, IL-1β and IFN-γ were used as well as TNF-α in the experiment above, the level of TNF-α used varied and

Alvarez et. al. performed the experiment on myotubes (Alvarez et al. 2001). Although Plaisance et. al. treated C2C12 myotubes for 24 hours with only TNF-α (10ng/ml), a significant increase in protein synthesis was also observed, albeit to a higher degree than that displayed above (Plaisance et al. 2008). What is clear though, is that these results presented above help explain why myoblasts consistently had more protein after 18 hours of LPS plus cytokine treatment, as seen in Figure 6.2a.

As discussed in previous sections in this chapter, the insulin-stimulated rise in protein synthesis was impaired after 18 hours of LPS plus cytokine treatment. During the time course experiment insulin was also included in the experimental model so as to assess at which time-point the insulin-resistant phenotype became apparent.

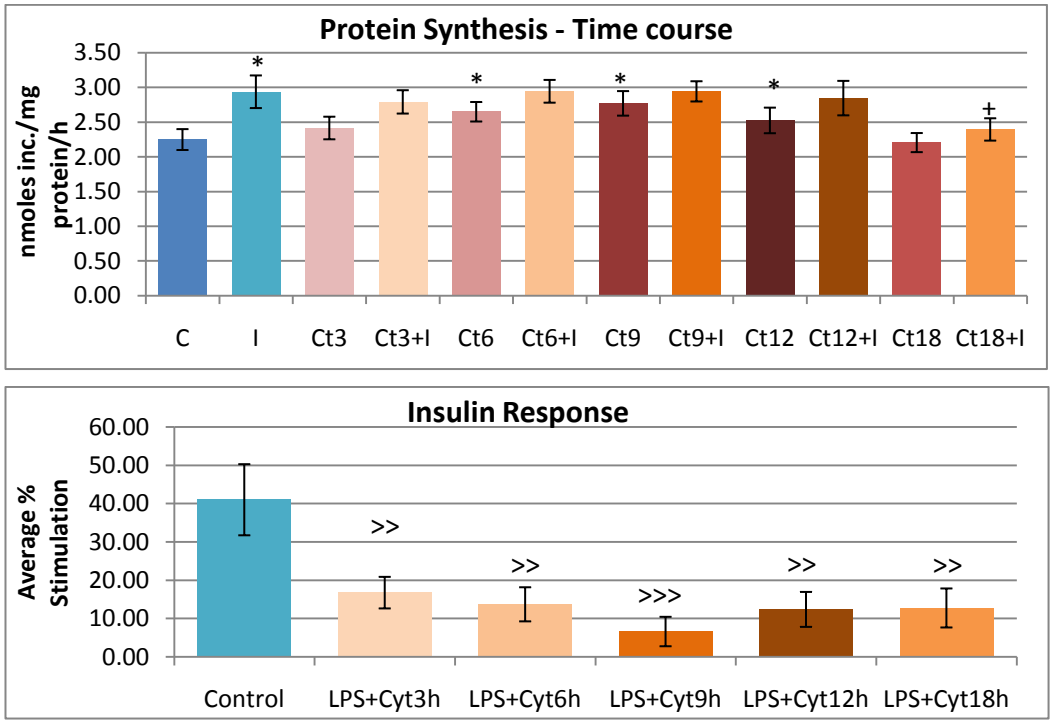

Fig. 6.4b+c. b: Effect of varying the time of LPS plus cytokine treatment on the insulin-stimulated protein synthesis in myoblasts. c: insulin response from the different LPS plus cytokine treatments. The results shown are the mean nmoles of methionine incorporated into protein over one hour ± SEM from 10-12 determinations from 4 independent experiments. Statistical significance is as described in Section 2.14.
* = Significance from control, + = Significance from Insulin, > = Significance from control insulin response
C=control; I=Insulin; Ct=LPS+Cytokine; Ct+I=LPS+Cyt+Insulin; 3,6,9,12,18=hours of treatment)

Figure 6.4b displays the rates of protein synthesis in myoblasts after varying times of LPS plus cytokine treatment, and the effect this had on the insulin response. In untreated cells insulin significantly raised the rate of protein synthesis by 31%, or from 2.25 to 2.94 nmoles inc./mg protein/h. The insulin induced rates after the various LPS plus cytokine treatments were not significantly different from the control insulin response, except after 18 hours of treatment at which point the insulin-induced rate of protein synthesis was significantly lower. Following LPS plus cytokine treatment, insulin failed to significantly upregulate protein synthesis, as can be seen by the lack of significance between basal and insulin-stimulated rates from the bar chart above. Figure 6.4c shows the average % stimulation induced by insulin in LPS plus cytokine treated cells for 3 – 18 hours, as well as the control value. For each treatment time-point, the insulin-induced stimulation was significantly different to the control insulin-induced stimulation. The average increment induced by insulin in untreated cells was 41%, while after 3, 6, 9, 12 and 18 hours of LPS plus cytokine treatment it decreased to 17, 14, 7, 12 and 13%, respectively. This could suggest that the insulin response was impaired following treatment, however since the LPS plus cytokine treatment raised the control rates, it is potentially a case of protein synthesis reaching a maximal rate. This was similar to the situation seen with the myoblast insulin-stimulated glycogen synthesis following LPS plus cytokine treatment for 3, 6, 9, 12 and 18 hours, discussed in Section 3.3.5.

As can be seen from Figure 6.4b the insulin-induced rate of protein synthesis at 18 hours of treatment dropped together with the 18 hour LPS plus cytokine-induced rate. This indicates that the drop in the insulin-induced rate of protein synthesis at 18 hours of treatment occurred simultaneously with the drop in basal protein synthesis. This could suggest that the reason for the insulin-induced rate after 18 hours of treatment being lower than the control insulin-induced rate is due to the fact that 18 hours of treatment no longer increased protein synthesis as did 6-12 hours of treatment. As the LPS plus cytokine-induced stimulation of protein synthesis ceased (after 12 hours), insulin-resistance began. Nevertheless it is difficult to address the insulin-resistant phenotype between 3 and 12 hours of treatment. Two studies in C2C12 myotubes reported insulin resistance after 70 minutes of TNF-α (20ng/ml) or 6 hours of TNF-α (100ng/ml) treatment (Alvarez et al. 2001; Williamson et al. 2005). In the studies performed by Williamson et. al., TNF-α failed to affect protein synthesis, which was also the case in TNF-α and insulin treated myotubes. While Alvarez et. al. observed a significant increase in protein synthesis following TNF-α treatment as well as insulin stimulation alone, but TNF-α treated myotubes stimulated with insulin failed to raise the rate of protein synthesis. The latter could be a similar situation as the one displayed above, where

insulin failed to increase the rate of protein synthesis in treated cells because the treatment increased the control rate which meant that protein synthesis had reached a maximal rate.

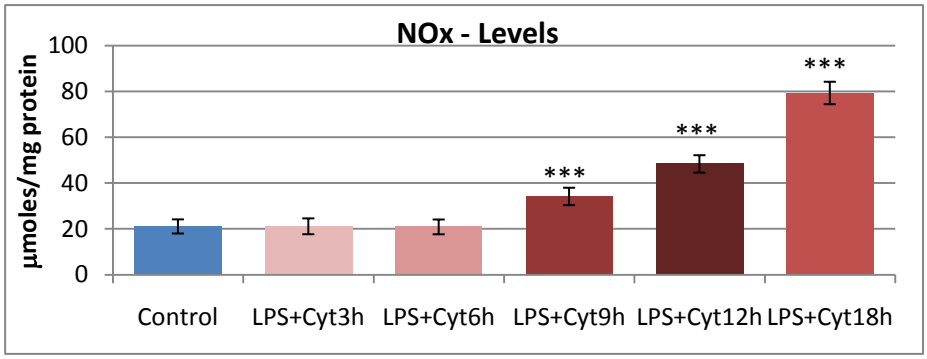

Fig. 6.4d. Effect of varying the time of LPS plus cytokine treatment on the accumulation of NOx in myoblasts. The results shown are the mean µmoles of NOx in the medium per mg protein ± SEM from 31-35 determinations from 6 independent experiments. Statistical significance is as described in Section 2.14
* = Significance from control

Figure 6.4d is the same as shown previously in Section 3.3.5. It shows the levels of NOx present in the medium following the different LPS plus cytokine treatment times. It was only after 9 hours of treatment that the levels of NOx accumulated to a significantly higher degree relative to the untreated control cells. This represented an increase of 62% (from 21µmoles to 34µmoles/mg protein). Following 12 and 18 hours of treatment the relative accumulated level of NOx was 128 and 276% higher than in the control cells, respectively. LPS plus cytokines significantly increased myoblast protein synthesis following 6 hours of treatment, which together with the NOx results presented above, indicates the upregulation was NO-independent. The insulin resistance induced by 18 hours of LPS plus cytokine treatment is unlikely to be due to NO production either, since NOx accumulated to significantly higher levels before the insulin-resistance phenotype was apparent. It has been shown however that NO inhibits the translational machinery through nitrosylation of Akt, impairing the mTOR pathway (Yasukawa et al. 2005; Frost et al. 2009). This would not have been apparent in the Western blot data related to Akt presented in Section 5.3.1 since Akt phosphorylation was still enabled but its activity was reduced (Yasukawa et al. 2005). It is therefore possible that the protein synthetic machinery was impaired towards the latter stages of the treatment with LPS plus cytokines, thus explaining why the rate of protein synthesis was only upregulated between 6 and 12 hours of treatment. This is however difficult to address from the results

shown in Figure 6.4d as the levels of NOx shown represent the levels of accumulated NOx. Moreover after 9 hours of LPS plus cytokine treatment there was a significantly higher level of NOx in the medium compared to the control wells, suggesting that iNOS expression was already resulting in NO production and potential inhibition of the Akt/mTOR pathway. Nevertheless there may have been a threshold level of NO reached, resulting in the LPS plus cytokine-induced increase in protein synthesis ceasing.

6.5 Effects of LPS and Pro-Inflammatory Cytokine Combinations on Protein Synthesis

Several pieces of literature referred to in this chapter treated cells in vitro or rats in vivo with one or two pro-inflammatory cytokines as well as utilising LPS in combination with one other cytokine. Although the purpose of the experimental model in this thesis was to mimic endotoxic shock, using particular combinations of cytokines and LPS can provide insight into which stimulants appear to be more important, if any. As a result C2C12 myoblasts were treated with various combinations of LPS, TNF-α, IL-1β and IFN-γ for 18 hours, and subsequently the rate of protein synthesis determined.

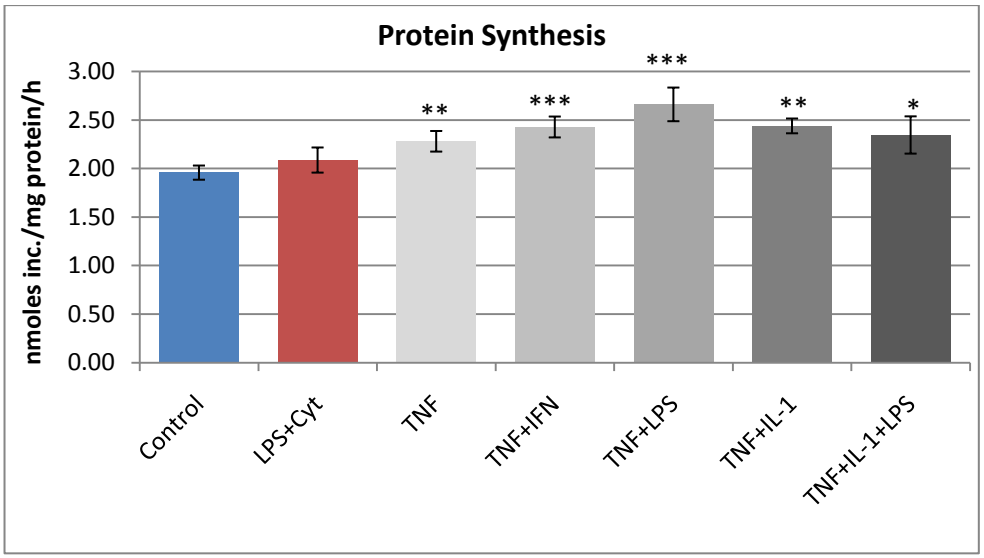

Fig. 6.5a. Effect of various combinations of LPS, TNF-α, IL-1β and IFN-γ on myoblast protein synthesis. The cells were treated for 18 hours with the combination of stimulants shown. The results shown are the mean nmoles of methionine incorporated into protein over one hour ± SEM from 13-15 determinations from 5 independent experiments (except TNF+IL-1+LPS: 6 determinations from 2 independent experiments. TNF+LPS and TNF+IL-1: 3 determinations from 1 experiment). Statistical significance is as described in Section 2.14. * = Significance from control,

Figure 6.5a displays the rates of protein synthesis in myoblasts following 18 hours of treatment with various combinations of cytokines and LPS. In this instance, TNF-α was used in combination with one of the following: IFN-γ, LPS, IL-1β; and then with IL-1β and LPS. The focus was on TNF-α due to the multitude of studies having used TNF-α due to its established effects on protein synthesis (Llovera et al. 1997; Alvarez et al. 2001; Lang et al. 2002; Williamson et al. 2005; Lang and Frost 2007; Austin et al. 2008; Eley et al. 2008; Plaisance et al. 2008). These experiments were done in parallel with the usual LPS plus all 3 cytokines treatment, to appropriately compare to the previous results presented in this chapter. As expected, LPS plus all 3 cytokines failed to significantly affect the rate of protein synthesis ($p = 0.19$), correlating with earlier data discussed in this chapter. The 5 other combinations however, significantly upregulated basal protein synthesis. TNF-α and TNF-α + IFN-γ treatment increased protein synthesis by 16 and 24%, respectively. This equated to a net increase of 0.32 and 0.47 nmoles inc./mg/h, respectively. TNF-α + LPS and TNF-α + IL-1β treatment upregulated protein synthesis by 36 and 25%, respectively, or a net increase of 0.7 and 0.48 nmoles inc./mg protein/h, respectively. Finally myoblasts treated with TNF-α, IL-1β and LPS increased the rate of protein synthesis by 19% (net increment of 0.38 nmoles inc./mg protein/h).

The treatment of myoblasts with TNF-α on its own displayed in Figure 6.5a correlates with two other studies. A 24 hour treatment with TNF-α (10ng/ml) upregulated protein synthesis by 67% (Plaisance et al. 2008). This paper used myotubes, treated for an extra 6 hours and used a 5 fold higher concentration of TNF-α, which could explain the variability between the results observed by Plaisance et. al. and those presented above. In the other study, C2C12 myotubes were treated for 6 hours with 100ng/ml of TNF-α and observed a similar 70% increase as that seen by Plaisance et. al., even though TNF-α levels were 10 fold higher and the incubation time with the cytokine was only 6 hours (Alvarez et al. 2001). In contrast to these papers, and the results presented above, a 24 hour treatment of C2C12 myotubes with TNF-α (50ng/ml) or with TNF-α and INF-γ (10ng/ml) significantly inhibited protein synthesis by 30% and 50%, respectively (Eley et al. 2008). Despite the conflicting results in the literature, the results presented in Figure 6.5a suggest TNF-α alone, as well as TNF-α in combination with either LPS, IFN-γ or IL-1β significantly increased protein synthesis after 18 hours of treatment. This is interesting since an 18 hour treatment with LPS and all 3

cytokines failed to do so, even if between 6 hours and 12 hours there was a significant increment induced by the full treatment (as discussed in Section 6.4).

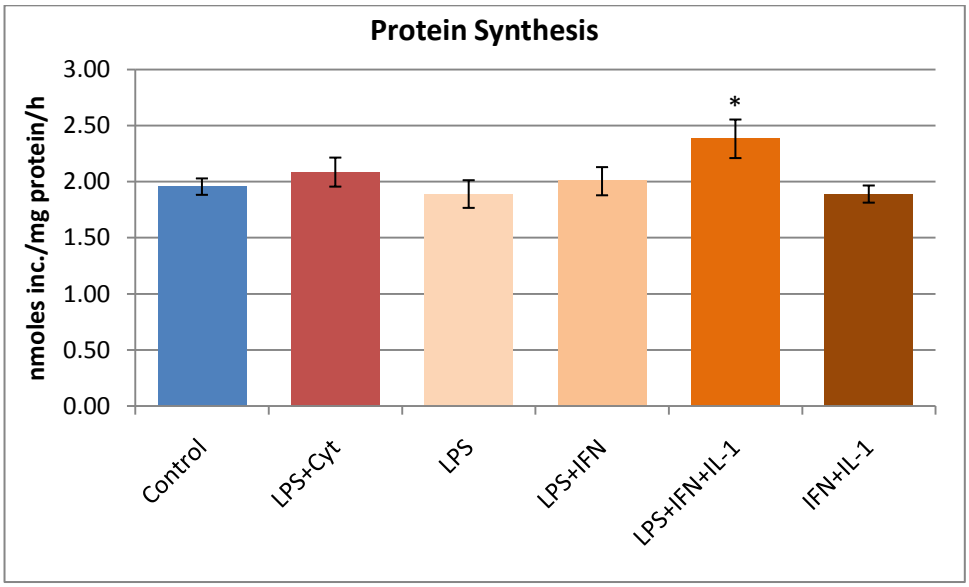

Fig. 6.5b. Effect of various combinations of LPS, TNF-α, IL-1β and IFN-γ treatment on myoblast protein synthesis. Cells were treated for 18 hours with the combination of stimulants shown. The results shown are the mean nmoles of methionine incorporated into protein over one hour ± SEM from 13-15 determinations from 5 independent experiments (except LPS+IFN and IFN+IL-1: 9 determinations from 3 independent experiments. LPS: 6 determinations from 2 independent experiments). Statistical significance is as described in Section 2.14.
* = Significance from control,

Figure 6.5b shows myoblast rates of protein synthesis after another set of 18 hour LPS and cytokine combination treatments. The only treatment that significantly affected the basal rate of synthesis was LPS, IFN-γ and IL-β, which brought about an upregulation of 21%, equating to a net increase of 0.42 nmoles inc./mg protein/h. This upregulation was not significantly different from the increments induced by the treatments presented in Figure 6.5a. Interestingly IFN-γ + IL-1β, and LPS + IFN-γ failed to upregulate protein synthesis, yet LPS + IFN-γ + IL-1β together succeeded in doing so. This would imply that it was critical to have all three there, however since the effect of just LPS with IL-1β was not determined, it cannot be excluded that it too may have been enough to stimulate protein synthesis. The surprising thing is that LPS and IL-1β stimulate very similar pathways, as discussed in the introduction to this thesis, suggesting that the presence of LPS and IL-1β in the system may have had an additive effect. Since the increments induced by these various treatments presented in the two figures above did not significantly differ from each other, it could point towards an overlapping

mechanism of action on protein synthesis. Although LPS, TNF-α and IFN-γ stimulate separate pathways, the routes overlap at particular signalling molecules as well as stimulating the regulation of similar transcription factors.

As discussed in Section 2.2.5, a significant increase in NOx accumulation required a combination of LPS, TNF-α, IFN-γ and IL-1β. This indicates that NO production did not contribute to the increase in protein synthesis induced by these various combinations shown in this section. Moreover, the increments induced by these treatments were not statistically different to the increments induced by 6, 9 and 12 hours of LPS plus all 3 cytokines discussed in Section 6.4, re-affirming the NO-independent effect as well as suggesting a similar underlying mechanism resulting in this increase in protein synthesis. This is surprising however, as 18 hours of LPS plus cytokine treatment failed to increase protein synthesis. This could re-affirm the concept that NO production was higher during the latter stages of LPS plus cytokine treatment, and that a threshold level was reached which stopped the treatment-induced increase in protein synthesis.

6.6 Summary

Myoblast protein synthesis was significantly (40%) higher than the rate in myotubes. The rate was unchanged for both myoblasts and myotubes following 18 hours of LPS plus cytokine treatment (Figure 6.2.1b). This was despite the fact that the treatment consistently increased the level of protein in myoblasts (Figure 6.2a). Insulin treatment significantly increased protein synthesis, by 38% in myoblasts and 13% in myotubes. Both these results correlate with the signalling data presented in Sections 5.3.1 and 5.3.2 where Akt, GSK3 and ERK1/2 phosphorylation were induced by insulin. The LPS plus cytokine treatment impaired the insulin response in myoblasts, indicating insulin resistance; the treatment decreased the insulin-induced increment from 38 to 5%. There appeared to be insulin resistance in the myotube results as well but the minimal insulin response made it difficult to determine. The impairment in the myoblasts was not due to an impairment of the insulin signalling cascade through Akt, as shown in Section 5.3.1 where insulin-induced Akt phosphorylation was unaltered by LPS plus cytokine treatment. Insulin-induced ERK1/2 phosphorylation on the other hand was considerably impaired by LPS plus cytokine treatment in myoblasts. This may well have reduced the synthesis of protein under insulin stimulation, due to the role played by ERK1/2 in the insulin signal cascade governing protein synthesis (as discussed in Section 6.1).

L-NAME was used to suppress the production of NO, reducing NO production by 72 and 86% in LPS plus cytokine treated myoblasts and myotubes, respectively. This brought no significant change to the LPS plus cytokine, insulin or LPS plus cytokine and insulin induced effects on myoblast or myotube protein synthesis. This indicated that the LPS plus cytokine-induced impairment of the insulin response in myoblasts was not NO-dependent.

4E-BP1 (BP1) is one of the routes of protein synthesis regulation as it can bind and sequester eIF4E preventing translation initiation (discussed in Section 6.1). Blotting for BP1 allows the visualisation of 3 possible bands: α, β and γ. The γ-band represents the hyperphosphorylated form which is indicative of eIF4E release, and therefore activation of translation initiation (Bodine 2006). In the myoblasts, 18 hours of LPS plus cytokine treatment partially decreased the γ-BP1 population, increased the level of β-BP1 and also slightly increased α-BP1 relative to the control. This would have contributed to a decrease in protein synthesis, however as seen in Figure 6.2.1b, the rate of protein synthesis was unchanged. Insulin stimulation in myoblasts considerably increased the level of γ-BP1, leaving almost no BP1 in the α or β form. This correlated with the results presented in Figure 6.2.2a where insulin significantly increased the rate of myoblast protein synthesis. This data also correlates with the insulin-induced phosphorylation of myoblast Akt and ERK1/2 (Figures 5.3.1e and 5.4.1g), which upon activation bring about BP1 phosphorylation via mTOR (Figure 6.1a). The LPS plus cytokine treatment had no effect on the insulin-mediated phosphorylation of BP1, indicating an unimpaired signal. This would correlate with the unimpaired insulin-induced phosphorylation of Akt in myoblasts (Figure 5.3.1e) following treatment but would contrast with the data in Figure 6.2.2b where LPS plus cytokines impaired the rate of insulin-mediated protein synthesis. In addition, ERK1/2 phosphorylation under insulin stimulation was impaired by the 18 hours treatment in myoblasts, contrasting with the BP1 result. The insulin resistance observed may be due to the inhibition of insulin-induced ERK1/2 phosphorylation involving the other downstream event of this activation besides mTOR/BP1 which is the activation of eIF4E via Mnk1, as described in Section 6.1.

The 18 hour LPS plus cytokine treatment also caused the dephosphorylation of myotube BP1, correlating with the myoblast data. The treatment increased α-BP1 (hypophosphorylated form), and reduced both the γ and β forms relative to control (Figure 6.2.4b). This would suggest a possible inhibition of protein synthesis, however as seen in Figure 6.2.1b protein synthesis was unchanged by the treatment, suggesting BP1 activation alone cannot inhibit protein synthesis. L-NAME prevented the LPS plus cytokine-induced dephosphorylation of myotube BP1 as seen by the lack of the α-BP1 band, suggesting this

effect was NO-dependent. As seen with the myoblasts, insulin stimulated the phosphorylation of BP1 with the prominent expression of γ-BP1, correlating with the insulin-induced increase in protein synthesis (Figure 6.2.2a), despite it being small. In contrast to the myoblast data however, LPS plus cytokines inhibited the insulin-induced phosphorylation of myotube BP1, suggesting insulin resistance, which was rescued by L-NAME. Due to the minor insulin response in myotube protein synthesis however insulin resistance was difficult to address. Although insulin-stimulated myotube Akt phosphorylation was not altered by LPS plus cytokine treatment, there was an impairment to the insulin-mediated phosphorylation of ERK1/2 which may have played a role in this treatment-induced impairment to BP1 signalling under insulin stimulation. Indeed the LPS plus cytokine-induced impairment of insulin-stimulated ERK1/2 was also NO-dependent, suggesting that this was likely to contribute to the impairment of BP1 phosphorylation under insulin treatment.

The fact that LPS plus cytokines failed to increase the rate of myoblast protein synthesis yet consistently increased the level of protein over the 18 hour period, lead to treating the myoblasts for shorter times in order to deduce when the increase in protein synthesis occurred. After 6 hours of LPS plus cytokine treatment, protein synthesis was significantly increased relative to control – by 18% (Figure 6.4a) – while a 9 and 12 hour incubation with LPS plus cytokines also significantly increased protein synthesis, by 23 and 12%, respectively. After 18 hours of incubation however, this significant LPS plus cytokine-induced upregulation of protein synthesis was no longer visible, correlating with the previous data presented which had not shown a change in protein synthesis after 18 hours of LPS plus cytokine treatment. This latter observation could indicate that the treatment-induced upregulation of glycogen synthesis discussed in Section 3.3.5 did not occur via the same mechanism as the upregulation of protein synthesis since glycogen synthesis was still increased after 18 hours of treatment. Nevertheless, as discussed, it is possible that a shared mechanism resulted in the upregulation of both myoblast protein and glycogen synthesis following treatment, but that the stimulation to protein synthesis was switched off by a different mechanism that had no effect on glycogen synthesis.

LPS plus cytokine-mediated insulin resistance in myoblasts treated for 3, 6, 9 and 12 hours was not clear. The insulin-induced stimulation of myoblast protein synthesis following these treatments was significantly lower than the control insulin-stimulated increment (Figure 6.4c), while the net insulin-induced rates of protein synthesis of these treatments were not statistically different to their respective basal rates. These facts could suggest an insulin impairment. However, the net rates of protein synthesis in LPS plus cytokine treated myoblasts (for 3, 6, 9 and 12 hours) stimulated with insulin were not statistically different to the insulin-

induced rate (Figure 6.4b). In addition LPS plus cytokines increased the basal rates, potentially suggesting that the rate of protein synthesis under insulin conditions in treated myoblasts reached a maximal rate. After 18 hours of treatment, the rate of protein synthesis returned to the basal rate, but the insulin-induced increment was statistically different to the control insulin stimulation, indicating a degree of insulin resistance, which correlates with the earlier data presented in Section 6.2.2. NOx accumulation became significantly higher than in untreated myoblasts following 9 hours of treatment, suggesting that the onset of LPS plus cytokine-stimulated protein synthesis at 6 hours of treatment was not due to NO. The insulin-impairment following 18 hours of LPS plus cytokine treatment did not appear to be NO-mediated since NOx levels had already accumulated to a significant amount after 9 hours of treatment, indicating iNOS expression and NO production. However it is possible that NO production was higher during the latter stages of treatment reaching a threshold level resulting in insulin resistance.

18 hours of LPS plus all 3 cytokines failed to increase protein synthesis, while an 18 hour treatment of various combinations of LPS, TNF-α, IL-1β and IFN-γ significantly increased protein synthesis (Figures 6.5a and 6.5b). These combinations were: TNF-α, TNF-α + IFN-γ, TNF-α + LPS, TNF-α + IL-1β, TFN-α + IL-1β + LPS and LPS + IFN-γ + IL-1β. On the other hand, other combinations – LPS, LPS + IFN-γ and IFN-γ + IL-1β – failed to significantly change the basal rate of protein synthesis. The stimulatory combinations upregulated protein synthesis by 18-32% depending on the actual combination, yet neither of these increments were significantly different from each other nor the increments induced by 6, 9 and 12 hours of LPS plus all 3 cytokines, potentially suggesting a similar mode of action. This is possible because although TNF-α, IFN-γ and LPS activate different pathways, there are numerous overlapping targets. Once again, NO was not responsible for this increment since NOx levels were only significantly higher than untreated cells in those treated with LPS plus all 3 cytokines (Figure 2.2.5a). Interestingly 18 hours with TFN-α + IL-1β + LPS and LPS + IFN-γ + IL-1β increased protein synthesis yet the combination of LPS and all 3 cytokines failed to affect protein synthesis following 18 hours of treatment. This suggests that having the combination of all 4 differed enough to prevent this upregulation in protein synthesis compared the combination of LPS and just two cytokines. One of the differences was NOx production, which failed to occur in any of the combinations used. This could suggest that 18 hours of LPS plus all 3 cytokines treatment failed to maintain the increase in protein synthesis due to a threshold level of NO production being reached in the latter stages of treatment.

Chapter Seven - Conclusion

7.1 Overview of the Present Studies

The aim of the present study was to investigate the effects of the later stages of endotoxic shock on skeletal muscle glycogen synthesis in order to shed light on possible causes of the dysregulation of glucose homeostasis associated with the syndrome and involvement of NO in the process. As a result, the rate of glycogen synthesis and processes known to regulate it were assessed in C2C12 myoblasts and myotubes following an 18 hour treatment with LPS plus cytokines (TNF-α, INF-γ and IL-1β). Previous studies in hepatocytes (Curran et al. 1990; Ceppi et al. 1996; Wallington et al. 2008) reported that in order to induce iNOS and therefore NO production that LPS and all 3 cytokines were required. This was also the case in the C2C12 cells as NO production was only produced in significant amounts upon treatment with LPS plus all 3 cytokines (Figure 2.2.5a). This treatment did not affect cell viability in either myoblasts or myotubes, indicating that changes associated with the treatment were not due to effects on cell viability (Table 3.2.2a).

The LPS plus cytokine treatment significantly increased myoblast glycogen synthesis (Figure 3.3.1a), which correlated with a comparable increase in glucose transport (Figure 4.2.1b). Neither of these effects was NO-dependent and the treatment-induced increase in glucose transport was not due to oxidative stress either, as neither Euk8 nor PDTC significantly affected the stimulation. This increase in glucose uptake correlated with reports that glucose transport was increased in skeletal muscle following 24 hours of endotoxic shock treatment in vitro (Lee et al. 1987; Bedard et al. 1997; Khanna et al. 1999). As seen by the total activities of GS and Phosphorylase, myotubes expressed more of each compared with myoblasts, in line with previous studies (Wahrmann et al. 1973; Halse et al. 2001). The activity ratios of GS and Phosphorylase were unchanged by the LPS plus cytokine treatment while phosphorylation at myoblast GS Site 3 was increased which indicated it was inactive (Figure 4.4h). This suggests that the activation state of either of these proteins was not responsible for the increase in myoblast glycogen synthesis following LPS plus cytokine treatment. It has been established that an increase in glucose uptake alone is enough to significantly increase glycogen synthesis (Ren et al. 1993; Hansen et al. 1995). Moreover, a study looking at L6 myoblast differentiation following alterations in glucose concentration – among other parameters – reported that an increase in intracellular glucose correlated with an increase in G-6-P levels and glycogen deposition over 4 hours, while GS-a levels decreased (Elsner et al. 1998). These studies suggest that the increase in myoblast glycogen synthesis is likely to be accounted for by the increase in glucose transport. This increase in glycogen synthesis was apparent as of 6 hours of LPS plus

cytokine treatment, indicating that the underlying mechanism of this stimulation occurred earlier than the 18 hour treatment (Figure 3.3.5a).

Insulin treatment in myoblasts significantly increased glycogen synthesis but failed to affect glucose uptake (Figures 3.3.2a and 4.2.2a), in spite of the fact that Akt was activated under insulin stimulation which should mediate GLUT4 translocation (Huang and Czech 2007). Nevertheless literature has reported that insulin-mediated glucose transport is difficult to measure in C2C12 cells (Schmitz-Peiffer et al. 1999; Tortorella and Pilch 2002; Nedachi and Kanzaki 2006; Lorenzo 2008). However, the Phosphorylase-a : Phosphorylase-b ratio was significantly decreased in response to insulin (Figure 4.4d), which would result in a slower rate of glycogen breakdown, thereby increasing apparent net glycogen synthesis. Surprisingly myoblast GS fractional activity was unchanged by insulin despite insulin-mediated inactivation of GSK3 (Figure 5.3.1g), suggesting GS phosphorylation was maintained by other GS-kinases. A candidate for this could be AMPK, as Western blot analysis indicated it was phosphorylated by insulin stimulation implying increased activity (Figure 5.2.1e). AMPK phosphorylation increased following LPS plus cytokine treatment as well, which may have contributed to the increase in glucose transport, yet the activation of AMPK under insulin stimulation failed to lead to a measurable increase in glucose transport, making AMPK an unlikely factor contributing to the stimulation of myoblast glucose transport following treatment. Since insulin failed to significantly increase glucose transport, it would suggest that LPS plus cytokine-mediated stimulation of glucose uptake may have occurred via GLUT1, correlating with previous studies reporting an increase in GLUT1 expression and activity (Vary et al. 1995; Bedard et al. 1997; Ciaraldi et al. 1998).

Relative to the control insulin response, the insulin-stimulated rate of myoblast glycogen synthesis was significantly lower following 6 hours of LPS plus cytokine treatment. This could either imply insulin-resistance or that insulin prevented the full LPS plus cytokine induced increase in glycogen synthesis. Since the combination of both stimulatory treatments did not result in an additive response, it could suggest that both mechanisms underlying this stimulation shared a common mechanism of action which would result in a maximal rate being reached. The rate of glycogen synthesis in LPS plus cytokine treated cells was significantly lower than the rate in insulin-stimulated myoblasts following treatment (Figure 3.3.2b). However their rates of glucose transport were the same (Figure 4.2.3a), while insulin failed to increase glucose uptake, suggesting that insulin and LPS plus cytokines did not stimulate glycogen synthesis in a similar fashion. These facts taken together would imply that either treatment is impairing the increase induced by the other. The insulin-induced ERK1/2 phosphorylation – that would lead to PP-1 activation – was impaired by LPS plus cytokine

treatment (Figure 5.4.1g), suggesting insulin resistance was the more probable impairment. Indeed this may well have contributed the lack of Phosphorylase inactivation induced by insulin in LPS plus cytokine treated myoblasts (Figure 4.4d), confirming potential insulin resistance in myoblasts following 18 hours of LPS plus cytokine treatment.

The LPS plus cytokine treatment affected myotubes differently since glycogen synthesis was significantly downregulated (Figure 3.3.1a). This effect cannot be explained by a change in glucose transport as the rate of glucose uptake remained the same in treated and untreated myotubes. The downregulation of glycogen synthesis was NO-dependent as determined by the reversal of the effect by L-NAME treatment (Figure 3.3.3e). This correlated with a significant increase in glucose transport following L-NAME and LPS plus cytokine treated myotubes, possibly explaining the L-NAME-mediated reversal of glycogen synthesis downregulation (Figure 4.2.3b). Moreover, this NO-dependent inhibition coincided with a NO-dependent phosphorylation of GS at Site 3 (Figure 4.4p), despite the fact that myotube GSK3 activity was surprisingly inhibited by LPS plus cytokines as judged by phosphorylation (Figure 5.3.2g), implying it was not responsible for the phosphorylation of GS. However, phosphorylation at Site 3 is also regulated by other kinases (DYRK and PASK) and dephosphorylation by PP-1 (Ragolia and Begum 1998; Skurat and Dietrich 2004; Wilson et al. 2005), indicating that a DYRK or PASK-mediated phosphorylation of GS Site 3, or an inhibition of PP-1 activity may be responsible for the LPS plus cytokine-induced phosphorylation of myotube GS. In addition to this, LPS plus cytokine treatment resulted in an NO-dependent phosphorylation of myotube AMPK – indicating it was activated (Figure 5.2.2c) – which could lead to phosphorylation and inhibition of GS at Site 2. Therefore this could also be contributing to the inhibition of myotube glycogen synthesis following LPS plus cytokine treatment. Nevertheless we failed to measure a change in myotube GS fractional activity (Figure 4.4c), indicating that there was no significant change in GS phosphorylation, making AMPK-mediated phosphorylation of GS an unlikely mechanism.

Insulin significantly upregulated myotube glycogen synthesis, correlating with insulin-mediated Akt, GSK3 and ERK1/2 phosphorylation. Part of this response was clearly impaired by LPS plus cytokine treatment. Akt and GSK3 signalling under insulin conditions remained intact following treatment, but insulin-stimulation of glycogen synthesis and ERK1/2 phosphorylation were impaired by the treatment. Interestingly, the former impairment was NO-independent (Figure 3.3.4b), however insulin-stimulation of ERK1/2 was impaired by LPS plus cytokines in a NO-dependent manner (Figure 5.4.2h). Similarly to the myoblast result, the inhibition of insulin-stimulation of ERK1/2 would result in the impairment of PP-1 activation, which could

affect insulin-induced glycogen synthesis. Since both processes differed with regards to the role played by NO, it indicates another underlying mechanism contributed to the insulin resistance.

No evidence was found to explain the increase in myotube glycogen synthesis following insulin treatment. However as described by Nedachi et. al., the basal rate of glucose uptake in C2C12 cells is particularly high, making it difficult to measure insulin-stimulation of glucose transport despite the presence of GLUT4 machinery (Nedachi and Kanzaki 2006). This could imply that insulin may have increased the rate of myotube glucose transport, albeit minimally, leading to the subsequent increase in G-6-P resulting in allosteric activation of GS as well as an increase in its substrate (UDP-glucose). It is therefore possible to suggest that this would have significantly increased glycogen synthesis, correlating with the fact that myotube Akt was activated by insulin.

The difference between myoblasts and myotubes throughout this study was interesting. The LPS plus cytokine treatment upregulated myoblast glycogen synthesis while downregulated it in myotubes, and the treatment increased myoblast glucose uptake but failed to affect myotube glucose transport. In addition Akt and GSK3 phosphorylation was induced by LPS plus cytokines in myotubes only. Finally NO appeared to play a more prominent role in the myotube effects observed while in myoblasts the inhibition of NO production made no significant changes to LPS plus cytokine induced effects. This is intriguing because the expression of iNOS was significantly higher in myotubes than myoblasts (Figure 3.2.3g), and glycogen synthesis was inhibited in myotubes in a NO-dependent manner, suggesting a higher level of NO production may have been the cause for the difference in effects. In support of this, a batch of C2C12 cells from a different source was used in parallel with the C2C12 batch used throughout this thesis and the rate of NOx production was found to differ substantially between both batches. The results are shown below in Figure 7.1a.

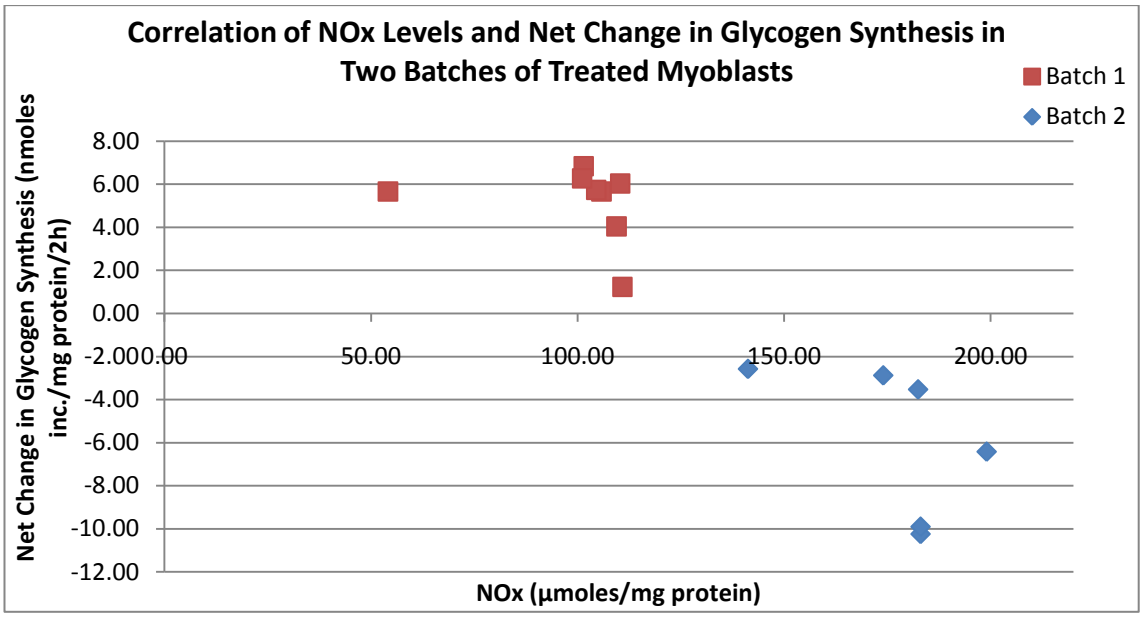

Figure 7.1a. Graph showing the correlation between NOx levels accumulated and the net change in glycogen synthesis induced by LPS plus cytokine treatment in two batches of C2C12 myoblast. Batch 1: batch of C2C12 cells used throughout this thesis. Batch 2: batch of C2C12 cells from a different source

Figure 7.1a shows the correlation between NOx levels accumulated in the medium and the net LPS plus cytokine induced effect on the rate of myoblast glycogen synthesis. Batch 1 represents the C2C12 myoblast batch used throughout this study whereas the second set (Batch 2) shows results from a batch of C2C12 cells that came from a different source. The figure shows that the LPS plus cytokine induced effect on glycogen synthesis was significantly different; the average net change in Batch 1 was 5.2 nmoles inc./mg/2h which differed significantly from the average net change in Batch 2 which was -6 nmoles inc./mg/2h. This correlated with a significant difference in NOx levels produced by both batches. The correlation coefficient of the points in the figure above was -0.89, indicating a negative correlation. These results would suggest that there was a biphasic effect with NO production; until NOx levels increased past a threshold, the LPS plus cytokine treatment induced an increase in glycogen synthesis while past the threshold, the increase was inhibited and glycogen synthesis downregulated. This concept would correlate with the myotube glycogen synthetic results presented in this thesis and with previous studies in our laboratory that investigated endotoxic shock in hepatocytes (Wallington et al. 2008).

LPS plus cytokine treatment consistently raised myoblast protein levels relative to the control, which was not evident in myotubes (Figure 6.2a) and unlikely due to a promotion of differentiation as suggested by some studies. Despite this increase in protein content, the rate

of myoblast protein synthesis following 18 hours of treatment failed to differ from the basal rate (Figure 6.2.1b). Following 6 hours of LPS plus cytokine treatment however, the rate of protein synthesis was significantly upregulated, and this was maintained up until 12 hours of treatment, returning to the basal rate after 18 hours of treatment (Figure 6.4a). The onset of this upregulation correlated with the onset of the LPS plus cytokine-induced upregulation of glycogen synthesis, suggesting both processes may be stimulated via a similar mechanism. Surprisingly, glycogen synthesis was upregulated at 18 hours, contrasting with the same time point for protein synthesis, indicating that if both stimulations occurred due to the same mechanism, the half life of each was different.

Insulin significantly stimulated protein synthesis in myoblasts, and was impaired following the 18 hour LPS plus cytokine treatment (Figure 6.2.2b). The inhibition of NO production failed to rescue this impairment, indicating it was NO-independent (Figure 6.2.3b). Insulin-mediated ERK1/2 phosphorylation leads to increased protein synthesis via two mechanisms: phosphorylation of BP1 and activation of eIF4E (as discussed in Section 6.1). Insulin mediated BP1 phosphorylation in myoblasts was unimpaired by the LPS plus cytokine treatment, indicating that a likely contributing factor to the insulin-resistance observed resulted from an impairment of the ERK1/2-mediated activation of eIF4E. This mechanism appeared to contribute to insulin resistance on glycogen synthesis discussed above. Interestingly, myotube BP1 phosphorylation following insulin-stimulation was impaired by the LPS plus cytokine treatment in a NO-dependent manner (Figure 6.3b). Due to the minimal insulin response in myoblast protein synthesis however, insulin-resistance was not easily addressed.

The insulin-induced increase in protein synthesis was significantly lower following 3 hours of LPS plus cytokine treatment, and remained the same following 6, 9, 12 and 18 hours of treatment. The net rate of insulin-stimulated protein synthesis however, was the same in all treatments except following 18 hours of LPS plus cytokine treatment. This 18 hour treatment coincided with disappearance of the LPS plus cytokine-stimulation on protein synthesis observed between 6 and 12 hours of treatment. As a result it is possible that the lower increment induced by insulin in cells treated for 3-12 hours was not due to a degree of resistance but due to a maximal rate being reached. This could imply that the LPS plus cytokine upregulation of protein synthesis following 6, 9 and 12 hours of treatment, occurred in a manner similar to the insulin-stimulation of protein synthesis.

An 18 hour treatment with various combinations of LPS, TNF-α, IFN-γ and IL-1β also increased myoblast protein synthesis, to a comparable degree as seen with the 6, 9 and 12 hours of treatment with LPS plus all 3 cytokines. TNF-α on its own and in combination with one

of the other stimulants or with LPS + IL-1β upregulated protein synthesis (Figure 6.5a). This indicated the importance of TNF-α in the upregulation of protein synthesis, however it was not the only stimulatory factor required since the combination of LPS + IFN-γ + IL-1β also upregulated protein synthesis to a similar degree (Figure 6.5b). These results were interesting because they showed that protein synthesis was indeed upregulated after 18 hours of treatment provided all 4 stimulants were not added. This meant that the difference between having 3 stimulants and 4 was enough to prevent the increase in protein synthesis following 18 hours of treatment. One difference between treating with LPS plus all 3 cytokines and the combinations used was the production of NO. Neither of these combinations significantly increased NOx levels, confirming the idea that the stimulation of protein synthesis occurred in a NO-independent manner. Although protein synthesis was increased following 9 hours of LPS plus cytokine treatment and NOx levels were significantly higher than the untreated control, it is possible that NO production at 18 hours was considerably higher than at 9 or 12 hours after treatment. If so this could imply that NO production may have prevented the treatment-induced increase in protein synthesis, explaining why 18 hours of treatment with any of the combinations discussed upregulated the rate.

7.2 Future Work

LPS plus cytokines significantly upregulated myoblast glucose transport. Time dependent studies would be interesting to assess whether glucose transport was increased at a similar time as myoblast glycogen synthesis, as if they did not coincide it would signify other underlying mechanisms were involved. Evidence suggests that endotoxic shock in vitro upregulates GLUT1 expression (Bedard et al. 1997; Ciaraldi et al. 1998). In order to determine whether this was the underlying mechanism for the increased glucose uptake it would be worth obtaining a better GLUT1 antibody to measure the levels by Western blot, and to determine expression levels of the transporter via qPCR studies.

A more sensitive method for analysing G-6-P, UDP-glucose and glycogen levels would help shed light on the suggestions made from the present studies. The assays of G-6-P and UDP-glucose levels would be necessary to confirm the suggested mode of increase in myoblast glycogen synthesis following treatment. Previous work has suggested sepsis in vivo increased skeletal muscle G-6-P levels (Vary et al. 1995). The measure of glycogen stores in control and treated cells would enable the deduction of whether a change in the total glycogen content

contributed to the increase in myoblast glycogen synthesis or the downregulation of myotube glycogen synthesis induced by LPS plus cytokine treatment.

Time dependent studies in myotubes would help elucidate the time of onset of glycogen synthesis downregulation following LPS plus cytokine treatment. This would also shed light on how important NO production was since NOx levels should not accumulate to a significant degree until approximately 9 hours of treatment. Western blot analysis of iNOS protein levels determined in a time-dependent fashion would compliment these studies to help deduce whether there was indeed a biphasic response to NO production as discussed in Section 7.1. This latter experiment could also be done in myoblasts as it could address the potential insulin resistance and disappearance of LPS plus cytokine-stimulation of myoblast protein synthesis seen after 18 hours of treatment.

Myotube GS was phosphorylated at Site 3 in a NO-dependent manner following LPS plus cytokine treatment. Results indicated that GSK3 activity was unlikely to be responsible for this, suggesting that either PASK or DYRK-mediated phosphorylation of GS Site 3 may be accountable, or perhaps an inhibition of basal PP-1 activity. It would therefore be relevant to address the activities of these three proteins to help determine the reason for the increased phosphorylation of myotube GS following LPS plus cytokine treatment. Another GS kinase, AMPK, was similarly phosphorylated (indicating activity) in a NO-dependent fashion suggesting it may have contributed to the phosphorylation of GS and thus to the inhibition of myotube glycogen synthesis. Depending on the results obtained regarding the onset of LPS plus cytokine-induced downregulation of glycogen synthesis, assessing AMPK activity following this time course would help confirm the potential role of AMPK in this effect. The use of an antibody for GS phosphorylation Site 2 would be an appropriate complimentary assay, while using an AMPK inhibitor – such as Compound C which has already been used in C2C12 myocytes (Frost et al. 2009) – in parallel with this would overcome the fact that numerous other kinases phosphorylate GS at Site 2. Compound C would also be worth using in myoblasts to see if AMPK had any effect on the increase in myoblast glucose uptake induced by the LPS plus cytokines, since it is said to activate glucose uptake (Li et al. 2004).

The lack of an insulin response on glucose transport was surprising, despite the evidence suggesting the difficulty in measuring it, since insulin stimulated glycogen synthesis in both myoblasts and myotubes. Serum-starving the cells prior to determining glucose uptake is a process often done before conducting metabolic experiments, and is said to be important

with regards to measuring a significant insulin-stimulated rate of glucose transport (Vishnu Prasad). This was not done in the present study as it would have been different to the conditions of the method regarding the determination of glycogen synthesis, however would be of use to elucidate whether this was the reason for the lack of insulin response. In addition the use of a more sensitive GLUT4 antibody in immunohistochemistry experiments would show whether or not insulin stimulated GLUT4 translocation to the membrane, as evidence suggests the GLUT4 machinery to be intact in C2C12 cells (Nedachi and Kanzaki 2006).

As discussed throughout this thesis, much research suggests sepsis, endotoxic shock and indeed pro-inflammatory cytokines induce insulin-resistance, as noted in some experiments in this study. In both myoblasts and myotubes the insulin-stimulation of Akt and GSK3 occurred unimpaired by the treatment, however ERK1/2 phosphorylation – as well as myotube BP1 phosphorylation – was impaired. Insulin-induced ERK1/2 stimulation results in PP-1 activation, the impairment of this process appeared to correlate with the insulin-resistance regarding myoblast Phosphorylase inactivation, myoblast protein synthesis, and myotube glycogen synthesis. Addressing PP-1 activity under these conditions would help deduce whether or not this was a potential underlying mechanism of insulin-resistance.

The work regarding the LPS and cytokine combinations on protein synthesis was very insightful as they exposed the fact that one or a combination of the stimulants (LPS, TNF-α, IFN-γ and IL-1β) were enough to increase protein synthesis. Such combinations would be interesting to look at with regards to glycogen synthesis and glucose transport in both myoblasts and myotubes in order to deduce which of the cytokines or which combinations give the same response as the results noted following treatment with LPS plus all 3 cytokines. This may narrow the search for potential contributing factors, while with the help of Western blot analysis, would allow for the formulation of a more accurate picture.

Chapter Eight - Bibliography

Adams, V., B. Nehrhoff, U. Spate, A. Linke, P. C. Schulze, A. Baur, S. Gielen, R. Hambrecht, and G. Schuler. 2002. Induction of iNOS expression in skeletal muscle by IL-1 beta and NF kappa B activation: an in vitro and in vivo study. *Cardiovascular Research* 54 (1):95-104.

Agius, L., M. Peak, and K. Alberti. 1990. Regulation of glycogen-synthesis from glucose and gluconeogenic precursors by insulin in periportal and perivenous rat hepatocytes. *Biochemical Journal* 266 (1):91-102.

Akira, S., S. Uematsu, and O. Takeuchi. 2006. Pathogen recognition and innate immunity. *Cell* 124 (4):783-801.

Al-Khalili, L., D. Kramer, P. Wretenberg, and A. Krook. 2004. Human skeletal muscle cell differentiation is associated with changes in myogenic markers and enhanced insulin-mediated MAPK and PKB phosphorylation. *Acta Physiologica Scandinavica* 180 (4):395-403.

Alderton, W. K., C. E. Cooper, and R. G. Knowles. 2001. Nitric oxide synthases: structure, function and inhibition. *Biochemical Journal* 357:593-615.

Alvarez, B., L. S. Quinn, S. Busquets, F. J. Lopez-Soriano, and J. M. Argiles. 2001. Direct effects of tumor necrosis factor alpha (TNF-alpha) on murine skeletal muscle cell lines. Bimodal effects on protein metabolism. *European Cytokine Network* 12 (3):399-410.

Annane, D., E. Bellissant, and J. M. Cavaillon. 2005. Septic shock. *Lancet* 365 (9453):63-78.

Antonescu, C. N., C. Huang, W. Niu, Z. Liu, P. A. Eyers, K. A. Heidenreich, P. J. Bilan, and A. Klip. 2005. Reduction of insulin-stimulated glucose uptake in L6 myotubes by the protein kinase inhibitor SB203580 is independent of p38MAPK activity. *Endocrinology* 146 (9):3773-3781.

Aschenbach, W. G., Y. Suzuki, K. Breeden, C. Prats, M. F. Hirshman, S. D. Dufresne, K. Sakamoto, P. G. Vilardo, M. Steele, J. H. Kim, S. L. Jing, L. J. Goodyear, and A. A. DePaoli-Roach. 2001. The muscle-specific protein phosphatase PP1G/R-GL(G(M)) is essential for activation of glycogen synthase by exercise. *Journal of Biological Chemistry* 276 (43):39959-39967.

Austin, R. L., A. Rune, K. Bouzakri, J. R. Zierath, and A. Krook. 2008. SiRNA-mediated reduction of inhibitor of nuclear factor-kappa B kinase prevents tumor necrosis factor-alpha-induced insulin resistance in human skeletal muscle. *Diabetes* 57 (8):2066-2073.

Azpiazu, I., J. Manchester, A. V. Skurat, P. J. Roach, and J. C. Lawrence. 2000. Control of glycogen synthesis is shared between glucose transport and glycogen synthase in skeletal muscle fibers. *American Journal of Physiology-Endocrinology and Metabolism* 278 (2):E234-E243.

Bagby, G. J., C. H. Lang, D. M. Hargrove, J. J. Thompson, L. A. Wilson, and J. J. Spitzer. 1988. Glucose kinetics in rats infused with endotoxin-induced monokines or tumor necrosis factor. *Circulatory Shock* 24 (2):111-121.

Balon, T. W., and J. L. Nadler. 1997. Evidence that nitric oxide increases glucose transport in skeletal muscle. *Journal of Applied Physiology* 82 (1):359-363.

Barnard, R. J., and J. F. Youngren. 1992. Regulation of Glucose-Transport in Skeletal-Muscle. *Faseb Journal* 6 (14):3238-3244.

Barnes, K., J. C. Ingram, O. H. Porras, L. F. Barros, E. R. Hudson, L. G. D. Fryer, F. Foufelle, D. Carling, D. G. Hardie, and S. A. Baldwin. 2002. Activation of GLUT1 by metabolic and osmotic stress: potential involvement of AMP-activated protein kinase (AMPK). *Journal of Cell Science* 115 (11):2433-2442.

Bedard, S., B. Marcotte, and A. Marette. 1997. Cytokines modulate glucose transport in skeletal muscle by inducing the expression of inducible nitric oxide synthase. *Biochemical Journal* 325:487-493.

Begum, N., and L. Ragolia. 1996. Effect of tumor necrosis factor-alpha on insulin action in cultured rat skeletal muscle cells. *Endocrinology* 137 (6):2441-2446.

Beutler, B. 2003. Science review: Key inflammatory and stress pathways in critical illness - the central role of the Toll-like receptors. *Critical Care* 7 (1):39-46.

Bodine, S. C. 2006. mTOR signaling and the molecular adaptation to resistance exercise. *Medicine and Science in Sports and Exercise* 38 (11):1950-1957.

Boehm, U., T. Klamp, M. Groot, and J. C. Howard. 1997. Cellular responses to interferon-gamma. *Annual Review of Immunology* 15:749-795.

Bonavida, B., S. Khineche, S. Huerta-Yepez, and H. Garban. 2006. Therapeutic potential of nitric oxide in cancer. *Drug Resistance Updates* 9 (3):157-173.

Borgs, M., M. Bollen, S. Keppens, S. H. Yap, W. Stalmans, and F. Vanstapel. 1996. Modulation of basal hepatic glycogenolysis by nitric oxide. *Hepatology* 23 (6):1564-1571.

Bouskila, M., M. F. Hirshman, J. Jensen, L. J. Goodyear, and K. Sakamoto. 2008. Insulin promotes glycogen synthesis in the absence of GSK3 phosphorylation in skeletal muscle. *American Journal of Physiology-Endocrinology and Metabolism* 294 (1):E28-E35.

Bradford, M. M. 1976. Rapid and sensitive method for quantitation of microgram quantities of protein utilizing principle of protein-dye binding. *Analytical Biochemistry* 72 (1-2):248-254.

Broussard, S. R., R. H. McCusker, J. E. Novakofski, K. Strle, W. H. Shen, R. W. Johnson, G. G. Freund, R. Dantzer, and K. W. Kelley. 2003. Cytokine-hormone interactions: Tumor necrosis factor alpha impairs biologic activity and downstream activation signals of the insulin-like growth factor I receptor in myoblasts. *Endocrinology* 144 (7):2988-2996.

Bryant, C. E., D. R. Spring, M. Gangloff, and N. J. Gay. 2010. The molecular basis of the host response to lipopolysaccharide. *Nature Reviews Microbiology* 8 (1):8-14.

Bubici, C., S. Papa, C. G. Pham, F. Zazzeroni, and G. Franzoso. 2004. NF-kappa B and JNK - An intricate affair. *Cell Cycle* 3 (12):1524-1529.

Camussi, G., E. Albano, C. Tetta, and F. Bussolino. 1991. The Molecular Action of Tumor-Necrosis-Factor-Alpha. *European Journal of Biochemistry* 202 (1):3-14.

Carlson, G. L. 2004. Insulin resistance in human sepsis: implications for the nutritional and metabolic care of the critically ill surgical patient. *Annals of the Royal College of Surgeons of England* 86 (2):75-81.

Casteleijn, E., J. Kuiper, H. C. J. Vanrooij, J. Kamps, J. F. Koster, and T. J. C. Vanberkel. 1988. Endotoxin stimulates glycogenolysis in the liver by means of intercellular communication. *Journal of Biological Chemistry* 263 (15):6953-6955.

Cazzolli, R., L. Carpenter, T. J. Biden, and C. Schmitz-Peiffer. 2001. A role for protein phosphatase 2A-like activity, but not atypical protein kinase C zeta, in the inhibition of protein kinase B/Akt and glycogen synthesis by palmitate. *Diabetes* 50 (10):2210-2218.

Cazzolli, R., D. L. Craig, T. J. Biden, and C. Schmitz-Peiffer. 2002. Inhibition of glycogen synthesis by fatty acid in C2C12 muscle cells is independent of PKC-alpha, -epsilon, and -theta. *American Journal of Physiology-Endocrinology and Metabolism* 282 (6):E1204-E1213.

Ceppi, E. D., F. S. Smith, and M. A. Titheradge. 1996. Effect of multiple cytokines plus bacterial endotoxin on glucose and nitric oxide production by cultured hepatocytes. *Biochemical Journal* 317:503-507.

Ceppi, E. D., F. S. Smith, and M. A. Titheradge. 1997. Nitric oxide, sepsis and liver metabolism. Paper read at Symposium on Xanthine Oxidase - Enzymology and Pathophysiology, at the 661st Meeting of the Biochemical-Society, Apr 10-11, at Bath, England.

Cerami, A., and B. Beutler. 1988. The Role of Cachectin/Tnf in Endotoxic-Shock and Cachexia. *Immunology Today* 9 (1):28-31.

Chavez, J. A., and S. A. Summers. 2003. Characterizing the effects of saturated fatty acids on insulin signaling and ceramide and diacylglycerol accumulation in 3T3-L1 adipocytes and C2Cl2 myotubes. *Archives of Biochemistry and Biophysics* 419 (2):101-109.

Chen, S. E., B. W. Jin, and Y. P. Li. 2007. TNF-alpha regulates myogenesis and muscle regeneration by activating p38 mapk. *American Journal of Physiology-Cell Physiology* 292 (5):C1660-C1671.

Ciaraldi, T. P., L. Carter, S. Mudaliar, and R. R. Henry. 2010. GSK-3 beta and control of glucose metabolism and insulin action in human skeletal muscle. *Molecular and Cellular Endocrinology* 315 (1-2):153-158.

Ciaraldi, T. P., L. Carter, S. Mudaliar, P. A. Kern, and R. R. Henry. 1998. Effects of tumor necrosis factor-alpha on glucose metabolism in cultured human muscle cells from nondiabetic and type 2 diabetic subjects. *Endocrinology* 139 (12):4793-4800.

Ciaraldi, T. P., S. E. Nikoulina, R. A. Bandukwala, L. Carter, and R. R. Henry. 2007. Role of glycogen synthase kinase-3 alpha in insulin action in cultured human skeletal muscle cells. *Endocrinology* 148 (9):4393-4399.

Cohen, P. 1993. Dissection of the protein-phosphorylation cascades involved in insulin and growth-factor action. *Biochemical Society Transactions* 21 (3):555-567.

Cohen, P. 2006. Timeline - The twentieth century struggle to decipher insulin signalling. *Nature Reviews Molecular Cell Biology* 7 (11):867-873.

Cohen, P., and S. Frame. 2001. The renaissance of GSK3. *Nature Reviews Molecular Cell Biology* 2 (10):769-776.

Cooney, R. N., G. O. Maish, T. Gilpin, M. L. Shumate, C. H. Lang, and T. C. Vary. 1999. Mechanism of IL-1 induced inhibition of protein synthesis in skeletal muscle. *Shock* 11 (4):235-241.

Crossland, H., D. Constantin-Teodosiu, S. M. Gardiner, D. Constantin, and P. L. Greenhaff. 2008. A potential role for Akt/FOXO signalling in both protein loss and the impairment of muscle carbohydrate oxidation during sepsis in rodent skeletal muscle. *Journal of Physiology-London* 586 (22):5589-5600.

Curran, R. D., T. R. Billiar, D. J. Stuehr, J. B. Ochoa, B. G. Harbrecht, S. G. Flint, and R. L. Simmons. 1990. Multiple Cytokines Are Required to Induce Hepatocyte Nitric-Oxide Production and Inhibit Total Protein-Synthesis. *Annals of Surgery* 212 (4):462-471.

Cvek, B., and Z. Dvorak. 2007. Targeting of nuclear Factor-kappa B and proteasome by dithiocarbamate complexes with metals. *Current Pharmaceutical Design* 13 (30):3155-3167.

D'Alessandris, C., R. Lauro, I. Presta, and G. Sesti. 2007. C-reactive protein induces phosphorylation of insulin receptor substrate-1 on Ser(307) and Ser(612) in L6 myocytes, thereby impairing the insulin signalling pathway that promotes glucose transport. *Diabetologia* 50 (4):840-849.

Danforth, W. H. 1965. Glycogen synthetase activity in skeletal muscle. *Journal of Biological Chemistry* 240 (2):588-&.

Dauphinee, S. M., and A. Karsan. 2006. Lipopolysaccharide signaling in endothelial cells. *Laboratory Investigation* 86 (1):9-22.

Dehoux, M., C. Gobier, P. Lause, L. Bertrand, J. M. Ketelslegers, and J. P. Thissen. 2007. IGF-I does not prevent myotube atrophy caused by proinflammatory cytokines despite activation of Akt/Foxo and GSK-3 beta pathways and inhibition of atrogin-1 mRNA. *American Journal of Physiology-Endocrinology and Metabolism* 292 (1):E145-E150.

Del Aguila, L. F., K. P. Claffey, and J. P. Kirwan. 1999. TNF-alpha impairs insulin signaling and insulin stimulation of glucose uptake in C2C12 muscle cells. *American Journal of Physiology-Endocrinology and Metabolism* 276 (5):E849-E855.

Dempsey, P. W., S. E. Doyle, J. Q. He, and G. H. Cheng. 2003. The signaling adaptors and pathways activated by TNF superfamily. *Cytokine & Growth Factor Reviews* 14 (3-4):193-209.

Dent, P., A. Lavoinne, S. Nakielny, F. B. Caudwell, P. Watt, and P. Cohen. 1990. The molecular mechanism by which insulin stimualtes glycogen-synthesis in mammalian skeletal-muscle. *Nature* 348 (6299):302-308.

Deshmukh, A. S., Y. C. Long, T. D. Barbosa, H. K. R. Karlsson, S. Glund, W. J. Zavadoski, E. M. Gibbs, H. A. Koistinen, H. Wallberg-Henriksson, and J. R. Zierath. 2010. Nitric oxide increases cyclic GMP levels, AMP-activated protein kinase (AMPK)alpha 1-specific activity and glucose transport in human skeletal muscle. *Diabetologia* 53 (6):1142-1150.

Doi, M., I. Yamaoka, T. Fukunaga, and M. Nakayama. 2003. Isoleucine, a potent plasma glucose-lowering amino acid, stimulates glucose uptake in C2C12 myotubes. *Biochemical and Biophysical Research Communications* 312 (4):1111-1117.

Donati, C., P. Nincheri, F. Cencetti, E. Rapizzi, M. Farnararo, and P. Bruni. 2007. Tumor necrosis factor-[alpha] exerts pro-myogenic action in C2C12 myoblasts via sphingosine kinase/S1P2 signaling. *Febs Letters* 581 (23):4384-4388.

Drenning, J. A., V. A. Lira, C. G. Simmons, Q. A. Soltow, J. E. Sellman, and D. S. Criswell. 2008. Nitric oxide facilitates NFAT-dependent transcription in mouse myotubes. *American Journal of Physiology-Cell Physiology* 294 (4):C1088-C1095.

Eley, H. L., S. T. Russell, and M. J. Tisdale. 2008. Attenuation of depression of muscle protein synthesis induced by lipopolysaccharide, tumor necrosis factor, and angiotensin II by beta-hydroxy-beta-methylbutyrate. *American Journal of Physiology-Endocrinology and Metabolism* 295 (6):E1409-E1416.

Elsner, P., B. Quistorff, T. S. Hermann, J. Dich, and N. Grunnet. 1998. Regulation of glycogen accumulation in L6 myotubes cultured under optimized differentiation conditions. *American Journal of Physiology-Endocrinology and Metabolism* 275 (6):E925-E933.

Ertel, W., M. H. Morrison, P. Wang, Z. F. Ba, A. Ayala, and I. H. Chaudry. 1991. The complex pattern of cytokines in sepsis - association between prostaglandins, cachectin, and interleukins. *Annals of Surgery* 214 (2):141-148.

Etgen, G. J., D. A. Fryburg, and E. M. Gibbs. 1997. Nitric oxide stimulates skeletal muscle glucose transport through a calcium/contraction- and phosphatidylinositol-3-kinase-independent pathway. *Diabetes* 46 (11):1915-1919.

Fan, J., Y. H. Li, M. M. Wojnar, and C. H. Lang. 1996. Endotoxin-induced alterations in insulin-stimulated phosphorylation of insulin receptor, IRS-1, and MAP kinase in skeletal muscle. *Shock* 6 (3):164-170.

Fantuzzi, G. 2005. Adipose tissue, adipokines, and inflammation. *Journal of Allergy and Clinical Immunology* 115 (5):911-919.

Feingold, K. R., Y. W. Wang, A. Moser, J. K. Shigenaga, and C. Grunfeld. 2008. LPS decreases fatty acid oxidation and nuclear hormone receptors in the kidney. *Journal of Lipid Research* 49 (10):2179-2187.

Ferrer, J. C., S. Baque, and J. J. Guinovart. 1997. Muscle glycogen synthase translocates from the cell nucleus to the cytosol in response to glucose. *Febs Letters* 415 (3):249-252.

Ferrer, J. C., C. Favre, R. R. Gomis, J. M. Fernandez-Novell, M. Garcia-Rocha, N. de la Iglesia, E. Cid, and J. J. Guinovart. 2003. Control of glycogen deposition. *Febs Letters* 546 (1):127-132.

Feve, B., and J. P. Bastard. 2009. The role of interleukins in insulin resistance and type 2 diabetes mellitus. *Nature Reviews Endocrinology* 5 (6):305-311.

Fleming, I., and R. Busse. 1999. NO: the primary EDRF. *Journal of Molecular and Cellular Cardiology* 31 (1):5-14.

Frame, S., and P. Cohen. 2001. GSK3 takes centre stage more than 20 years after its discovery. *Biochemical Journal* 359:1-16.

Fraser, C. S., V. M. Pain, and S. J. Morley. 1999. Cellular stress in Xenopus kidney cells enhances the phosphorylation of eukaryotic translation initiation factor (eIF)4E and the association of eIF4F with poly(A)-binding protein. *Biochemical Journal* 342:519-526.

Frost, R. A., G. J. Nystrom, and C. H. Lang. 2003a. Lipopolysaccharide (LPS) and proinflammatory cytokines stimulate interleukin-6 expression in skeletal muscle and C2C12 myoblasts via a Jun-N-terminal kinase (JNK) pathway. *Faseb Journal* 17 (4):A439-A439.

Frost, R. A., G. J. Nystrom, and C. H. Lang. 2003b. Tumor necrosis factor-alpha decreases insulin-like-growth factor-I messenger ribonucleic acid expression in C2C12 myoblasts via a Jun N-terminal kinase pathway. *Endocrinology* 144 (5):1770-1779.

Frost, R. A., G. J. Nystrom, and C. H. Lang. 2004. Lipopolysaccharide stimulates nitric oxide synthase-2 expression in murine skeletal muscle and C2C(12) myoblasts via Toll-like receptor-4 and c-Jun NH2-terminal kinase pathways. *American Journal of Physiology-Cell Physiology* 287 (6):C1605-C1615.

Frost, R. A., G. J. Nystrom, and C. H. Lang. 2009. Endotoxin And Interferon-Gamma Inhibit Translation In Skeletal Muscle Cells By Stimulating Nitric Oxide Synthase Activity. *Shock* 32 (4):416-426.

Fujii, N., N. Jessen, and L. J. Goodyear. 2006. AMP-activated protein kinase and the regulation of glucose transport. *American Journal of Physiology-Endocrinology and Metabolism* 291 (5):E867-E877.

Furchgott, R. F., and J. V. Zawadzki. 1980. The Obligatory Role Of Endothelial-Cells In The Relaxation Of Arterial Smooth-Muscle By Acetylcholine. *Nature* 288 (5789):373-376.

Furnsinn, C., S. Neschen, O. Wagner, M. Roden, M. Bisschop, and W. Waldhausl. 1997. Acute and chronic exposure to tumor necrosis factor-alpha fails to affect insulin-stimulated glucose metabolism of isolated rat soleus muscle. *Endocrinology* 138 (7):2674-2679.

Gamelli, R. L., H. Liu, L. K. He, and C. A. Hofmann. 1996. Augmentations of glucose uptake and glucose transporter-1 in macrophages following thermal injury and sepsis in mice. *Journal of Leukocyte Biology* 59 (5):639-647.

Gath, I., J. Ebert, U. Godtel-Armbrust, R. Ross, A. B. Reske-Kunz, and U. Forstermann. 1999. NO synthase II in mouse skeletal muscle is associated with caveolin 3. *Biochemical Journal* 340:723-728.

Geppert, T. D., C. E. Whitehurst, P. Thompson, and B. Beutler. 1994. Lipopolysaccharide Signals Activation of Tumor-Necrosis-Factor Biosynthesis through the Ras/Raf-1/Mek/Mapk Pathway. *Molecular Medicine* 1 (1):93-103.

Ghosh, N., N. Patel, K. Jiang, J. E. Watson, J. Cheng, C. E. Chalfant, and D. R. Cooper. 2007. Ceramide-activated protein phosphatase involvement in insulin resistance via Akt, serine/arginine-rich protein 40, and ribonucleic acid splicing in L6 skeletal muscle cells. *Endocrinology* 148 (3):1359-1366.

Glund, S., A. Deshmukh, Y. C. Long, T. Moller, H. A. Koistinen, K. Caidahl, J. R. Zierath, and A. Krook. 2007. Interleukin-6 directly increases glucose metabolism in resting human skeletal muscle. *Diabetes* 56 (6):1630-1637.

Gomis, R. R., E. Cid, M. Garcia-Rocha, J. C. Ferrer, and J. J. Guinovart. 2002. Liver glycogen synthase but not the muscle isoform differentiates between glucose 6-phosphate produced by glucokinase or hexokinase. *Journal of Biological Chemistry* 277 (26):23246-23252.

Goodfellow, I. G., and L. O. Roberts. 2008. Eukaryotic initiation factor 4E. *International Journal of Biochemistry & Cell Biology* 40 (12):2675-2680.

Gough, D. J., D. E. Levy, R. W. Johnstone, and C. J. Clarke. 2008. IFN-gamma signaling-Does it mean JAK-STAT? *Cytokine & Growth Factor Reviews* 19 (5-6):383-394.

Green, L. C., D. A. Wagner, J. Glogowski, P. L. Skipper, J. S. Wishnok, and S. R. Tannenbaum. 1982. Analysis of Nitrate, Nitrite, and [N-15]-Labeled Nitrate in Biological-Fluids. *Analytical Biochemistry* 126 (1):131-138.

Greenberg, C. C., M. J. Jurczak, A. M. Danos, and M. J. Brady. 2006. Glycogen branches out: new perspectives on the role of glycogen metabolism in the integration of metabolic pathways. *American Journal of Physiology-Endocrinology and Metabolism* 291 (1):E1-E8.

Grimes, C. A., and R. S. Jope. 2001. The multifaceted roles of glycogen synthase kinase 3 beta in cellular signaling. *Progress in Neurobiology* 65 (4):391-426.

Groves, J. T., and C. C. Y. Wang. 2000. Nitric oxide synthase: models and mechanisms. *Current Opinion in Chemical Biology* 4 (6):687-695.

Grzelkowska-Kowalczyk, K., and W. Wieteska-Skrzeczynska. 2009. Treatment with TNF-alpha and IFN-gamma alters the activation of SER/THR protein kinases and the metabolic response to IGF-I in mouse c2c12 myogenic cells. *Cellular & Molecular Biology Letters* 15 (1):13-31.

Guha, M., and N. Mackman. 2001. LPS induction of gene expression in human monocytes. *Cellular Signalling* 13 (2):85-94.

Halse, R., L. G. D. Fryer, J. G. McCormack, D. Carling, and S. J. Yeaman. 2003. Regulation of glycogen synthase by glucose and glycogen - A possible role for AMP-activated protein kinase. *Diabetes* 52 (1):9-15.

Halse, R., S. L. Pearson, J. G. McCormack, S. J. Yeaman, and R. Taylor. 2001. Effects of tumor necrosis factor-alpha on insulin action in cultured human muscle cells. *Diabetes* 50 (5):1102-1109.

Hansen, P. A., E. A. Gulve, B. A. Marshall, J. P. Gao, J. E. Pessin, J. O. Holloszy, and M. Mueckler. 1995. Skeletal-muscle glucose-transport and metabolism are enhanced in transgenic mice overexpressing the glut4 glucose-transporter. *Journal of Biological Chemistry* 270 (4):1679-1684.

Hardie, D. G., S. A. Hawley, and J. Scott. 2006. AMP-activated protein kinase - development of the energy sensor concept. *Journal of Physiology-London* 574 (1):7-15.

Hargreaves, M. 2004. Muscle glycogen and metabolic regulation. *Proceedings of the Nutrition Society* 63 (2):217-220.

Heyneman, R., and R. Vercauteren. 1997. Lipopolysaccharides and endotoxic shock: Recent developments, new perspectives. *Vlaams Diergeneeskundig Tijdschrift* 66 (1):14-20.

Higaki, Y., M. F. Hirshman, N. Fujii, and L. J. Goodyear. 2001. Nitric oxide increases glucose uptake through a mechanism that is distinct from the insulin and contraction pathways in rat skeletal muscle. *Diabetes* 50 (2):241-247.

Hill, M., and R. McCallum. 1991. Altered transcriptional regulation of phosphoenolpyruvate carboxykinase in rats following endotoxin treatment. *Journal of Clinical Investigation* 88 (3):811-816.

Ho, R. C., O. Alcazar, N. Fujii, M. F. Hirshman, and L. J. Goodyear. 2004. p38 gamma MAPK regulation of glucose transporter expression and glucose uptake in L6 myotubes and mouse skeletal muscle. *American Journal of Physiology-Regulatory Integrative and Comparative Physiology* 286 (2):R342-R349.

Holloszy, J. O. 2003. A forty-year memoir of research on the regulation of glucose transport into muscle. *American Journal of Physiology-Endocrinology and Metabolism* 284 (3):E453-E467.

Hotamisligil, G. S., D. L. Murray, L. N. Choy, and B. M. Spiegelman. 1994. Tumor-necrosis-factor-alpha inhibits signaling from the insulin-receptor. *Proceedings of the National Academy of Sciences of the United States of America* 91 (11):4854-4858.

Hotamisligil, G. S., P. Peraldi, A. Budavari, R. Ellis, M. F. White, and B. M. Spiegelman. 1996. IRS-1-mediated inhibition of insulin receptor tyrosine kinase activity in TNF-alpha- and obesity-induced insulin resistance. *Science* 271 (5249):665-668.

Huang, F. L., and S. H. Tao. 1980. Glycogen-metabolism in myogenic cells in culture - presence of inhibitors for dephosphorylation of glycogen-synthase and glycogen-phosphorylase. *Archives of Biochemistry and Biophysics* 199 (1):123-132.

Huang, S., and M. P. Czech. 2007. The GLUT4 Glucose Transporter. *Cell Metabolism* 5 (4):237-252.

Huber-Lang, M., U. Waidner, U. Knippschild, D. Henne-Bruns, and A. Wolf. 2009. Adipokines and Adipose Tissue Derided Hormones: Sepsis Related Changes. *Obesity Surgery* 19 (8):992-992.

Inoki, K., H. Ouyang, Y. Li, and K. L. Guan. 2005. Signaling by target of rapamycin proteins in cell growth control. *Microbiology and Molecular Biology Reviews* 69 (1):79-+.

Jackson, R. J., C. U. T. Hellen, and T. V. Pestova. 2010. The mechanism of eukaryotic translation initiation and principles of its regulation. *Nature Reviews Molecular Cell Biology* 11 (2):113-127.

Jensen, J., E. Jebens, E. O. Brennesvik, J. Ruzzin, M. A. Soos, E. M. L. Engebretsen, S. O'Rahilly, and J. P. Whitehead. 2006. Muscle glycogen inharmoniously regulates glycogen synthase activity, glucose uptake, and proximal insulin signaling. *American Journal of Physiology-Endocrinology and Metabolism* 290 (1):E154-E162.

Jensen, J., Lai, YC. 2009. Regulation of muscle glycogen synthase phosphorylation and kinetic properties by insulin, exercise, adrenaline and role in insulin resistance. *Archives of Physiology and Biochemistry* 115 (1):13-21.

Ji, S. Q., S. Neustrom, G. M. Willis, and M. E. Spurlock. 1998. Proinflammatory cytokines regulate myogenic cell proliferation and fusion but have no impact on myotube protein metabolism or stress protein expression. *Journal of Interferon and Cytokine Research* 18 (10):879-888.

Jobgen, W. S., S. K. Fried, W. J. Fu, C. J. Meininger, and G. Wu. 2006. Regulatory role for the arginine-nitric oxide pathway in metabolism of energy substrates. *The Journal of Nutritional Biochemistry* 17 (9):571-588.

Jope, R. S., C. J. Yuskaitis, and E. Beurel. 2007. Glycogen synthase kinase-3 (GSK3): Inflammation, diseases, and therapeutics. *Neurochemical Research* 32 (4-5):577-595.

Jorgensen, S. B., J. N. Nielsen, J. B. Birk, G. S. Olsen, B. Viollet, F. Andreelli, P. Schjerling, S. Vaulont, D. G. Hardie, B. F. Hansen, E. A. Richter, and J. F. P. Wojtaszewski. 2004. The alpha 2-5 ' AMP-activated protein kinase is a site 2 glycogen synthase kinase in skeletal muscle and is responsive to glucose loading. *Diabetes* 53 (12):3074-3081.

Jorgensen, S. B., and A. J. Rose. 2008. How is AMPK activity regulated in skeletal muscles during exercise? *Frontiers in Bioscience* 13:5589-5604.

Katz, A. 2007. Modulation of glucose transport in skeletal muscle by reactive oxygen species. *Journal of Applied Physiology* 102 (4):1671-1676.

Kelleher, D. L., B. C. Fong, G. J. Bagby, and J. J. Spitzer. 1982. Metabolic and hormonal changes following endotoxin administration to diabetic rats. *American Journal of Physiology* 243 (1):R77-R81.

Kelm, M. 1999. Nitric oxide metabolism and breakdown. *Biochimica Et Biophysica Acta-Bioenergetics* 1411 (2-3):273-289.

Khamzina, L., A. Veilleux, S. Bergeron, and A. Marette. 2005. Increased activation of the mammalian target of rapamycin pathway in liver and skeletal muscle of obese rats: Possible involvement in obesity-linked insulin resistance. *Endocrinology* 146 (3):1473-1481.

Khanna, S., S. Roy, L. Packer, and C. K. Sen. 1999. Cytokine-induced glucose uptake in skeletal muscle: redox regulation and the role of alpha-lipoic acid. *American Journal of Physiology-Regulatory Integrative and Comparative Physiology* 276 (5):R1327-R1333.

Kilbourn, R. G., D. L. Traber, and C. Szabó. 1997. Nitric oxide and shock. *Disease-a-Month* 43 (5):279-348.

Kim, J. S., V. Saengsirisuwan, J. A. Sloniger, M. K. Teachey, and E. J. Henriksen. 2006. Oxidant stress and skeletal muscle glucose transport: Roles of insulin signaling and p38 MAPK. *Free Radical Biology and Medicine* 41 (5):818-824.

Kleinert, H., A. Pautz, K. Linker, and P. M. Schwarz. 2004. Regulation of the expression of inducible nitric oxide synthase. *European Journal of Pharmacology* 500 (1-3):255-266.

Knowles, R. G., S. J. Beevers, and C. I. Pogson. 1986. The roles of glucagon, insulin and glucocorticoid hormones in the effects of sublethal doses of endotoxin on glucose-homeostasis in rats. *Biochemical Pharmacology* 35 (22):4043-4048.

Knowles, R. G., J. P. McCabe, S. J. Beevers, and C. I. Pogson. 1987. The characteristics and site of inhibition of gluconeogenesis in rat-liver cells by bacterial-endotoxin - stimulation of phosphofructokinase-1. *Biochemical Journal* 242 (3):721-728.

Kramer, H. F., and L. J. Goodyear. 2007. Exercise, MAPK, and NF-kappa B signaling in skeletal muscle. *Journal of Applied Physiology* 103 (1):388-395.

Kramer, H. F., C. A. Witczak, N. Fujii, N. Jessen, E. B. Taylor, D. E. Arnolds, K. Sakamoto, M. F. Hirshman, and L. J. Goodyear. 2006. Distinct signals regulate AS160 phosphorylation in response to insulin, AICAR, and contraction in mouse skeletal muscle. *Diabetes* 55 (7):2067-2076.

Kroder, G., B. Bossenmaier, M. Kellerer, E. Capp, B. Stoyanov, A. Muhlhofer, L. Berti, H. Horikoshi, A. Ullrich, and H. Haring. 1996. Tumor necrosis factor-alpha- and hyperglycemia-induced insulin resistance - Evidence for different mechanisms and different effects on insulin signaling. *Journal of Clinical Investigation* 97 (6):1471-1477.

Kuma, Y., D. G. Campbell, and A. Cuenda. 2004. Identification of glycogen synthase as a new substrate for stress-activated protein kinase 2b/p38 beta. *Biochemical Journal* 379:133-139.

Kumar, H., T. Kawai, and S. Akira. 2009. Pathogen recognition in the innate immune response. *Biochemical Journal* 420:1-16.

Lai, Y. C., J. T. Stuenaes, C. H. Kuo, and J. Jensen. 2007. Glycogen content and contraction regulate glycogen synthase phosphorylation and affinity for UDP-glucose in rat skeletal muscles. *American Journal of Physiology-Endocrinology and Metabolism* 293 (6):E1622-E1629.

Lai, Y. C., E. Zarrinpashneh, and J. Jensen. 2010. Additive effect of contraction and insulin on glucose uptake and glycogen synthase in muscle with different glycogen contents. *Journal of Applied Physiology* 108 (5):1106-1115.

Lang, C. H. 1992. Sepsis-induced insulin resistance in rats is mediated by a beta-adrenergic mechanism. *American Journal of Physiology* 263 (4):E703-E711.

Lang, C. H., R. Cooney, and T. C. Vary. 1996a. Central interleukin-1 partially mediates endotoxin-induced changes in glucose metabolism. *American Journal of Physiology-Endocrinology and Metabolism* 34 (2):E309-E316.

Lang, C. H., C. Dobrescu, and K. Meszaros. 1990. Insulin-mediated glucose-uptake by individual tissues during sepsis. *Metabolism-Clinical and Experimental* 39 (10):1096-1107.

Lang, C. H., J. Fan, R. Cooney, and T. C. Vary. 1996b. IL-1 receptor antagonist attenuates sepsis-induced alterations in the IGF system and protein synthesis. *American Journal of Physiology-Endocrinology and Metabolism* 270 (3):E430-E437.

Lang, C. H., and R. A. Frost. 2007. Sepsis-induced suppression of skeletal muscle translation initiation mediated by tumor necrosis factor alpha. *Metabolism-Clinical and Experimental* 56 (1):49-57.

Lang, C. H., R. A. Frost, L. S. Jefferson, S. R. Kimball, and T. C. Vary. 2000. Endotoxin-induced decrease in muscle protein synthesis is associated with changes in eIF2B, eIF4E, and IGF-I. *American Journal of Physiology-Endocrinology and Metabolism* 278 (6):E1133-E1143.

Lang, C. H., R. A. Frost, A. C. Nairn, D. A. MacLean, and T. C. Vary. 2002. TNF-alpha impairs heart and skeletal muscle protein synthesis by altering translation initiation. *American Journal of Physiology-Endocrinology and Metabolism* 282 (2):E336-E347.

Lang, C. H., R. A. Frost, and T. C. Vary. 2007. Regulation of muscle protein synthesis during sepsis and inflammation. *American Journal of Physiology-Endocrinology and Metabolism* 293 (2):E453-E459.

Lang, C. H., G. Nystrom, and R. A. Frost. 2008. beta-adrenergic blockade exacerbates sepsis-induced changes in tumor necrosis factor alpha and interleukin-6 in skeletal muscle and is associated with impaired translation initiation. *Journal of Trauma-Injury Infection and Critical Care* 64:477-486.

Langen, R. C. J., A. Schols, M. Kelders, E. F. M. Wouters, and M. W. Janssen-Heininger. 2001. Inflammatory cytokines inhibit myogenic differentiation through activation of nuclear factor-kappa B. *Faseb Journal* 15 (7):1169-1180.

Langlois, W. J., T. Sasaoka, A. R. Saltiel, and J. M. Olefsky. 1995. Negative feedback-regulation and desensitization of insulin-stimulated and epidermal growth factor-stimulated p21(ras) activation. *Journal of Biological Chemistry* 270 (43):25320-25323.

Lee, J. D., S. W. Cho, and O. Y. Hwang. 1993. Interleukin-1-Beta Regulates Glycogen-Metabolism In Primary Cultured Rat Hepatocytes. *Biochemical and Biophysical Research Communications* 191 (2):515-522.

Lee, J. K., S. S. Choi, J. S. Won, and H. W. Suh. 2003. The regulation of inducible nitric oxide synthase gene expression induced by lipopolysaccharide and tumor necrosis factor-alpha in C6 cells: involvement of AP-1 and NF kappa B. *Life Sciences* 73 (5):595-609.

Lee, M. D., A. Zentella, P. H. Pekala, and A. Cerami. 1987. Effect of Endotoxin-Induced Monokines on Glucose-Metabolism in the Muscle-Cell Line-L6. *Proceedings of the National Academy of Sciences of the United States of America* 84 (9):2590-2594.

Li, J., X. Y. Hu, P. Selvakumar, R. R. Russell, S. W. Cushman, G. D. Holman, and L. H. Young. 2004. Role of the nitric oxide pathway in AMPK-mediated glucose uptake and GLUT4 translocation in heart muscle. *American Journal of Physiology-Endocrinology and Metabolism* 287 (5):E834-E841.

Li, Y. P., R. J. Schwartz, I. D. Waddell, B. R. Holloway, and M. B. Reid. 1998. Skeletal muscle myocytes undergo protein loss and reactive oxygen-mediated NF-kappa B activation in response to tumor necrosis factor alpha. *Faseb Journal* 12 (10):871-880.

Lira, V. A., Q. A. Soltow, J. H. D. Long, J. L. Betters, J. E. Sellman, and D. S. Criswell. 2007. Nitric oxide increases GLUT4 expression and regulates AMPK signaling in skeletal muscle. *American Journal of Physiology-Endocrinology and Metabolism* 293:E1062-E1068.

Liu, M. L., A. L. Olson, N. P. Edgington, W. S. Moyerowley, and J. E. Pessin. 1994. Myocyte Enhancer Factor-2 (Mef2) Binding-Site Is Essential for C2c12 Myotube-Specific Expression of the Rat Glut4 Muscle-Adipose Facilitative Glucose-Transporter Gene. *Journal of Biological Chemistry* 269 (45):28514-28521.

Liu, M. S., and G. F. Kang. 1987. Liver-glycogen metabolism in endotoxin-shock .1. Endotoxin administration decreases glycogen-synthase activities in dog livers. *Biochemical Medicine and Metabolic Biology* 37 (1):61-72.

Llovera, M., N. Carbo, J. Lopez-Soriano, C. Garcia-Martinez, S. Busquets, B. Alvarez, N. Agell, P. Costelli, F. J. Lopez-Soriano, A. Celada, and J. M. Argiles. 1998. Different cytokines modulate ubiquitin gene expression in rat skeletal muscle. *Cancer Letters* 133 (1):83-87.

Llovera, M., C. GarciaMartinez, N. Agell, F. J. LopezSoriano, and J. M. Argiles. 1997. TNF can directly induce the expression of ubiquitin-dependent proteolytic system in rat soleus muscles. *Biochemical and Biophysical Research Communications* 230 (2):238-241.

Lorenzo, M. F.-V. S., Vila-Bedmar R, Garcia-Guerra L, De Alvaro C, Nieto-Vazquez I. 2008. Insulin resistance induced by tumor necrosis factor-alpha in myocytes and brown adipocytes. 86 (14 Suppl):E94-104.

Lu, Y. C., W. C. Yeh, and P. S. Ohashi. 2008. LPS/TLR4 signal transduction pathway. *Cytokine* 42 (2):145-151.

Lydyard, P. M., Whelan, A., Fanger, M. W. 2000. Instant Notes in Immunology.

MacEwan, D. J. 2002. TNF receptor subtype signalling: Differences and cellular consequences. *Cellular Signalling* 14 (6):477-492.

Maitra, S. R., M. L. Gestring, M. R. El-Maghrabi, C. H. Lang, and M. C. Henry. 1999. Endotoxin-induced alterations in hepatic glucose-6-phosphatase activity and gene expression. *Molecular and Cellular Biochemistry* 196 (1-2):79-83.

Maitra, S. R., M. M. Wojnar, and C. H. Lang. 2000. Alterations in tissue glucose uptake during the hyperglycemic and hypoglycemic phases of sepsis. *Shock* 13 (5):379-385.

Manchester, J., A. V. Skurat, P. Roach, S. D. Hauschka, and J. C. Lawrence. 1996. Increased glycogen accumulation in transgenic mice overexpressing glycogen synthase in skeletal muscle. *Proceedings of the National Academy of Sciences of the United States of America* 93 (20):10707-10711.

Mannick, J. B., and C. M. Schonhoff. 2002. Nitrosylation: the next phosphorylation? *Archives of Biochemistry and Biophysics* 408 (1):1-6.

Marette, A. 2002. Mediators of cytokine-induced insulin resistance in obesity and other inflammatory settings. *Current Opinion in Clinical Nutrition and Metabolic Care* 5 (4):377-383.

Markovits, J., B. P. Roques, and J. B. Lepecq. 1979. Ethidium Dimer - New Reagent For The Fluorimetric Determination Of Nucleic-Acids. *Analytical Biochemistry* 94 (2):259-264.

McGettrick, A. F., and L. A. J. O'Neill. 2004. The expanding family of MyD88-like adaptors in Toll-like receptor signal transduction. *Molecular Immunology* 41 (6-7):577-582.

McManus, E. J., K. Sakamoto, L. J. Armit, L. Ronaldson, N. Shpiro, R. Marquez, and D. R. Alessi. 2005. Role that phosphorylation of GSK3 plays in insulin. *Embo Journal* 24 (8):1571-1583.

Natanson, C., P. W. Eichenholz, R. L. Danner, P. Q. Eichacker, W. D. Hoffman, G. C. Kuo, S. M. Banks, T. J. MacVittie, and J. E. Parrillo. 1989. Endotoxin and tumor necrosis factor challenges in dogs simulate the cardiovascular profile of human septic shock. *J Exp Med* 169 (3):823-832.

Nedachi, T., and M. Kanzaki. 2006. Regulation of glucose transporters by insulin and extracellular glucose in C2C12 myotubes. *American Journal of Physiology-Endocrinology and Metabolism* 291 (4):E817-E828.

Niesler, C. U., K. H. Myburgh, and F. Moore. 2007. The changing AMPK expression profile in differentiating mouse skeletal muscle myoblast cells helps confer increasing resistance to apoptosis. *Experimental Physiology* 92 (1):207-217.

Nikoulina, S. E., T. P. Ciaraldi, S. Mudaliar, P. Mohideen, L. Carter, and R. R. Henry. 2000. Potential role of glycogen synthase kinase-3 in skeletal muscle insulin resistance of type 2 diabetes. *Diabetes* 49 (2):263-271.

Nishiki, Y., T. Kono, K. Fukao, K. Sato, K. Takahashi, M. Toyomizu, and Y. Akiba. 2008. Nitric oxide (NO) is involved in modulation of non-insulin mediated glucose transport in chicken skeletal muscles. *Comparative Biochemistry and Physiology Part B: Biochemistry and Molecular Biology* 149 (1):101-107.

Novogrodsky, A., A. Vanichkin, M. Patya, A. Gazit, N. Osherov, and A. Levitzki. 1994. Prevention Of Lipopolysaccharide-Induced Lethal Toxicity By Tyrosine Kinase Inhibitors. *Science* 264 (5163):1319-1322.

O'Neill, L. A. J. 2006. How Toll-like receptors signal: what we know and what we don't know. *Current Opinion in Immunology* 18 (1):3-9.

O'Neill, L. A. J. 2008. The interleukin-1 receptor/Toll-like receptor superfamily: 10 years of progress. *Immunological Reviews* 226:10-18.

Orellana, R. A., S. R. Kimball, A. Suryawan, J. Escobar, H. V. Nguyen, L. S. Jefferson, and T. A. Davis. 2007. Insulin stimulates muscle protein synthesis in neonates during endotoxemia despite repression of translation initiation. *American Journal of Physiology-Endocrinology and Metabolism* 292 (2):E629-E636.

Pain, V. M. 1996. Initiation of protein synthesis in eukaryotic cells. *European Journal of Biochemistry* 236 (3):747-771.

Palmer, R. M., M. G. Thompson, R. M. Knott, G. P. Campbell, A. Thom, and K. S. Morrison. 1997. Insulin and insulin-like growth factor-I responsiveness and signalling mechanisms in C2C12 satellite cells: Effect of differentiation and fusion. *Biochimica Et Biophysica Acta-Molecular Cell Research* 1355 (2):167-176.

Palsson-McDermott, E. M., and L. A. J. O'Neill. 2004. Signal transduction by the lipopolysaccharide receptor, Toll-like receptor-4. *Immunology* 113 (2):153-162.

Pardridge, W. M., M. B. Davidson, and D. Casanelloertl. 1978. Glucose and amino-acid metabolism in an established line of skeletal-muscle cells. *Journal of Cellular Physiology* 96 (3):309-317.

Passonneau, V. J., and O. H. Lowry. 1993. *Enzymatic Analysis*: Humana Press.

Pirola, L., A. M. Johnston, and E. Van Obberghen. 2004. Modulation of insulin action. *Diabetologia* 47 (2):170-184.

Plaisance, I., C. Morandi, C. Murigande, and M. Brink. 2008. TNF-alpha increases protein content in C2C12 and primary myotubes by enhancing protein translation via the TNF-R1, PI3K, and MEK. *American Journal of Physiology-Endocrinology and Metabolism* 294 (2):E241-E250.

Plomgaard, P., K. Bouzakri, R. Krogh-Madsen, B. Mittendorfer, J. R. Zierath, and B. K. Pedersen. 2005. Tumor necrosis factor-alpha induces skeletal muscle insulin resistance in healthy human subjects via inhibition of Akt substrate 160 phosphorylation. *Diabetes* 54 (10):2939-2945.

Poltorak, A., X. L. He, I. Smirnova, M. Y. Liu, C. Van Huffel, X. Du, D. Birdwell, E. Alejos, M. Silva, C. Galanos, M. Freudenberg, P. Ricciardi-Castagnoli, B. Layton, and B. Beutler. 1998. Defective LPS signaling in C3H/HeJ and C57BL/10ScCr mice: Mutations in Tlr4 gene. *Science* 282 (5396):2085-2088.

Proud, C. G. 2007. Signalling to translation: how signal transduction pathways control the protein synthetic machinery. *Biochemical Journal* 403:217-234.

Ragolia, L., and N. Begum. 1998. Protein phosphatase-1 and insulin action. *Molecular and Cellular Biochemistry* 182 (1-2):49-58.

Ranganathan, S., and M. B. Davidson. 1996. Effect of tumor necrosis factor-alpha on basal and insulin-stimulated glucose transport in cultured muscle and fat cells. *Metabolism-Clinical and Experimental* 45 (9):1089-1094.

Rees, D. D., S. Cellek, R. M. J. Palmer, and S. Moncada. 1990. Dexamethasone Prevents The Induction By Endotoxin Of A Nitric-Oxide Synthase And The Associated Effects On Vascular Tone - An Insight Into Endotoxin-Shock. *Biochemical and Biophysical Research Communications* 173 (2):541-547.

Ren, J. M., B. A. Marshall, E. A. Gulve, J. P. Gao, D. W. Johnson, J. O. Holloszy, and M. Mueckler. 1993. Evidence from transgenic mice that glucose-transport is rate-limiting for glycogen deposition and glycolysis in skeletal-muscle. *Journal of Biological Chemistry* 268 (22):16113-16115.

Ribe, D., J. Yang, S. Patel, F. O. Koumanov, S. W. Cushman, and G. D. Holman. 2005. Endofacial competitive inhibition of glucose transporter-4 intrinsic activity by the mitogen-activated protein kinase inhibitor SB203580. *Endocrinology* 146 (4):1713-1717.

Roach, P. 2002. Glycogen and its Metabolism. *Current Molecular Medecine* 2 (2):101-120.

Roach, P. J. 1990. Control Of Glycogen-Synthase By Hierarchical Protein-Phosphorylation. *Faseb Journal* 4 (12):2961-2968.

Roach, P. J., J. L. William, and M. D. Lane. 2004. Glycogen Metabolism. In *Encyclopedia of Biological Chemistry*. New York: Elsevier, 244-248.

Roberts, C., Barnard RJ, Scheck SH, Balon TW. 1997. Exercise-stimulated glucose transport in skeletal muscle is nitric oxide dependent. *American Journal of Physiology* 273:E220-225.

Roher, N., V. Samokhvalov, M. Diaz, S. MacKenzie, A. Klip, and J. V. Planas. 2008. The proinflammatory cytokine tumor necrosis factor-alpha increases the amount of glucose transporter-4 at the surface of muscle cells independently of changes in interleukin-6. *Endocrinology* 149 (4):1880-1889.

Roy, D., M. Perreault, and A. Marette. 1998. Insulin stimulation of glucose uptake in skeletal muscles and adipose tissues in vivo is NO dependent. *American Journal of Physiology-Endocrinology and Metabolism* 274 (4):E692-E699.

Rui, L. Y., V. Aguirre, J. K. Kim, G. I. Shulman, A. Lee, A. Corbould, A. Dunaif, and M. F. White. 2001. Insulin/IGF-1 and TNF-alpha stimulate phosphorylation of IRS-1 at inhibitory Ser(307) via distinct pathways. *Journal of Clinical Investigation* 107 (2):181-189.

Schmitz-Peiffer, C., D. L. Craig, and T. J. Biden. 1999. Ceramide generation is sufficient to account for the inhibition of the insulin-stimulated PKB pathway in C2C12 skeletal muscle cells pretreated with palmitate. *Journal of Biological Chemistry* 274 (34):24202-24210.

Schroder, K., P. J. Hertzog, T. Ravasi, and D. A. Hume. 2004. Interferon-gamma: an overview of signals, mechanisms and functions. *Journal of Leukocyte Biology* 75 (2):163-189.

Shangraw, R. E., F. Jahoor, H. Miyoshi, W. A. Neff, C. A. Stuart, D. N. Herndon, and R. R. Wolfe. 1989. Differentiation between septic and postburn insulin resistance. *Metabolism-Clinical and Experimental* 38 (10):983-989.

Shaw, R. J. 2008. mTOR signaling: RAG GTPases transmit the amino acid signal. *Trends in Biochemical Sciences* 33 (12):565-568.

Silva, A. T., and J. Cohen. 1992. Role of interferon-gamma in experimental gram-negative sepsis. *Journal of Infectious Diseases* 166 (2):331-335.

Skurat, A. V., and A. D. Dietrich. 2004. Phosphorylation of Ser(640) in muscle glycogen synthase by DYRK family protein kinases. *Journal of Biological Chemistry* 279 (4):2490-2498.

Smith, F. S., E. D. Ceppi, and M. A. Titheradge. 1997. Inhibition of cytokine-induced inducible nitric oxide synthase expression by glucagon and cAMP in cultured hepatocytes. *Biochemical Journal* 326:187-192.

Smith, P. K., R. I. Krohn, G. T. Hermanson, A. K. Mallia, F. H. Gartner, M. D. Provenzano, E. K. Fujimoto, N. M. Goeke, B. J. Olson, and D. C. Klenk. 1985. Measurement of Protein Using Bicinchoninic Acid. *Analytical Biochemistry* 150 (1):76-85.

Somwar, R., M. Perreault, S. Kapur, C. Taha, G. Sweeney, T. Ramlal, D. Y. Kim, J. Keen, C. H. Cote, A. Klip, and A. Marette. 2000. Activation of p38 mitogen-activated protein kinase alpha and beta by insulin and contraction in rat skeletal muscle - Potential role in the stimulation of glucose transport. *Diabetes* 49 (11):1794-1800.

Sonenberg, N., and T. E. Dever. 2003. Eukaryotic translation initiation factors and regulators. *Current Opinion in Structural Biology* 13 (1):56-63.

Spitzer, J. J., G. J. Bagby, K. Meszaros, and C. H. Lang. 1989b. Altered control of carbohydrate metabolism in endotoxemia. *Prog Clin Biol Res* 286:145-165.

Stadler, J., D. Barton, H. Beilmoeller, S. Diekmann, C. Hierholzer, W. Erhard, and C. D. Heidecke. 1995. Hepatocyte nitric-oxide biosynthesis inhibits glucose output and competes with urea synthesis for l-arginine. *American Journal of Physiology-Gastrointestinal and Liver Physiology* 31 (1):G183-G188.

Stamler, J. S., and G. Meissner. 2001. Physiology of nitric oxide in skeletal muscle. *Physiological Reviews* 81 (1):209-237.

Subramaniam, S., C. Stansberg, and C. Cunningham. 2004. The interleukin 1 receptor family. *Developmental and Comparative Immunology* 28 (5):415-428.

Sugita, H., M. Fujimoto, T. Yasukawa, N. Shimizu, M. Sugita, S. Yasuhara, J. A. J. Martyn, and M. Kaneki. 2005. Inducible nitric-oxide synthase and NO donor induce insulin receptor substrate-1 degradation in skeletal muscle cells. *Journal of Biological Chemistry* 280 (14):14203-14211.

Sugita, H., M. Kaneki, E. Tokunaga, M. Sugita, C. Koike, S. Yasuhara, R. G. Tompkins, and J. A. J. Martyn. 2002. Inducible nitric oxide synthase plays a role in LPS-induced hyperglycemia and insulin resistance. *American Journal of Physiology-Endocrinology and Metabolism* 282 (2):E386-E394.

Sweeney, G., R. Somwar, T. Ramlal, A. Volchuk, A. Ueyama, and A. Klip. 1999. An inhibitor of p38 mitogen-activated protein kinase prevents insulin-stimulated glucose transport but not glucose transporter translocation in 3T3-L1 adipocytes and L6 myotubes. *Journal of Biological Chemistry* 274 (15):10071-10078.

Syed, N. A., and R. L. Khandelwal. 2000. Reciprocal regulation of glycogen phosphorylase and glycogen synthase by insulin involving phosphatidylinositol-3 kinase and protein phosphatase-1 in HepG2 cells. *Molecular and Cellular Biochemistry* 211 (1-2):123-136.

Takaoka, A., and H. Yanai. 2006. Interferon signalling network in innate defence. *Cellular Microbiology* 8 (6):907-922.

Taniguchi, S., K. Takahashi, and S. Noji. 1985. *In Methods of Enzymatic Analysis*. Edited by J. a. G. Bergmeyer. Vol. 7.

Thain, M., Hickman, M. 2000. The Penguin Dictionary of Biology. Tenth Edition.

Tiao, G., J. Fagan, V. Roegner, M. Lieberman, J. J. Wang, J. E. Fischer, and P. O. Hasselgren. 1996. Energy-ubiquitin-dependent muscle proteolysis during sepsis in rats is regulated by glucocorticoids. *Journal of Clinical Investigation* 97 (2):339-348.

Titheradge, M. A. 1998. Nitric oxide protocols. *New Jersey, Humana Press*.

Titheradge, M. A. 1999. Nitric oxide in septic shock. *Biochimica Et Biophysica Acta-Bioenergetics* 1411 (2-3):437-455.

Tognarini, M., and E. Villa-Moruzzi. 1998. Protein phosphatase 1 isoforms in differentiating C2C12 myocytes. *European Journal of Cell Biology* 76 (3):212-219.

Tolosa, L., M. Morla, A. Iglesias, X. Busquets, J. Llado, and G. Olmos. 2005. IFN-[gamma] prevents TNF-[alpha]-induced apoptosis in C2C12 myotubes through down-regulation of TNF-R2 and increased NF-[kappa]B activity. *Cellular Signalling* 17 (11):1333-1342.

Toole, B. J., and P. T. W. Cohen. 2007. The skeletal muscle-specific glycogen-targeted protein phosphate 1 plays a major role in the regulation of glycogen metabolism by adrenaline in vivo. *Cellular Signalling* 19 (5):1044-1055.

Tortorella, L. L., and P. F. Pilch. 2002. C2C12 myocytes lack an insulin-responsive vesicular compartment despite dexamethasone-induced GLUT4 expression. *American Journal of Physiology-Endocrinology and Metabolism* 283 (3):E514-E524.

Towler, M. C., and D. G. Hardie. 2007. AMP-activated protein kinase in metabolic control and insulin signaling. *Circulation Research* 100 (3):328-341.

Tracey, K. J., and A. Cerami. 1994. Tumor-necrosis-factor - a pleiotropic cytokine and therapeutic target. *Annual Review of Medicine* 45:491-503.

Tracey, K. J., H. Wei, K. R. Manogue, Y. M. Fong, D. G. Hesse, H. T. Nguyen, G. C. Kuo, B. Beutler, R. S. Cotran, A. Cerami, and S. F. Lowry. 1988. Cachectin tumor necrosis factor induces cachexia, anemia, and inflammation. *Journal of Experimental Medicine* 167 (3):1211-1227.

Tremblay, F., M. J. Dubois, and A. Marette. 2003. Regulation of GLUT4 traffic and function by insulin and contraction in skeletal muscle. *Frontiers in Bioscience* 8:D1072-D1084.

Tsakiridis, T., C. Taha, S. Grinstein, and A. Klip. 1996. Insulin activates a p21-activated kinase in muscle cells via phosphatidylinositol 3-kinase. *Journal of Biological Chemistry* 271 (33):19664-19667.

Turban, S., V. A. Beardmore, J. M. Carr, K. Sakamoto, E. Hajduch, J. S. C. Arthur, and H. S. Hundal. 2005. Insulin-stimulated glucose uptake does not require p38 mitogen-activated protein kinase in adipose tissue or skeletal muscle. *Diabetes* 54 (11):3161-3168.

Ueki, K., T. Kondo, and C. R. Kahn. 2004. Suppressor of cytokine signaling 1 (SOCS-1) and SOCS-3 cause insulin resistance through inhibition of tyrosine phosphorylation of insulin receptor substrate proteins by discrete mechanisms. *Molecular and Cellular Biology* 24 (12):5434-5446.

Uematsu, S., and S. Akira. 2007. Toll-like receptors and type I interferons. *Journal of Biological Chemistry* 282 (21):15319-15323.

Ulloa, L., and K. J. Tracey. 2005. The 'cytokine profile': a code for sepsis. *Trends in Molecular Medicine* 11 (2):56-63.

Valente, G., L. Ozmen, F. Novelli, M. Geuna, G. Palestro, G. Forni, and G. Garotta. 1992. Distribution of interferon-gamma receptor in human tissues. *European Journal of Immunology* 22 (9):2403-2412.

Vary, T. C., G. Deiter, and S. R. Kimball. 2002. Phosphorylation of eukaryotic initiation factor eIF2B epsilon in skeletal muscle during sepsis. *American Journal of Physiology-Endocrinology and Metabolism* 283 (5):E1032-E1039.

Vary, T. C., G. Deiter, and C. H. Lang. 2004. Diminished Erk 1/2 and p38 MAPK phosphorylation in skeletal muscle during sepsis. *Shock* 22 (6):548-554.

Vary, T. C., D. Drnevich, C. Jurasinski, and W. A. Brennan. 1995. Mechanisms regulating skeletal-muscle glucose-metabolism in sepsis. *Shock* 3 (6):403-410.

Vary, T. C., L. S. Jefferson, and S. R. Kimball. 2001. Insulin fails to stimulate muscle protein synthesis in sepsis despite unimpaired signaling to 4E-BP1 and S6K1. *American Journal of Physiology-Endocrinology and Metabolism* 281 (5):E1045-E1053.

Vary, T. C., and S. R. Kimball. 1992. Sepsis-induced changes in protein-synthesis - differential-effects on fast-twitch and slow-twitch muscles. *American Journal of Physiology* 262 (6):C1513-C1519.

Verstrepen, L., T. Bekaert, T. L. Chau, J. Tavernier, A. Chariot, and R. Beyaert. 2008. TLR-4, IL-1R and TNF-R signaling to NF-kappa B: variations on a common theme. *Cellular and Molecular Life Sciences* 65 (19):2964-2978.

Victor, V. M., M. Rocha, and M. De la Fuente. 2004. Immune cells: free radicals and antioxidants in sepsis. *International Immunopharmacology* 4 (3):327-347.

VillarPalasi, C., and J. J. Guinovart. 1997. The role of glucose 6-phosphate in the control of glycogen synthase. *Faseb Journal* 11 (7):544-558.

Virkamaki, A., and H. Ykijarvinen. 1994. Mechanisms of insulin-resistance during acute endotoxemia. *Endocrinology* 134 (5):2072-2078.

Virkamaki, A., and H. Ykijarvinen. 1995. Role of Prostaglandins in Mediating Alterations in Glucose-Metabolism During Acute Endotoxemia in the Rat. *Endocrinology* 136 (4):1701-1706.

Vishnu Prasad, C. . Personal Communication.

Wahrmann, J. P., F. Gros, and D. Luzzati. 1973. Phosphorylase And Glycogen Synthetase During Myoblast Differentiation. *Biochimie* 55 (4):457-463.

Wallach, D., Arumugam T.U., Boldin M.P., Cantarella G. *et.al.* 2002. How are the regulators regulated? The search for mechanisms that impose specificity on induction of cell death and NF-κB activation by members of the TNF/NGF receptor family. *Arthritis Research* 4 (suppl 3):S189-S196.

Wallington, J. 2004. The regulation of hepatic carbohydrate metabolism during endotoxic shock. *Biochemistry* Brighton (University of Sussex).

Wallington, J., J. Ning, and M. A. Titheradge. 2008. The control of hepatic glycogen metabolism in an in vitro model of sepsis. *Molecular and Cellular Biochemistry* 308 (1-2):183-192.

Wiernan, H. L., J. A. Wofford, and J. C. Rathmell. 2007. Cytokine stimulation promotes glucose uptake via phosphatidylinositol-3 kinase/Akt regulation of Glut1 activity and trafficking. *Molecular Biology of the Cell* 18 (4):1437-1446.

Williams, G., T. Brown, L. Becker, M. Prager, and B. P. Giroir. 1994. Cytokine-induced expression of nitric-oxide synthase in c2c12 skeletal-muscle myocytes. American Journal of Physiology-Regulatory Integrative and Comparative Physiology 267 (4):R1020-R1025.

Williamson, D. L., S. R. Kimball, and L. S. Jefferson. 2005. Acute treatment with TNF-alpha attenuates insulin-stimulated protein synthesis in cultures of C2C12 myotubes through a MEK1-sensitive mechanism. American Journal of Physiology-Endocrinology and Metabolism 289 (1):E95-E104.

Wilson, W. A., A. V. Skurat, B. Probst, A. de Paoli-Roach, P. J. Roach, and J. Rutter. 2005. Control of mammalian glycogen synthase by PAS kinase. Proceedings of the National Academy of Sciences of the United States of America 102 (46):16596-16601.

Woodgett, J. R., and P. S. Ohashi. 2005. GSK3: an in-Toll-erant protein kinase? Nature Immunology 6 (8):751-752.

Yaffe, D., and O. Saxel. 1977. Serial passing and differentiation of myogenic cells isolated from dystrophic mouse muscle. Nature 270 (5639):725-727.

Yasukawa, T., E. Tokunaga, H. Ota, H. Sugita, J. A. J. Martyn, and M. Kaneki. 2005. S-nitrosylation-dependent inactivation of Akt/protein kinase B in insulin resistance. Journal of Biological Chemistry 280 (9):7511-7518.

Ykijarvinen, H., D. Mott, A. A. Young, K. Stone, and C. Bogardus. 1987. Regulation of glycogen-synthase and phosphorylase activities by glucose and insulin in human skeletal-muscle. Journal of Clinical Investigation 80 (1):95-100.

Young, M. E., G. K. Radda, and B. Leighton. 1997. Nitric oxide stimulates glucose transport and metabolism in rat skeletal muscle in vitro. Biochemical Journal 322:223-228.

Zhang, J. H., Z. L. Xie, Y. Z. Dong, S. X. Wang, C. Liu, and M. H. Zou. 2008. Identification of nitric oxide as an endogenous activator of the AMP-activated protein kinase in vascular endothelial cells. Journal of Biological Chemistry 283 (41):27452-27461.

Zhang, J. N., J. Hiken, A. E. Davis, and J. C. Lawrence. 1989. Insulin Stimulates Dephosphorylation Of Phosphorylase In Rat Epitrochlearis Muscles. Journal of Biological Chemistry 264 (29):17513-17523.